

**Unravelling the antidiabetic effects of polyphenols in
chamomile: the gastrointestinal tract as a potential site
of action.**

Jose Alberto Villa Rodriguez

Submitted in accordance with the requirements for the degree of Doctor of
Philosophy

The University of Leeds
School of Food Science and Nutrition

November, 2017

*The best preparation for tomorrow
is doing your best today*

H. Jackson Brown, Jr.

The candidate confirms that the work submitted is his own, except where work which has formed part of jointly-authored publications has been included. The contribution of the candidate and the other authors to this work has been explicitly indicated below. The candidate confirms that appropriate credit has been given within the thesis where reference has been made to the work of others.

Publications

Chapter 2 and 3 and 4 contain work which has also been used in the publications

Villa-Rodriguez, J.A., Kerimi, A., Abranko, L., C., & Williamson, G. (2015) German chamomile (*Matricaria chamomilla*) extract and its major polyphenols inhibit intestinal alpha-glycosidases *in vitro*. *FASEB Journal*, **21(1)**, LB323.

Nyambe-Silavwe, H*., **Villa-Rodriguez, J.A*.**, Ifie, I*., Holmes, M., Aydin, E., Jensen, J.M. & Williamson, G. (2015). Inhibition of human α -amylase by dietary polyphenols. *Journal of Functional Foods*, **19**, 723-732. (*equal contribution).

Villa-Rodriguez, J.A*., Aidyn E*., Gauer, J.S., M., Pyner, A., Williamson, G., & Kerimi, A. (2017) Green and chamomile teas, but not acarbose, attenuate glucose and fructose transport via inhibition of GLUT2 and GLUT5. *Molecular Nutrition & Food Research*. doi: 10.1002/mnfr.201700566 (*equal contribution).

Villa-Rodriguez, J.A., Kerimi, A., Abranko, L., Ford, L., M., Blackburn, R., Rayner, C., & Williamson, G. Acute metabolic actions of the major polyphenols in chamomile: an *in vitro* mechanistic study on their potential to attenuate postprandial hyperglycaemia. *Manuscript under peer review in Scientific Reports*.

Conference abstracts

Villa-Rodriguez, J.A., Kerimi, A., Abranko, L., C., & Williamson, G. German chamomile (*Matricaria chamomilla*) extract and its major polyphenols inhibit intestinal alpha-glycosidases in vitro. Experimental Biology Conference, Boston, MA, USA, 2015.

Villa-Rodriguez, J.A., Kerimi, A., Abranko, L., C., & Williamson, G. German chamomile extract and its major polyphenols inhibit carbohydrate digestion and absorption *in vitro*. VII International Conference on Polyphenols and Health, Tours, France, 2015.

Villa-Rodriguez, J.A., Kerimi, A., Abranko, L., Ford, L., M., Blackburn, R., Rayner, C., & Williamson, G. Potential effects of chamomile polyphenols to modulate carbohydrate digestion and absorption: targeted analysis on (*Z*), and (*E*)-methoxycinnamic acid glucoside, apigenin and apigenin 7-*O*-glucoside. 1st International Conference on Food Bioactives and Health, Norwich, UK, 2016.

Konic-Ristic, A., Nyambe-Silavwe, H., **Villa-Rodriguez, J.A.,** Ifie, I., Williamson, G. Interactions between polyphenols as inhibitors of human α -amylase. 1st International Conference on Food Bioactives and Health, Norwich, UK, 2016.

Acknowledgements.

I would like to take this opportunity to thank the people who have helped and supported me over the last four years.

First of all, I am very grateful to my supervisor, Professor Gary Williamson for giving me the opportunity to conduct my doctoral work in his world-renowned group and for all his mentorship, guidance and contribution to the research work but most importantly for sharing his broad knowledge and enthusiasm for science. I also want to thank him for providing the scientific environment to explore the effects of polyphenols on energy metabolism, which has proven to be an exciting journey.

My deepest gratitude goes to all the people that shared with me their intellectual and technical knowledge for the successful completion of this research work. I would like to particularly recognise the contribution of Dr. Asimina Kerimi for sharing with me the technical skills to perform cell culture experiments, for her intellectual input to the work and for her endless disposal for discussion. I acknowledge Dr. Laszlo Abranko, Professor Christopher Rayner and Ms Lauren Ford for our collaborative work and for their analytical expertise in this project. I also extend my gratitude to Dr. Sharka Tumova for her approachable attitude and willingness to help at any moment.

Thanks to all my past and present colleagues, especially to Idolo Ifie, Michael Houghton, Julia Gauer, Alison Pyner, Hilda Nyambe Aleksandra Konic Ristic and Samantha Gardner. You guys have been my family in Leeds, I have been fortunate to spend such an amazing time with you.

I want to thank to the School of Food Science and Nutrition and its entire staff.

Special thanks are reserved for Ms. Justine Segui who motivated and encouraged me throughout my PhD but most importantly, I want to thank you for your patient and understanding. It has not been easy for you travelling to Leeds nearly every weekend and I want to dedicate this work to you. Special thanks are also to my family, for their consistent love and support.

Finally, I would like to acknowledge CONACYT Mexico for funding my PhD studies.

Abstract.

Background and objective: Polyphenol-rich foods and extracts have been proposed of being capable of lower imbalance in energy metabolism and type 2 diabetes risk by mitigating postprandial glycaemia. However, this physiological action is still controversial due to conflicting *in vivo* evidence which is partially due to their limited characterisation in terms of active constituents, their targets and efficacies. This study systematically investigated the potential of a polyphenol rich-extract (chamomile) to blunt postprandial sugar rise, the compounds involved and biochemical pathways affected.

Methods: A combination of HPLC and LC/QTOF were used to characterise the polyphenol profile of aqueous chamomile extract. The inhibition of carbohydrate-digesting enzymes was determined using an isolated human salivary α -amylase and acetone rat intestinal powder under optimal kinetic conditions. The inhibition of sugar transporters and cholesterol uptake was assessed in the well-characterised intestinal cell models Caco-2/TC7 and Caco-2 respectively.

Results: When assessed by inhibition of α -amylase and maltase activities, the active components were apigenin-7-*O*-glucoside, apigenin, and (*Z*) and (*E*)-2-hydroxy-4-methoxycinnamic acid glucosides. The latter two compounds were purified and characterised. Molecular docking studies showed that apigenin and cinnamic acids present totally different poses in the active site of α -amylase which determined their potency. In differentiated Caco-2/TC7 cell monolayers, apigenin-7-*O*-glucoside and apigenin strongly inhibited D-[U-¹⁴C]-glucose and D-[U-¹⁴C]-sucrose transport, and less effectively D-[U-¹⁴C]-fructose transport, whereas the cinnamic acids were ineffective on all sugar transport. Inhibition of D-[U-¹⁴C]-glucose transport by apigenin was stronger under Na⁺-depleted conditions, suggesting interaction with the GLUT2 transporter and competitive binding studies with molecular probes indicate interaction primarily at the exofacial-binding site. The attenuation of glucose absorption had a knock on effect on [4-¹⁴C]-cholesterol uptake by downregulating Niemann-Pick C1 Like 1 protein.

Conclusion: Chamomile extract containing apigenin and apigenin 7-*O*-glucoside or the individual components thereof, could potentially reduce glucose absorption and availability within the enterocyte attenuating the glucose and cholesterol-rich chylomicron particles during the postprandial phase.

Table of contents.

Acknowledgements	iv
Abstract	v
Table of contents	vii
List of figures	xiii
List of tables	xvii
List of abbreviations	xviii
Chapter 1 Literature review	1
1.1 Introduction.....	1
1.2 Carbohydrate and lipid metabolism: an their interplay in the development of type 2 diabetes and cardiovascular disease.....	2
1.3 Polyphenols: from antioxidants to modulators of human metabolism.	6
1.4 Importance of polyphenol characterisation to establish their health effects.....	9
1.5 Botanical extracts as a source of polyphenols to promote metabolic health: the case of chamomile and type 2 diabetes.....	11
1.5.1 <i>In vivo</i> evidence of the metabolic protection of chamomile and apigenin.....	11
1.5.2 <i>In vitro</i> evidence of the metabolic protection of chamomile and apigenin.....	15
1.6 Metabolic regulation by the GI tract: a potential site of action for polyphenols and polyphenol rich-foods and extracts on diabetes.....	19
1.6.1 The GI tract in carbohydrate intake and sensing for controlling energy homeostasis: the significance of the postprandial state.....	20
1.6.2 Postprandial glycaemia and polyphenols.	26
1.7 Aim and objectives of the thesis	33

Chapter 2 Identification and quantification of major polyphenols in chamomile: isolation and structural characterisation of two hydroxycinnamic acid derivatives.....	35
2.1 Abstract.....	35
2.2 Introduction.....	36
2.3 Materials and methods.....	38
2.3.1 Materials.....	38
2.3.2 Methods.....	38
2.3.2.1 Preparation of ChE for high performance liquid chromatography analysis and semi-preparative isolation.	38
2.3.2.2 Identification and quantification of major polyphenols in ChE... ..	38
2.3.2.3 Method development for the isolation of hydroxycinnamic acid derivatives from ChE by semi-preparative RP-HPLC chromatography.	40
2.3.2.4 Semi-preparative isolation of hydroxycinnamic acid derivatives	42
2.3.2.5 Chemical characterisation of hydroxycinnamic acid derivatives.. ..	44
2.3.2.5.1 HPLC/MS ² and QTOFMS.....	44
2.3.2.5.2 Acid hydrolysis.....	44
2.3.2.5.3 Determination of the monosaccharide moiety.....	45
2.3.2.5.4 NMR.....	46
2.3.2.5.5 Synthesis of (<i>E</i>)-2-hydroxy-4-methoxycinnamic acid. ...	48
2.3.3 Statistical analysis.	49
2.4 Results and discussion.....	50
2.4.1 Analytical and semipreparative HPLC-DAD analysis.....	50

2.4.2	Chemical characterisation of the hydroxycinnamic acid derivatives.....	53
2.5	Conclusion.....	61
Chapter 3 Assessment of the inhibition of carbohydrate-digesting enzymes by polyphenols and chamomile extract <i>in vitro</i>: optimisation of α-amylase activity using the 3, 5-dinitrosalicylic acid method and determination of molecular interactions <i>in silico</i>.....		
3.1	Abstract.....	62
3.2	Introduction.....	64
3.3	Materials and methods.....	68
3.3.1	Materials.....	68
3.3.2	Methods.....	68
3.3.2.1	Determination of K_m and V_{max}	68
3.3.2.2	Enzyme concentration and reaction time.....	69
3.3.2.3	Effect of polyphenols on colour reagent.....	69
3.3.2.4	Retention efficiency of Solid Phase Extraction cartridges by HPLC-PDA.....	70
3.3.2.5	Human salivary α -amylase inhibition assay.....	71
3.3.2.6	Preparation of maltodextrin-free ChE.....	74
3.3.2.7	Inhibition of α -glucosidase activity by ChE and its individual major polyphenols.....	74
3.3.2.8	Molecular Modelling.....	77
3.3.3	Statistical analysis.....	79
3.4	Results and discussion.....	80
3.4.1	Effect of enzyme and substrate concentration on inhibition.....	80
3.4.2	Kinetic studies on amylose and amylopectin.....	83
3.4.3	Interference of polyphenols with the DNS reagent.....	84

3.4.4	Inhibitory effect of selected polyphenols on human salivary α -amylase activity.....	86
3.4.5	Inhibitory effect of ChE and individual major polyphenols on human salivary α -amylase and α -glucosidase activity.....	89
3.4.6	Modelling studies.....	94
3.5	Conclusion.....	102
Chapter 4 Chamomile, apigenin and apigenin 7-O-glucoside attenuate monosaccharide transport across Caco-2/TC7 cell monolayers: a mechanistic study for the identification of the target transporter.....		
4.1	Abstract.....	103
4.2	Introduction.....	104
4.3	Materials and methods.....	107
4.3.1	Materials.....	107
4.3.2	Methods.....	107
4.3.2.1	Preparation of ChE for bioactivity studies.....	107
4.3.2.2	Cell culture.....	107
4.3.2.3	Transport assay of monosaccharides in Caco-2/TC7 cells... ..	108
4.3.2.4	Differential mRNA and protein expression levels of GLUT5 in Caco-2 and Caco-2/TC7 cells.....	111
4.3.2.5	Characterisation of the main glucose transporter in Caco-2/TC7 cells and its inhibition by ChE, apigenin and apigenin 7-O-glucoside.....	115
4.3.2.6	Detection of GLUT2 in Caco-2/TC7 cells by immunofluorescence staining.....	115
4.3.2.7	<i>In vitro</i> conversion of apigenin 7-O-glucoside to apigenin by Caco-2/TC7 cells.....	116
4.3.3	Statistical analysis.....	116
4.4	Results and discussion.....	117

4.4.1	Inhibitory effect of ChE and polyphenols on glucose, sucrose and fructose transport.....	117
4.4.2	Identification of the main glucose transporter protein in Caco-2/TC7 cells and the effect of ChE, apigenin and apigenin 7- <i>O</i> -glucoside on its activity.....	124
4.5	Conclusion.....	134

Chapter 5 Glucose stimulates cholesterol uptake in Caco-2 cells *via* upregulation of NPC1L1 protein receptor and this response is attenuated by the acute inhibition of glucose absorption by Chamomile and apigenin 7-*O*-glucoside
..... 135

5.1	Abstract.....	135
5.2	Introduction.....	136
5.3	Materials and methods.....	140
5.3.1	Materials.....	140
5.3.2	Methods.....	140
5.3.2.1	Preparation of ChE for bioactivity studies.....	140
5.3.2.2	Cell culture.....	140
5.3.2.3	Preparation of mixed-micelles.....	140
5.3.2.4	Acute inhibition of D-[U- ¹⁴ C]-glucose uptake.....	143
5.3.2.5	Gene expression analysis of cholesterol flux transporters....	144
5.3.3	Statistical analysis.....	144
5.4	Results and discussion.....	145
5.4.1	Glucose promote [4- ¹⁴ C]-cholesterol uptake in Caco-2 cells.....	145
5.4.2	[4- ¹⁴ C]-cholesterol uptake in Caco-2 cells is attenuated by acute inhibition of glucose absorption by ChE and apigenin 7- <i>O</i> glucoside.....	149
5.5	Conclusion.....	157

Chapter 6 Polyphenols and type 2 diabetes :perspectives and conclusion.	158
6.1 Advances in polyphenol research: the GI tract as a prime site of action?.....	160
6.1.1 Perspective.....	162
6.1.2 Concluding comments	168
List of references.	170
Appendix A. Assay parameters used for measuring the inhibition of human salivary α-amylase by polyphenols. Adapted from Nyambe-Silavwe <i>et al.</i> (2015).	192
Appendix B. Assay parameters used for measuring the inhibition of porcine α-amylase by polyphenols. Adapted from Nyambe-Silavwe <i>et al.</i> (2015)..	193
Appendix C. Assay parameters used for measuring the inhibition of microorganism α-amylase by polyphenols. Adapted from Nyambe-Silavwe <i>et al.</i> (2015).....	194

List of figures

Figure 1.1 The role of obesity on tissue-specific metabolic dysregulations leading to type 2 diabetes and cardiovascular disease.....	4
Figure 1.2 Absorption, metabolism and excretion of polyphenols in the human body..	7
Figure 1.3 Postprandial metabolic effects occurred from 2-6 h post-ingestion of high GI foods.	22
Figure 2.2 Basic configuration of the AKTA purifier system used to isolate the hydroxycinnamic acid derivatives from ChE.	40
Figure 2.3 Chromatographic separation of polyphenols present in ChE.	41
Figure 2.4 Chromatographic separation of polyphenols present in ChE using the C6 phenyl column.....	42
Figure 2.5 LC-MS of isolated compounds from ChE.....	43
Figure 2.6 HPLC-DAD chromatograms of PMP derivatives of standard monosaccharides.....	46
Figure 2.7 HPLC-DAD and LC-MS analysis of chemically synthesised (<i>E</i>)-2-hydroxy-4-methoxycinnamic acid.....	49
Figure 2.8 Analysis of polyphenols in ChE.	51
Figure 2.9 Semi-preparative purification of the two hydroxycinnamic acid derivatives (HCA) from ChE using the AKTA system.....	53
Figure 2.10 Fragmentation pattern of isolated ion at m/z 711.....	55
Figure 2.11 Analysis of hydroxycinnamic acid derivative 2 (HCA 2) after acid hydrolysis.....	56
Figure 2.12 Acid hydrolysis of hydroxycinnamic acid derivative 2 (HCA 2).....	56
Figure 2.13 Comparison of the resulting compounds after acid hydrolysis with authentic standards of monosaccharides.....	58
Figure 2.14 NOESY analysis of hydroxycinnamic acid derivative 2.....	59

Figure 3.1 Steps involved in the digestion of starch and the disaccharides sucrose and lactose leading to the appearance of glucose in circulation.....	65
Figure 3.2 Reaction of DNS with reducing sugars.	66
Figure 3.3 Representative example of maltose standard calibration curve.	69
Figure 3.4 Retention efficacy of OASIS solid phase extraction cartridges.	70
Figure 3.5 Schematic representation of human α -amylase inhibition assay.....	72
Figure 3.6 Enzymatic determination of glucose by hexokinase-linked reaction.	76
Figure 3.7 Representative example of glucose standard calibration curve.....	76
Figure 3.8 Validation of the docking parameters using the crystal structure analyses of human α -amylases.	78
Figure 3.9 Time-dependence rate of hydrolysis by human α -amylase.	81
Figure 3.10 Inhibition of human α -amylase by acarbose.....	82
Figure 3.11 Lineweaver–Burk plot for action of human α -amylase.....	83
Figure 3.12 Reaction of selected polyphenols with the DNS reagent solution.	85
Figure 3.13 Relationship between the number of OH groups and colour development by DNS reagent solution.....	85
Figure 3.14 Inhibition of human α -amylase by polyphenols.	87
Figure 3.15 Dixon plot kinetic analysis of EGCG on human α -amylase.	88
Figure 3.16 Inhibition of human α -amylase activity by ChE and polyphenols.	90
Figure 3.17 Enzymatic hydrolysis of kaempferol 3- <i>O</i> -glucoside (positive control) and (<i>E</i>)-MCAG.....	92
Figure 3.18 Inhibition of rat maltase activity by ChE and polyphenols.	93
Figure 3.19 Structural comparison between the residues forming chemical interactions with the co-crystal structures of human salivary (1MFV) and human pancreatic α -amylase (1CPU).	97
Figure 3.20 The binding pose and chemical interactions of polyphenols with human salivary α -amylase.	98

Figure 3.21 Substrate binding pose of strong polyphenol inhibitors of human salivary α amylase.	99
Figure 4.1 Schematic representation of glucose and fructose absorption in the small intestine.	104
Figure 4.2 Schematic representation of Transwell® permeable support.	109
Figure 4.3 Schematic representation of the experimental design for assessing the inhibition of D-[U- ¹⁴ C]-monosaccharide transport across differentiated Caco-2/TC7 cell monolayers.	110
Figure 4.4 Representative example of ddPCR data viewed as a 1-D plot with each droplet from a sample plotted on the graph of fluorescence intensity vs droplet number.	112
Figure 4.5 Schematic representation of the integration of all steps equivalent to a traditional Western blot in the automated capillary ProteinSimple system ‘Wes’.	113
Figure 4.6 Concentration-dependent detection of multiplexed claudin-1 and GLUT5 in whole cell lysate.	114
Figure 4.7 Monosaccharide transport under Na ⁺ conditions across differentiated Caco-2/TC7 cells monolayers.	117
Figure 4.8 Inhibition of D-[U- ¹⁴ C]-fructose transport by ChE across differentiated Caco-2 cell monolayers.	119
Figure 4.9 Differential mRNA and protein expression levels of GLUT5 in differentiated Caco-2 and Caco-2/TC7 cell monolayers.	120
Figure 4.10 Inhibition of monosaccharide transport under Na ⁺ conditions across differentiated Caco-2/TC7 cell monolayers by individual polyphenols.	121
Figure 4.11 Inhibition of monosaccharide transport by ChE and combined inhibition of apigenin and apigenin 7- <i>O</i> -glucoside (A7G).	123
Figure 4.12 Concentration-dependent inhibition of D-[U- ¹⁴ C]-sucrose transport by the antidiabetic drug acarbose across differentiated Caco-2/TC7 cell monolayers.	124

Figure 4.13 Characterisation of the main D-[U- ¹⁴ C]-glucose transporter in Caco-2/TC7 cell monolayers	125
Figure 4.14 Inhibition D-[U- ¹⁴ C]-glucose transport across differentiated Caco-2/TC7 cell monolayers under Na ⁺ -free conditions	126
Figure 4.15 <i>In vitro</i> conversion of apigenin 7- <i>O</i> -glucoside to apigenin by Caco-2/TC7 cells.....	128
Figure 4.16. Immunofluorescence detection of GLUT2 in differentiated Caco-2/TC7 cell monolayers.....	130
Figure 4.17 Characterisation of the potential binding site of apigenin and apigenin 7- <i>O</i> -glucoside (A7G) on GLUT2.....	131
Figure 4.18 Effects of ChE and apigenin on D-[U- ¹⁴ C]-glucose transport across differentiated Caco-2/TC7 cell monolayers.....	132
Figure 5.1 Cholesterol metabolism in the human body.	136
Figure 5.2 Formation of mixed-micelle containing cholesterol as assessed by particle size and distribution.	141
Figure 5.3 Effect of type of plate on [4- ¹⁴ C]-cholesterol uptake in Caco-2 cells...	143
Figure 5.4 Effect of glucose concentration and incubation time on [4- ¹⁴ C]-cholesterol uptake in Caco-2 cells.....	146
Figure 5.5 Effect of glucose concentration on [4- ¹⁴ C]-cholesterol uptake in Caco-2 cells.....	147
Figure 5.6 Time-dependence effect of glucose concentration on [4- ¹⁴ C]-cholesterol uptake in Caco-2 cells.....	148
Figure 5.7 Effect of acute inhibitors of glucose absorption on [4- ¹⁴ C]-cholesterol uptake.....	150
Figure 5.8 Representative examples of ABCG5/G8 and TBP ddPCR expression analysis following incubation in media with different glucose concentrations.	153
Figure 5.9 Quantitative mRNA expression analysis of NPC1L1 in differentiated Caco-2 cells following incubation in media containing 5, 10 and 25 mM glucose and with and without inhibitors of glucose uptake.....	154

List of tables

Table 1.1 <i>In vivo</i> studies of the antidiabetic effects of chamomile and apigenin.	12
Table 2.1 Polyphenol profile of aqueous ChE.	50
Table 2.2 Identification and quantification of targeted polyphenols in ChE.	51
Table 2.3. Q/TOF-MS/MS of isolated hydroxycinnamic acid derivatives (HCA) from ChE.	54
Table 3.1 Experimental IC ₅₀ values of acarbose, selected polyphenols and green tea extract.	82
Table 3.2 Docking scores of polyphenols on human salivary and pancreatic α -amylase.	95

List of abbreviations

[M-H] ⁻ ... Negatively charged molecular ion.	HHydrogen.
~.....Approximately.	HbA1cHaemoglobin A1c.
°C.....Celsius degree.	HCLHydrochloric acid.
μCi.....Microcurie.	HisHistidine.
μL.....Microlitre.	HPLCHigh performance liquid chromatography.
μM.....Micromole.	HzHertz.
AktProtein kinase B.	ICInhibition constant.
Apo-BApolipoprotein B.	ICAM-1 .Intercellular Adhesion Molecule 1.
AREAntioxidant response element.	IDInternal diameter.
AspAspartame.	IL-1βInterleukin 1 beta.
CACalifornia.	IL-6Interleukin 6.
Ca⁺Calcium ion.	KKelvin.
CaCl₂Calcium chloride.	K⁺Potassium ion.
Caco-2Colorectal adenocarcinoma cell line.	KClPotassium chloride.
CD38Cluster of differentiation 38.	KEAP1Kelch-like ECH-associated protein 1.
cDNAComplementary DNA.	Ki ... Inhibitor-enzyme dissociation constant.
CoACoenzyme A.	K_mHalf of the V _{max} .
COX-2Cyclooxygenase 2.	LCLiquid chromatography.
CVColumn volume.	LC-MSLiquid chromatography-mass spectrometry.
DaDalton.	LeuLeucine.
DADDiode array detector.	m/zMass to charge ratio.
DMSODimethyl sulfoxide.	MAMassachusetts.
DNADesoxyribonucleic acid.	mAUMilli absorbance unit.
EDTAEthylenediaminetetracetic acid.	mgMilligram.
eNOSEndothelial nitric oxide synthase.	MHzMegahertz.
FWHMFull width at half maximum.	MinMinutes.
GluGlutamine.	mL :.....Millilitre.
GLUT2Glucose transporter protein 2.	mMMillimolar.
GLUT5Glucose transporter protein 5.	
GlyGlycine.	

mm.....Millimeter. **STOP-NIDDM**.....Study to prevent non-
mRNA.....Messenger RNA. insulin dependent diabetes mellitus.
MS.....Mass spectrometry. **T1R2-T1R3**....Sweet taste receptor dimers.
Na⁺.....Sodium ion. **TEER**.....Trans epithelial resistance.
NaCl.....Sodium chloride. **TFA**.....Trifluoroacetic acid.
NAD⁺...Nicotinamide adenine dinucleotide. **TNF- α**Tumour Necrosis factor alpha.
NADH.....Reduced nicotinamide adenine **TOF**.....Time of flight.
dinucleotide. **Trp**.....Tryptophan.
NaHCO₃.....Sodium carbonate. **Tyr**.....Tyrosine.
NaOH.....Sodium hydroxide. **U**.....Units.
NF- κ B.....Nuclear factor- κ B. **UK**.....United Kingdom.
nm.....Nanometre. **USA**.....United States of America.
Nrf2.....Nuclear factor erythroid 2-related **UV**.....Ultraviolet.
factor 2. **v/v**.....Volume/volume.
PBS.....Phosphate buffer saline. **VCAM-1**...Vascular cell adhesion protein 1.
PGE₂.....Prostaglandin E2. **Vis**.....Visible.
PI3K.....Phosphatidylinositol-4,5- **Vmax**.....Maximal velocity.
bisphosphate 3-kinase. **WHO**.....World health organisation.
PKA.....Protein Kinase A. **μ m**.....Micrometre.
PKC ϵProtein kinase C epsilon.
ppm.....Parts per million.
PTFE.....Polytetrafluoroethylene.
Q.....Quadrupole analyser.
RNA.....Ribonucleic acid.
RPC.....Reverse phase chromatography.
SEM.....Standard error of mean.
SGLT1.....Sodium-dependent glucose
cotransporter 1.
siRNA.....Small interfering RNA.
SIRT.....Sirtuin.
SLC2A5.....Solute carrier family 5 member
gene 1.

Chapter 1 Literature review.

1.1 Introduction.

Intake of high-calorie foods and sedentary lifestyles are important contributors in today's society to the prevalence of cardiometabolic disturbances such as obesity, type 2 diabetes and cardiovascular disease. It has been predicted that 90 % of obesity-related type 2 diabetes and 80 % of coronary heart disease conditions are preventable by decreasing caloric intake and increasing expenditure (Willett, 2002).

Epidemiological evidence supports that dietary habits rich in fruits and vegetables and plant-derived food products could be inversely associated with the risk of developing type 2 diabetes and cardiovascular disease (Ley *et al.*, 2014; Amiot *et al.*, 2016; Bertoia *et al.*, 2016). A common attribute of a plant-derived diet is its polyphenol content and thus polyphenols have been postulated as key mediators of the underlined health effects. Polyphenols present variable bioavailability, are highly metabolised and their biotransformation in the gastrointestinal (GI) tract is heterogeneous across individuals (Manach *et al.*, 2016; Williamson and Clifford, 2017). This has been a major shortcoming to establish functional connections between plasma metabolites and the vast range of claimed metabolic changes, limiting our understanding of their biological actions in the human body, including their cardiometabolic protection. The GI tract has postprandially the highest concentration of polyphenols compared to any other site in the body by one or more orders of magnitude (Williamson, 2013) and therefore it could be a major site where polyphenols can mediate cardiometabolic protection by for example, reducing postprandial sugar excursions.

This literature review will present and integrate the current understanding of diet-related factors contributing to metabolic disorders and describe the recent advancements and limitations in the study of polyphenols, which are exemplified by studies conducted in chamomile, a significance source of these molecules. Moreover, a prospective view is provided for the translational application to protect and/or manage the metabolic

phenotype observed in type 2 diabetes, emphasising the GI tract as a short-term realistic target.

1.2 Carbohydrate and lipid metabolism: an interplay in the development of type 2 diabetes and cardiovascular disease.

The current concept of metabolic disorders is that ‘high caloric diets’ cause a disruption in normal cell energy metabolism resulting in the development of cardiometabolic diseases such as type 2 diabetes. Sugars and fats are energy-dense nutrients that contribute ~75 % of the total calorie intake in a diet; therefore it is not surprising that the interaction between carbohydrate and lipid metabolism which are intimately interlinked through the intersection of metabolic pathways is fundamental for energy balance.

After a meal, upon digestion and absorption by α -glycosidases and membrane transporters respectively (for a detailed description of carbohydrate digestion and absorption see chapter 3 and 4, respectively), simple carbohydrates are delivered to the liver *via* the lymphatic system. The liver processes a substantial part of these sugars through the glycolysis, glycogenesis and *de novo* lipogenesis (DNL) pathways producing energy, glycogen and lipids respectively (Vacca *et al.*, 2015). In the case of lipids, a proportion is stored in the adipose tissue and the remaining part exported into circulation as very low-density lipoproteins (VLDL) particles to cardiac and skeletal muscle for energy consumption (Harwood, 2012).

In a similar way, dietary lipids travel to the liver forming part of chylomicron particles after a series of reactions that take place in the small intestine (see chapter 5 for a comprehensive description). These include hydrolysis by pancreatic and intestinal lipases, uptake by the enterocytes, re-esterification and conjugation with apolipoprotein B48 in the enterocyte to form the chylomicrons (Dash *et al.*, 2015). Once in circulation, the chylomicron-triglyceride component is hydrolysed by lipoprotein lipase (LPL) expressed on the surface of peripheral tissues such as adipocyte, myocytes, and macrophages, producing the low-density lipoproteins (LDL). The triglyceride component is used for

energy production, stored in the liver or adipocytes *via* lipogenesis or exported back into circulation as a VLDL component (Vacca *et al.*, 2015; Bays *et al.*, 2016).

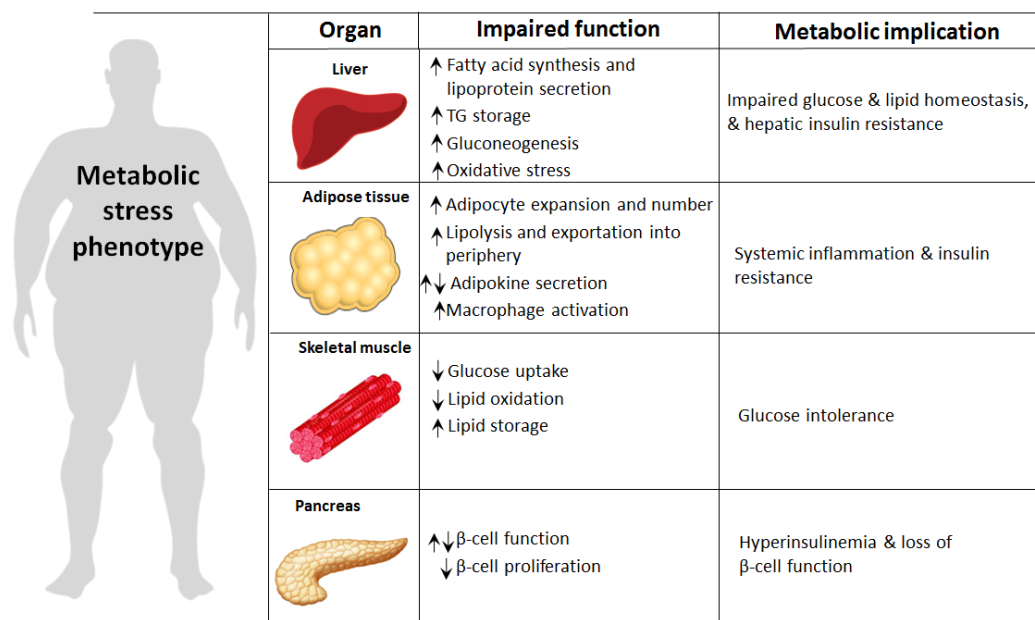
Therefore, systemic glucose and lipid levels are in a constant state of flux, with overall levels ultimately dependent on the balance between glucose and lipid acquisition and removal (regulated by a complex system of network of transcription factors, signal transducer proteins and metabolic enzymes) governed by highly active metabolic tissues such as the liver (Cheng *et al.*, 2015; Vacca *et al.*, 2015), adipocytes (Harwood, 2012), myocytes and pancreas (Muio and Newgard, 2008; Taylor, 2013). However, in situations of chronic energy excess (high calorie diets), a dysregulation of glucose and lipids flux occurs contributing to a coordinated breakdown in cellular functions.

The biochemical pathways linked to type 2 diabetes have been deciphered and it is consensual that the major pathogenesis factor is the accumulation of lipids in the liver and adipose tissue. Chronic excess of calorie intake in the form of carbohydrates (which are ultimately metabolised to glucose) overactivates the DNL pathway through the action of insulin facilitating the synthesis of fatty acids. The excess of fatty acids are primarily stored and exported into circulation (to counterbalance the accumulation of lipids) due to the inhibition of β -oxidation by the malonyl-CoA produced during DNL (Taylor, 2013).

Fatty acids are therefore esterified with glycerol to produce mono-, di-, and triglycerides where raised levels of diacylglycerol have been implicated in an impaired insulin action (Taylor, 2013). Moreover, when the storage capability of the adipose tissue is reached (normally occurring in the obesity condition), there is a dysregulated secretion of adipokines (i.e. adiponectin, leptin, resistin, retinol binding protein 4) along with the gain of a proinflammatory state (promotion of adipocytokines), resulting in an increased fatty acid release from adipocytes (Harwood, 2012). These adipocyte-derived fatty acids and the circulating fraction originating from the DNL are taken up and stored in the liver. Thus irregularities in the DNL and adipose tissue dysfunction during metabolic stress promotes the inundation of lipids in the liver and an inflammatory response, which ultimately impairs insulin signalling resulting in systemic insulin resistance; a pathophysiological state where cells fail to respond to the normal actions of insulin.

Although whether insulin resistance arises first in the peripheral tissues or in the liver is still a matter of debate.

Insulin exerts a variety of physiological effects to integrate nutrient processing and energy assimilation. Insulin promotes hepatic glucose uptake, glycolysis, glycogenesis and inhibits gluconeogenesis, promotes DNL, free fatty acid influx and efflux of VLDL (Vacca *et al.*, 2015). Thus the insulin resistant state leads to uncontrolled gluconeogenesis and reduced catabolism of circulating VLDL and chylomicron remnants, which seems to be mediated by an aberrant adipose tissue hormonal function (Harwood, 2012) driving to hyperglycaemia and dyslipidaemia. Hyperglycaemia and dyslipidaemia lead to systemic increases in oxidative stress, produces a pro-inflammatory state predominantly resulting in increased levels of TNF- α , IL-6 and C-reactive protein which increase lipid deposition and the development of endothelial dysfunction and atherosclerotic plaque (Lumeng and Saltiel, 2011). Thus, type 2 diabetes results from a vicious cycle of conditions such as hyperglycaemia, hyperinsulinemia, systemic inflammation, dyslipidaemia and insulin resistance, ultimately ensuing the loss of β -cell function (figure 1.1).







Organ	Impaired function	Metabolic implication
 Liver	↑ Fatty acid synthesis and lipoprotein secretion ↑ TG storage ↑ Gluconeogenesis ↑ Oxidative stress	Impaired glucose & lipid homeostasis, & hepatic insulin resistance
 Adipose tissue	↑ Adipocyte expansion and number ↑ Lipolysis and exportation into periphery ↑↓ Adipokine secretion ↑ Macrophage activation	Systemic inflammation & insulin resistance
 Skeletal muscle	↓ Glucose uptake ↓ Lipid oxidation ↑ Lipid storage	Glucose intolerance
 Pancreas	↑↓ β -cell function ↓ β -cell proliferation	Hyperinsulinemia & loss of β -cell function

Figure 1.1 The role of obesity on tissue-specific metabolic dysregulations leading to type 2 diabetes and cardiovascular disease. The interplay between sugar and lipid metabolism responsible for the metabolic dysregulations described in the text. Increase ↑; decrease ↓; altered ↑↓. TG: triglycerides.

Type 2 diabetes is a condition that affects over ~420 million people worldwide (WHO, 2016) and is rapidly becoming a global epidemic with a projected increase of ~55 % by 2035 (Guariguata *et al.*, 2014). Overweight and obesity are the two main risk factors associated with this disease (Forouzanfar *et al.*, 2015). Findings from meta-analyses indicate that consumption of readily absorbable sugars such as sucrose, fructose and glucose increases the prospect of body fat gain *via* changes in energy intake (Te Morenga *et al.*, 2013) and independently of adiposity, they contribute to type 2 diabetes onset (Imamura *et al.*, 2015).

In support of this, two independent meta-analyses suggest that carbohydrate quality, rather than quantity, as evidenced by the glycaemic index (GI) and the glycaemic load, has a greater impact on type 2 diabetes risk (Livesey *et al.*, 2008; Bhupathiraju *et al.*, 2014) and management (Brand-Miller *et al.*, 2003; Livesey *et al.*, 2008). Reduced sugar intake, consumption of low glycaemic index diets and regular exercise have been suggested as effective modifiable factors to avoid type 2 diabetes (Ley *et al.*, 2014). However, the rising numbers of cases indicates compliance is poor and other actions are needed.

Dietary patterns that include the consumption of plant-based food items such as coffee, tea, fruits and vegetables and plant extracts have been associated with a reduced risk of developing type 2 diabetes (Liu *et al.*, 2013; Ding *et al.*, 2014; Salas-Salvadó *et al.*, 2014; Bertoia *et al.*, 2016; Martel *et al.*, 2016). For instance, consumption of a Mediterranean diet with extra virgin olive oil without calorie restriction has shown to reduce the incidence of type 2 diabetes by 40 % (Salas-Salvadó *et al.*, 2014). Common dietary constituents of these diets are polyphenols, a group of molecules which are not included in the classical definition of a nutrient, but which are plausible mediators of the underlined health effects. This has placed polyphenols in the spotlight for the prevention and treatment of type 2 diabetes, and worldwide efforts are being conducted to establish functional connections between *in vitro* and *in vivo* studies in order to prove causation.

1.3 Polyphenols: from antioxidants to modulators of human metabolism.

Since the establishment of the free radical theory, which stated the role of free radicals and other 'reactive oxygen species (ROS)' in the development of many human diseases (Harman, 1956), the belief that molecules with antioxidant properties would delay or prevent disease risk started emerging in the minds of the scientific community. Polyphenols, naturally-occurring compounds *in planta* belonging to the group of the so called *phytochemicals* (for a comprehensive review on their biosynthesis and content in certain plant-base foods and beverages see Crozier *et al.* (2009)) were among these molecules. Recognition that polyphenols, due to their inherent chemical antioxidant activity (conferred by the availability OH groups), were responsible for protecting biomolecules for oxidation helping to maintain key cellular process, provided the scientific basis to explain the epidemiological evidence stating an association between the consumption polyphenol-rich foods (fruits, vegetables, cocoa and cereals) and the prevention/reduction of some chronic and degenerative diseases. However, as soon as bioavailability studies started to be conducted, an increasing awareness about the biological relevance of such findings emerged, and the paradigm of their mode of action started to change.

The process of absorption, metabolism and excretion of the most abundant polyphenols after dietary intake is well understood (figure 1.2). Bioavailability studies on polyphenols revealed that they are extensively metabolised during absorption from the small intestine, resulting in the formation of glucuronides, sulphates (Wong *et al.*, 2010) and methyl metabolites (Lotito *et al.*, 2011), while in the colon breakdown to phenolic acids and non-phenolic catabolites occurs (Roowi *et al.*, 2010). As such, the compounds that are found in the circulatory system and reach the peripheral tissues are chemically different from the dietary form, and therefore, they do not retain the same *in vitro* antioxidant capacity (Lotito *et al.*, 2011).

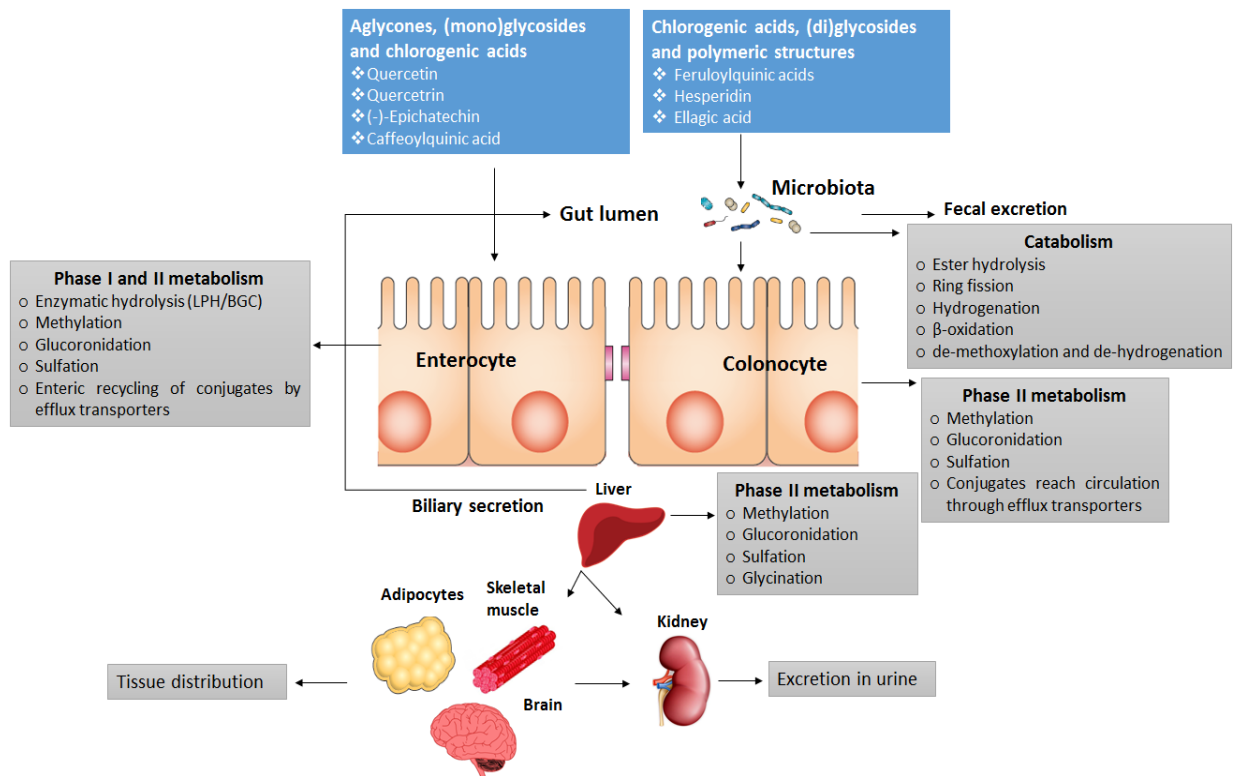


Figure 1.2 Absorption, metabolism and excretion of polyphenols in the human body. The absorption of polyphenols is associated with cleavage and release of the aglycone by the action of lactase phloridzin hydrolase (LPH) in the small intestine and by an alternative step mediated by β -glucosidase (BGC) within the epithelial cells (Day *et al.*, 1998; Day *et al.*, 2000; Crozier *et al.*, 2009), thus allowing passage through enterocytes and then to the blood stream *via* efflux transporters. Before this last, the aglycones undergo phase II metabolism forming sulfate, glucuronide, and/or methylated metabolites *via* the action of phenol sulfotransferases, UDP glucucosyl transferase and catechol-*O*-methyltransferase, respectively (Wong *et al.*, 2010). The conjugates formed can be excreted back into the intestinal lumen by efflux transporters. Once in the bloodstream, metabolites rapidly reach the liver, where they can be subjected to further phase II metabolism and then secreted into circulation where they can reach and be absorbed in other peripheral tissues or excreted in the urine or bile. Conjugated polyphenols (i.e sugars and organic acids) that are resistant to the action of LPH/BGC are not absorbed in the small intestine and pass to the colon (Day *et al.*, 1998; Day *et al.*, 2000; Crozier *et al.*, 2009). Once in the colon, the colonic microbiota transform these polyphenols into absorbable products yielding different catabolites although predominant groups (i.e phenolic acids with zero to three aromatic hydroxyls, or their mono- or di-methoxy analogues) originated from varying substrates (i.e chlorogenic acids, flavanols, proanthocyanidins, theaflavins) can be found (Williamson and Clifford, 2017).

Moreover, polyphenols are absorbed with an estimated maximum concentration of 10 μM in plasma for metabolites and 1 μM for total aglycones (Clifford, 2004), suggesting that their biological activity once absorbed goes beyond the modulation of oxidative stress and therefore, their mechanism of action might be far more complex. Because of the relatively concentration of absorbed aglycones, it is widely acknowledged that metabolites are the active forms, although it has also been proposed that aglycones can mediate biological functions after intracellular deconjugation as evidenced for quercetin (Menendez *et al.*, 2011; Dueñas *et al.*, 2013).

The current view of the cellular effects of dietary polyphenols and their metabolites is that they interact with specific proteins central to intracellular signalling cascades. These interactions, through the activation of specific genes, either directly or indirectly, are associated with the modulation of cellular functions related to oxidative processes, inflammation, insulin resistance, energy metabolism and mitochondrial function (Kerimi and Williamson, 2016). As such, there are multiple and complex metabolic pathways affected making almost an impossible task to establish a clear association between aglycones, plasma metabolites (rarely available for mechanistic studies) and the overwhelming range of induced metabolic changes in peripheral tissues such as the pancreas, liver, skeletal muscle and adipose tissue. This is further complicated by our very limited understanding of the distribution and concentrations reached in these organs. Although this issue is currently being addressed with the use of metabolomics, one of the main challenges is to obtain robust predictive biomarkers of exposure since large interpersonal variation exist (Manach *et al.*, 2016). Furthermore, the development of these biomarkers has been further complicated by the incomplete qualitative and quantitative characterisation of polyphenol-rich foods and extracts. The metabolites present in circulation are determined in the first instance by the precursor polyphenol in *planta* and so, in order to strengthen the evidence for a specific food containing polyphenols, and indeed, a specific polyphenol and human health, a reliable and full characterisation is required.

1.4 Importance of polyphenol characterisation to establish their health effects.

As products of plant secondary metabolism, polyphenols are present in virtually all foods of plant origin and many phenolic structures have been reported so far (Crozier *et al.*, 2009). This huge diversity of chemical structures of polyphenols is one of the main limitations to estimate their content in foodstuff, estimate their daily average intake and establish a clear relationship between their intake and health and disease state.

There are many factors than can affect the polyphenol profile and content *in planta* and in food items. These include the species, geographic distribution, seasonal variation and processing and storage conditions. Certain polyphenols are widely distributed, whereas others are specific to a particular plant or food. All these factors make the qualitative and quantitative estimation of polyphenols a challenging task and it has been regarded as the main limitation to correlate the insights obtained from epidemiological studies to those observed in *in vitro* studies using a particular polyphenol, polyphenol-rich food or extract (Crozier *et al.*, 2009).

In planta, polyphenols are generally found conjugated to sugars and organic acids. They are hydroxylated, methoxylated, and/or glycosylated derivatives and the linked sugar is often glucose or rhamnose (Crozier *et al.*, 2009). The number of sugar moieties ranges from one to two or three, and there are several positions of substitution on the polyphenol (Singh *et al.*, 2008). Therefore, a complex mixture of chemical structures can be found *in planta* and so highly specialised and costly analytical instrumentation are required to characterise the polyphenol constituents in a plant matrix. Instrumentation requirements have been addressed with the development of powerful techniques such as LC-ESI-MS and tandem MS which have provided the necessary measurements to selectively characterise compounds in a complex matrix (Gosslau *et al.*, 2011; Joven *et al.*, 2013). However, the development of suitable standards required for a confident and rigorous identification and quantification has not been fully overcome. Arguably, surrogate standards supported by LC-MS data providing retention time, UV-Vis spectrum, molecular mass, and mass fragmentation data can be employed to fingerprint and

unequivocally identify polyphenols in plant matrices (Clifford and Madala, 2017). This information is open to interpretation and therefore, very often can result in the identification of erroneous polyphenol structures without a careful interpretation of the analytical data. This is clearly demonstrated by the polyphenol characterisation of chamomile where two abundant compounds were mistakenly identified by Mulinacci *et al.* (2000) and this work has served as a reference for the identification of these compounds in further studies (discussed in chapter 2).

Polyphenols are natural compounds and consequently, their content and distribution will vary in *planta* and will do so in plant-based foods and extracts that are used *in vivo* and *in vitro* studies for exploring their effects on health. This could explain the heterogeneity of results reported in the literature for polyphenol-rich foods and extracts on putative health benefits. An example could be cocoa polyphenols, particularly flavan-3-ols, where a health claim on their vasodilatory effects has been accepted by the European Commission (Tallon, 2015). The claim indicates that intake of 200 mg of cocoa flavanols with a degree of polymerisation of 1-10 can help to maintain the elasticity of blood vessels contributing to normal blood flow. More than 20 oligomers with a degree of polymerisation from 2-20 have been reported in cocoa (Porter *et al.*, 1991) and their composition, content and bioavailability are greatly influenced by processing techniques (Payne *et al.*, 2010). This implies that the vasodilatory effects of cocoa may be present or totally absent since it is elusive which of the polymers is likely responsible for the activity and so, the proposed physiological effect may not be sustained from batch to batch. Therefore a full and reliable characterisation of the polyphenol source under investigation seems to be a first and necessary step in order to establish functional links between active constituents, their molecular targets and mode(s) of action. Only with this data, will we be able to formulate polyphenol-nutritional approaches for lowering the risk and managing cardiometabolic diseases such as type 2 diabetes.

1.5 Botanical extracts as a source of polyphenols to promote metabolic health: the case of chamomile and type 2 diabetes.

Botanicals represent a valuable source of polyphenols that can be employed to promote metabolic health. Chamomile (*Matricaria recutita L*) epitomises a remarkable example as evidenced by recent human, animal and *in vitro* studies. Chamomile is widely used throughout the world and its consumption in the form of tea has been estimated over 1 million cups per day (Srivastava and Gupta, 2009). Thus it contributes significantly to dietary exposure of polyphenols, particularly the flavone apigenin and its glucoside and acylated derivatives which represent the predominant examples (Švehlíková *et al.*, 2004). In the following sections, the most recent evidence supporting the health effects of chamomile and/or apigenin and the potential mechanism involved in metabolic benefits in relation to type 2 diabetes will be presented and discussed.

1.5.1 *In vivo* evidence of the metabolic protection of chamomile and apigenin.

In recent years, a number of animal studies have suggested the potential of chamomile for regulating carbohydrate and lipid metabolism in experimental diabetes (table 1.1). In streptozotocin-induced diabetic rats, where diabetes is induced by the irreversible destruction of the β -islet cells of the pancreas by streptozotocin (a naturally produced antibiotic from *Streptomyces achromogenes*), the administration of an hydroalcoholic chamomile extract (36/64 v/v) for 14 days decrease postprandial hyperglycaemia as compared with control diabetic rats, with an overall decreased ranging ~20-25 % depending on the dose (5-100 mg/kg) (Cemek *et al.*, 2008). Interestingly, the effect observed by chamomile at the highest concentration in diabetic rats was superior to that of glibenclamide (5 mg/kg), an antidiabetic drug that stimulates insulin release from the pancreas. The authors also observed an improvement of other metabolic parameters (doses ranging from 20-100 mg/kg) including reduced levels of oxidative stress as evidenced by the lower blood levels of malondialdehyde, along with an increase in the activity of antioxidant enzymes (superoxide dismutase, catalase), the levels of dietary antioxidants (vitamin C and β -carotene) and protection of β -cell function.

The results described above suggest that chamomile protection is mediated through the attenuation of glucose absorption, preventing hyperglycaemia and the associated oxidative stress and thus protecting β -cell function. Indeed, the findings of an independent subsequent study support the aforementioned pathway. Using the same experimental model, Kato *et al.* (2008) showed that acute chamomile intervention (water extract, 500 mg/kg) decreased postprandial glucose peak levels by ~15% after a sucrose loading test where the effect was evidenced after 30 min, and reaching baseline levels at 120 min. In the same study, chronic administration of chamomile for 21 days using the same dose reduced fasting glucose levels (~24%) and increased hepatic glycogen content (~3.6 fold).

Table 1.1 *In vivo* studies of the antidiabetic effects of chamomile and apigenin.

Test material*/compound	Model	Dose	Duration (weeks)	Biomarkers positively affected	Reference
Chamomile	Streptozotocin-induced diabetic rats	20 mg/kg/d	2	Fasting blood glucose Glucose intolerance	Eddouks et al. (2005)
Chamomile	Streptozotocin-induced diabetic rats	20-100 mg/kg/d	2	Glucose intolerance Malondialdehyde blood levels Oxidative stress	Cemek et al. (2008)
Chamomile	Streptozotocin-induced diabetic rats	500 mg/kg/d	3	Fasting blood glucose	Kato et al. (2008)
Chamomile	Streptozotocin-induced diabetic rats	500 mg/kg/d	3	Postprandial blood glucose	Kato et al. (2008)
Apigenin	Streptozotocin-induced diabetic rats	4 mg/kg/d	1	Fasting blood glucose Glucose intolerance Liver injury Renal dysfunction	Rauter et al. (2010)
Apigenin	Diet-induced obese mice (C57BL/6)	100 mg/kg (intraperitoneal injection)	1	Fasting blood glucose Glucose intolerance Blood glucose concentration Hepatic triglycerides	Escande et al. (2013)
Chamomile	Diet-induced obese mice (C57BL/6)	200 mg/kg/d	6	Fasting blood glucose Glucose intolerance Plasma triglycerides Insulin resistance Adipose dysfunction	Weidner et al. (2013)
Chamomile	Lean high-fat fed mice (C57BL/6)	200 mg/kg/d	20	Fasting blood glucose Glucose intolerance Insulin resistance Hepatic non-esterified fatty acids in the liver Hepatic triglycerides	Weidner et al. (2013)
Apigenin	Type 2 diabetic subjects	3000 mg (20 mg/mL) 3 times/day after each meal	8	Fasting glucose and insulin HbA1C Insulin resistance Plasma cholesterol Plasma triglycerides Plasma LDL-cholesterol Malondialdehyde blood levels Oxidative stress	Rafraf et al. (2015) Zemestani et al. (2016)
Apigenin	Streptozotocin-induced diabetic rats fed with a high-fat diet	50 and 100 mg/kg/d	6	Fasting glucose and insulin HbA1C Insulin resistance Plasma cholesterol Plasma triglycerides Plasma LDL-cholesterol Malondialdehyde blood levels Oxidative stress Endothelial function	Ren et al. (2016)

*The chemical composition of the extract used during the study was not reported.

These results provide more robust evidence about the modulation of glucose by chamomile, suggesting an attenuation of glucose absorption in the intestine and a direct/indirect effect in the liver through the modulation of gluconeogenesis.

The protective effect of chamomile on peripheral tissues such as the liver and adipose tissue has been recently demonstrated in a lean high fat-fed C57BL/6 mice. In this animal model, high fat diet is provided in order to induce obesity and the associated metabolic disorders (discussed in section 1.3). Chronic chamomile intervention (200 mg/kg/day, 20 weeks) inhibited the high fat diet-induced insulin resistance by ~35% and the accompanying increase in fasting plasma glucose and improved dyslipidaemia evidenced by a decrease of circulating free fatty acids and triacylglycerol as compared to control mice (Weidner *et al.*, 2013). Although body weight changes were not observed between controls and treated mice, hepatic analysis at the functional level suggest that chamomile promotes adequate lipid oxidation and utilisation. Hepatic tissue of high fat-fed mice over 20 weeks showed increases in liver triacylglycerols and non-esterified fatty acids along with signs of liver inflammation and fatty liver formation. Chamomile treatment efficiently attenuated the metabolic stress caused by the high-fat diet with reductions of ~72% and ~64% of triacylglycerols and free fatty acids respectively, and a decrease in the protein expression of TNF- α (~54%) which attenuated the signs of fatty liver formation (reduction of ~64%).

Interestingly, the protective effects of chamomile remained in obese mice which have already developed a pathophysiological phenotype (i.e insulin resistance). Chronic treatment with chamomile (200 mg/kg/d) substantially reduced insulin resistance (~36%), fasting glucose levels and glucose intolerance (~15%), plasma triacylglycerol (~35%), free fatty acids (53%), total cholesterol (16%) and LDL/VLDL cholesterol (~43%). Gene expression analysis of adipose tissue of mice treated with chamomile showed an upregulation of important genes participating in lipid metabolism and so, the aforementioned affects could have been mediated by reduction of adipocyte dysfunction (Weidner *et al.*, 2013).

Although not conclusive, the most convincing evidence about the potential of chamomile to attenuate metabolic dysregulation characteristic of diabetes state comes from a recent

human intervention study (Rafraf *et al.*, 2015). In a single blinded, randomized, parallel controlled clinical trial, type 2 diabetes subjects consumed one cup of chamomile tea (20 mg/mL) three times a day immediately after meals for 8 weeks. Compared to baseline values, subjects who consumed chamomile tea showed an improvement of metabolic parameters characterised by reductions in fasting serum glucose (~11 %) and insulin levels (~39%), the levels of glycated haemoglobin (HbA1c, ~5%), and insulin resistance (~40%). Similar improvements were observed in lipid profile with reductions of total cholesterol, total triglycerides and LDL-cholesterol by ~18, 5.6 and 9 %, respectively. These metabolic improvements were related with a reduction of oxidative stress as evidenced by lower serum malondialdehyde and higher activity of antioxidant enzymes (Zemestani *et al.*, 2016) as previously reported in streptozotocin-induced diabetic rats (Cemek *et al.*, 2008).

It is important to mention that during the human study, the type 2 diabetic subjects were consuming their normal dose of the antidiabetic drug metformin, indicating that the metabolic effects elicited by chamomile were complementary. This highlights the potential of botanicals in general, and chamomile in particular, to complement the use of antidiabetic drugs and maximise effects while lowering deleterious side effects, providing everyday maintenance.

Most of the *in vivo* evidence on the positive effects of chamomile to prevent and attenuate the metabolic dysregulation of diabetic state comes from animal studies. These effects seem to be translated in humans, although more studies are needed to validate these findings. These studies should consider the dose-response effects as well as to employ standardised formulation based on active constituent(s), which is still a matter of investigation since all the presented studies failed to provide compositional data. Apigenin and its derivatives appears to be strong candidates considering they are present in higher amounts than any other polyphenol in chamomile and their bioactivity is supported by *in vitro* studies.

1.5.2 *In vitro* evidence of the metabolic protection of chamomile and apigenin.

The effect of polyphenols on energy metabolism is likely through a variety of different mechanisms including reduction on postprandial glucose, enhanced insulin secretion and improved insulin sensitivity, modification of hepatic glucose release, activation of insulin receptors and glucose uptake and modulation of signalling pathways and gene expression and modulation of gut microbiota (Hanhineva *et al.*, 2010; Kim *et al.*, 2016). So how do chamomile polyphenols modulate energy metabolism? Most of the mechanistic evidence indicates that chamomile works by interacting with transcription factors and the proteins of cell signalling pathways affecting gene expression patterns, although careful interpretation of the *in vitro* data needs to be conducted when extrapolating to the effects found *in vivo*.

A study conducted by Weidner *et al.* (2013) pointed out the protective effects of chamomile on type 2 diabetes *via* activation of fatty acid sensors that control metabolic programs and regulate energy homeostasis. In this study, using a combination of *in vitro* assays, the authors showed that the chemical constituents of an ethanolic extract of chamomile interact and activate nuclear receptor peroxisome proliferator-activated receptors (PPARs). In a competitive binding assay, chamomile extract interacted with relatively the same strength with different PPARs with binding constants of ~6, 9 and 10 $\mu\text{g/mL}$ for PPAR γ , PPAR β/δ and PPAR α respectively. However, this was not proportional to the activation of PPARs where the half-maximal concentration to activate PPAR γ was ~ 14 and 44-fold lower than PPAR α and PPAR β/δ respectively in a reporter gene assay.

In adipocytes, chamomile upregulated the expression of genes involved in adipose differentiation, lipid uptake and storage and inflammation whereas in hepatocytes, increased expression of genes promoting β -oxidation were observed. Knockdown of PPAR γ and PPAR α with siRNA in adipocytes and hepatocytes respectively, led to a significant reduction of gene expression by chamomile. Deletion of PPAR γ and PPAR α in mice fed a high-fat diet has been associated with the development of hypertriglyceridemia, increased susceptibility to high fat diet-induced steatosis,

hyperinsulinemia, and insulin resistance; conversely, their activation with pharmacological agents protected mice against these metabolic dysregulations (He *et al.*, 2003; Su *et al.*, 2014). Thus, PPAR γ and PPAR α could represent one of the potential molecular targets through which chamomile exerts metabolic protection, preserving adipose tissue and liver normal functions under metabolic stress conditions (chronic overnutrition). However, from this study, it is not clear whether there is a direct activation of PPARs or their activation is *via* modulation of the activity of downstream SIRT1 target peroxisome proliferator-activated receptor-coactivator 1 α (an activator of PPARs) by altering intracellular NAD⁺ levels. Apigenin (10-40 μ M) maintained adequate levels of NAD⁺ by inhibiting CD38 activity and promoting SIRT1 activity in A549 cells and in primary CD38 wild-type and knockout mouse embryonic fibroblasts (Escande *et al.*, 2013). This was associated with improved glucose homeostasis and reduces lipid content in the liver of high-fat diet-induced obesity mice.

Obesity and early stages of type 2 diabetes, are characterised by a low-grade systemic inflammation and oxidative stress, which in turn are associated with adipose tissue dysfunction, insulin resistance, endothelial dysfunction and liver damage. Existing data suggest that the metabolic protection observed in *in vivo* studies with chamomile may be complementary mediated through alleviating inflammation and oxidative burst.

In lipopolysaccharide (LPS)-activated RAW 264.7 cells, aqueous chamomile extract reduced the synthesis of prostaglandins (PGE₂) in a time (0-24 h) and dose-dependent (5-40 μ g/mL) manner. This effect was described to be through the inhibition of the COX-2 pathway by inhibiting the synthesis and activity of the enzyme (Srivastava *et al.*, 2009) by apigenin 7-*O*-glucoside, which constituted ~90% of the polyphenol content in the extract. In support of this, in LPS-THP1 macrophages, apigenin at doses of 10-50 μ M drastically suppressed the release of IL-6, IL-1 β and TNF- α (70-90%), however when chamomile extract was tested, this effect was nearly suppressed owing to the low content of apigenin (0.8 μ M) (Drummond *et al.*, 2013). In an independent study, apigenin reduced NF- κ B activation, ICAM-1 mRNA expression and increased insulin-mediated nitric oxide (NO) production in endothelial cells after palmitic acid treatment (Ren *et al.*, 2016). Apigenin attenuated the protein levels of lectin-like oxidized LDL receptor-1 elicited by high glucose and TNF- α in endothelial cells *via* downregulation of mRNA expression

(Yamagata *et al.*, 2011) and reducing phosphorylation of protein kinase C β II, oxidative stress and apoptosis along with increased NO levels (Qin *et al.*, 2016); this effect was mediated *via* the PI3K/Akt/eNOS pathway. These *in vitro* results suggest that chamomile/apigenin can confer metabolic protection by mitigating inflammation and oxidative stress caused by hyperglycaemia. This antioxidant response could be mediated through the Keap1/Nrf2/ARE pathway thus, increasing the expression of antioxidant enzymes (Bhaskaran *et al.*, 2013).

Postprandial glycaemia is associated with metabolic dysregulation by altering nutrient partitioning, promoting fat storage in metabolic tissues (liver, adipose tissue and skeletal muscle), and insulin resistance (Ludwig, 2002; Blaak *et al.*, 2012). An intensive area of research on polyphenols and type 2 diabetes has focused on their ability to attenuate carbohydrate digestion and absorption which could help to ameliorate metabolic stress (Williamson, 2013); this could represent one of the mechanism by which chamomile confers metabolic protection. In fact, in human intervention studies (Rafraf *et al.*, 2015; Zemestani *et al.*, 2016), chamomile tea was taken after every meal, underlining the possibility that the metabolic effects observed can be related with the attenuation of postprandial glycaemia. An aqueous chamomile extract inhibited porcine pancreatic α -amylase and rat maltase and sucrase activity with IC₅₀ values of ~5200, ~2600 and ~900 μ g/mL, respectively (Kato *et al.*, 2008). This represents the only mechanistic study looking at the modulation of postprandial glucose by chamomile and so, its potential to modulate this metabolic pathway needs further scientific investigation.

Despite the valuable mechanistic information that has been generated on the antidiabetic potential of chamomile, most of it is relevant only in a pharmacological context rather than in reducing type 2 diabetes risk by a dietary approach. In these studies, chamomile extract was directly applied to cells reaching concentrations and chemical forms of polyphenols that are not normally expected when they undergo normal metabolism after consumption. For instance, the evident inhibition of COX-2 expression and activity was observed when chamomile was applied at concentrations of 10 and 20 μ g/mL containing ~40 and ~80 μ M of apigenin 7-*O*-glucoside (Srivastava *et al.*, 2009). This polyphenol is unlikely to be present in the blood stream since it undergoes deglycosylation and microbial metabolism resulting in the formation of phase II conjugates (Teng *et al.*, 2012)

and microbial catabolites such as 3-(4-hydroxyphenyl)propionic acid (Hanske *et al.*, 2009). Maximum apigenin plasma concentration in rats consuming an oral dose of ~15 μM was ~ 0.185 μM indicating that only ~1.23 % is bioavailable (Teng *et al.*, 2012). The *in vitro* studies on apigenin report an average effective dose of ~10-50 μM which could not possibly have been achieved by the oral administration of chamomile in the *in vivo* studies conducted in rats and mice (assuming that apigenin is present mainly as glycoside derivative and underwent mammalian metabolism) and so, they do not support the metabolic protection observed in these animal models. This conclusion can be generalised for many other *in vitro* studies employing pure polyphenols and polyphenol-rich extracts where the doses applied are not achievable through the diet, and so they do not entirely represent what occurs *in vivo* after repetitive dietary intakes.

Growing scientific consensus converges on the notion that metabolites rather than the parent polyphenol (chemical form *in planta*) are the ones influencing metabolism after absorption. Certainly, deciphering the molecular targets and metabolic pathways of these metabolites in terms of type 2 diabetes risk prevention is not an easy task, since the chemical types and concentrations that reach systemic circulation are a function of the individual's genetic profile and microbiota capabilities. Understanding their *true* mechanism of action requires the development of *in vitro* models that better represent the chronic effect as normally happens after dietary intake, rather than the current *pharmacological* approach adopted for most of the studies so far. As a consequence, we have a very limited knowledge of the systemic action of polyphenols and polyphenol-rich foods and extracts, and so it certainly will take some few years until we partially define robust functional connections between circulating polyphenol metabolites and human health and disease state.

Emerging evidence is starting to unmask the contribution and significance that GI dysregulation plays on the body's energy balance, suggesting that it can be a prime target for therapeutic actions. Unlike other organs, the knowledge generated on the actions of polyphenols and polyphenol-rich foods and extracts including chamomile can be directly applied at this site, since postprandial concentrations of parent compounds can reach the mM range (Williamson, 2013). Recognition of this therapeutic potential as a core activity of these molecules is of primary importance for the development of new products with

relevant nutritional characteristics. They can also provide an increase of daily polyphenol intake and may guarantee the health benefits attributed to plant-based diets. These formulations could provide a window to effective clinical nutrition acting subtly but broadly given significant changes in energy balance over a life time period and preventing and managing cardiometabolic diseases including type 2 diabetes (Brown *et al.*, 2015).

1.6 Metabolic regulation by the GI tract: a potential site of action for polyphenols and polyphenol rich-foods and extracts on diabetes.

It has started to be widely acknowledged that altered GI function is a significant contributor of aberrant metabolism leading to metabolic stress and the subsequent progression to type 2 diabetes and associated comorbidities. Intervention studies in humans and animals, as well as mechanistic studies in cell models, have provided scientific evidence for the protective effects of polyphenols acting at different sites in the GI tract, positively influencing physiological processes that protect against type 2 diabetes. This can be achieved on two main fronts, i) lowering postprandial and total glucose excursions and ii) preserving intestinal barrier function. The latter can be accomplished by offsetting LPS-mediated inflammation, increasing the expression of junctional proteins and remodelling microbiota ecology (Cani *et al.*, 2008; Cani *et al.*, 2009). Interestingly, some *in vitro* studies suggests that modulation of these biochemical pathways may represent two of the true mechanism by which polyphenols in general, and chamomile in particular, confer metabolic protection against type 2 diabetes. However, a full discussion of these topics is outside the scope of this thesis, and only the metabolic functions of the GI tract in carbohydrate digestion and sugar and the effect of polyphenols on these pathways will be discussed.

1.6.1 The GI tract in carbohydrate intake and sensing for controlling energy homeostasis: the significance of the postprandial state.

The GI tract contains differentiated specialized cell types including enterocytes, enteroendocrine, goblet, and paneth cells. Enterocytes are absorptive cells responsible for transporting nutrients into circulation. Enteroendocrine cells coordinate gut functioning through specific peptide hormone secretion (GI hormones) which regulate nutrient absorption and utilisation while goblet and paneth cells are responsible for protecting against chemical damage and modulating the innate immunity respectively (van der Flier and Clevers, 2009). The GI tract is thus responsible for the sensing, digestion and absorption of nutrients evoking complex neural and endocrine responses that control energy metabolism while also functioning as a barrier, preventing antigens and pathogens entering the mucosal tissues and potentially causing disease.

Throughout the GI tract, carbohydrates and lipids are sensed *via* G protein-coupled taste receptors (GPCRs) expressed in enteroendocrine cells (originally identified in the oral epithelium) increasing intracellular Ca^{2+} (Sternini *et al.*, 2008; Reimann *et al.*, 2012). Intracellular Ca^{2+} spikes release GI hormones from secretory granules at the basolateral membrane which activate nearby vagal- and spinal afferent fibres from neurons and/or enter the bloodstream to conduct their hormonal function including the regulation of sugar absorption and its metabolism (Sternini *et al.*, 2008; Reimann *et al.*, 2012). GI hormones described to regulate these pathways include cholecystokinin (CCK), glucose-dependent insulinotropic peptide (GIP), glucagon-like peptides (GLPs) and peptide YY (PYY).

Upon reaching the upper small intestine, partially hydrolysed carbohydrates activate GPCRs expressed on 'I' and 'K' enteroendocrine cells releasing CCK and GIP respectively. CCK induces the secretion of α -amylase from the pancreas (Sternini *et al.*, 2008), thus achieving efficient carbohydrate digestion by converting starch into smaller oligosaccharides, dextrans and disaccharides which require a further step involving the action of α -glucosidase enzymes (maltase-glucoamylase and sucrase-isomaltase) to produce absorbable glucose. When the dietary sugar is sucrose (glucose linked to fructose), the absorbable products are glucose and fructose after hydrolysis by sucrase-isomaltase. Likewise, released GIP stimulates distal GLP-1 *via* neural signals in the distal

ileum which act together to boost the secretion of insulin from pancreatic β cells (Reimann *et al.*, 2012) ensuring efficient buffering of absorbed glucose exported into circulation. This is mediated through apically-located transporters SGLT1 (for glucose), GLUT2 (glucose and fructose) and GLUT5 (fructose). PPY presents the same biphasic release pattern as GLP-1 which seems to be facilitated by CCK (Lin *et al.*, 2000) (Lin and Taylor, 2004). Unlike CCK, PYY can reduce carbohydrate digestion and absorption by inhibiting pancreatic and intestinal secretion as well as glucose-stimulated insulin secretion and sensitivity (Boey *et al.*, 2007). Unabsorbed carbohydrates are further catabolised by the microbiota in the distal small intestine and colon producing short chain fatty acids (SCFA; mainly acetate, propionate and butyrate) that can stimulate gluconeogenesis and DNL in the liver, although the exact mechanism remains elusive (Samuel *et al.*, 2008; Marchesi *et al.*, 2016).

During excessive caloric intake (characteristic of the current 'Western' lifestyle), lipids and sugars presents a metabolic challenge for the body's bioenergetics, and so the metabolic functions of the GI tract are essential for regulating its supply and utilisation in the body. The postprandial phase is particularly relevant since during this period, the body has to respond with regulatory mechanisms to restore normal energy levels in order to maintain homeostasis. High postprandial lipid and sugar excursions can challenge the correct functioning of these mechanisms altering the normal transition from the postprandial to the postabsorptive state. For instance, in a recent study it was demonstrated that an acute and single dose of fat similar to that found in a high fat meal such a burger or pizza was sufficient to reduce insulin sensitivity in the whole body of healthy individuals by 25 %, altering energy metabolism and promoting hepatic glucose release and lipid storage (Hernández *et al.*, 2017). These results indicate that high postprandial calorie intake, including high sugar excursions can prepare the path for the development of metabolic irregularities. In fact, persistent postprandial glucose spikes have been proposed as an independent risk factor of developing type 2 diabetes and cardiovascular disease (Barclay *et al.*, 2008; Ceriello and Colagiuri, 2008; Vinoy *et al.*, 2016). (figure 1.3).

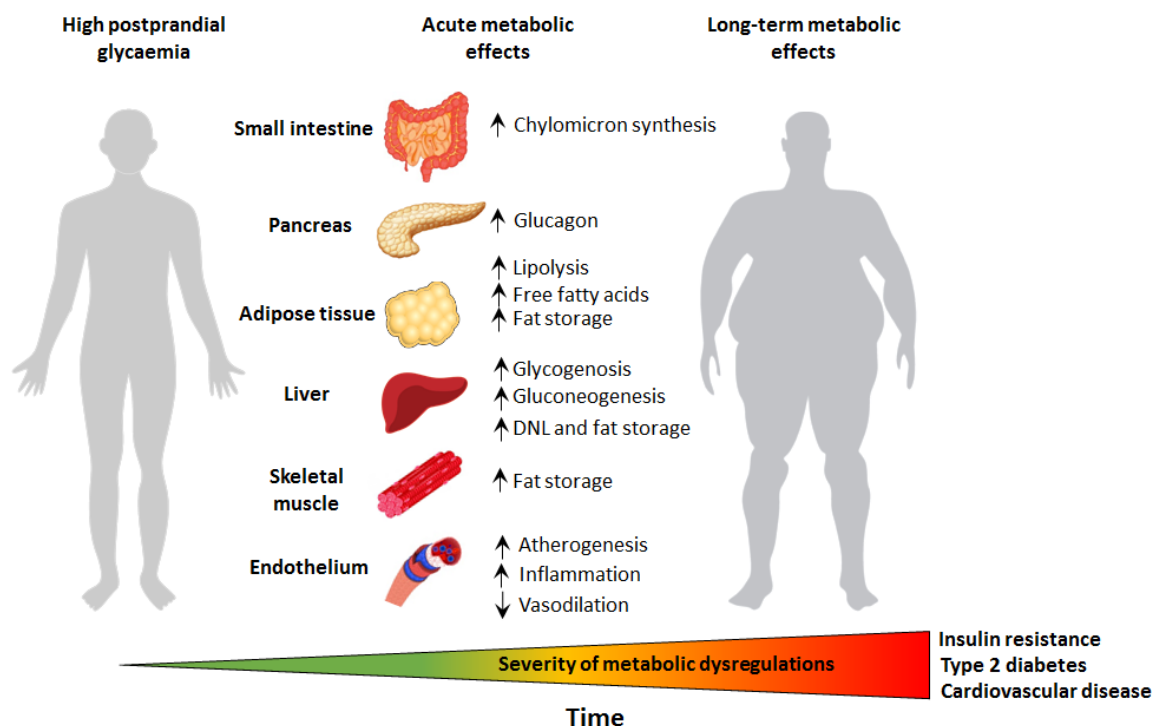


Figure 1.3 Postprandial metabolic effects occurred from 2-6 h post-ingestion of high GI foods. Postprandial sugar concentrations after the consumption of a high glycaemic food can be twice as high as compared with a low GI food with similar levels of nutrients and energy (Ludwig, 2002). This rapid flux of glucose exacerbates the secretion of GIP and GLP-1 secretion, which along with glucose itself, potentiates insulin release from the pancreas promoting its physiological effects on nutrient processing and energy assimilation; as a result, glucose uptake in peripheral tissues, glycogenesis and DNL is enhanced while gluconeogenesis is suppressed. The up-and downregulation of these pathways are maintained even after the total glucose ingested has been processed due to the initial boost of insulin, causing a temporal (middle postprandial phase, 2-4 h) low glucose state or even hypoglycaemic levels (Lev-Ran and Anderson, 1981; Brun *et al.*, 1995; Ludwig, 2002). Since hyperinsulinemia reduces lipolysis, the fuel levels of the body are low and need to be restored. This happens by activating anabolic and catabolic pathways including glycogenesis, gluconeogenesis and lipolysis through the secretion of counterregulatory hormones ensuing physiological responses that are normally reached after many hours without food (Cahill Jr, 1970; Ludwig, 2002). As such, lipolysis and DNL can be overactive in the late postprandial phase (4-6 h after ingestion) stimulating chylomicron synthesis and secretion (which can be upregulated by glucose, independently of circulating fatty acid levels) (Dash *et al.*, 2015) yielding an hyperlipidaemic and inflammatory state, causing vascular injury and the accumulation of fat in peripheral tissues. These postprandial metabolic events happen several times a day resulting in prolonged and persistent hyperglycaemia, hyperlipidaemia and metabolic stress that,

over time supersede the body's capacity to manage the rise of short and long-term glucose and lipid excursions leading to the onset of overt diabetes.

Several plausible mechanisms have been proposed for this association including altered energy partitioning, increased oxidative stress, low-grade inflammation and endothelial dysfunction. For instance, studies conducted in animal models have shown that high GI starch diets promote weight gain, visceral adiposity and higher concentrations of lipogenic enzymes than do isoenergetic, macro nutrient controlled, low GI-starch. In humans, high GI diets promote weight gain as compared with equivalent diets with a low GI (Brand-Miller *et al.*, 2002). In healthy, impaired glucose tolerance and type 2 diabetic subjects, postprandial hyperglycaemia after ingestion of 75 g of glucose increased nitrotyrosine, ICAM-1, VCAM-1, and E-selectin plasma levels, indicating oxidative stress and activation of inflammatory pathways (Ceriello *et al.*, 2004).

Decreased endothelium-dependent vasodilation after an oral glucose challenge concomitant with a decrease in NO availability was observed in healthy, early stages of diabetes and type 2 diabetic individuals (Kawano *et al.*, 1999). Hyperlipidaemia and hypertriglyceridaemia are common features of the postprandial state after a high GI diet (Harbis *et al.*, 2001; Aslam *et al.*, 2016) and are well known for evoking the production of proinflammatory cytokines, recruitment of neutrophils, and generation of oxidative stress, thus provoking endothelial dysfunction (Ansar *et al.*, 2011; Nakamura *et al.*, 2016).

The pathological events initiated by hyperglycaemia during the postprandial phase are thought to be related to exaggerated hormonal responses caused by the rapid rise and fall of blood glucose levels. This is first initiated with the development of an hypoglycaemic state due to hyperinsulinemia (Lev-Ran and Anderson, 1981; Brun *et al.*, 1995) that in turn triggers glucagon secretion and gluconeogenesis along with overactivation of lipolysis and DNL (Ludwig, 2002; Blaak *et al.*, 2012) causing hyperlipidaemia and hypertriglyceridemia. These upregulated physiological responses are not observed in individuals after having a low GI meal which produce smaller postprandial glucose rise, leading to smaller fluctuations in blood glucose levels and more gentle decreases; thus the hypoglycaemic state is evaded (Ludwig, 2002) and dyslipidaemia is attenuated (Harbis *et*

al., 2001). The metabolic events during the postprandial phase last for approximately 6 h before reaching fasting levels (Ludwig, 2002; Nakamura *et al.*, 2016), so for those who consume three meals a day spend most the days and their lives in this phase. Therefore persistent postprandial hyperglycaemia can disrupt energy metabolism in peripheral tissues and perhaps can be involved in the gradual failure of metabolic control in the GI tract.

Recent findings suggest that alteration of endocrine output could occur *via* chronic stimulation of GPCRs with high sugar diets, and it could be an important contributor of postprandial metabolic stress. Both, SGLT1 and GLUT2 are regulated through T1R2-T1R3. High sucrose increased SGLT1 mRNA and protein expression by 2-fold, and glucose absorptive capacity in wild-type mice, but not in knockout mice lacking T1R3 (Margolskee *et al.*, 2007). Activation of T1R2-T1R3 by glucose (75 mM) resulted in a rapid 3-fold increase in apical GLUT2 in rat jejunum (Mace *et al.*, 2007) and this effect was also observed for sucrose (Gouyon *et al.*, 2003). Importantly, T1R2 expression decreases markedly in response to glucose during hyperglycaemia in healthy subjects but increased in type 2 diabetics (Young *et al.*, 2013) indicating that disrupted signalling under metabolic stress could contribute to the abnormal expression and/or function of glucose transporters observed in obesity (Seimon *et al.*, 2013), experimental diabetes (Tobin *et al.*, 2008) and type 2 diabetic subjects (Ait-Omar *et al.*, 2011). Moreover, metabolic adaptations in the GI tract can occur in response to carbohydrate intake (Perry *et al.*, 2007) which will in turn enhance their processing and transport into circulation contributing to postprandial metabolic stress. Studies conducted in human vascular cells indicates that these adaptations can occur during transient hyperglycaemia and persevere even after restoration of normoglycaemia (El-Osta *et al.*, 2008), which can also presumably occur in enterocytes.

In addition to promote hyperglycaemia, *in vitro* and *in vivo* evidence indicates that high flux of glucose into absorptive cells may dysregulate the assembly and export of chylomicrons carrying triglycerides and cholesterol during the postprandial phase. Luminal cholesterol is taken up by the Niemann-Pick C1 Like 1 (NPC1L1) receptor and studies in the intestinal cell model Caco-2 suggest that its expression is modulated by glucose concentration and metabolism (Altmann *et al.*, 2004; Davis and Veltri, 2007; Jia

et al., 2011) and overexpressed in insulin resistance and type 2 diabetes (Adeli and Lewis, 2008; Tomkin and Owens, 2011; Veilleux *et al.*, 2014; Tomkin and Owens, 2015). This is supported by the established observation that excessive postprandial glucose excursions in impaired glucose tolerance and in type 2 diabetics are associated with a cascade of pro-atherogenic events. Furthermore, enterocytes are capable of storing dietary lipid in the cytosol (Chavez–Jauregui *et al.*, 2010; D'Aquila *et al.*, 2016) and subsequently mobilise and release them as part of chylomicrons hours after in response to an acute glucose stimuli (Robertson *et al.*, 2003). This is in line with the observation that chylomicron synthesis in healthy individuals is increased in response to luminal glucose and insulin levels (Harbis *et al.*, 2001; Xiao *et al.*, 2013; Xiao *et al.*, 2016).

The atherogenic process has been proposed to be a postprandial event caused by the accumulation of remnant cholesterol into sub-endothelial space, leading to inflammation and vascular injury (Nordestgaard and Varbo, 2014) increasing the risk of cardiovascular disease (Jørgensen *et al.*, 2012; Varbo *et al.*, 2013). Hypertriglyceridaemia, which has been suggested to be a marker of circulating remnants rich in cholesterol (Nordestgaard and Varbo, 2014) is a common feature of high glucose influx into circulation (Harbis *et al.*, 2001; Aslam *et al.*, 2016) evoking the production of proinflammatory cytokines, recruitment of neutrophils, and generation of oxidative stress, thus provoking endothelial dysfunction (Ansar *et al.*, 2011; Nakamura *et al.*, 2016). Therefore dysregulation of cholesterol-rich chylomicrons might be the root cause of the low-grade inflammation and endothelial dysfunction observed during the postprandial phase mediated by hyperglycaemia and the concomitant hyperinsulinemia. Thus the acute but persistent postprandial metabolic disorders such as hyperglycaemia, dyslipidaemia, inflammation and endothelial dysfunction could be preceded by sustained and repeated exposure to high GI diets which will ultimately lead to chronic insulin resistance and decline of cardiometabolic health.

In the light of present eating patterns, the GI tract represents an organ that can drive metabolic disorder by increasing energy availability, glycaemic impact and dyslipidaemia. Nevertheless, it also represents an opportunity for protection and intervention. The low bioavailability of polyphenols entails that they are delivered in the GI tract in relatively high concentrations in their native chemical form. This can favour

chemical interactions with proteins altering the digestion and absorption processes of carbohydrates and sugars, and thus attenuating the hormonal response caused by high postprandial sugar excursions and the cluster of metabolic dysregulations.

1.6.2 Postprandial glycaemia and polyphenols.

Reducing or delaying glucose absorption could prevent impaired glucose tolerance in healthy individuals while potentially lowering demands on β cells in insulin resistance and type 2 diabetic state. This can be achieved by inhibiting the carbohydrate-digesting enzymes α -amylase and α -glucosidase and glucose transporters SGLT1 and GLUT2.

Over the past decade, evidence from many *in vitro* studies has supported the potential of polyphenols to attenuate the activity of α -amylase (Nyambe-Silavwe *et al.*, 2015) and α -glucosidase enzymes (Xiao *et al.*, 2013). Most of these studies have been conducted using polyphenol-rich extracts without clearly identifying the active(s) constituents. While this approach may be useful to identify potential dietary sources that can attenuate postprandial sugar levels, it also constitutes a basis for ambiguity and is prone to conflicting results, due to the inherent variability of these molecules *in planta*. For example, significant variation on the inhibition of α -amylase and α -glucosidase activity was observed in different cultivars of fig (Wojdyło *et al.*, 2016), apple pulp and peel (Barbosa *et al.*, 2010) and grape pomace extracts (Kadouh *et al.*, 2016) while no inhibition was also reported for an apple peel extract (Nyambe-Silavwe and Williamson, 2016). The same discrepancy has been reported for hibiscus extracts on α -amylase and in black currant extracts on α -glucosidase were positive (Boath *et al.*, 2012; Ademiluyi and Oboh, 2013) and negligible inhibition was observed (Ifie *et al.*, 2016; Nyambe-Silavwe and Williamson, 2016). Thus, the literature in this field is overwhelmed by conflicting observations of polyphenol-rich extracts that may be capable of reducing carbohydrate digestion (Etxeberria *et al.*, 2012; Martel *et al.*, 2016). Whereas the assessment of the total extracts considers polyphenol interactions and synergism, it is of interest to examine specific compounds that greatly contribute to the total activity, which may guide the quest for potent compounds and help to reduce the aforementioned variability in fruit and plant extracts.

In silico studies have shown that the chemical nature of polyphenols and OH substitution pattern and number play a pivotal role in the inhibitory activity against carbohydrate-digesting enzymes. For human α -amylase, a detailed structure-activity analysis for flavonoids described a competitive mechanism where hydrogen bonds between the hydroxyl groups of the polyphenol and the catalytic triad, and the formation of a conjugated π -system are key for the inhibitory activity (Lo Piparo *et al.*, 2008). As for α -glucosidases, appropriate *in silico* studies are more difficult to conduct since the enzyme is membrane-bound, so special attention should be paid when extrapolating results from studies conducted using non-mammalian enzymes, which have very different specificities to human or porcine enzymes (Williamson, 2013). This can mislead the identification of molecules that lack physiological relevance and *vice versa*. However, a similar mechanism of inhibition as for human α -amylase has been described using a bacterial enzyme (Ahmed *et al.*, 2014).

Docking studies suggest that polyphenols with complex phenolic cores (i.e. high number of OH groups and hydrophobic or π interactions) are likely to be effective inhibitors of carbohydrate-digesting enzymes. A remarkable example is the strongest α -amylase polyphenol inhibitor described so far, 'montbretin A' with $K_i = 8$ nM' (Tarling *et al.*, 2008; Williams *et al.*, 2015) which is comprised of a phenolic core of caffeic acid and myricetin. Other well-established polyphenol structures where modelling predictions have been experimentally verified include quercetin, epigallocatechin gallate (EGCG) and luteolin. There are some other polyphenols with reported inhibitory activity of α -amylase and α -glucosidase however, as for plant extracts, the data includes contradictory results. Cyandin-3-sambubioside was very effective at inhibiting α -amylase and α -glucosidase and surprisingly, it was ~48 and 28 times more potent than acarbose for both enzymes (Ho *et al.*, 2017). Conversely, it has also been reported to be ineffective at attenuating α -amylase activity while its inhibition on α -glucosidase was ~200 fold lower than the previous report (Ifie *et al.*, 2016). Even for EGCG whose inhibitory potential against α -amylase is well established, negative results still can be found in the literature (Yasuda *et al.*, 2014).

The *in vitro* studies conducted on the potential of polyphenols and polyphenol-rich extracts provide valuable insights about their potential to attenuate α -glycosidase activity.

However, recognition and ranking of effective specific compounds or extracts have been difficult to establish since there are wide inconsistencies in both assay methods and experimental outcomes (see appendix A-C). Very often, synthetic substrates are employed to assess the inhibition of polyphenols on α -glycosidase activity. While they are useful to assess enzymatic activity, their affinity and binding properties are different when compared to physiological substrates (Williamson, 2013) representing a limitation for inhibition assays, especially for competitive inhibitors. In the case of inhibition assays on α -glucosidase activity, *p*-nitrophenyl-glucoside is mostly used which indicates a general α -glucosidase activity, and no distinction between maltase and sucrase activity can be established. Physiologically relevant substrates are also often used however, the heterogeneity of assay conditions has led to wide inconsistencies, even when the same natural substrate and inhibitor are under study. This irreproducibility of results has been a major shortcoming for the translation of polyphenols into nutritional therapeutic formulations since there is no robust evidence to relate the effect of a particular polyphenol-rich food, plant extract or single compound on this pathway.

The potential of polyphenols to reduce postprandial sugar excursions goes beyond the inhibition of digestive enzymes. Polyphenols can form complexes with brush-border membrane transporters altering the entry and transport of intestinal sugars across the small intestine. The first direct evidence about the interaction of a polyphenol with an intestinal sugar transporter dates back to the 1960s where phlorizin, a polyphenol present in apple competitively inhibited intestinal glucose transport in everted hamster's rings (Alvarado and Crane, 1962). Further studies on the mechanism of phlorizin inhibition on membrane sugar transport led to the identification of the sodium–glucose transport mechanism (Vick *et al.*, 1973) and gained its recognition as a specific SGLT inhibitor.

Extending the observation on the similarity with acarbose (an antidiabetic drug that inhibits α -amylase and α -glucosidase enzymes) to blunt intestinal glucose absorption, it has been demonstrated that acute administration of phlorizin suppresses postprandial blood glucose levels in mice (Takii *et al.*, 1997; Shirotsaki *et al.*, 2012). This finding has been further supported by three independent pilot studies in healthy volunteers where apple juice (Johnston *et al.*, 2002) and apple extract (Schulze *et al.*, 2014; Makarova *et al.*, 2015) attenuated postprandial glucose and insulin levels as compared with control meals,

which can be mainly attributed to the inhibition of glucose uptake by phlorizin, according to *in vitro* mechanistic studies conducted in intestinal models (Williamson, 2013; Schulze *et al.*, 2014). Like phloridzin, there are other example of polyphenols that have been described to inhibit intestinal glucose uptake *in vitro* through their interaction with SGLT1 and/or GLUT2 including EGCG, (-)-epicatechin, quercetin, myricetin, naringenin, and some of their glucoside derivatives (Kobayashi *et al.*, 2000; Johnston *et al.*, 2005; Kottra and Daniel, 2007; Schulze *et al.*, 2014; Schulze *et al.*, 2015). The inhibition constants on both transporters have been reported to be in the range of ~10-1000 μM which are realistic as intestinal intraluminal concentrations (Williamson, 2013). Hence, intake of the right polyphenol or polyphenol mixture could possibly inhibit, to some extent, the glucose influx into the enterocyte and circulation. The *in vitro* studies on the inhibition of sugar transporters by polyphenols are more limited than those conducted for α -glycosidase enzymes and so more studies are needed to validate already reported candidates. Although there seems to be a consensus on this matter, conflicting results still can be found. For instance, in Caco-2 cells, (-)-epicatechin inhibited SGLT1 mediated glucose uptake with an IC_{50} value of ~100 μM (Johnston *et al.*, 2005) while no inhibition was observed in a latter study in the same cell model even at a concentration >500 μM (Manzano and Williamson, 2010).

Although there are still some discrepancies when linking the *in vitro* with *in vivo* results, as to whether polyphenols act synergistically in the various steps of the process of carbohydrate digestion and absorption, some evidence from animal studies clearly indicate that these compounds limit the postprandial sugar flux into circulation. This has been reflected by decreases in postprandial peak and blood glucose and insulin levels (Forester *et al.*, 2012; Goto *et al.*, 2012; Murase *et al.*, 2012) and in the secretion of GIP incretin hormone (Murase *et al.*, 2012). In particular, the decrease in postprandial glucose and insulin along with GIP secretion by an extract of coffee polyphenols was related with changes in energy partitioning (Murase *et al.*, 2012), suggesting that polyphenols can improve metabolic management of glucose, maintaining an adequate equilibrium between the rate of carbohydrate oxidation and utilisation preserving a healthy phenotype.

Most of the effects of polyphenols in postprandial glycaemia were related to the inhibition of α -amylase and α -glucosidase enzymes (without distinguishing between

maltase and sucrase) with the exception of the study of Goto and co-workers, that also related the effects with the inhibition of the sugar transporters SGLT1 and GLUT2 (Goto *et al.*, 2012). Surprisingly, when EGCG was co-administered with maltose or glucose to mice, no changes were observed in postprandial blood glucose (Forester *et al.*, 2012) suggesting no effect on α -glucosidase activity and SGLT1 and/or GLUT2 transporters, despite the fact these activities have been reported for this molecule (Hossain *et al.*, 2002; Johnston *et al.*, 2005; Nyambe-Silavwe and Williamson, 2016).

Despite the promising results observed in rodents, the answer to the question as to whether polyphenols can actually reduce postprandial glucose input with long-term metabolic effects in humans remains ambiguous (Suksomboon *et al.*, 2011; de Bock *et al.*, 2012; Amiot *et al.*, 2016). For instance, opposing conclusions were obtained in two systematic reviews evaluating the association of the consumption of polyphenol-rich foods, or beverages, with a carbohydrate source on acute postprandial glycaemia and/or insulin concentrations (Burton-Freeman, 2010; Coe and Ryan, 2016). The intake of cranberry juice, wild blueberry, strawberry and a fruit meal of banana, kiwi or apple, red wine or red wine components did not reduce postprandial glucose levels while mixed results were observed regarding insulin, although without reaching significant differences in most of the cases (Burton-Freeman, 2010). On the other hand, Coe and Ryan (2016) concluded that polyphenol sources such as coffee, black tea, different types of berries, apple and aracá juice reduced the peak and early-phase glycaemic and insulin response, however with varying degrees of effectiveness depending on the polyphenol-carbohydrate combination.

The conflicting results presented above can be partially explained by the inconsistent and limited characterisation of polyphenol-rich extracts in terms of active constituents, their targets and efficacies, restricting the rational design of human intervention studies and validation of potential physiological effects. Therefore very few human studies have selected individual polyphenols or polyphenol-rich extract with specific mechanisms of effect in mind, yet some examples do exist. For instance, a designed polyphenol-rich meal with a combination and concentration of polyphenols capable of inhibiting the different stages of starch digestion and absorption as observed *in vitro*, reduced glucose and insulin postprandial levels (~ 50 %) in healthy individuals in a randomised, cross-over

intervention (Nyambe-Silavwe and Williamson, 2016). In a similar design, 4 g of green tea extract (EGCG content –257.6 mg) with an active concentration of ~0.26 mg/mL considering an intestinal volume of 1 L (Nyambe-Silavwe and Williamson, 2016) reduced blood glucose by ~30 % after a corn starch meal. In both studies, the concentration of the active constituents were at least ~100 times higher than the experimental inhibition constants obtained *in vitro*, which perhaps are needed in order to account for possible interactions with other macromolecules if positive results are to be obtained.

Hyperlipidaemia is a common feature during high postprandial glycaemia, probably involved in the endothelial dysfunction observed under this condition by promoting oxidative stress, atherogenesis and inflammation (Ludwig, 2002; Nordestgaard and Varbo, 2014). Due to this intrinsic relationship, the effect of polyphenols on postprandial glycaemic impact could attenuate to some extent the levels of circulating lipids and cholesterol rich-lipoproteins during the postprandial phase. Indeed, epidemiological studies suggest a lower risk of cardiovascular disease by polyphenol intake (Hertog *et al.*, 1997; McCullough *et al.*, 2012; Kishimoto *et al.*, 2013) and human intervention studies indicate that polyphenols regulates postprandial lipid metabolism (Annuzzi *et al.*, 2014). For instance, postprandial ApoB48 (a specific marker of chylomicrons and their remnants) was reduced by acute non-alcoholic red wine consumption in dyslipidaemic postmenopausal woman 6 h after eating (Pal and Naissides, 2004). Similarly, a polyphenol-rich diet composed of decaffeinated green tea and coffee, dark chocolate, blueberry jam, artichokes, onions, spinach, rocket, and extra-virgin olive oil reduced postprandial triglyceride and chylomicron cholesterol in obese/overweight individuals after 8 weeks intervention (Annuzzi *et al.*, 2014). Impaired lipid availability in enterocytes by the inhibiting digestive lipases and impairing cholesterol solubility has been linked with the reduction in intestinal chylomicron production. However, since glucose metabolism in enterocytes increase cholesterol absorption, lipogenesis and chylomicron assembly and secretion (Robertson *et al.*, 2003; Ravid *et al.*, 2008; Malhotra *et al.*, 2013; Xiao *et al.*, 2013), it is possible that attenuation of glucose influx has a knock on effect on maintaining a fine tune on this biosynthetic pathway. Therefore, *in vitro* experiments evaluating the effect of polyphenols on postprandial glycaemia should contemplate the pleiotropic effect of polyphenols on lipoprotein assembly and secretion since there is a plausible association between these metabolic pathways.

More studies are needed to validate the effects of polyphenols on postprandial glycaemic and lipid response in healthy individuals as well as in those at risk and with type 2 diabetes. These studies should consider the assessment of standardised preparations based on both active constituents and inhibition constants (active concentrations) as well as targeting all the steps of the digestion and absorption process, which can potentially give subtle but multiple inhibition resulting in a significant overall response. The complexity and diversity of polyphenol structures pose a challenge on this matter, which can only be overcome with an appropriate chemical characterisation of the polyphenol source that is under investigation. This will help to conduct targeted *in vitro* experiments in order to identify the most likely class of molecule(s) responsible for the activity and information about potential synergy with other molecules. The *in vitro* experiments must be conducted under the highest standards of methodological rigor if consistent results, and recognition on the potential of a particular polyphenol are to be obtained. In this regard, the *in vitro* assays have to be conducted under optimal conditions and using physiological substrates which will aid in reducing the current variability that exist in the literature in terms of inhibition potencies. By identifying and validating the action of specific polyphenols, we will move forward to develop standardised polyphenol-based formulations with reproducible actions to achieve an effective clinical nutrition through the attenuation of persistent high postprandial glycaemia.

1.7 Aim and objectives of the thesis

Plant food supplements are concentrated sources of botanical preparations which could provide everyday maintenance. However their use is of concern amongst scientific and regulatory communities since there is a lack of scientific substantiation of their bioactive constituents and the product itself. The research work of this thesis was developed under the framework of the EU project PlantLIBRA with the aim to establish the potential health benefits of some plant food supplements using advanced *in vitro* approaches.

Type 2 diabetes is a growing epidemic and alternatives to reduce the risk of this metabolic disease are much needed. *In vivo* evidence has shown that chamomile can positively modulate energy metabolism, suggesting it can be used to provide everyday health maintenance. Polyphenols are abundant constituents in chamomile and cumulative studies propose they can attenuate the short-term metabolic disturbance caused by high postprandial sugar excursions, an important metabolic pathway to maintain long-term energy balance. This thesis aimed to investigate whether the *in vivo* effects of chamomile on type 2 diabetes prevention and management can be partially mediated by attenuating carbohydrate digestion and sugar absorption and to identify the potential polyphenol candidates acting on these pathways by *in vitro* mechanistic studies.

Hypothesis: Chamomile can attenuate the activity of carbohydrate-digestive enzymes and sugar transporters *in vitro* and these effects are mediated by the most abundant polyphenol constituents.

The objectives of this research project were:

- i) Identify and quantify the major polyphenols present in chamomile leading to confirm the identity of two abundant hydroxycinnamic acid derivatives present.
- ii) Assess the effect of chamomile extract and the most abundant polyphenols to attenuate the activity of human salivary α -amylase and rat α -glucosidase (maltase, sucrase and isomaltase) employing physiologically relevant substrates under optimised assay conditions, identifying individual

contributions for each polyphenol. *In silico* studies were conducted to establish the structure-activity relationship.

- iii) Assess the effect of chamomile extract and its major polyphenols to reduce the rate of glucose, sucrose and fructose transport using the well characterised Caco-2/TC7 cell model and to delineate through mechanistic experiments the transporter protein mostly affected and the active compounds.
- iv) Explore the effect of attenuating glucose uptake on cholesterol absorption and in the expression of genes regulating cholesterol transporter proteins in Caco-2 cells.

Chapter 2 Identification and quantification of major polyphenols in chamomile: isolation and structural characterisation of two hydroxycinnamic acid derivatives.

2.1 Abstract.

Botanical extracts represent a rich source of bioactive small molecules which can be used to provide everyday health maintenance and lower disease risk. Nonetheless, a major drawback in this field has been the inadequate determination of the chemical composition of the starting plant material resulting in wide inconsistencies across studies. Moreover, many of these small molecules remain undiscovered or unexplored for their potential biological activity due to their commercial unavailability. Chamomile is a rich source of small molecules, especially polyphenols and their chemical characterisation and identification is still a work in progress. This chapter summarises the identification and quantification of the main polyphenol constituents in a chamomile extract and the isolation and chemical characterisation of two hydroxycinnamic acid derivatives whose identity was uncertain. LC-MS/MS, LC-QTOF and HPLC-DAD revealed the presence of apigenin, apigenin 7-*O*-glucoside and two hydroxycinnamic acid derivatives as the main polyphenol constituents. The two hydroxycinnamic acid derivatives were purified by semi-preparative column chromatography, and identified as (*Z*) and (*E*)-2-hydroxy-4-methoxycinnamic acid glucoside based on accurate mass TOFMS, ¹H-¹³C NMR, nuclear Overhauser effect spectroscopy and chemical synthesis of the (*E*)-methoxycinnamic acid skeleton. Quantitative analysis revealed that these compounds are present ~ at the same levels as apigenin 7-*O*-glucoside, the predominant example reported in chamomile until now and so, they may contribute to the therapeutic effects of chamomile preparations.

2.2 Introduction.

Natural plant extracts provide a rich source for therapeutic discovery which is supported by empirical knowledge generated through their use in folklore medicine. Nowadays, there is a growing perception that the use of natural bioactive constituents may elicit fewer side effects and be similar or more effective than single synthetic chemical entities (Gosslau *et al.*, 2011). Thus, they have become a major focus in the field of clinical nutritional research to develop multicomponent botanical therapeutic preparations, functional foods and nutraceuticals with good safety profiles that can complement conventional pharmaceuticals in the treatment and reduction of disease risk. However, the development of these safe and effective therapeutic formulations is currently being slowed down by the lack of rigorous or poorly documented science, including setbacks in their chemical characterisation and biological activity, often resulting in irreproducible effects or conflicting results (Raskin *et al.*, 2002; Gosslau *et al.*, 2011; Atanasov *et al.*, 2015). For instance, green tea extract showed positive effects on reducing postprandial glycaemic response (Weber *et al.*, 2008) while no effects were also observed (Josic *et al.*, 2010) in healthy subjects.

Chamomile it is one of the oldest, most widely used and well-documented medicinal plants in the world. It belongs to the Asteraceae/Compositae family and it is represented by two common varieties *viz.* German Chamomile (*Matricaria recutita*) and Roman Chamomile (*Chamaemelum nobile*) (McKay and Blumberg, 2006; Srivastava *et al.*, 2010). It is an annual herbaceous plant indigenous to Europe and Western Asia that has been naturalised in Australia, UK and the United States and cultivated in Germany, Hungary, Russia and other Southern and Eastern European countries for the flower heads (Shukla and Gupta, 2010). The recognition of its medicinal properties is exemplified by its listing as an official drug in the pharmacopoeias of 26 countries including the UK (Ross, 2008). Its medicinal application is mainly established on its anti-inflammatory, anti-septic, anti-spasmodic and wound-healing effects, particularly in gastrointestinal disorders where its therapeutic effects have been recognised by the German Commission E and approved to treat various inflammatory illness (Ross, 2008). Other health effects of chamomile that possess scientific substantiation include its chemopreventive (Srivastava

and Gupta, 2007; Srivastava and Gupta, 2009; Srivastava *et al.*, 2010) and antidiabetic activity (Kato *et al.*, 2008; Weidner *et al.*, 2013; Rafraf *et al.*, 2015).

Several phytochemicals have been identified in chamomile where polyphenols constitute the principal group (McKay and Blumberg, 2006). Among them, the flavone apigenin and its derivatives (glucosides and acetates) have been reported as the predominant examples with levels ~17 % on a dry weight basis of the total flower (Mulinacci *et al.*, 2000; Švehlíková *et al.*, 2004; Srivastava and Gupta, 2007). Consequently, apigenin and its precursor apigenin-7-*O*-glucoside which are commercially available, have been selected, studied and related with some of the biological activities of chamomile including anti-inflammation (Srivastava *et al.*, 2009) and chemoprevention (Srivastava and Gupta, 2007; Srivastava and Gupta, 2009; Matić *et al.*, 2013). However, several hydroxycinnamic acid derivatives have been identified and quantified by several independent research groups indicating that they are present in higher amounts than total flavonoids, making up to 64.8 % (dry weight) of the total polyphenol content (Mulinacci *et al.*, 2000; Guimarães *et al.*, 2013; Matić *et al.*, 2013). In particular, the presence of two of these derivatives makes ~ 50 % of the total hydroxycinnamic acids and so, they may modulate and/or participate to some extent in the biological activity of chamomile preparations; something that remains unexplored so far. It is important to underline that the identity of these two compounds is debatable and uncertain based on various tentative identifications which have suggested several chemical structures such as isomeric and dimeric structures of ferulic acid derivatives (Mulinacci *et al.*, 2000; Guimarães *et al.*, 2013) and isomeric structures of 2- β -D-glucopyranosyloxy-4-methoxycinnamic acid (Weber *et al.*, 2008). Thus the chemical information that has been generated and used to characterise and identify the chemical structure of these compounds to date remains insufficient and controversial.

The aim of this study was to identify and quantify the major polyphenol constituents in German chamomile extract (ChE) and fully and positively identify the two hydroxycinnamic acid derivatives to provide adequate compositional data.

2.3 Materials and methods.

2.3.1 Materials.

The ChE and authentic standards of apigenin and apigenin 7-*O*-glucoside were obtained from the plantLIBRA partner PhytoLab Co. KG.h (Vestenbergsgreuth, Germany) as a lyophilised powder. 7-methoxycoumarin, LC grade solvents acetonitrile and methanol, the analytical reagent formic acid, 1-phenyl-3-methyl-5-pyrazolone, D-mannose, D-galactose and D-xylose were obtained from Sigma-Aldrich Co., Ltd., Dorset, U.K. The analytical reagents D-glucose and TFA were purchased from Fisher Scientific (Loughborough, Leicestershire, UK). Distilled water was used for all the experiments (Millipore UK Ltd., Hertfordshire, UK). All the reagents were of the highest purity and standards were ≥ 98 % according to the manufacturer.

2.3.2 Methods.

2.3.2.1 Preparation of ChE for high performance liquid chromatography analysis and semi-preparative isolation.

The ChE was prepared in tubes (14 mL) by adding room temperature water to reach a desired concentration of 1 mg/mL. The suspension was mixed vigorously and vortexed for 1 min. Then the suspension was centrifuged at 17000 *g* for 10 min at 4 °C and the supernatant was recovered. Thereafter, the supernatant was filtered through 0.2 μ m syringe-drive PTFE filters and the filtrate used for the subsequent analysis.

2.3.2.2 Identification and quantification of major polyphenols in ChE.

Identification and quantification of major polyphenols in ChE was performed on an HPLC-DAD system (1200 series; Agilent Technologies, Berkshire, UK) equipped with a kinetex C18 analytical column (150x2.10 mm I.D., 2.6 μ m; Phenomenex, Cheshire, UK) maintained at 35 °C. ChE was prepared as previously described in section 2.3.2.1 at 1 mg/mL and 10 μ L was injected and separated using a 41 min gradient of premixed 5 % acetonitrile in water (5:95, v/v) (A) and premixed 5% water in acetonitrile (5:95, v/v) (B), both modified with 0.1 % formic acid at 0.25 mL/min. The gradient utilized started at 0 % solvent B and increased to 10 % (5 min), 25 % (10 min), 35 % (20 min), 50 % (25 min), and held at a plateau up to 30 min. The gradient was increased 100 % at 30.5 min and returned to 0 % solvent B over 5.5 min before initial starting conditions were resumed for

a 6 min column re-equilibration. Double online detection was carried out using 280 and 320 nm and chromatograms acquired at 320 nm were used for quantification and presentation.

Identification of apigenin and apigenin-7-*O*-glucoside was performed by comparison of retention time with those of authentic standards. For the two hydroxycinnamic acid derivatives, the identification was based on the deprotonated molecular ions previously reported for those compounds at *m/z* 355 and 711 (Mulinacci *et al.*, 2000; Guimarães *et al.*, 2013) on a Shimadzu LC-2010 HT coupled with 2020 quadrupole mass spectrometer equipped with an ESI interface under the chromatographic conditions described above. Nitrogen was used as nebulizing (45 psig; 1.50 L/min) and drying gas (15.0 L/min); gas and vapourizer temperature was 250 °C; detector -1.80 kV, DL temperature 250°C. Quantitative analysis of the targeted compounds was conducted by comparison with those of authentic standards using an external five-point linear calibration curve (figure 2.1).

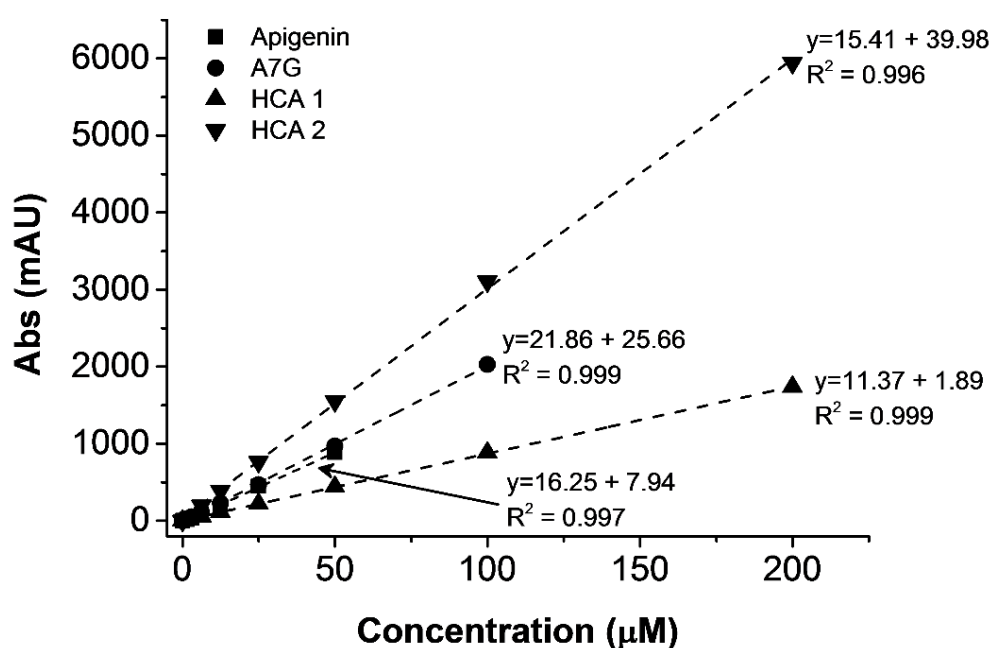


Figure 2.1 Representative example of the standard calibration curves generated and used for the quantification of apigenin, apigenin 7-*O*-glucoside (A7G) and hydroxycinnamic acid derivatives (HCA) in ChE. Due to its limited solubility, the standard curve of apigenin was prepared in the range of 0-50 µM. The values shown are averages of triplicate assays ± SEM. Where not visible, error bars are smaller than the size of the data point.

The limit of detection (LOD) and the limit of quantitation (LOQ) were calculated by $LOD=(3.3*\text{intercept})/\text{slope}$ and $LOQ=(10*\text{intercept})/\text{slope}$, respectively for the individual polyphenols.

2.3.2.3 Method development for the isolation of hydroxycinnamic acid derivatives from ChE by semi-preparative RP-HPLC chromatography.

An ÄKTA Purifier System (GE Healthcare, Fairfield, CT, USA) controlled by a PC running GE Unicorn software (5.11), equipped with an UV detector UV-900, pH/conductivity detector pH/C-900, fraction collector Frac-950, gradient mixer, and pump P-900 was employed. The basic configuration of the system is shown in figure 2.2.

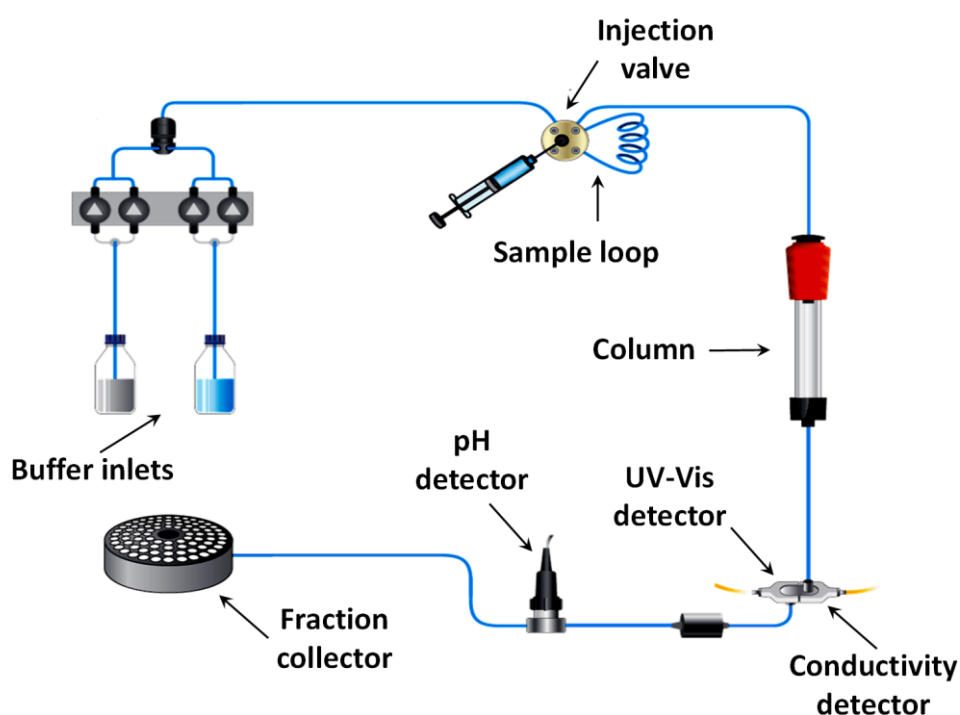


Figure 2.2 Basic configuration of the AKTA purifier system used to isolate the hydroxycinnamic acid derivatives from ChE. The separation unit of the chromatography system has four main modules: 1) a binary high performance gradient pump, 2) a multi-wavelength UV-Vis monitor for simultaneous monitoring of up to 3 wavelengths in the range of 190-700 nm, 3) a combined monitor for on-line conductivity and pH monitoring and 4) a fraction collector with capacity to collect up to 175 fractions. For method optimisation, the sample was loaded through a sample loop of 0.1 mL. For isolation, the capacity of the sample loop was increased to 1 mL and the flow rate adjusted accordingly (section 2.3.2.4).

Two different bonded-phase chemistries were used for the development of the method. The first column was a μ RPC C2/C18 ST LC column 4.6x100mm I.D. (GE Healthcare, Fairfield, CT, USA) which has been demonstrated to be suitable for the determination of glycosylated polyphenols (Courts, 2011). The second column was a Gemini C6 phenyl column 4.6x150mm i.d. which has a higher selectivity for aromatic compounds (Phenomenex, Cheshire, UK). Different chromatographic conditions (flow rate, mobile phase, and gradients) were tested using ChE as test sample before the best resolution was achieved. This was obtained using the Gemini C6 phenyl column using water containing 0.1% TFA (solvent A) and acetonitrile (Solvent B) as mobile phase and a gradient program as follows: 1.5 column volumes (cv), 5–24% B, 1.5 cv, 24% B, 3 cv, 24–38% B, 3 cv 38-100% B, 1.5 cv, 100% B, 0.1 cv, 100-5% B, 4 cv, 5% B) at 0.8 mL/min (figure 2.3).

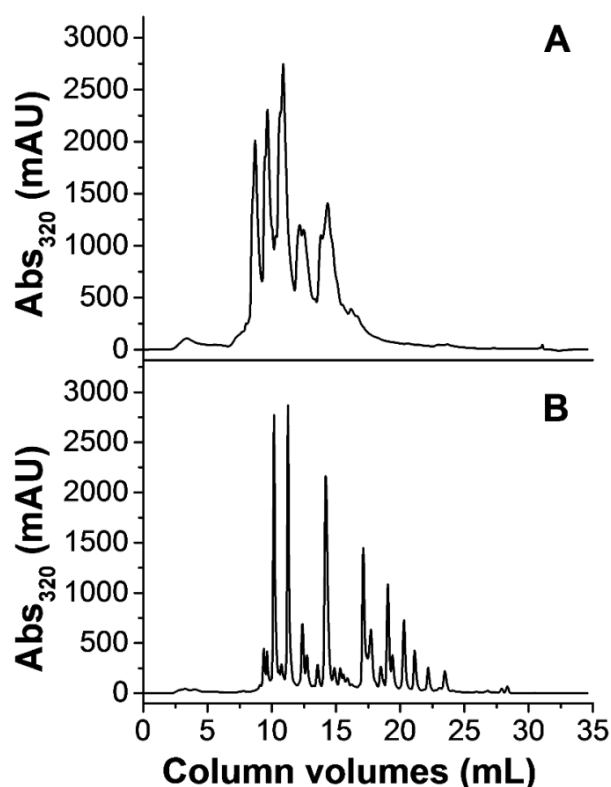


Figure 2.3 Chromatographic separation of polyphenols present in ChE. (A) The separation was conducted using a μ RPC C2/C18 column. (B) The separation was done with a phenyl C6 column. The same chromatographic conditions were employed with both columns and the separation was performed using a mobile phase composed of H₂O (0.1% TFA) and the separation

was performed using a mobile phase composed of H₂O (0.1% TFA) and acetonitrile using the gradient described in section 2.3.2.3.

For the purification of the hydroxycinnamic acid derivatives, solvent B was changed for methanol in order to increase the selectivity and separation factor (α) to those polyphenols close to the target compounds (figure 2.4).

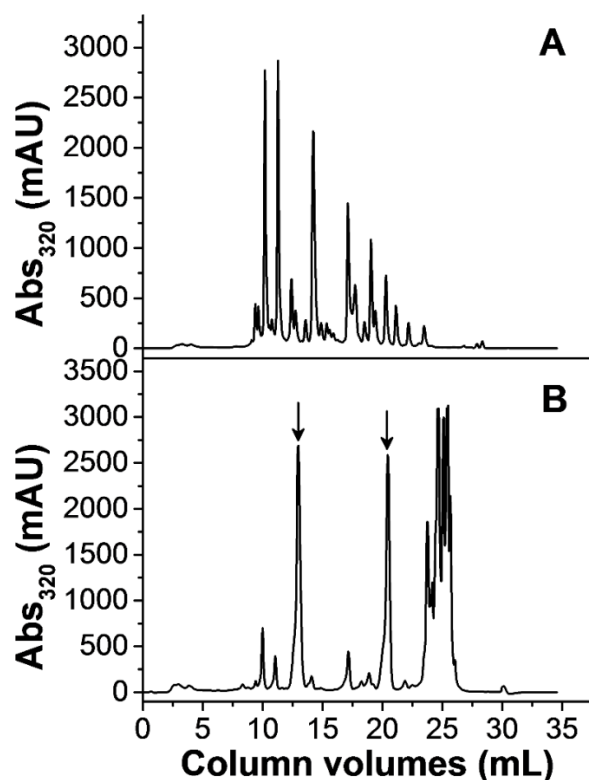


Figure 2.4 Chromatographic separation of polyphenols present in ChE using the C6 phenyl column. The chromatogram shows the difference between (A) acetonitrile and (B) methanol as mobile phase. The same chromatographic gradient was used for both mobile phases. Targeted peaks for isolation are indicated with arrows in panel B.

2.3.2.4 Semi-preparative isolation of hydroxycinnamic acid derivatives.

The two hydroxycinnamic acid derivatives were isolated using the instrument and chromatographic conditions previously described in section 2.3.2.3 with the following modifications: 1) the system was equipped with a semi-preparative column Gemini C6

phenyl (250 x 10 mm i.d., 5 μ m; Phenomenex, Cheshire, UK), and 2) ChE (150 mg/mL) was loaded manually (1 mL) using a syringe through a sample loop of 1 mL and eluted using water containing 0.1% TFA (solvent A) and methanol (Solvent B) at a flow rate of 2.3 mL/min. The elution was followed at 320 nm and fractions containing the separated compounds were collected and analysed for purity by LC-MS (figure 2.5) as described in section 2.3.2.2.

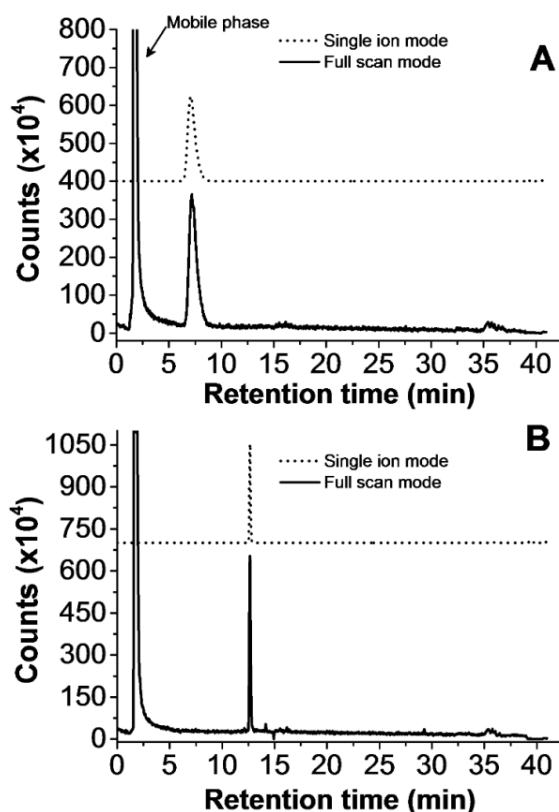


Figure 2.5 LC-MS of isolated compounds from ChE.(A) Hydroxycinnamic acid derivative 1 and (B) hydroxycinnamic acid derivative 2. The spectra obtained for both fractions reveals that the compounds were at least >95 % pure at the moment of the isolation as assessed by the total ion count in LC-MS. For figure (A) the peak observed presented a m/z (⁻) of 355 Da while (B) was characterised by a predominant m/z (⁻) of 711 Da.

Multiple semi-preparative separations were conducted and the fractions for each peak combined, freeze-dried, and stored at -20 °C until use for structure characterisation.

2.3.2.5 Chemical characterisation of hydroxycinnamic acid derivatives.

2.3.2.5.1 HPLC/MS² and QTOFMS.

Initial analysis of the purified hydroxycinnamic acid derivatives were carried out using an Agilent 1200 HPLC coupled with a 6410-MS triple quadrupole (Agilent Technologies, Berkshire, UK) and equipped with a dual spray ESI source operating in negative mode. An isocratic separation was conducted with a mixture of water-acetonitrile (4:1 v/v) employing reversed phase HPLC using a kinetex C18 analytical column, 150x2.10 mm I.D., 2.6 μ m; Phenomenex maintained at 35 °C. Data were obtained from full-scan MS peak spectra acquired in the mass range of m/z 50-1100. Next, manually selected ion peaks of the MS spectra were subjected to MS² analysis under different fragmentor and collision energy conditions to characterise the resulting product ion peak spectra from the isolated compounds. Complementary LC-QTOFMS analysis were performed by Dr. Laszlo Abranko at the Department of Applied Chemistry at the Corvinus University of Budapest. The analysis were conducted in a Agilent 1200 series HPLC system (Agilent Technologies, Waldbronn, Germany) coupled to an Agilent 6530 Q/TOF mass spectrometer (Agilent Technologies, Santa Clara, CA, USA) using the chromatographic conditions described above. Elemental formulae of compounds were determined with the aid of MassHunter software based on high-resolution (> 20,000 FWHM) accurate mass (<5 ppm) data completed with evaluation of isotope abundance matching and isotope spacing. Data were obtained from full-scan TOF-only peak spectra acquired in the mass range of m/z 50-1100. Next, manually selected ion peaks of the TOF-only spectra were subjected to Q/TOFMS analysis and elemental formulae of fragments were determined based on accurate mass (<20 ppm) data obtained from product ion peak spectra. Since the data obtained with both mass analysers was essentially the same and due to the greater mass resolution, sensitivity and accuracy of the TOF analyser, only data acquired with this instrument was included to avoid repetition.

2.3.2.5.2 Acid hydrolysis.

An aliquot of the purified hydroxycinnamic acid derivative 2 was dissolved in HCl (2 M) to reach a concentration of 500 μ M (based on the previously reported neutral mass of 356 Da by Mulinacci *et al.* (2001)) and subjected to hydrolysis for 2 h at 60 °C. The reaction mixture was concentrated to dryness under reduced pressure and reconstituted in water (1

mL) and analysed by HPLC-DAD using the chromatographic conditions previously described in section 2.3.2.2.

2.3.2.5.3 Determination of the monosaccharide moiety.

An aliquot of the hydroxycinnamic acid derivative 2 (200 μ M) was subjected to acid hydrolysis as previously described in 2.3.2.5.2 and concentrated to dryness. The released hexose was chemically tagged with 1-phenyl-3-methyl-5-pyrazolone (PMP) as described elsewhere (Shen and Perreault, 1998; Lv *et al.*, 2009) with minor modifications. PMP powder was dissolved in methanol containing 0.5 % of HCL (11.65 M) to reach a final concentration of 0.5 M. After, 0.5 mL of the PMP solution and 0.5 mL of NaOH (0.3 M) were added to the dried hydrolysed sample and heated for 2 h at 70 °C, cooled down to room temperature and neutralised with 0.5 mL of HCl (1 M). Thereafter, water (0.5 ml) and chloroform were added (1:2, v/v), the mixture was vortexed and the organic phase discarded. The process was repeated for approximately six times until the excess of PMP was removed. The remaining aqueous phase containing the PMP-hexose complex was concentrated to dryness and reconstituted in water (0.25 mL). The derivatised monosaccharide was analysed on HPLC-DAD equipped with a C18 analytical column (250 x 4.6 mm I.D., 5 μ m, Phenomenex, Cheshire, UK) and UV detection at 250 nm. A 10 μ L sample was eluted with 0.1 mM ammonium acetate buffer (pH 5.5)–acetonitrile (78:22, v/v) at 1 mL/min. The identification of the monosaccharide component was achieved by comparing the retention time with those of authentic standards (D-mannose, D-glucose, D-galactose and D-xylose) (figure 2.6).

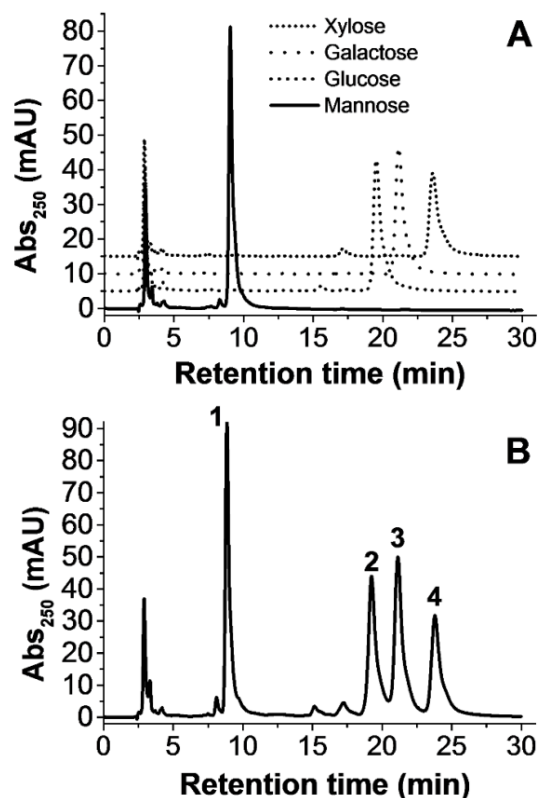


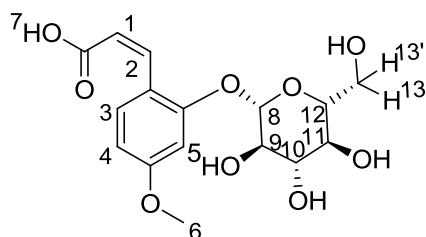
Figure 2.6 HPLC-DAD chromatograms of PMP derivatives of standard monosaccharides.

The four standard monosaccharides were chemically tagged and separated under the experimental conditions described. (A) Standard monosaccharides were derivatised and analysed individually, (B) Standard monosaccharides were derivatised and analysed as a mixture, Peaks: 1. D-mannose; 2. D-glucose; 3. D-galactose; 4. D-xylose.

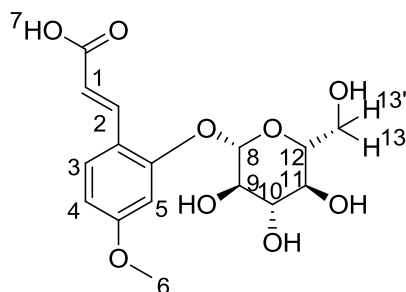
2.3.2.5.4 NMR.

The NMR analyses were performed in collaboration with Ms. Lauren Ford and Professor Christopher Rayner from the school of Chemistry at the University of Leeds. Purified samples were dissolved in d_6 DMSO and placed in a 5 mm OD NMR tube. All NMR data were recorded on a Bruker Avance 500 spectrometer (^1H frequency 500.573 MHz, ^{13}C frequency 125.878 MHz) temperature controlled at 299.3 K. Chemical shifts are expressed in ppm and are reported with reference to the residual solvent peak. Multiplicities are reported with coupling constants and are given to the nearest 0.1 Hz. Where needed, two-dimensional correlation spectroscopy (2D-COSY), heteronuclear single quantum coherence spectroscopy (HSQC) and heteronuclear multiple bond

correlation spectroscopy (HMBC) and nuclear Overhauser effect spectroscopy (NOESY) was performed.



(*Z*)-2-D-glucopyranosyloxy-4-methoxycinnamic acid present as a mixture of *E* and *Z* in a ~ 1:3 ratio, *E* peaks eliminated and *Z* peaks picked at: ^1H NMR (501 MHz, DMSO- d_6) δ 7.70 (d, $J = 8.5$ Hz, 1H, H3), 7.19 (d, $J = 12.5$ Hz, 1H, *cis*-alkene, H2), 6.74 (d, $J = 2.5$ Hz, 1H, H5), 6.56 (dd, $J = 8.5, 2.5$ Hz, 1H, H4), 5.78 (d, $J = 12.5$ Hz, 1H, *cis*-alkene, H1), 4.85 (d, $J = 7.5$ Hz, 1H, anomeric proton, H8), 3.77 (s, 3H, H6), 3.72 (broad d, $J = 11.7$ Hz, 1H, H13), 3.47 (broad dd, $J = 11.7, 6.0$ Hz, 1H, H13'), 3.38 (ddd, $J = 10.0, 6.2, 1.6$ Hz, 1H, H12), 3.34-3.29 (m, 2H, H9 & H10)*, 3.16 (apparent t, $J = 8.8$ Hz, 1H, H11). ^{13}C NMR (126 MHz, DMSO- d_6) δ 167.7, 161.0, 160.7, 156.7, 136.32, 131.1, 117.53, 116.73, 101.11, 100.5, 77.24, 76.86, 73.27, 69.81, 60.72, 55.33. *Overlaid by strong signal from water. ESI-MS: m/z 355.1035 $[\text{M}-\text{H}]^-$.

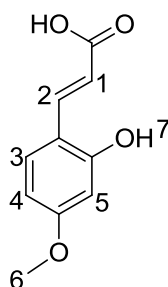
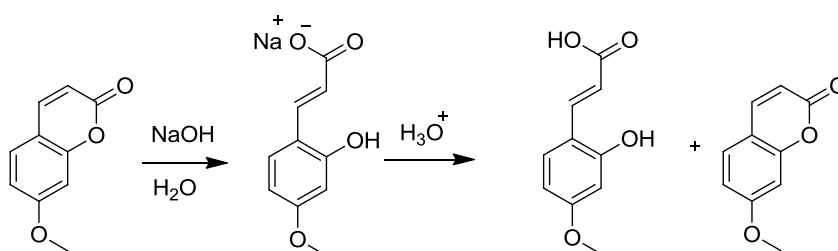


Analysis of pure (*E*)-2- β -D-glucopyranosyloxy-4-methoxycinnamic acid: ^1H NMR (501 MHz, DMSO- d_6) δ 12.00 (s, 1H, H7), 7.82 (d, $J = 16.2$ Hz, 1H, *trans*-alkene, H2), 7.62 (d, $J = 8.7$ Hz, 1H, H3), 6.76 (d, $J = 2.4$ Hz, 1H, H5), 6.62 (dd, $J = 8.6, 2.4$ Hz, 1H, H4), 6.39 (d, $J = 16.2$ Hz, 1H, *trans*-alkene, H1), 5.16 (broad s, 1H (OH)), 4.98 (d, $J = 7.5$ Hz, 1H, anomeric proton, H8), 4.89 (broad s, 2H (OH)), 4.58 (broad s, 1H, (OH)), 3.78 (s, 3H, H6), 3.72 (broad d, $J = 11.7$ Hz, 1H, H13), 3.47 (broad dd, $J = 11.7, 6.0$ Hz, 1H, H13'), 3.38 (ddd, $J = 10.0, 6.2, 1.6$ Hz, 1H, H12), 3.34-3.29 (m, 2H, H9 & H10)*, 3.16 (apparent t, $J = 8.8$ Hz, 1H, H11). ^{13}C NMR (126 MHz, DMSO- d_6) δ 168.08, 162.08, 157.07, 138.76, 129.32, 116.73, 116.05, 108.03, 101.11, 100.02, 77.24, 76.86, 73.27,

69.81, 60.72, 55.33. *Overlaid by strong signal from water. ESI-MS: m/z 355.1035 [M-H]⁻.

2.3.2.5.5 Synthesis of (*E*)-2-hydroxy-4-methoxycinnamic acid.

7-Methoxycoumarin (0.44 g) was dissolved in an aqueous solution of 0.5 M NaOH (20 mL, 2.5 mM) and stirred for 4 h at room temperature. Aliquots were taken and showed full conversion to the *trans* carboxylate by NMR in D₂O. The solution was then acidified with 1 M aqueous HCl and extracted with dichloromethane (3 × 10 mL). The solvent was then evaporated and eluted with ethyl acetate on a flash silica column. This yielded the (*E*)-2-hydroxy-4-methoxycinnamic acid (32 mg, 0.165 mM, 6.6 % yield). The low yield was due to the ring closing to reform the coumarin in acidic conditions. The schematic representation of the chemical synthesis of shown below.



¹H NMR (500 MHz, Acetone) δ 9.25 – 9.21 (broad s, 1H, H7), 7.95 (d, J = 16.1 Hz, 1H, H2), 7.54 (d, J = 8.5 Hz, 1H, H3), 6.40 (d, J = 2.2 Hz, 1H, H5), 6.37 (dd, J = 2.2, 8.5 Hz, 1H, H4) 6.33 (d, J = 16.1 Hz, 1H, H1), 3.66 (s, 3H, H6). The synthesised compound was analysed by HPLC-DAD. ESI-MS: m/z 193.06 [M-H]⁻ (figure 2.7).

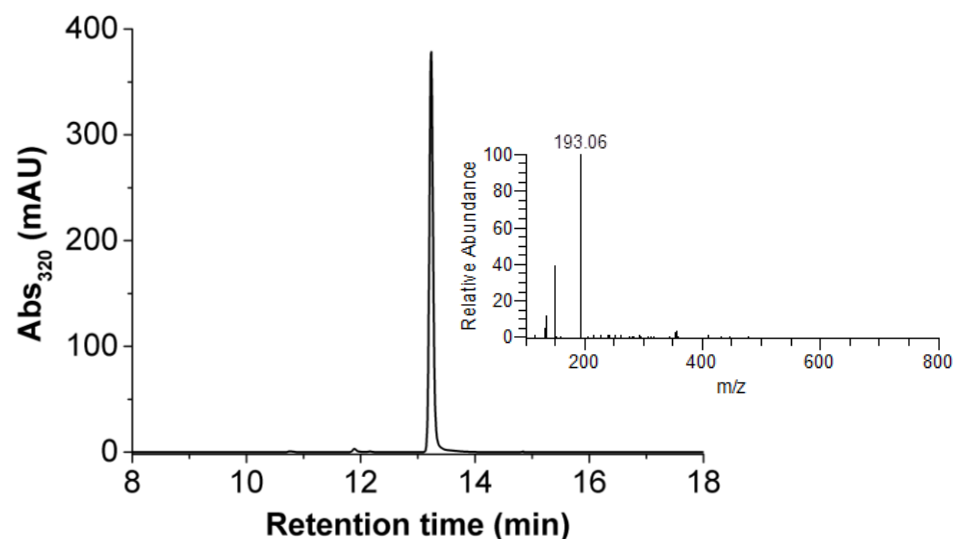


Figure 2.7 HPLC-DAD and LC-MS analysis of chemically synthesised (*E*)-2-hydroxy-4-methoxycinnamic acid. The synthesised standard was dissolved in 5 % acetonitrile in water (5:95, v/v) and analysed under the conditions described in section 2.3.2.2 for both HPLC-DAD and LC-MS. The insert shows the deprotonated molecular mass of the synthesised compound.

2.3.3 Statistical analysis.

Statistical analyses were performed by one-way analysis of variance using the Number Cruncher Statistical System version 6.0 software (NCSS, LLC). Significant differences were assessed with the Tukey–Kramer multiple comparison test ($p < 0.05$). The data are expressed as the mean \pm SEM of at least three independent experiments with three technical replicates each.

2.4 Results and discussion.

2.4.1 Analytical and semipreparative HPLC-DAD analysis.

Initial detection of the major polyphenols in ChE was based on previous analysis conducted in ChE where apigenin, apigenin 7-*O*-glucoside and two peaks with [M-H]⁻ ion masses at *m/z* 355 and 711 showed the highest intensity among the polyphenols detected (Villa-Rodriguez *et al.*, 2017). Table 2.1 shows the polyphenol profile of the ChE used in this study as reported in Villa-Rodriguez *et al.* (2017).

Table 2.1 Polyphenol profile of aqueous ChE.

Compound	[M-H] ⁻	MS ²
Protocatechuic acid	153	109
Umbelliferone aglycone*	161	133
Ferulic acid*	193	149
Apigenin*	269	151
Luteolin*	285	133
Kaempferol*	285	151
Quercetin*	301	151
Isorhamnetin	315	300
Coumaroyl quinic acid	337	191
4- <i>O</i> -CQA	353	173
3- <i>O</i> -CQA	353	179
5- <i>O</i> -CQA	353	191
cis/trans ferulic acid hexoside	355	193
5- <i>O</i> -feruloylquinic acid	367	194
Dimethoxy-cinnamic acid hexoside	369	189
Luteolin 7 <i>O</i> -glucoside*	447	285
Quercetin 3 <i>O</i> -glucoside*	443	301
Quercetin 3 <i>O</i> -glucuronide	477	301
Myricetin <i>O</i> -hexoside	479	317
Luteolin <i>O</i> -acylhexoside	489	285
di-CQA*	515	353
Kaempferol 3 <i>O</i> -rutinoside	593	285
Quercetin 3 <i>O</i> -rutinoside	609	301
FA hexoside dimer	711	355, 193

The polyphenols were identified using authentic standards when available (*). Otherwise, the identification was conducted by comparing the characteristic transition ions with those reported in the literature (Mulinacci *et al.*, 2000; Lin and Harnly, 2012; Guimarães *et al.*, 2013).

Figure 2.8A shows an HPLC-DAD chromatographic analysis of ChE demonstrating the presence of four major polyphenols previously identified (Villa-Rodriguez *et al.*, 2017) and targeted in this study; their descriptive characteristics are presented in table 2.2.

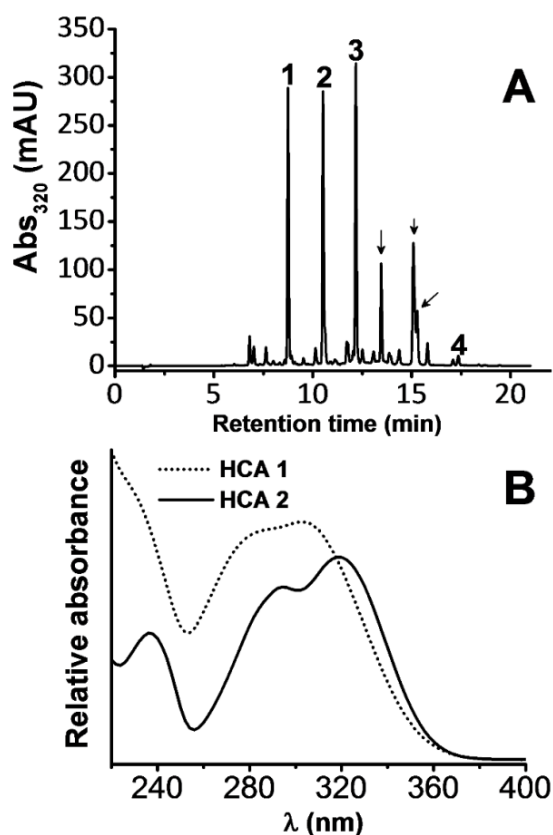


Figure 2.8 Analysis of polyphenols in ChE. (A) HPLC-DAD chromatogram of polyphenols in ChE. Compounds are referred according to the retention time sequence, 1) hydroxycinnamic acid derivative (HCA) 1; 2) HCA 2; 3) apigenin 7-*O*-glucoside; 4) apigenin. The peaks indicated with arrows were tentatively identified as apigenin acetyl derivatives according to LC-MS analysis (data not shown). (B) UV-Vis spectrum of the abundant HCAs (peaks 1 and 2).

Table 2.2 Identification and quantification of targeted polyphenols in ChE.

Compound	Rt (min)	Concentration (μ M)	LOD (μ M)	LOQ (μ M)
1*	8.7	257.0 \pm 2.2	0.42	1.32
2	10.5	200.9 \pm 2.0	0.46	1.43
3	12.1	148.7 \pm 2.0	2.62	8.18
4	15.8	12.22 \pm 0.08	2.48	7.75

*The quantification was conducted with the isolated standard with an estimated purity of >80 % based on quantitative information of compound 2. An isomerisation reaction took place where the hydroxycinnamic acid derivative changed to the most thermodynamically stable form (*trans*)

which accounts for the impurity detected. There were significant differences ($p < 0.05$) in the content of the polyphenols in ChE.

In line with previous observations, apigenin 7-*O*-glucoside and its derivatives were the predominant examples in chamomile (Mulinacci *et al.*, 2000; Švehlíková *et al.*, 2004; Guimarães *et al.*, 2013; Villa-Rodriguez *et al.*, 2017). Additionally, we detected two abundant peaks with UV-Vis absorption spectra of those previously shown to have [M-H]⁻ ion masses at m/z 355 and 711 (Mulinacci *et al.*, 2000) and which are characteristic of hydroxycinnamic acid derivatives (compound 1 and 2). An important work reporting the presence of these compounds was conducted by Mulinacci *et al.* (2000) who assigned their identity as ferulic acid-1-*O*-glucoside and ferulic acid-7-*O*-glucoside and their work has served as a reference for the identification of these compounds in further studies (Lin and Harnly, 2012; Matic *et al.*, 2013). LC-MS by itself usually does not provide sufficient structural information for unambiguous identification of a particular chemical constituent in a plant extract. Therefore it is intriguing to considerer how Mulinacci and co-workers assigned the identity of these compounds based solely on spectroscopic analysis and comparison with structurally-related compounds without complementary analytical techniques. Similarly, Guimarães *et al.* (2013) tentatively identified these compounds as ferulic acid derivatives and they suggested the presence of a ferulic acid hexoside dimer based on the predominant deprotonated molecular ion peak observed at m/z 711 which gives a mass difference of 355 units. On the other hand, Weber *et al.* (2008) reported the presence of isomeric structures of 2-(glucosyloxy)-4-methoxy-cinnamic acid which possess the same deprotonated molecular mass of the isomers of ferulic acid previously identified in the work of Mulinacci and co-workers. Since the exact identity of these molecules is controversial, here the isolation of the hydroxycinnamic acid derivatives on a semi-preparative scale was conducted in order to establish their chemical identity, their content in ChE and their potential bioactivity (described in chapter 3 and 4).

The two hydroxycinnamic acid derivatives were successfully semi-preparatively separated (figure 2.9), isolated and concentrated, yielding enough material to perform chemical analysis and future *in vitro* experiments. The purity after pooling the collected fractions and freeze-dried concentration, was >80 % for compound 1 and >99 % for

compound 2. Moreover, the quantitative analysis revealed that compound 1 and 2 are present at higher levels than apigenin 7-*O*-glucoside suggesting that they might contribute to certain extent to the biological activity of chamomile.

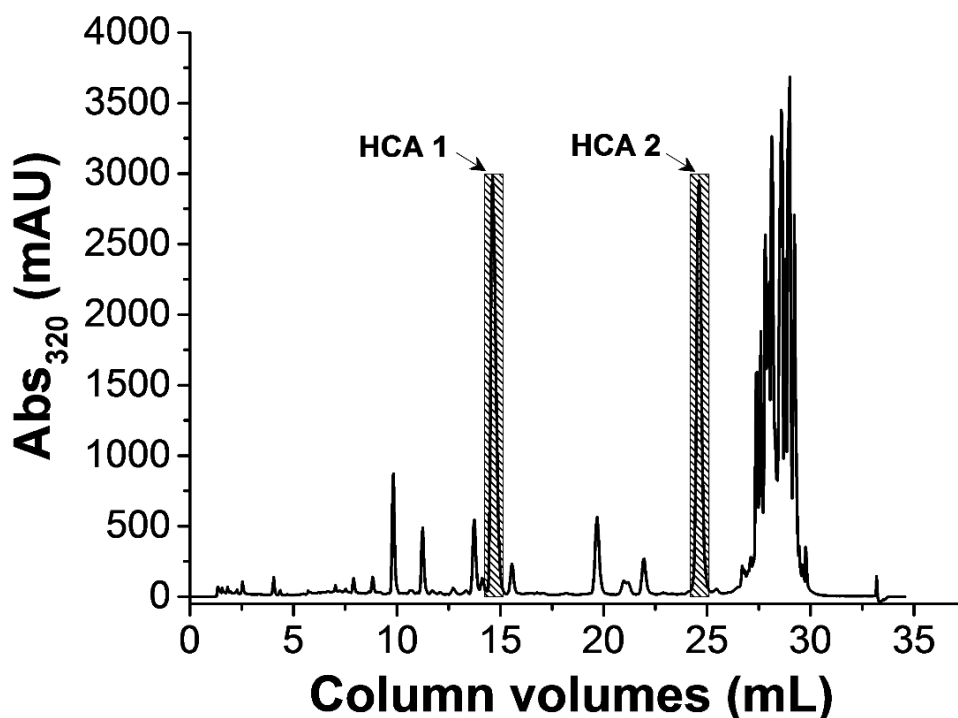


Figure 2.9 Semi-preparative purification of the two hydroxycinnamic acid derivatives (HCA) from ChE using the AKTA system. The chromatographic separation was conducted using the gradient described in section 2.3.2.4. Isolated peaks are highlighted with dashed lines.

2.4.2 Chemical characterisation of the hydroxycinnamic acid derivatives.

The identity of the hydroxycinnamic acid derivatives was assigned based on HPLC-DAD/QTOFMS, ^1H and ^{13}C NMR, NOESY and chemical synthesis. The full-scan TOF spectra of both compounds showed prominent ions at m/z 355.1035 and 711.2136, which were assigned as $[\text{M}-\text{H}]^-$ and $[2\text{M}-\text{H}]^-$ respectively (table 2.3). This assignment could be further confirmed by the appearance of the $[\text{M}+\text{Cl}]^-$ ion at m/z 391.0801 in the spectrum of hydroxycinnamic acid derivative 2. The (neutral) elemental formula of the two hydroxycinnamic acid derivatives was established as $\text{C}_{16}\text{H}_{20}\text{O}_9$. Both compounds showed identical fragment ions in the Q/TOF product ion spectra at m/z 193.0506 $[\text{M}-\text{hexosyl}-\text{H}]^-$ and 149.0608 $[\text{M}-\text{hexosyl}-\text{CO}_2]^-$ (table 2.3). These results clarified that neither of the compounds are dimeric ferulic hexosides as suggested by Guimarães *et al.* (2013) based

on the predominant ion at m/z 711 for the hydroxycinnamic acid derivative 2 but a pseudo-molecular created in the interface during the ionisation process.

Table 2.3. Q/TOF-MS/MS of isolated hydroxycinnamic acid derivatives (HCA) from ChE.

Compound	[M-H]-	MS ²	Elemental formula	Measured m/z	Exact mass	Error (ppm)
1	355	[M-hexosyl-CO2]-	C ₉ H ₉ O ₂	149.0599	149.0608	-6.04
	355	[M-hexosyl]-	C ₁₀ H ₉ O ₄	193.0496	193.0506	-5.18
	355	[M-H]-	C ₁₆ H ₁₉ O ₉	355.1017	355.1035	-5.07
	711	[M-hexosyl]-	C ₁₀ H ₉ O ₄	193.0497	193.0506	-4.66
	711	[M-H]-	C ₁₆ H ₁₉ O ₉	355.1029	355.1035	-1.69
	711	[2M-H]-	C ₃₂ H ₃₉ O ₁₈	711.2152	711.2136	2.25
2	355	[M-hexosyl-CO2]-	C ₉ H ₉ O ₂	149.0599	149.0608	-6.04
	355	[M-hexosyl]-	C ₁₀ H ₉ O ₄	193.0493	193.0506	-6.73
	355	[M-H]-	C ₁₆ H ₁₉ O ₉	355.1034	355.1035	-0.28
	711	[M-hexosyl]-	C ₁₀ H ₉ O ₄	193.0494	193.0506	-6.22
	711	[M-H]-	C ₁₆ H ₁₉ O ₉	355.1022	355.1035	-3.66
	711	[2M-H]-	C ₃₂ H ₃₉ O ₁₈	711.2114	711.2136	-3.09

It is noted that covalently bound ‘dimeric ferulic acids’ are well characterised compounds, which act as polysaccharide cross-linking agents in cell walls (Kennedy *et al.*, 1999; Andreassen *et al.*, 2000). Thus their (di)glycosides structures also can be theoretically expected in plant extracts. However, their predicted ion formula should be [C₃₂H₃₇O₁₈]⁻ resulting in a monoisotopic ion mass of m/z 709.1985 in negative ion mode. Confirmatory Q/TOF fragmentation of the m/z 711.2136 was performed that provided fragments only at m/z 355 and 193 (table 2.3, figure 2.10) lending further support to the original assumption that the elemental formula of the two hydroxycinnamic acid derivatives is C₁₆H₂₀O₉.

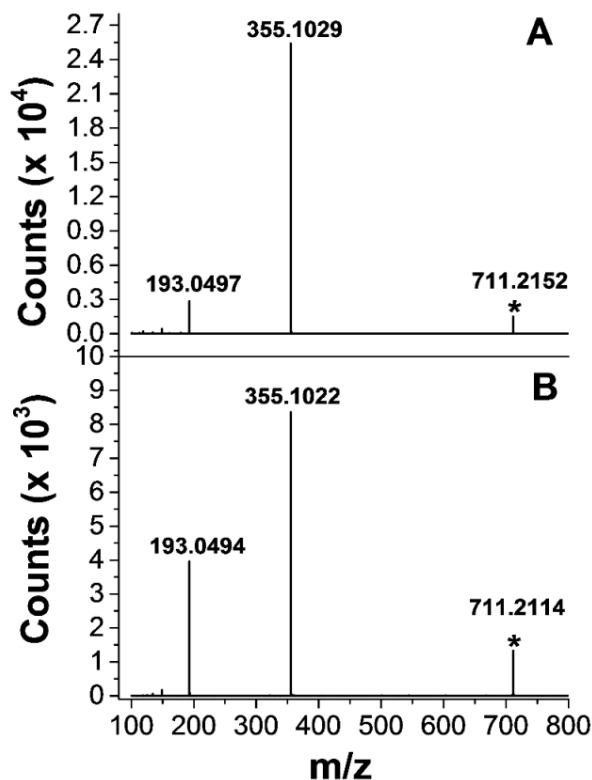


Figure 2.10 Fragmentation pattern of isolated ion at m/z 711.(A) hydroxycinnamic acid derivative 1 and (B) hydroxycinnamic acid derivative 2. The resulting ions are due to i) the cleavage of the glycosidic bond between the hydroxycinnamic acid and glucose (m/z 193), ii) cleavage of the pseudo-molecular deprotonated dimer ion formed ($[2M - H]^-$) in the interface during the ion generation (m/z 355).

Nevertheless, these results did not invalidate the presumed isomeric structures of ferulic acid glucosides previously reported (Mulinacci *et al.*, 2000). The diagnostic MS^2 fragments displayed by these polyphenols logically suggest that they are ferulic acid glycosides. However, acid hydrolysis of these compounds did not result in the release of ferulic acid (figure 2.11A) but a compound with a m/z of 193 eluting at 13.4 min with an UV-Vis spectra characteristic of hydroxycinnamates was detected (figure 2.11B). We also observed a peak with a UV-Vis spectra distinctive of coumarins (figure 2.11B) (Cho *et al.*, 2009) eluting at 15.3 min which was later confirmed as 7-methoxycoumarin by comparison with the authentic standard (figure 2.12).

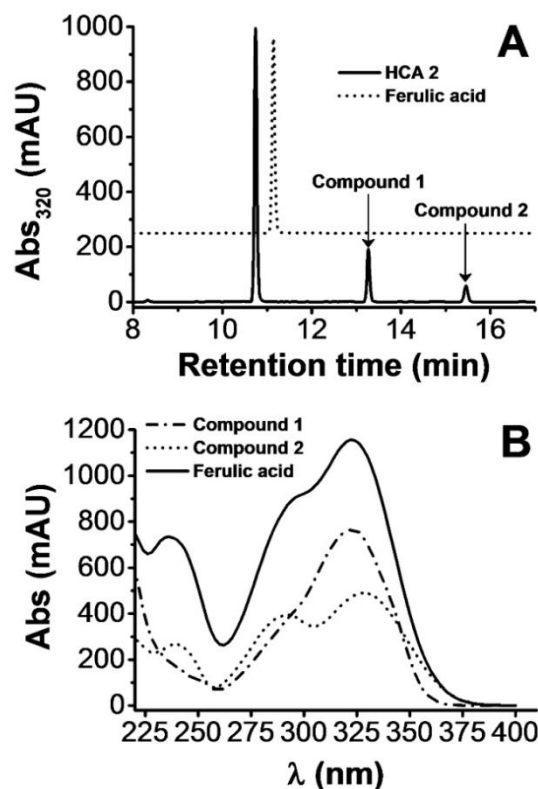


Figure 2.11 Analysis of hydroxycinnamic acid derivative 2 (HCA 2) after acid hydrolysis. (A) HPLC-DAD chromatogram of the hydrolysed fraction and comparison of the resulted compounds with ferulic acid standard. Released products after the hydrolysis are marked as compound 1 and 2. (B) UV-Vis spectra of ferulic acid standard and compounds resulting from acid hydrolysis.

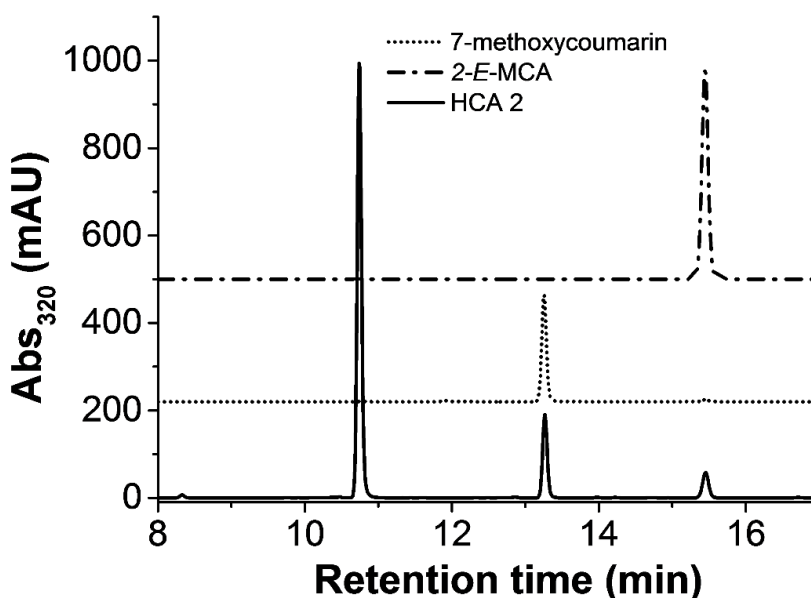


Figure 2.12 Acid hydrolysis of hydroxycinnamic acid derivative 2 (HCA 2).The products resulting from the hydrolysis were identified as (*E*)-2-hydroxy-4 methoxycinnamic acid (2-*E*-MCA) and 7-methoxycoumarin by comparison with authentic standards.

The presence of 7-methoxycoumarin was indicative of the release of a *O*-hydroxycinnamate after hydrolysis where part of it underwent intramolecular cyclization catalysed by the acid conditions (Cho *et al.*, 2009). A previous study (Weber *et al.*, 2008) identified the presence of (*Z*) and (*E*)-2- β -D-glucopyranosyloxy-4-methoxycinnamic acid (*Z* and *E*-MCAG) in chamomile which possesses the same molecular mass of the isolated hydroxycinnamic acid derivatives; this would explain the compounds detected after hydrolysis and their mistaken identification as ferulic acid derivatives. Moreover, these compounds have been reported to be the precursor of 7-methoxycoumarin (Repčák *et al.*, 2001) which clarify the appearance of this molecule after acid hydrolysis. Indeed, further confirmation of the identity of the cinnamate moiety was obtained by chemical synthesis and comparison with the released aglycone after acid hydrolysis (figure 2.12) indicating that the compound with a deprotonated molecular mass of 193 is an isomer of ferulic acid identified as 2-hydroxy-4-methoxy-*trans*-cinnamic acid.

The $^1\text{H-NMR}$ data displayed spectroscopic signals for a free carboxylic group, which was identified from the detection of the signal at δ 12.00. The presence of a (*Z*) and (*E*)-alkene group in the structure of hydroxycinnamic acid derivative 1 and 2 were identified from the signals at δ 7.19 and 5.78 ($J=12.7$ Hz), and δ 7.82 and 6.39 ($J=16.2$ Hz), respectively. The spectrum also showed three aromatic protons in the ABD substitution pattern characteristic of the coupling constants of $J=8.5$ -8.6 (ortho) and $J=2.4$ -2.5 (meta) (Weber *et al.*, 2008). Acid hydrolysis of both compounds resulted in the release of D-glucose (figure 2.13). The ^1H chemical shift in the range 4.85 (*Z*-isomer) and 4.98 (*E*-isomer) with coupling constants of $J=7.5$ Hz from the anomeric protons indicate a β -glycosidic linkage and the location of the D-glucose moiety was assigned at the phenolic ring by the observed NOE enhancements (figure 2.14).

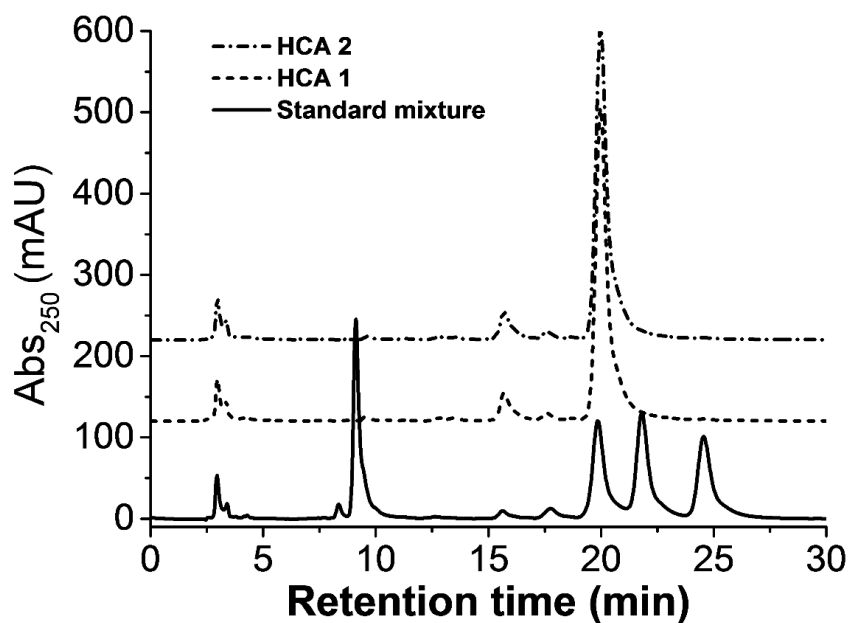


Figure 2.13 Comparison of the resulting compounds after acid hydrolysis with authentic standards of monosaccharides. The hexose was identified as D-glucose (for elution pattern see figure 6). HCA 1: hydroxycinnamic acid derivative 1; HCA 2: hydroxycinnamic acid derivative 2.

The NOE enhancements gave an indication of the position of the other functional groups around the ring. The ¹³C NMR data showed 16 carbon resonances for the phenolic moiety in isolated compound 2, suggesting the presence of (*Z*) and (*E*)-2-β-D-glucopyranosyloxy-4-methoxycinnamic acid (*Z* and-*E*-MCAG) as previously reported by Weber *et al.* (2008).

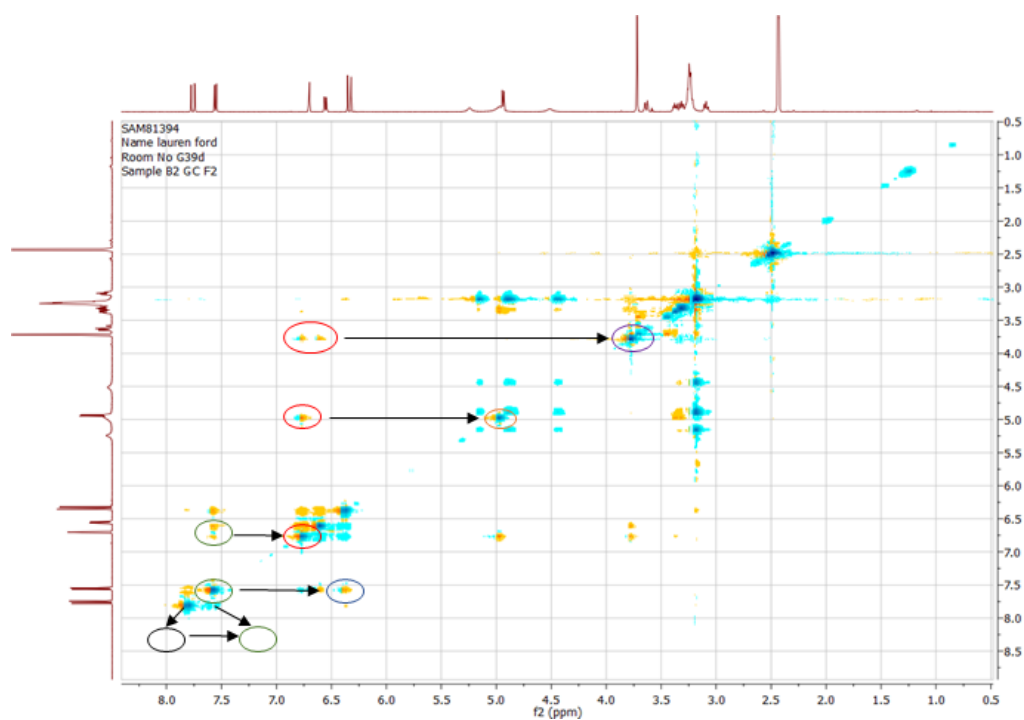
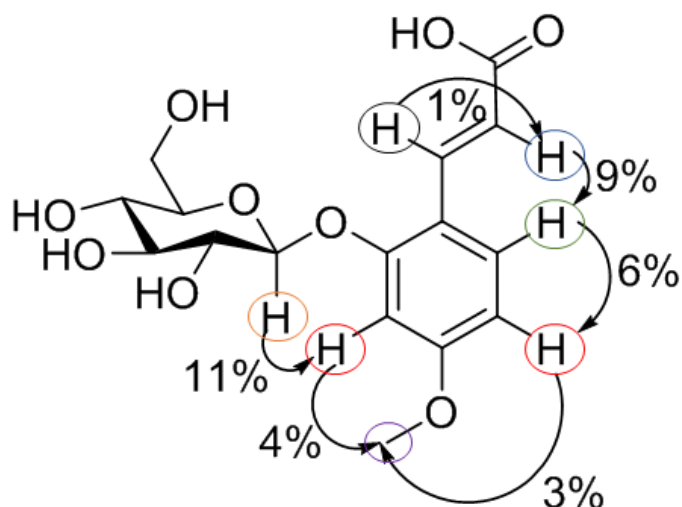
A**B**

Figure 2.14 NOESY analysis of hydroxycinnamic acid derivative 2.(A) Key NOESY correlations are indicated with arrows and circles. The colour of the circles represents the protons interacting in (B). (B) Key NOESY correlations are indicated with arrows and percentage enhancements.

In the present study conclusive evidence is provided that demonstrates unambiguously the chemical identity of the two hydroxycinnamic acids. The combination of analytical techniques indicates that the identity of the two hydroxycinnamic acid derivatives is (*Z*) and (*E*)-MCAG. This information adds to the previous one reported by Weber *et al.* (2008) who did not state the adduct formation [2M-H]⁻ with a deprotonated molecular mass of *m/z* 711 for both compounds, which is crucial for efficient data-mining. Moreover, it has been demonstrated through acid hydrolysis and the use of an authentic standard that *Z*-MCAG is the precursor of 7-methoxycoumarin, commonly known as herniarin. The characteristic chromatographic pattern observed after acid hydrolysis along with their formation of 7-methoxy coumarin and distinctive UV spectrum of the MCA can be used to identify the presence of these compounds in the absence of authentic standards.

Insufficient evidence regarding the analytical information obtained to identify and characterise the hydroxycinnamic acids in previous publications is perhaps the main reason why the identity of the hydroxycinnamic acid derivatives in chamomile remained obscure. In this sense, it is important to mention that the presence of these compounds was first described more than 20 years ago (Ohe *et al.*, 1994; Repčák *et al.*, 2001) but without fully providing the chemical information obtained to assigned their chemical identity (HPLC, LC-MS and NMR). This tendency has continued in some recent publications where the presence of (*Z*) and (*E*)-MCAG has been described in chamomile without giving enough chemical information (Kováčik and Repčák, 2008; Avula *et al.*, 2014).

2.5 Conclusion

The combination of analytical techniques used in this study confirmed that the $m/z^{(-)}$ at 711 is a pseudo-molecular dimer ion formed in the interface from both compounds. The hydroxycinnamic acid derivatives were identified as (*Z*) and (*E*)-MCAG and the quantitative analysis revealed for the first time that they can be present at higher levels than apigenin 7-*O*-glucoside. For (*Z*)-MCAG, the content can vary according to chamomile handling since deglycosylation results in 7-methoxycoumarin formation. In addition, the content of these major polyphenols in chamomile can be affected by different stresses, locations, climates, microenvironments and physical and chemical stimuli altering any activity resulting from their interaction. Therefore, suitable characterisation of botanical preparations from chamomile is mandatory to unravel and assure reproducible biological activity in screening assays.

Chapter 3 Assessment of the inhibition of carbohydrate-digesting enzymes by polyphenols and chamomile extract *in vitro*: optimisation of α -amylase activity using the 3, 5-dinitrosalicylic acid method and determination of molecular interactions *in silico*.

3.1 Abstract.

Botanical preparations, functional foods and nutraceuticals offer the possibility to modulate the absorption of sugars, leading to benefits for healthy individuals and diabetics. As part of the characterisation of such foods, inhibition of carbohydrate-digesting enzymes (acarbose-like activity) is used to assess components for their potential ability to modify the postprandial glycaemic response. Many publications on polyphenols as potential inhibitors report widely varying assay conditions leading to variable estimates of inhibition. The first part of this chapter describes the optimisation of an *in vitro* human salivary α -amylase inhibition assay and, in particular, it is show the importance of removing certain polyphenols after the enzymatic reaction when using 3,5-dinitrosalicylic acid solution since they interfere with this reagent. There was a substantial ~5-fold effect on acarbose IC₅₀ values when working outside optimal conditions. This shows that inappropriate assay parameters, such as excess of enzyme, greatly influence inhibition constants and could explain some discrepancies in the current existing literature.

The optimised α -amylase inhibition assay along with a α -glucosidase assay were used to assess the acarbose-like activity of ChE and identified the active polyphenols participating in this metabolic pathway. The four major polyphenols inhibited human salivary α -amylase, with apigenin exhibiting the strongest effect (competitive inhibition, $K_i = 17 \mu\text{M}$) followed by apigenin 7-*O*-glucoside (competitive inhibition, $K_i = 146 \mu\text{M}$) while (*Z*) and (*E*)-MCAG presented mild inhibitory activity (maximum ~25 % at 100-500 μM). When the four polyphenols were combined at the concentrations equivalent to those present in the ChE, the activity was enhanced by ~20 % as compared with the whole

extract. Molecular docking was performed to investigate the interactions taking place between the polyphenols and the enzyme and rationalise the inhibition observed for all the tested molecules. The rat intestinal maltase activity was modestly inhibited; neither ChE nor the individual polyphenols reached 50 %, while no inhibition of rat intestinal sucrase and isomaltase activities was observed. These results suggest that ChE as a herbal plant extract that combines (*Z*)-(*E*)-MCAG, apigenin and apigenin 7-*O*-glucoside, can potentially help to attenuate postprandial hyperglycaemia.

3.2 Introduction.

Persistent high postprandial glucose spikes have been proposed as independent risk factors for developing insulin resistance and progression to type 2 diabetes (Barclay *et al.*, 2008; Vinoy *et al.*, 2016). Plausible mechanisms suggested for this association include acute altered energy partitioning (Brand-Miller *et al.*, 2002), increased oxidative stress (Ceriello *et al.*, 2004), low-grade inflammation (Ceriello *et al.*, 2004) and endothelial dysfunction (Kawano *et al.*, 1999) that, over time, orchestrate a coordinated breakdown in cellular functions. Therefore, the modulation of absorption of sugars in the intestine has now been seen as a therapeutic target for reducing insulin resistance and type 2 diabetes risk (Ceriello and Colagiuri, 2008; Vinoy *et al.*, 2016).

The attenuation of carbohydrate digestion in the intestine by the antidiabetic drug acarbose (figure 3.1) has shown to reduce the risk of type 2 diabetes and cardiovascular events by 25 and 49 % respectively (Chiasson *et al.*, 2002; Chiasson *et al.*, 2003), proving the clinical relevance of this approach to manage blood glucose levels. Unfortunately the use of this drug very often is marked with severe GI side-effects including abdominal pain, meteorism, flatulence and diarrhea (Chiasson *et al.*, 2002; Bethel *et al.*, 2015) resulting in poor patient compliance and adherence to the treatment. This highlights the need for the identification of new small molecules that could decrease not only carbohydrate digestion but also sugar uptake in the gut which can be used as an alternative to acarbose or act as coadjuvants. Furthermore, considering the current western lifestyle patterns, the incorporation of these small molecules in foods represent a technical advantage over the use of low GI foods since postprandial glycaemic goals can be achieved without altering the carbohydrate and sugar composition of diets. Therefore these molecules can aid to control hyperglycaemia not only in persons with a pathophysiological phenotype, but also in healthy individuals.

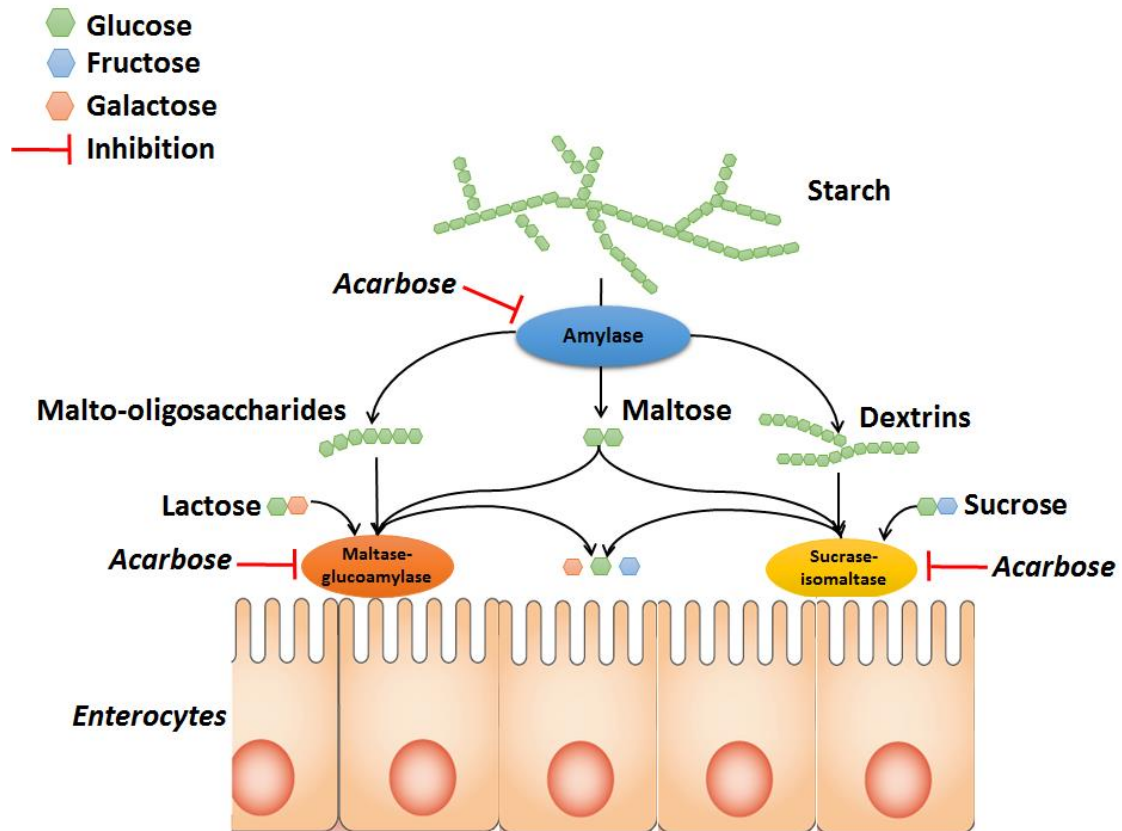


Figure 3.1 Steps involved in the digestion of starch and the disaccharides sucrose and lactose leading to the appearance of glucose in circulation. Starch is a polysaccharide formed of amylose and amylopectin. Amylose is made of linear chains of glucose molecules, joined by α -1–4 linkages whereas amylopectin is constituted of branched chains of glucose, joined by both α -1–4 and α -1–6 linkages (Guzmán-Maldonado *et al.*, 1995). Partial hydrolysis of starch is accomplished by salivary α -amylase, with major cleavage provided by human pancreatic α -amylase in the gut, generating malto-oligosaccharides (two or more α -1,4-linked glucose units) and dextrins (α -1,6-linked glucose units along with attached α -1,4-linked glucose units) (Butterworth *et al.*, 2011). These resulting products from starch hydrolyses as well as sucrose and lactose are in turn broken down to glucose by maltase-glucoamylase and sucrase-isomaltase (generally known as α -glucosidases) that are attached to the epithelium of the small intestine (Robayo–Torres *et al.*, 2006). Both enzymes are composed of duplicated catalytic domains showing overlapping substrate specificities for α -1,4-oligosaccharides. In addition, sucrase-isomaltase shows specificity for α -1,2 and α -1,6-glycosidic bonds and so, it mediates the conversion of sucrose and isomaltose respectively to the corresponding monosaccharides glucose and fructose (Sim *et al.*, 2010). The drug acarbose reduce and slows-down plasma glucose levels by inhibiting α -amylase and α -glucosidases.

Many reports indicate that polyphenol-rich extracts inhibit α -amylase (reviewed in Nyambe-Silavwe *et al.* 2015, appendix A-C). However, these studies used different methods of detection and assay conditions (reaction time and temperature, pH, enzyme concentration and source, substrate concentration and source) which have a pronounced impact on the reported data. The most commonly used method for measuring α -amylase activity involves the 3,5-dinitrosalicylic acid (DNS) reagent for detection of reducing sugars. The presence of a free carbonyl group in reducing sugars enables them to participate in an oxidation-reduction reaction with DNS (figure 3.2). However, due to the reducing potential of polyphenols, they could interfere with the development of the colour and thus the results of the assay. Therefore the development and optimisation of bioassays with high levels of reliability is essential to evaluate the acarbose-like activity of polyphenols and polyphenol-rich extracts in order to consider them as real candidates for attenuating hyperglycaemia. For instance, recent reports have indicated positive effects of chamomile in experimental diabetes and type 2 diabetic subjects (Cemek *et al.*, 2008; Weidner *et al.*, 2013; Rafraf *et al.*, 2015; Zemestani *et al.*, 2016). However it is yet elusive whether the antidiabetic and in particular, the antihyperglycaemic effect of chamomile is partially mediated through the modulation of carbohydrate metabolism at the small intestinal site.

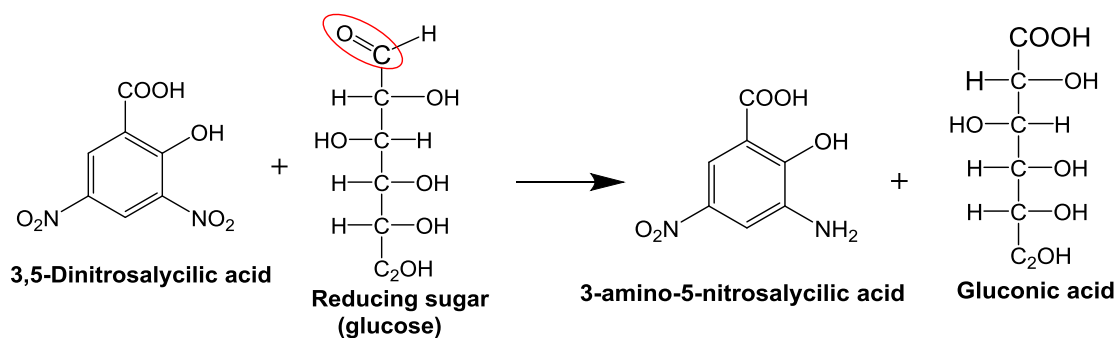


Figure 3.2 Reaction of DNS with reducing sugars. The aldehyde functional group of the reducing sugar (highlighted in circle) is oxidized into a carboxyl group and the 3, 5-dinitrosalicylic acid is reduced to 3-amino-5-nitrosalicylic acid. This reaction cause a colour change from yellow to orange or red, depending on the concentration of the reducing sugars present in the sample. By reading absorbance of the resulting reducing sugars, the amount of maltose equivalents can be calculated using a standard curve with different concentrations of maltose.

The *in vitro* results can be complemented with computational methods to provide mechanistic investigation by predicting the interaction between polyphenols and α -amylase. Molecular docking is a widely used computational method which allows to characterise the behaviour of small molecules in the binding site of target proteins through the use of efficient sampling algorithms and scoring functions (Kitchen *et al.*, 2004). The algorithms generate a predicted binding pose by exploring the ligand conformational space and interactions within a pocket of the protein surface. The binding modes associated with the lowest energy scores are predicted to be the binding modes, and the corresponding energy scores are used to evaluate the binding affinity and to predict the biological activity (Kitchen *et al.*, 2004; Meng *et al.*, 2011). Therefore molecular docking allows to model the interaction between a protein and small molecules including polyphenols, pointing out important features of the structure of the ligand that could be very useful to rationalise structure-activity relationships and to guide experimental research.

With a view to identify potential inhibitors of carbohydrate digestion, and to elucidate whether the antidiabetic effects of chamomile can be partially mediated by acting at this pathway, the combination of the two optimised *in vitro* assays along with molecular docking was used to assess the inhibitory activity of different classes of polyphenols including those in chamomile on α -amylase and α -glucosidase enzymes.

3.3 Materials and methods.

3.3.1 Materials.

3,5-Dinitrosalicylic acid reagent, potassium sodium tartrate, chromatographically purified human salivary α -amylase type IX-A (A0521), acetone extract of rat intestine (i1630), hesperidinase from *Aspergillus niger* (H8137), pancreatin from porcine pancreas (P3292), maltose, epigallocatechin 3-*O*-gallate, quercetin, amylose and amylopectin from potato, D-sucrose, D-maltose, D-glucose, glucose hexokinase and Bradford reagent were all purchased from Sigma-Aldrich. Co., Ltd., Dorset, UK. Phloridzin, quercetin-3-*O*-glucoside and luteolin were purchased from Extrasynthase, Genay, France. Gallic acid was obtained from Alfa Aesar, Lancashire, UK. Green tea, ChE, apigenin and apigenin 7-*O*-glucoside were obtained from PhytoLab Co. KG.h while *Z* and *E*-MCAG were purified from the ChE according to the procedure described in chapter 2, section 2.3.2.4. Oasis MAX cartridge 1 mL (30 mg) and 3 mL (60 mg) were purchased from Waters Corporation Ltd., Milford, MA, U.S.A. The DNS reagent solution was prepared by adding to 12 mL water, 20 mL of 96 mM DNS in water and 5.3 M sodium potassium tartrate solution (12 g in 8 mL of 2 M sodium hydroxide). All the reagents were of the highest purity and standards were $\geq 98\%$.

3.3.2 Methods.

3.3.2.1 Determination of K_m and V_{max} .

The kinetic parameters K_m and V_{max} were determined by using a chosen enzyme concentration and incubation times giving linear rates of reaction where enzyme activity is determined accurately. The substrate concentrations ranged from 0 to 1 mg/mL in the final assay volume. Maltose standard curve was obtained by adding 1 mL of the DNS reagent to a total volume of 500 μ L of different maltose concentrations (0-1.5 mg/mL,) and then heated (100 °C for 10 min). The absorbance was recorded at 540 nm in a PHERAstar FS microplate reader (BMG Labtech, Inc., Cary, NC, USA), and the amount of maltose produced was calculated against a five-point linear calibration curve (figure 3.3). The Lineweaver-Burk plot was used to calculate K_m and V_{max} .

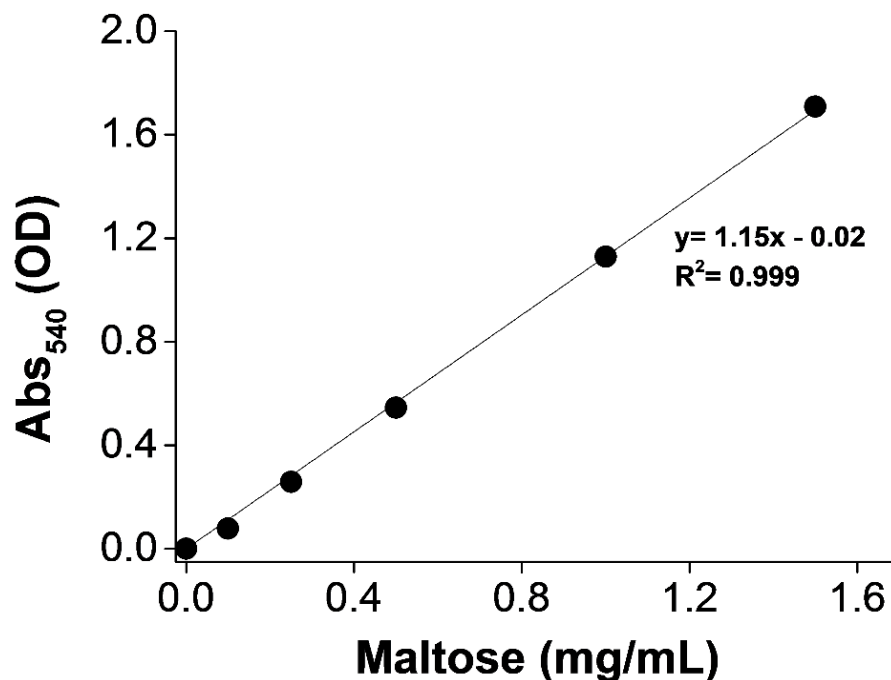


Figure 3.3 Representative example of maltose standard calibration curve. The calibration curve was used to quantify the reducing sugars (mainly maltose) produced from amylose and amylopectin after hydrolysis with human salivary α -amylase. Each data point represents the average of at least three independent determinations \pm SEM. Where not visible, error bars are smaller than the size of the data point.

3.3.2.2 Enzyme concentration and reaction time.

Optimal enzyme units and incubation time were determined by using different enzyme concentrations (0.5, 1.0, 1.5 and 2.0 U/mL). Assay mixtures were incubated for different times (0, 3, 6, 9, 12 and 15 min) and the results were plotted as absorbance versus time to obtain a combination that would give a linear relationship.

3.3.2.3 Effect of polyphenols on colour reagent.

The interference of polyphenols on the development of the colour by the DNS was determined by adding 1 mL of DNS reagent to an assay mixture containing 450 μ L phosphate buffer saline (PBS, 0.01 M, pH 6.9) and 50 μ L of different concentrations of different polyphenols (0-1 mM). The absorbance was recorded as described in section 3.2.2.2.

3.3.2.4 Retention efficiency of Solid Phase Extraction cartridges by HPLC-PDA.

HPLC analysis for efficiency of retention of polyphenols by the Oasis MAX solid phase extraction (SPE) cartridge was carried out with EGCG by Dr. Idolo Ifie (figure 3.4). The analysis were performed in a UFLC_{XR} Shimadzu system (Shimadzu, Japan) consisting of binary pump, a photodiode array with multiple wavelength SPD-20A and a LC-20AD solvent delivery module coupled with an online unit degasser DGU-20A3/A5 and a thermostat autosampler/injector unit SIL-20A (C). The column used was a 5 μ m Gemini C₁₈ (250 x 4.6 mm, i.d.) with a flow rate of 1 mL/min, column temperature set at 35 °C with an injection volume of 10 μ L and detection at 280 nm. A two phase gradient system consisting of water with 0.1% TFA as mobile phase A and acetonitrile containing 0.1 % TFA as mobile phase B. The gradient conditions were as follows: the initial conditions started with 92% A and increasing to 18 % solvent B at 3.50 min, 32% B at 18 min, 60% B at 28 min reaching to 100% B at 32 min for 4 min, returning to the initial conditions for 3.5 min.

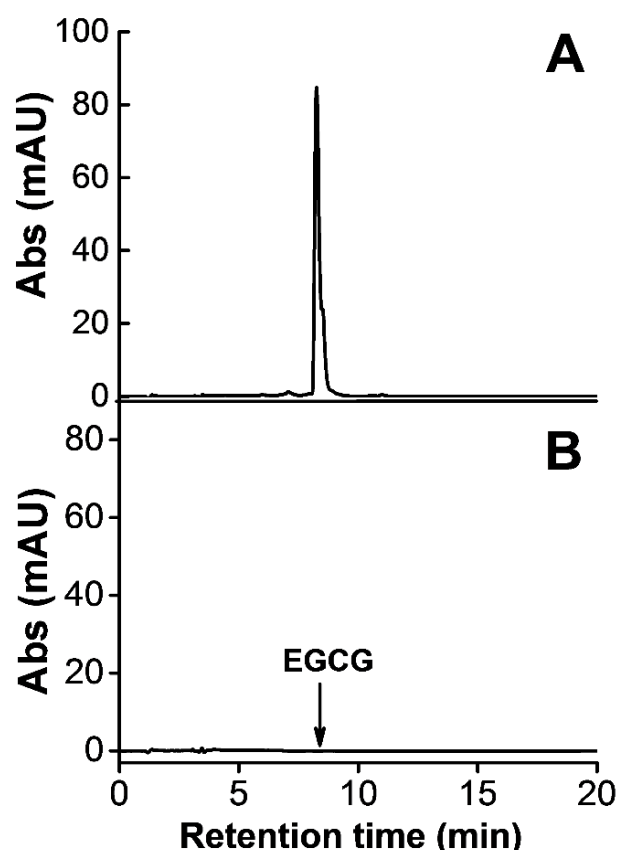


Figure 3.4 Retention efficacy of OASIS solid phase extraction cartridges. The efficiency was tested using EGCG as the test sample. (A) HPLC analysis of EGCG standard (200 μ M) SPE. (B) HPLC analysis of EGCG standard after solid phase extraction.

3.3.2.5 Human α -amylase inhibition assay.

For α -amylase, 1 “Sigma-defined” unit will liberate 1.0 mg of maltose from starch in 3 min at pH 6.9 at 20 °C, and this was the basis of the initial experiments to optimise the assay. The enzyme preparation on this basis contained 276 Sigma-units per mg protein as estimated by Bradford assay. The assay contained 200 μ L each of substrate (amylose or amylopectin) and enzyme, 50 μ L PBS and 50 μ l of inhibitor of different concentrations. For the control assay, the inhibitor was replaced by an equal volume of PBS. Stock amylose and amylopectin solutions (2.5 mg/mL) were prepared in water by heating at 90 °C on a hot plate until it was dissolved (normally 5-10 min). A second stock solution of amylopectin was prepared at 0.925 mg/mL. Human salivary α -amylase stock solution (1.25 U/mL) was prepared in PBS. The enzyme stock solution and the assay mixture containing the inhibitor, PBS and substrate were pre-incubated at 37 °C for 10 min and the reaction was started by adding the enzyme to the assay solution. The reaction was carried out at 37 °C for 10 min with α -amylase at 0.5 U/ mL, substrate at 1 mg/mL and varying concentrations of the inhibitor up to 1 mM (depending on solubility). The reaction was stopped by placing the samples in a water bath at 100 °C for 10 min where no further reaction occurred, transferred to ice to cool down to room temperature and centrifuged for 5 min at 14000 g. The resulting sample was used for SPE to remove polyphenols before adding the DNS reagent. Thereafter, 1 mL of the DNS reagent was added and heated at 100 °C for 10 min. After cooling to room temperature, 250 μ L from each sample was placed in a 96 well plate (Nunc A/S., Roskilde, Denmark) and the absorbance was recorded at 540 nm. Figure 3.5 summarises the different stages involved in the human salivary α -amylase protocol.

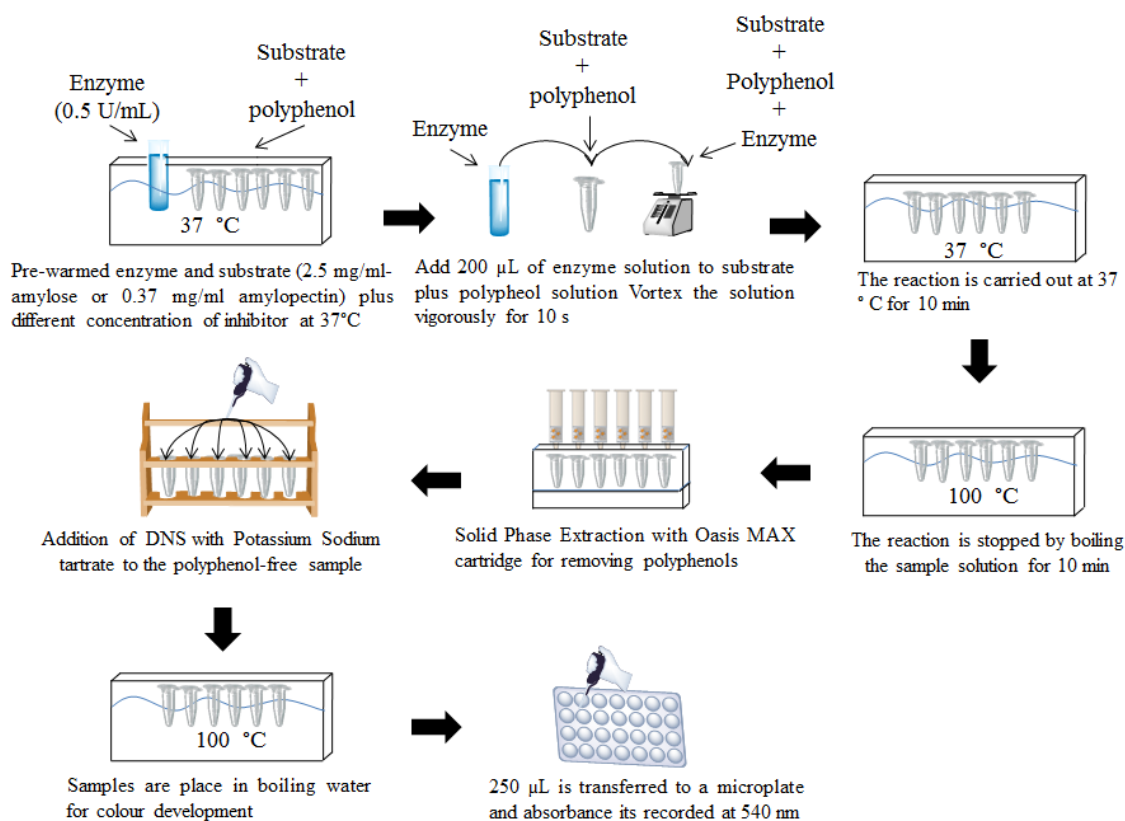


Figure 3.5 Schematic representation of human α -amylase inhibition assay. Critical steps that were optimised in order to get reliable inhibition constants include the concentration of enzyme and the removal of polyphenols to avoid interferences with the DNS reagent solution.

The rate of enzyme inhibition was calculated as a percentage of the control (without inhibitor) using the formula:

$$\% = ((\text{Abs Control} - \text{Abs sample}) / \text{Abs control}) \times 100$$

The half maximal inhibitory concentration (IC_{50}) was calculated graphically by dose-dependent inhibition. For K_i values, the Dixon plot method was employed (Dixon, 1953). K_i values were obtained by calculating the intersection point having an associated standard deviation supplying the uncertainties on the estimate using the following equations:

$$y_i = m_i x_i + c_i, \quad i = \{1, 2, 3, \dots, n\}$$

(Assuming n non-parallel regressions)

Intersections (x_{ij} , y_{ij}) of each pair-wise combination i, j ;

$$x_{ij} = \left(\frac{c_j - c_i}{m_i - m_j} \right), \quad y_{ij} = m_i \left(\frac{c_j - c_i}{m_i - m_j} \right) + c_i,$$

$$i, j = \{1, 2, 3, \dots, n\} \quad i \neq j$$

This provides precisely ${}^n C_2 = \frac{n!}{2!(n-2)!} = N$, unique, i.e. non-repetitive pair-wise combinations.

Defining the mean (\mathbf{x}, \mathbf{y}) and standard deviations (s_x, s_y) of the unique intersection coordinates x_{ij}, y_{ij} , as

$$\mathbf{x} = \frac{1}{N} \sum_{\substack{i, j=1 \\ i \neq j}}^n x_{ij}, \quad \mathbf{y} = \frac{1}{N} \sum_{\substack{i, j=1 \\ i \neq j}}^n y_{ij}$$

$$s_x^2 = \frac{1}{N-1} \sum_{\substack{i, j=1 \\ i \neq j}}^n (x_{ij} - \mathbf{x})^2, \quad s_y^2 = \frac{1}{N-1} \sum_{\substack{i, j=1 \\ i \neq j}}^n (y_{ij} - \mathbf{y})^2$$

provides the expected intersection point of the regressions and associated standard deviation to supply the uncertainties on the estimate. The lines of each data point were fitted to the intersection point obtained from the equation. This mathematical equation was designed with the collaboration of Dr. Melvin Holmes from the School of Food Science and Nutrition at the University of Leeds.

The α -amylase inhibition assay was employed to test the potential of ChE and its major polyphenols to attenuate carbohydrate digestion. ChE contained 50 % maltodextrin consisting of a variable length of D-glucose units linked by α -1,4 glycosidic bonds. Therefore, maltodextrin represent a substrate for intestinal enzymes and can interfere with the measurement of inhibition. The procedure employed to remove maltodextrin is described in the next section. For the α -amylase inhibition assay, ChE stock solution free of maltodextrin was reconstituted in DMSO while the individual polyphenols were prepared in a water-ethanol solution (50:50, v/v). The maximum concentration of the

organic solvents in the assay solution was 2 and 1 % for DMSO and ethanol respectively, which did not affect the activity of the enzyme as assessed in control incubations.

In order to evaluate the possibility of the release of 2-*E*-MCA after hydrolysis by digestive enzymes in the gastrointestinal tract and therefore its potential role as inhibitor of carbohydrate-digestive enzymes, 2-*E*-MCA was subjected to enzymatic hydrolysis using hesperidinase and acetone extract from rat small intestine. The enzymatic hydrolyses were conducted with 50 mg/mL of the respective enzyme (the enzyme solution was prepared in PBS as described for α -amylase) and the reaction was conducted for 3 h at 37 °C. The released products were analysed by HPLC under the chromatographic conditions described in chapter 2, section 2.3.2.2. Kaempferol 3-*O*-glucoside was used as positive control.

3.3.2.6 Preparation of maltodextrin-free ChE.

The maltodextrin in the chamomile preparation was removed using the ÄKTA Purifier System described in Chapter 2 section 2.3.2.3. ChE was loaded manually using a syringe through a sample loop of 0.1 mL and eluted using water containing 0.1% TFA (solvent A) and acetonitrile (Solvent B) at a flow rate of 0.75 mL/min as follows: 0-3 min linear gradient from 5 to 24 % B; 3-6 min isocratic at 24 % B; 6-18 min linear gradient to 40 % B; 18-24 min isocratic at 40 % B, 24-30 min linear gradient to 100 % B; 30-35 min isocratic at 100 % B, 35-38 min linear gradient to 5 % B, 38-41 min isocratic at 5 % B. The elution was followed at 280 nm and the polyphenol fraction was collected yielding a maltodextrin-free extract. Multiple semi-preparative collections were done, combined, freeze-dried, and stored at -20 °C until the enzymatic assays were conducted.

3.3.2.7 Inhibition of α -glucosidase activity by ChE and its individual major polyphenols.

For α -glucosidase activity, maltase, sucrase and isomaltase were assessed. The assay was optimised for linearity in terms of enzyme and substrate concentration by other members of the laboratory (Aydin, 2015; Nyambe-Silavwe, 2016) as described for human salivary

α -amylase. The apparent K_m values for maltose, sucrose and isomaltose were 3, 16 and 6 mM respectively as determined using the Lineweaver–Burk plot with a chosen enzyme concentration and incubation times giving linear rates of reaction. These concentrations were used to conduct the enzymic assays.

Acetone extract from rat small intestine was used as the enzyme source and inhibitors were prepared as described for human salivary inhibition assay. The reaction mixture contained 0.2 mL of enzyme solution (4 mg/mL powder in 0.01 M PBS, pH 7.0 for maltase and 20 mg/mL for sucrase and iso-maltase), 0.2 mL of substrate (3 mM maltose, 16 mM sucrose and 6 mM isomaltose), 0.05 mL of inhibitor (varying concentrations) and 0.05 mL of PBS. In the control sample, inhibitor was replaced by an equal volume of PBS. The enzyme solution and the assay mixture containing the maltose, inhibitor and PBS were pre-incubated at 37 °C for 10 min and the reaction started by adding the enzyme to the assay mixture. The reaction was carried out and stopped as reported for α -amylase assay after 20 min reaction time and cooled down to room temperature before the inhibitors were removed by solid phase extraction (polyphenols interfere with the enzymatic determination of glucose probably by enhancing NADH production yielding erroneous absorbance readings in their presence). The glucose produced was determined enzymatically (figure 3.6 and 3.7) by placing 0.01 mL of the reaction mixture in 96 well plate (Chimney well, Germany), adding 0.25 mL of hexokinase reagent, incubating for 15 min at 30 °C and recording the absorbance at 340 nm according to Encarnaç o (2015).

Enzyme inhibition (%) was calculated according to the equation:

$$\% = ((\text{Abs Control} - \text{Abs sample}) / \text{Abs control}) \times 100$$

where A_{sample} is absorption of the sample and A_{control} is absorption of the control (without inhibitor). The inhibition constants were calculated as previously described for human α -amylase.

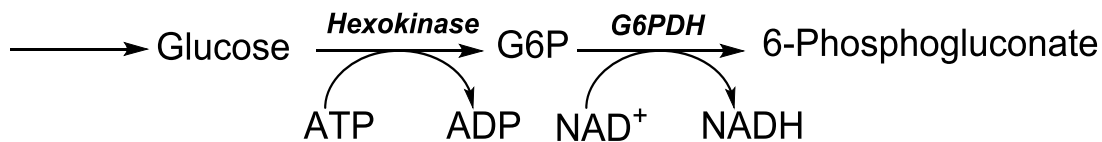


Figure 3.6 Enzymatic determination of glucose by hexokinase-linked reaction. Glucose is phosphorylated by adenosine triphosphate (ATP) in the reaction catalysed by hexokinase. Glucose- 6-phosphate (G6P) is then oxidized to 6-phosphogluconate in the presence of oxidized nicotinamide adenine dinucleotide (NAD) in a reaction catalysed by glucose-6-phosphate dehydrogenase (G6PDH). During this oxidation, an equimolar amount of NAD⁺ is reduced to NADH. The consequent increase in absorbance at 340 nm is directly proportional to glucose concentration.

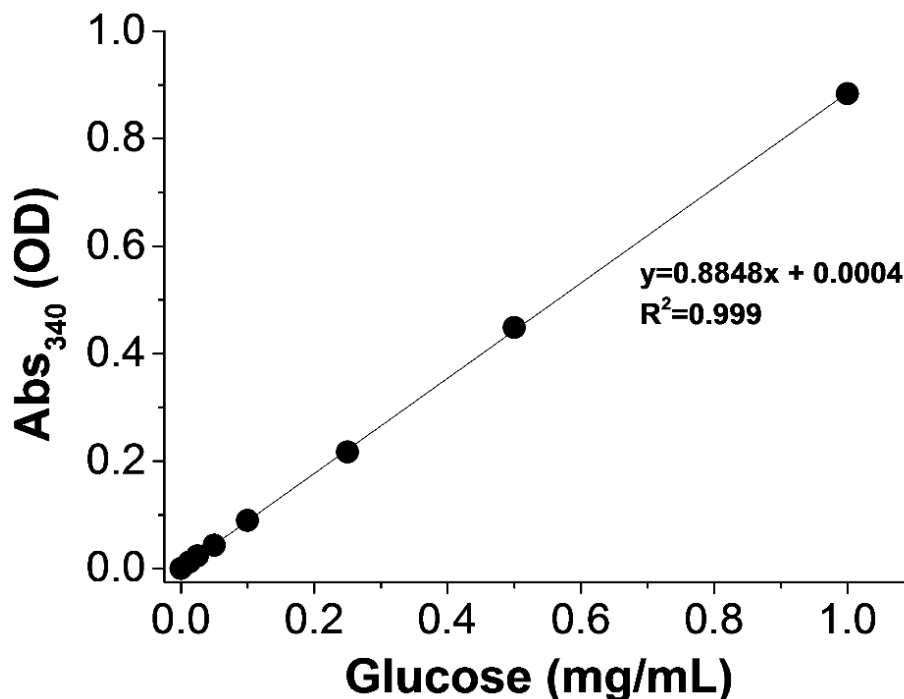


Figure 3.7 Representative example of glucose standard calibration curve. The calibration curve was used to quantify the glucose produced from maltose, sucrose and isomaltose after hydrolysis with acetone extract from rat small intestine. Each data point represents the average of at least three independent determinations \pm SEM. When not visible, the error bars are smaller than the data point.

3.3.2.8 Molecular Modelling.

We investigated the interactions of polyphenols with human salivary and pancreatic α -amylase using the three-dimensional crystal structure 1MFV (Ramasubbu *et al.*, 2003) and 1CPU (Brayer *et al.*, 2000) deposited in the RCSB Protein Data Bank (<http://www.rcsb.org/pdb/home/home>), respectively. They contain a modified form of the α -amylase inhibitor acarbose that was co-crystallised in the binding pocket. The 1MFV and 1CPU were superimposed applying the CLC drug discovery workbench 3.0.2 molecular modelling program (CLC Bio-Qiagen, Aarhus, Denmark) and the binding site residues were located in similar conformation for both enzymes. The α -amylase structures were prepared for docking by removing from the crystallographic structures water molecules and any other co-crystallised ligand. No constraints were introduced and the default parameters were used in this study (binding site: within 13 Å radius around acarbose, scoring function: PLANTS_{PLP} score, genetic algorithm: 100% search efficiency). The score mimics the potential energy change (ΔG), when the protein and the ligand (acarbose or polyphenol) come together. This means that a very negative score corresponds to a strong binding and *vice versa*. These interactions consist of (i) hydrogen-bond interaction, (ii) lone-pair metal ion interactions and (iii) non-polar interactions. The number of docking iterations for evaluation of the preferred binding pose was set at 500. This was optimised for the search space, as the binding poses generated after 500 iterations did not change. The ten best docked poses per docking calculation were analysed based on their docking score and the top ranked pose for each ligand was selected for further analysis. Ligand-receptor interactions were visualised within the CLC workbench and Discovery Studio (BIOVIA, Client version 2016).

Validation of the docking parameters was performed by docking the co-crystal modified structures of acarbose into the active site of each protein. The molecular mechanical energy of the extracted structures were minimised using the impact energy minimization option of Avogadro graphical interface applying the conjugate gradient algorithm before conducting the docking. For the co-crystal structure extracted from 1CPU, hydrogen atoms were added. The corresponding ligand was successfully docked in the binding pocket of 1MFV and 1CPU (1MFV= -74.07 and 1CPU= -73.99 Kcal/mol) with a root mean square deviation (RMSD) of 1.36 and 1.11 Å respectively, and establishing similar

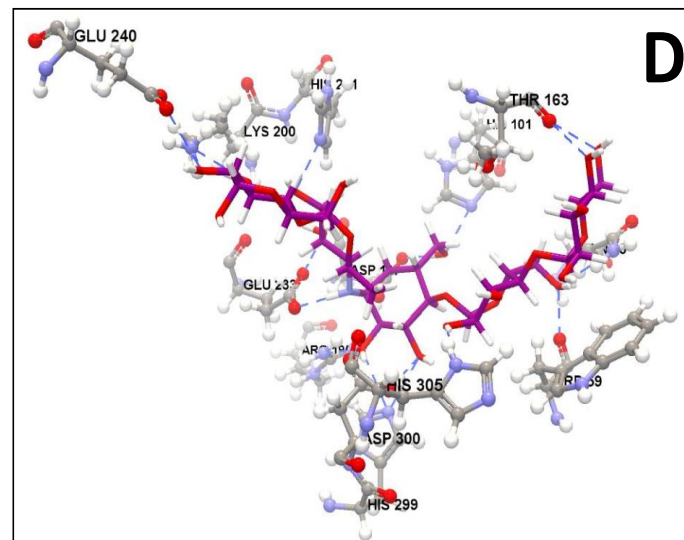
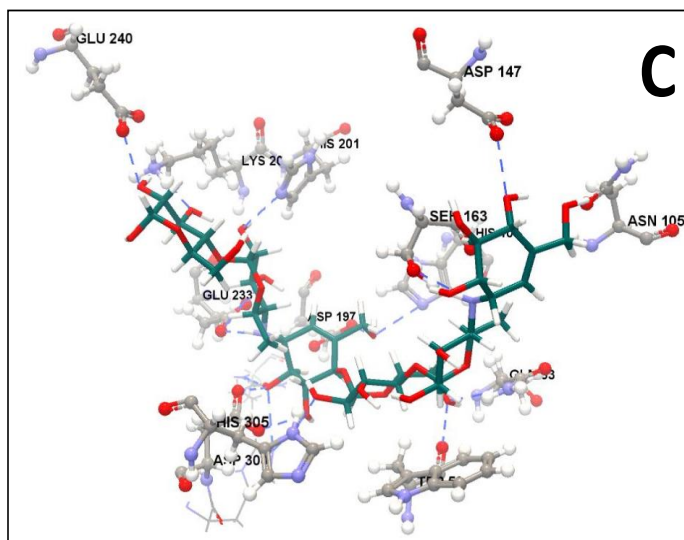
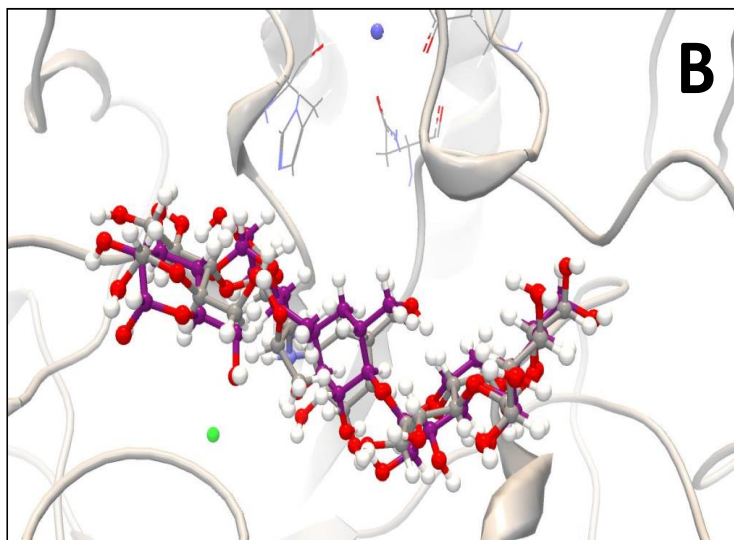
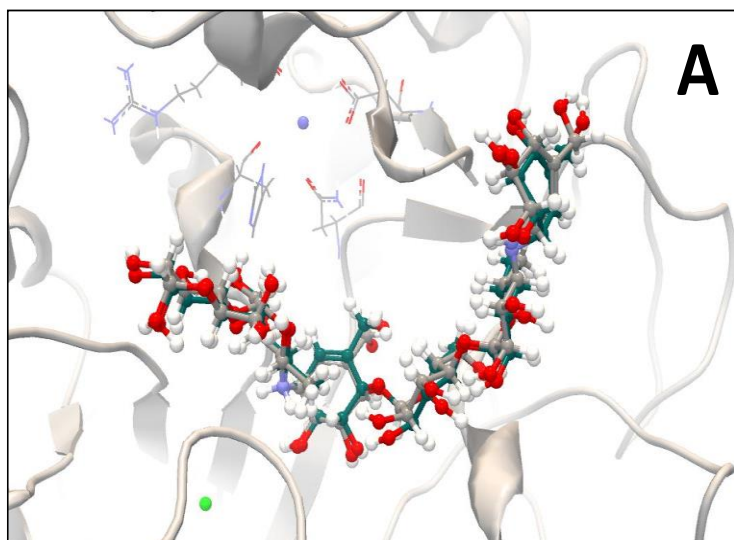


Figure 3.8 Validation of the docking parameters using the crystal structure analyses of human α -amylases. (A) human salivary (1MFV) and (B) human pancreatic α -amylase (1CPU) protein complexed with a modified acarbose ligand, showing the superimposition of native conformation (in grey) with the docked one (in turquoise and purple) in the active site. The RMSD of both docked structures were within the acceptance deviation with values of 1.36 and 1.11 Å for salivary and pancreatic α -amylase respectively. The small spheres in blue (calcium) and green (chlorine) represent cofactors. Figures on the right shows the H-bond formed between the co-crystal structures of (C) salivary and (D) pancreatic α -amylase in the binding pocket. H-bonds are indicated with blue dotted lines.

similar interactions (figure 3.8). Docking programs are considered reliable if they are able to return the re-docked pose below the RMSD value of 2 Å (Murumkar *et al.*, 2013). These results indicate that the CLC workbench was capable of reproducing the native crystallised pose of the ligands. After validation of the docking parameters, the atomic structure of each polyphenol molecule was obtained from PubChem database and the mechanical energy minimised before docking studies.

3.3.3 Statistical analysis.

Statistical analyses were performed by one-way analysis of variance using the Number Cruncher Statistical System version 6.0 software (NCSS, LLC). Significant differences were assessed with the Tukey–Kramer multiple comparison test ($p < 0.05$). The data are expressed as the mean \pm SEM of at least three independent experiments with three technical replicates each.

3.4 Results and discussion.

3.4.1 Effect of enzyme and substrate concentration on inhibition.

There are many *in vitro* examples of positive results on the inhibition of digestive enzymes by pure polyphenols and polyphenol-rich extracts. However the recognition and ranking of specific molecules and extracts have been difficult to establish since there are wide inconsistencies in both assay methods and experimental outcomes (Nyambe-Silavwe *et al.*, 2015).

The IC_{50} of an inhibitor is very dependent on the assay conditions including enzyme concentration, type of substrate, reaction time, temperature and pH. While temperature and pH have been standardised in most of the published studies on α -amylase inhibition to 37 °C and 6.9 respectively, there is no consensus regarding the other parameters. In this regard, the effect of acarbose, a well-known α -amylase inhibitor, was tested under two different assay conditions to determine the effect on the inhibition constant. Concentrations of 0.5 and 3.0 U/mL of enzyme were chosen to conduct this experiment where the former represents a suitable concentration of enzyme (linear range) and the latter a sub-optimal condition (where the substrate is rapidly mostly consumed during the mixing and/or starting procedure) under this experimental setting. This experiment was conducted on amylose and amylopectin as substrate (figure 3.9).

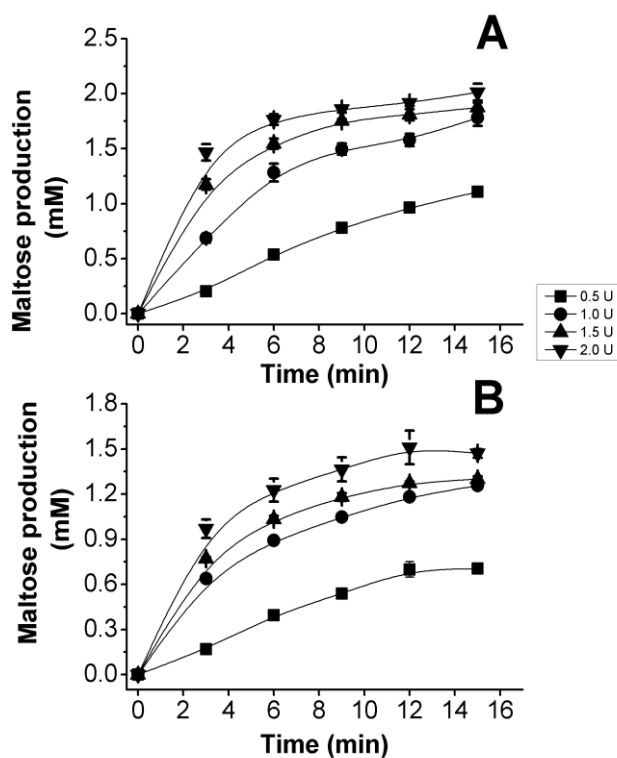


Figure 3.9 Time-dependence rate of hydrolysis by human α -amylase. The rate of hydrolysis at different incubation times was measured using two different substrates (A) amylose and (B) amylopectin. The hydrolysis of both substrates was measured by the amount of maltose-produced at four different concentrations of enzyme. Each data point represents the mean \pm SEM of three independent experiments conducted in triplicate ($n=3$). When not visible, the error bars are smaller than the data point.

As depicted in figure 3.10, the two different enzyme concentrations had an effect ($p<0.05$) on the apparent IC_{50} value exhibited by acarbose, and this was more pronounced when amylopectin was used as substrate. The IC_{50} value of acarbose under non-optimal conditions was ~ 7 to 8-fold higher than that obtained under optimal conditions for both substrates. Reducing the concentration of amylopectin from 1 mg/mL to 0.37 mg/mL to give the same ratio of K_m value versus concentration in comparison to amylose also caused an apparent increase in the inhibitory activity of acarbose, and the same pattern was observed for green tea (lower IC_{50}) (table 3.1). These results demonstrate that any enzymatic inhibition assay must be performed within the area of the initial linear progression of the reaction since the following non-linear phase will produce misleading results (Bisswanger, 2014). Furthermore, changes in the type of substrate and

concentration affect the apparent potency of an inhibitor due to the varying catalytic efficiencies (K_m) of the enzyme for the substrate, as exemplified with acarbose, EGCG and green tea extract.

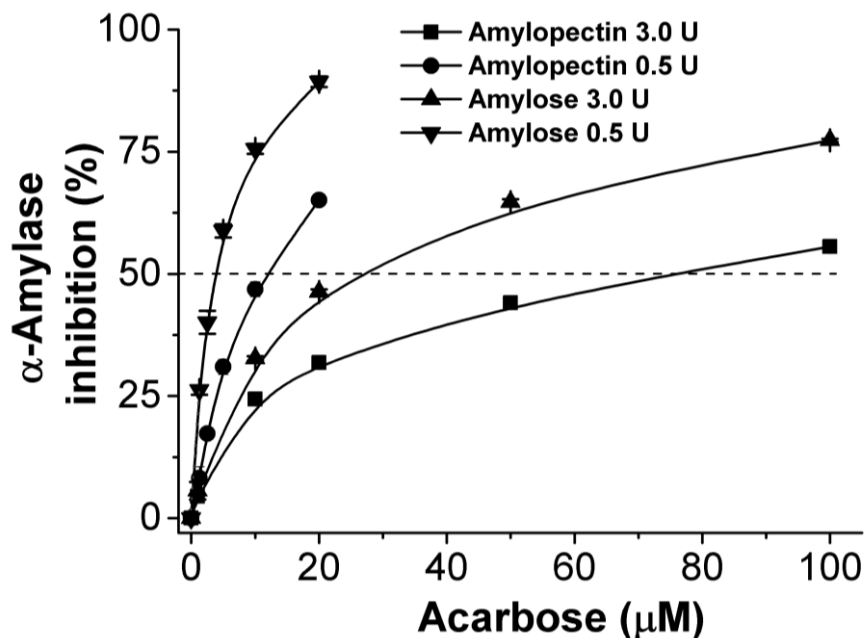


Figure 3.10 Inhibition of human α -amylase by acarbose. The experiment was conducted using amylose and amylopectin at a concentration of 1 mg/mL. Amylase activity inhibition varied according to the units utilized during the enzymic assay (units defined as described in section 1.3.2.5). Results are expressed as % compared to the reducing sugars produced in control incubations (no inhibitor; normalised to 100 %). Each data point represents the mean \pm SEM of three independent experiments conducted in triplicate ($n=3$). When not visible, the error bars are smaller than the data point.

Table 3.1 Experimental IC_{50} values of acarbose, selected polyphenols and green tea extract.

Inhibitor	Substrate		
	Amylose (1 mg/mL)	Amylopectin (1 mg/mL)	Amylopectin (0.37 mg/mL)
Acarbose	3.5 ± 0.3	10 ± 1	6.7 ± 0.8
EGCG	5 ± 0.6	72 ± 2	10 ± 4
Quercetin	20 ± 0.3	83 ± 7	22 ± 1
Luteolin	28 ± 0.3	75 ± 1	42 ± 9
Green tea	9 ± 0.6	60 ± 2	25 ± 1

The IC_{50} value of pure compounds is expressed in μM while for green tea is $\mu\text{g/mL}$.

3.4.2 Kinetic studies on amylose and amylopectin

The time-dependence hydrolysis assessed for different concentrations of enzyme was linear for up to 15 min for amylose and up to 12 min for amylopectin using 0.5 U of enzyme as depicted in figure 3.9. Therefore, 10 min and 0.5 U of enzyme were chosen as the optimum assay conditions to obtain the kinetic parameters, with 1 mg/mL substrate concentration. Using Lineweaver–Burk plots (figure 3.11), the values obtained are: amylose, $K_m = 12.9$ mg/mL and $V_{max} = 1.67$ mmol/min per mg of protein; amylopectin, $K_m = 4.8$ mg/mL and $V_{max} = 0.67$ mmol/min per mg of protein.

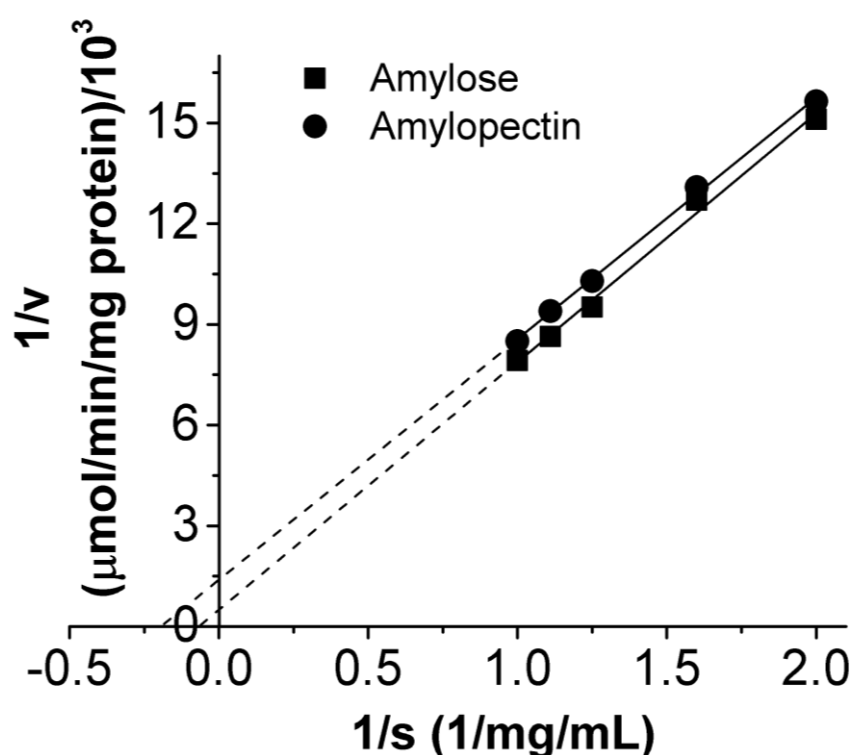


Figure 3.11 Lineweaver–Burk plot for action of human α -amylase. The kinetic parameters of α -amylase were calculated with using amylose and amylopectin as substrates with concentrations that ranged from 0-2 mg/mL (2 mg/mL was the maximum soluble concentration for both substrates). Each data point represents the mean \pm SEM of at least three independent experiments conducted in triplicate ($n = 3$). When not visible, the error bars are smaller than the data point.

The results obtained for the human α -amylase inhibition show the importance of determining the effect of enzyme concentration and the kinetic parameters K_m and V_{max} before measuring inhibition constants. These parameters are then used for assay

optimisation and are critical to the interpretation of correct and comparable IC₅₀ values (Acker and Auld, 2014). For instance, reducing the concentration of amylopectin from 1 mg/mL to 0.37 mg/mL to give the same ratio of K_m value versus concentration in comparison to amylose caused an apparent increase in the inhibitory activity of acarbose, and the same pattern was observed for green tea (lower IC₅₀).

3.4.3 Interference of polyphenols with the DNS reagent.

The use of the DNS reagent is one of the most widely reported methods to quantify the content of reducing sugars, and it has been largely applied to measure the inhibition of α -amylase from activity from different species by many compounds including polyphenols. For the optimisation of the assay, three different classes of polyphenols with different reduction potentials were tested to corroborate this fact (figure 3.12). Significant differences ($p < 0.05$) were observed between EGCG, gallic acid and phlorizin. EGCG caused the most interference with the DNS reagent solution in a dose-dependent manner, followed by gallic acid and phlorizin. The extent of the interference strongly correlates with the number of OH groups in the chemical structure of the polyphenol (figure 3.13), which also partially predicts their reduction potential (Rice-Evans *et al.*, 1996). This result implies that polyphenol molecules with high reduction potential (antioxidant activity) will interfere with the assay. Indeed, EGCG which contains the highest number of OH groups of the tested compounds, gave the greatest effect and ferulic acid, with the lowest number of OH groups did not react.

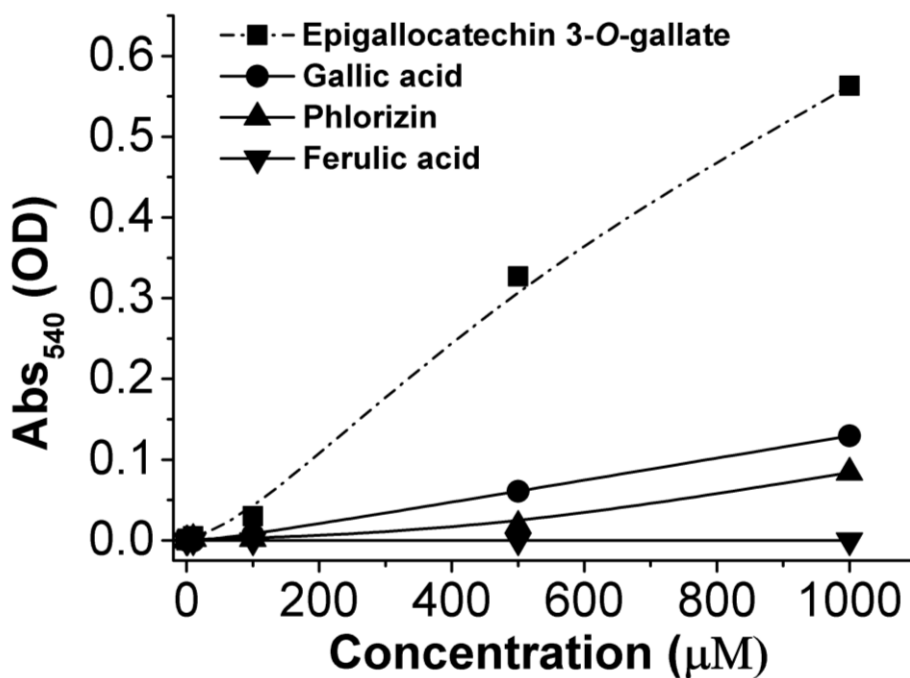


Figure 3.12 Reaction of selected polyphenols with the DNS reagent solution. For establishing the interference, different polyphenols with varying reduction potentials (judged by the number of OH groups in the chemical structure (Rice-Evans *et al.*, 1996)) were tested in the absence of any reducing sugar. Each data point represents the mean \pm SEM of at three independent experiments conducted in triplicate ($n = 3$). When not visible, the error bars are smaller than the data point.

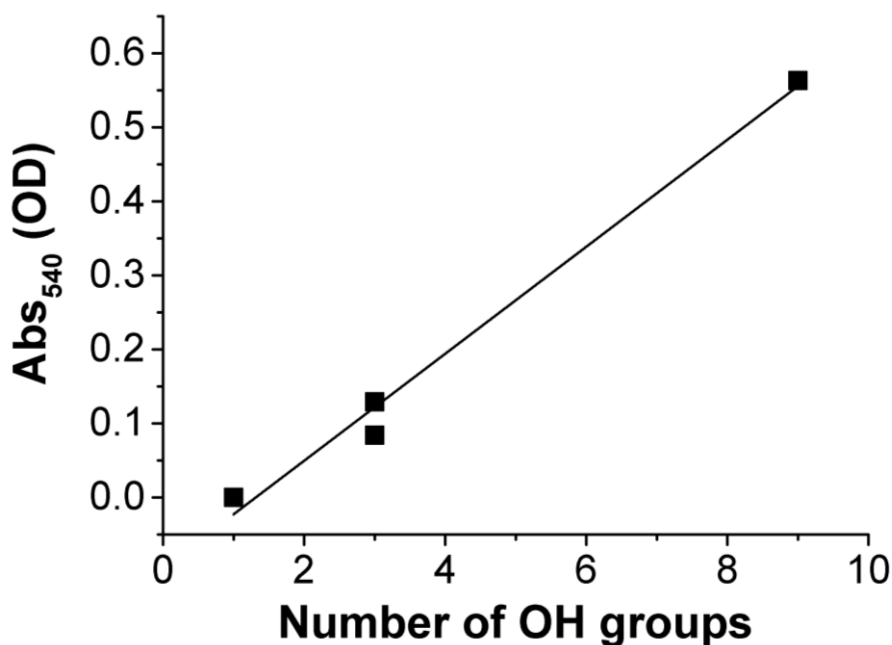


Figure 3.13 Relationship between the number of OH groups and colour development by DNS reagent solution. The Pearson correlation coefficient of linear regression between the num-

-ber of OH groups and absorbance at 100, 500 and 1000 μM of selected polyphenols gave a strong correlation ($r^2= 0.98$; $R^2= 0.9892$). Each data point represents the mean \pm SEM of three independent experiments conducted in triplicate ($n=3$). When not visible, the error bars are smaller than the data point.

While this relationship may not hold for all polyphenols, their removal should be considered in pre-tests involving the DNS reagent solution. This is something that has been ignored in many published studies and may account for the variation in the reported inhibition of α -amylase for EGCG (reviewed in Nyambe-Silavwe *et al.* 2015), since it interacts very strongly with the DNS reagent. Ignoring this contribution would decrease the apparent inhibition, i.e. raise IC_{50} and K_i values. This may explain the discrepancy between data in the literature, where, for example, EGCG was estimated to be far less potent compared with the result of this study with an IC_{50} value of 1.5 mM using the DNS reagent as detection method (Koh *et al.*, 2009).

3.4.4 Inhibitory effect of selected polyphenols on human α -amylase activity.

Assays under optimal conditions of enzyme concentration and incubation time were carried out to test the inhibitory activity of selected polyphenols using amylose and amylopectin as substrate and compared to those reported in the literature for those compounds (summarised in appendix A-C). Polyphenols were removed from the reaction solution using SPE, and the efficiency is shown in figure 3.4 for EGCG as an example. The same procedure was carried out with quercetin and luteolin with the same removal efficiency. All of the tested polyphenols showed dose-dependent inhibition of α -amylase activity on both substrates, and therefore the IC_{50} values could be calculated (figure 3.14).

The inhibitory activity of quercetin, EGCG and luteolin was higher when amylose was used as substrate. EGCG showed the highest inhibition with maximum inhibition at 20 μM and no significant difference ($p>0.05$) was observed above that concentration. For quercetin and luteolin, the highest inhibition was recorded at the highest concentration tested (100 μM) owing to limits in solubility, showing significant difference ($p<0.05$)

among the tested concentrations. No differences ($p>0.05$) were observed between the three tested polyphenols at a concentration of 100 μM using amylose as substrate.

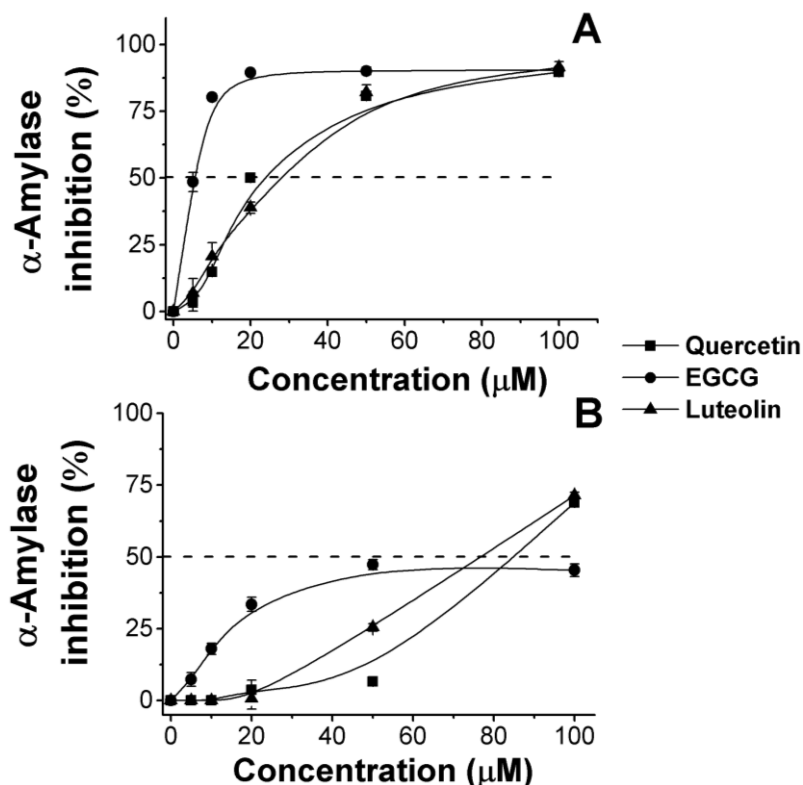


Figure 3.14 Inhibition of human α -amylase by polyphenols. Selected polyphenols were assessed for their inhibition of human salivary α -amylase using (A) amylose and (B) amylopectin as substrate at 1 mg/mL. The IC_{50} is indicated by the dotted line in (A) and (B). Different trends of inhibition are observed according to the substrate used which is due to the difference in the substrate/ K_m ratio (using the same ratio gave very similar inhibition values). Results are expressed as % compared to the reducing sugars produced in control incubations (no inhibitor; normalised to 100 %). Data points represent the mean \pm SEM of three independent experiments conducted in triplicate ($n=3$). When not visible, the error bars are smaller than the data point. For visualisation purposes, statistical significance are not indicated in the graph, instead they are described in the main text.

With amylopectin as substrate, IC_{50} values were higher. The differences in the inhibition behaviour of the polyphenols on α -amylase between amylose and amylopectin could be related to the differences in the affinity (K_m) for each type of substrate. This is another variable that partially explain the discrepancy in the literature regarding the inhibitory

potential of polyphenols. Even for acarbose which is an established α -amylase inhibitor, the reported differences in the IC_{50} values ranged from 0.9 to 23,100 μ M, and when results are compared with same-source enzymes, the range vary from 0.9– 6.9 and 1.24– 23,079 μ M for human and porcine, respectively (Nyambe-Silavwe *et al.*, 2015). Hence the need to calculate the K_i which, for competitive inhibition, represents the dissociation constant of the enzyme–inhibitor complex independently of substrate employed. There was no significant difference ($p>0.05$) between K_i values for amylose and amylopectin (figure 3.15) suggesting that the K_i should always be considered for measuring the inhibition efficacy of pure compounds in order to minimise some of the potential differences between laboratories.

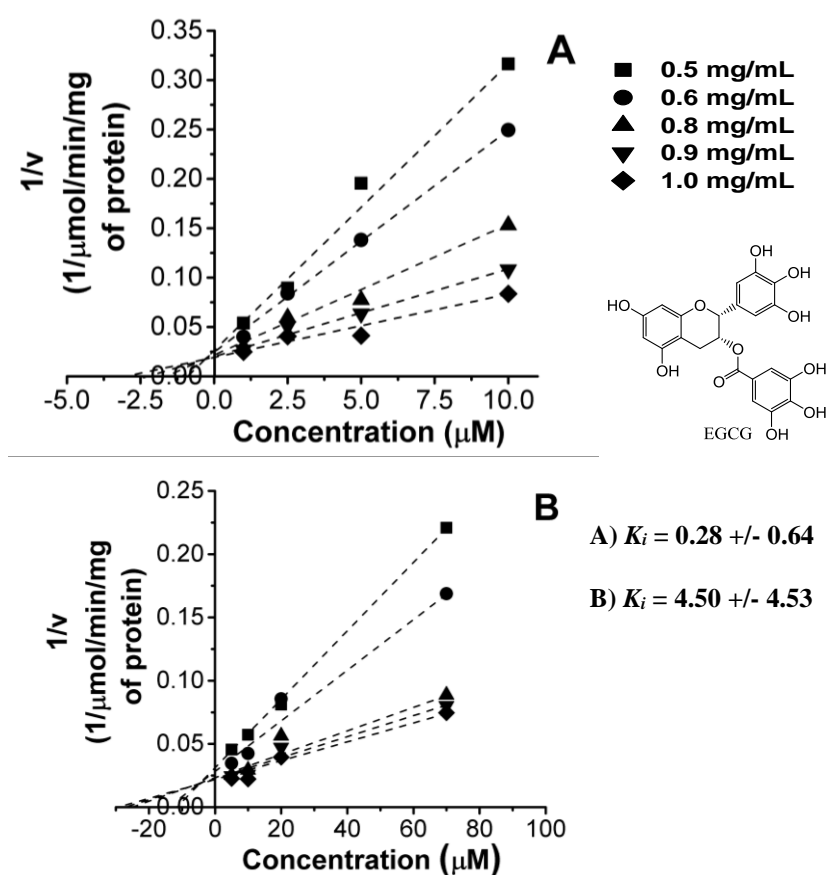


Figure 3.15 Dixon plot kinetic analysis of EGCG on human α -amylase. The kinetic analysis were conducted on both amylase substrates (A) amylose and (B) amylopectin at varying concentrations as indicated in the figure legend. The mean intercept value represents $-K_i$ which was calculated according to the equation described in section 1.3.2.5. The K_i are shown as inserts below the EGCG 2D chemical structure illustration. Data points represent the mean \pm SEM of th-

-ree independent experiments conducted in triplicate (n = 3). When not visible, the error bars are smaller than the data point.

Most of the research regarding the inhibition of α -amylase activity by polyphenols has been carried out using an enzyme from porcine pancreas, which possesses 14 % different amino acid composition to that of human origin (Brayer, Luo, & Withers, 1995), and data on the effect of polyphenols on human α -amylase are much more limited when compared to porcine (Lo Piparo *et al.*, 2008). In a previous study, acarbose, luteolin and quercetin competitively inhibited human salivary α -amylase with IC_{50} of ~1, 18 and 21 μ M respectively, similar to those obtained in this study when amylose was used as substrate (Lo Piparo *et al.*, 2008). Lo Piparo and co-workers utilised the same type of substrate (potato starch high in amylose to amylopectin ratio) as in this study which may partially explain the similarity of the results for the polyphenols and acarbose. These results indicate that when similar assay conditions are used, the experimental outcomes do not vary greatly.

3.4.5 Inhibitory effect of ChE and individual major polyphenols on human salivary α -amylase and α -glucosidase activity.

The inhibitory effect of ChE and individual polyphenols against human salivary α -amylase and rat α -glucosidase activity are shown in figure 3.16 and 3.17. The addition of ChE resulted in a dose-dependent inhibition of human salivary α -amylase activity by ~35, 45, 61 and 60 % at concentrations of 0.125, 0.25, 0.5 and 1 mg/mL respectively. The IC_{50} value for human α -amylase was 0.29 ± 0.052 mg/mL (figure 3.16A).

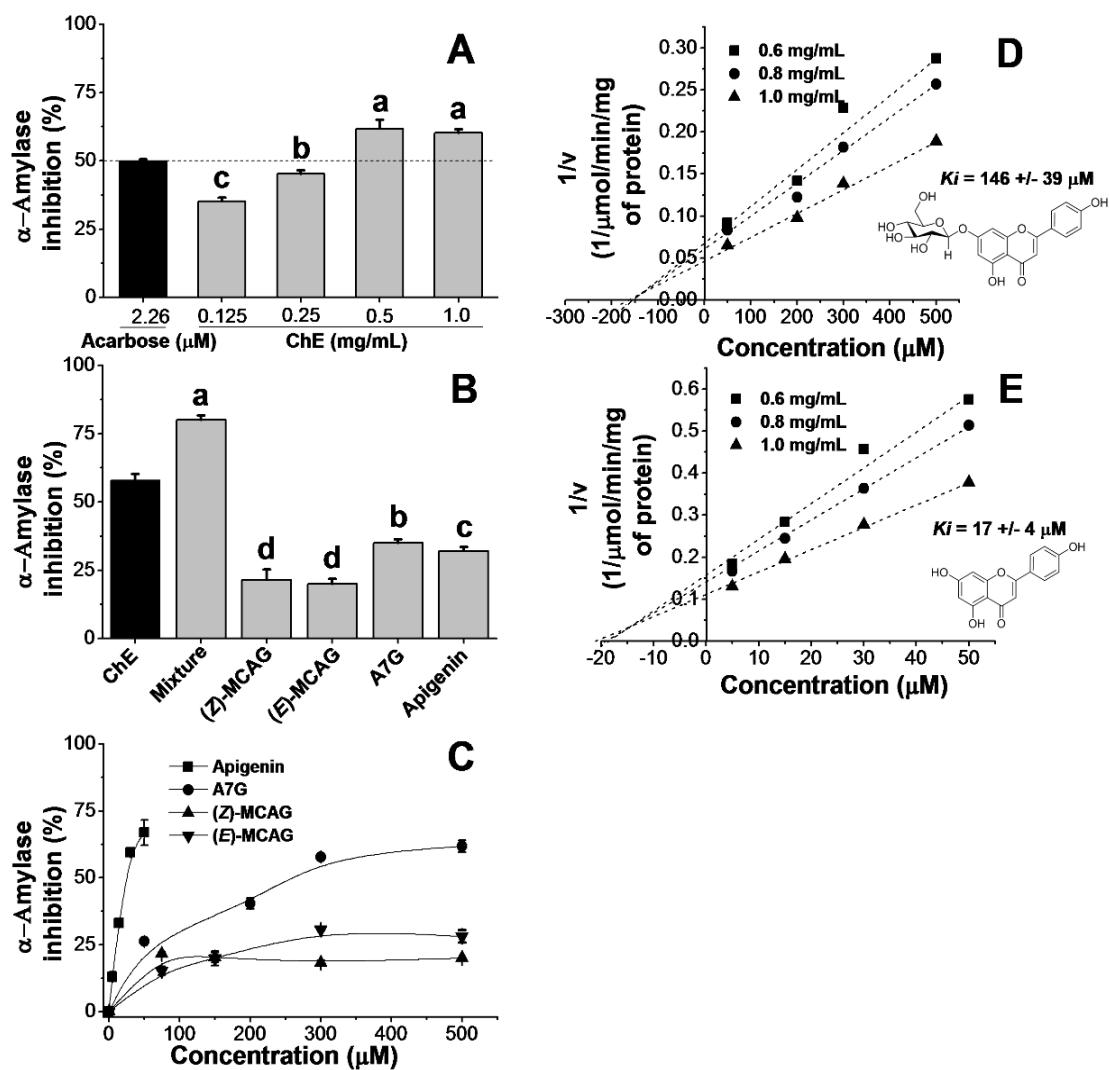


Figure 3.16 Inhibition of human α -amylase activity by ChE and polyphenols.(A) Dose-dependent inhibition of ChE. IC_{50} for acarbose was obtained and used as positive control. (B) Combined and individual inhibition effect of polyphenols at concentrations equivalent to those present in the ChE: (Z)-MCAG, 257 μM ; (E)-MCAG, 200 μM ; apigenin 7-*O*-glucoside (A7G), 148 μM ; apigenin, 12 μM . (C) Dose-dependent inhibition of individual polyphenols. (D, E) Dixon plot showing the kinetic analysis of apigenin and A7G against human salivary α -amylase. The intercept value represents $-K_i$. In panel A-C, results are expressed as % compared to the reducing sugars produced in control incubations (no inhibitor; normalised to 100 %). Data points represent the mean \pm SEM of three independent experiments conducted in triplicate ($n = 3$). When not visible, the error bars are smaller than the data point. Different letters denotes significant difference among treatments.

For the individual polyphenols, apigenin and its precursor apigenin 7-*O*-glucoside exhibited the most potent inhibition against human salivary α -amylase with IC_{50} of ~ 22.8 and $248 \mu\text{M}$ respectively (figure 3.16C). However, when the four polyphenols were combined at concentrations equivalent to those quantified in the extract, apigenin 7-*O*-glucoside showed the highest contribution ($p < 0.05$) (figure 3.16B). Moreover, the combination of the four polyphenols resulted in an increase on the inhibitory activity by $\sim 20\%$ as compared to the whole ChE. This result highlights that even when subtle inhibition is observed by a particular compound, any additive/synergistic effect can potentiate the overall response.

In order to gain a better understanding of the inhibitory effects of apigenin and apigenin 7-*O*-glucoside on human salivary α -amylase, a kinetic assessment was performed. K_i values were calculated at ~ 17 and $146 \mu\text{M}$ for apigenin and apigenin 7-*O*-glucoside respectively from the intercept of a Dixon plot (figure 3.17D and E). The potential inhibition of 2-(*E*)-MCA on carbohydrate-digestive enzymes was not assessed since this chemical form is very unlikely to be present in the small intestine given that *E*-MCA was resistant to digestive hydrolytic enzymes (figure 3.17).

The final step of starch digestion is catalysed by α -glucosidases (maltase-glucoamylase and sucrase-isomaltase). Their combined catalytic activities hydrolyse linear and branched malto-oligosaccharides after the action of pancreatic α -amylase (Sim *et al.*, 2010); in addition, sucrase-isomaltase hydrolyses sucrose, producing glucose and fructose. Their inhibition can provide complementary action for blunting the rise of these readily absorbable sugars whose intake increase the prospect of type 2 diabetes onset (Te Morenga *et al.*, 2013; Imamura *et al.*, 2015). The results indicate only a modest inhibition on maltase-glucoamylase activity using maltose as substrate while no inhibitory effect was observed on sucrase and isomaltase (figure 3.18A). Even at a concentration of 2 mg/mL , rat maltase was inhibited only by $\sim 33\%$. As expected, maltase-glucoamylase was weakly inhibited by the individual polyphenols (figure 3.17B and C). A dose response inhibition was observed and apigenin 7-*O*-glucoside was the principal contributor ($p < 0.05$), although apigenin seems to have a more potent inhibitory effect, its poor solubility did not allow testing at higher concentrations (figure 3.17C). Neither the individual polyphenols nor their combination reached 50% inhibition.

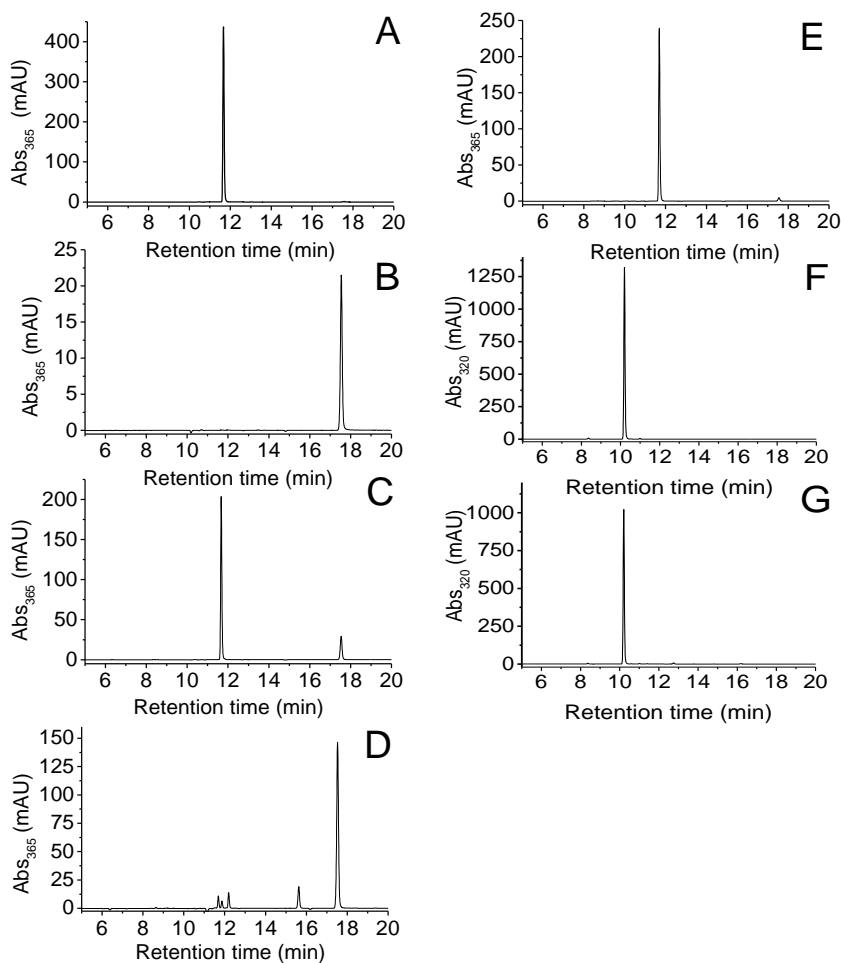


Figure 3.17 Enzymatic hydrolysis of kaempferol 3-*O*-glucoside (positive control) and (*E*)-MCAG. Kaempferol 3-*O*-glucoside standard (300 μM). (B) Kaempferol standard (100 μM) (C) Kaempferol 3-*O*-glucoside hydrolysed with hesperidinase. (D) Kaempferol 3-*O*-glucoside hydrolysed with acetone rat intestinal extract. (E) Kaempferol 3-*O*-glucoside hydrolysed with pancreatin. (F) (*E*)-MCAG (500 μM) hydrolysed with hesperidinase. (G) (*E*)-MCAG (500 μM) hydrolysed with acetone rat intestinal extract. Three independent experiments in triplicate were conducted (n=3). Representative chromatograms of the hydrolysis of each compound were randomly selected and presented in this figure.

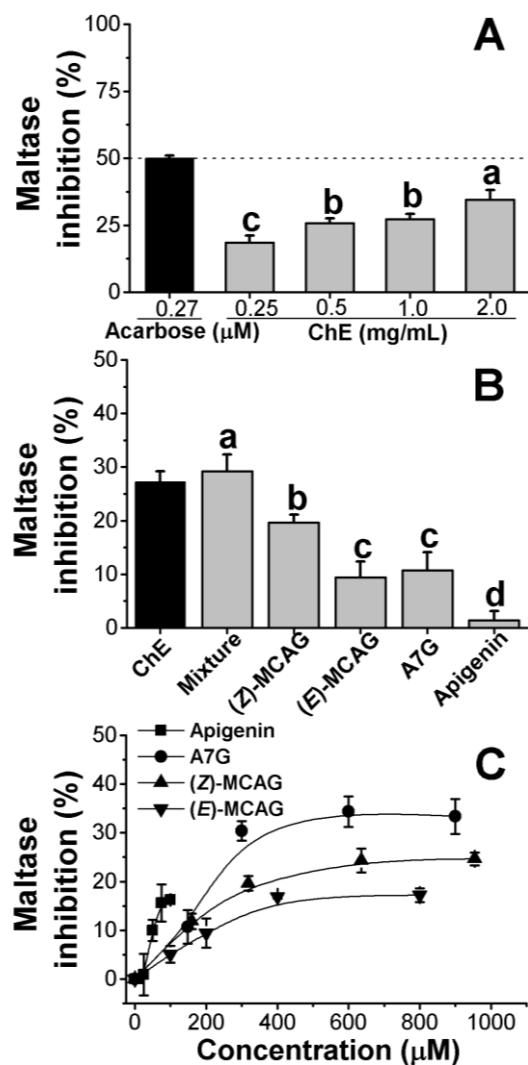


Figure 3.18 Inhibition of rat maltase activity by ChE and polyphenols.(A) Dose-dependent inhibition of ChE. IC_{50} for acarbose was obtained and used as positive control. (B) Combined and individual inhibition effect of polyphenols at concentrations equivalent to those present in the ChE: (Z)-MCAG, 257 μ M; (E)-MCAG, 200 μ M; apigenin 7-O-glucoside (A7G), 148 μ M; apigenin, 12 μ M. (C) Dose-dependent inhibition of individual polyphenols. Results are expressed as % compared to the reducing sugars produced in control incubations (no inhibitor; normalised to 100 %). Data points represent the mean \pm SEM of three independent experiments conducted in triplicate (n = 3). When not visible, the error bars are smaller than the data point.

There is limited studies designed at identifying potential inhibitors of carbohydrate digestion in chamomile (Kato *et al.*, 2008). In contrast to the present study, Kato and co-workers reported a more potent inhibition on α -glucosidase (IC_{50} = 2.6 mg/mL and sucrase = 0.9 mg/mL) than α -amylase activity (IC_{50} = 5.2 mg/mL) by chamomile.

However as reported here, apigenin showed the strongest effect although the inhibition was ~17 times lower (42 % at 400 μM). As for α -glucosidase, the authors suggest that this effect was driven by the presence of esculetin (maltase $\text{IC}_{50} = 534 \mu\text{M}$; sucrase $\text{IC}_{50} = 72 \mu\text{M}$) and quercetin aglycone (maltase $\text{IC}_{50} = 216 \mu\text{M}$; sucrase $\text{IC}_{50} = 71 \mu\text{M}$). However, other data on chamomile composition indicate that these compounds, if present at all, are unlikely to be effective since they are several orders of magnitude below the concentrations necessary for inhibition (Raal *et al.*, 2012; Guimarães *et al.*, 2013; Guimarães *et al.*, 2013).

There are several reasons that can explain the conflicting results which are related to the assay parameters as well as the ChE itself. First, the authors did not report the assay conditions to perform the inhibition with the exception of the pH. Consequently, the assay cannot be replicated and therefore it is difficult to ascertain whether the assays were conducted under optimal conditions. Second, the inhibition assays were conducted using different sources of enzyme. While human α -amylase and a commercial acetone rat intestinal powder for α -glucosidase was employed in the present study, Kato and co-workers used pancreatic porcine α -amylase and brush border membranes prepared from rat small intestine. Since kinetic parameters were not reported, it is impossible to have an idea of the specific activity and so the performance of the enzyme preparations. Third, as pointed out in chapter 2, the composition and content of the plant material must be reported. Kato and co-workers did not give any information on the phytochemical profile and content of the ChE tested and so, it is possible that the opposite results are due to variations in the chemical constituents. A caveat of failing to report compositional data is the identification of compounds that lack any physiological relevance (e.g. negligible or low levels as compared with the inhibition constants obtained) in plant extracts.

3.4.6 Modelling studies.

Molecular docking studies were further carried out to get a molecular insight of the interactions that occur between the tested ligands, human and pancreatic α -amylase in order to support the experimental findings. In general, all the docking scores were in line with the experimental results where the most potent inhibitors showed the lowest binding energy (table 3.2). A remarkable exception was apigenin 7-*O*-glucoside that showed a

very similar score to acarbose for both enzymes but its experimental inhibition value was ~71.5-fold times lower.

Table 3.2 Docking scores of polyphenols on human salivary and pancreatic α -amylase.

Molecule	Hydrogen bond score	Metal interaction score	Steric interaction score	Ligand conformation penalty	Total score
<i>IMFV</i>					
A7G	-14	0.00	-59.74	2.1	-71.46
Acarbose	-18.35	0.00	-63.03	10.34	-71.04
EGCG	-16.37	0.00	-57.67	5.6	-68.44
Luteolin	-9.7	0.00	-55.44	1.34	-63.79
Quercetin	-11.91	0.00	-51.36	1.41	-61.87
Apigenin	-7.86	0.00	-53.12	1.3	-59.68
(<i>E</i>)-MCAG	-24.57	0.00	-35.61	2.44	-57.75
(<i>Z</i>)-MCAG	-16.63	0.00	-40.55	3.92	-53.25
<i>ICPU</i>					
Acarbose	20.03	0.00	-56.28	7.35	-68.97
A7G	-14.49	0.00	-55.2	3.66	-66.02
EGCG	-13.6	0.00	-50.84	3.98	-60.46
Luteolin	-11.32	0.00	-48.15	1.47	-58
Quercetin	-13.31	0.00	-45.6	1.32	-57.6
Apigenin	-8.19	0.00	-48.27	1.6	-54.86
(<i>E</i>)-MCAG	-15.91	0.00	-40.33	0.94	-55.31
(<i>Z</i>)-MCAG	-9.38	0.00	-45.56	6.04	-48.9

The contribution from hydrogen bond interactions is presented as ‘hydrogen bond score’. The contribution from lone-pair-metal ion interactions is listed as ‘metal interaction score’. The non-polar interactions, non-polar–polar contacts, and the repulsive contacts are combined in the ‘steric interaction score’. The software punishes internal heavy atom clashes in the ligand and strain resulting from non-favourable bond rotations and is listed as ‘Ligand conformation penalty’. A7G: apigenin 7-*O*-glucoside.

A drawback of the scoring function is that it takes into account all the interactions between the ligand and the receptor, and so a large ligand can get a better score than a small one. Therefore docking score does not necessarily reflect the potency of a particular inhibitor as is the case of apigenin 7-*O*-glucoside. This is something to bear in mind specially when conducting a virtual docking screening to identify potential inhibitors for a particular receptor, where a combination of docking score and most importantly, the binding interactions within the catalytic pocket (if competitive inhibitors are assessed) has

to be considered. Luteolin showed slightly better score than quercetin and apigenin, however among them, it presented the higher IC₅₀ (lower inhibition activity). Nonetheless, this cannot be considered a bias from the software since both the docking scores and the experimental IC₅₀ values were very close to each other (quercetin= 20 μM; apigenin= 23; luteolin= 28 μM). Moreover, although the ligands were not experimentally tested on human pancreatic α-amylase, the binding energy scores and the comparison of the binding cavity and orientation of the catalytic residues (Asp¹⁹⁷, Glu²³³ and Asp³⁰⁰) suggest that the enzyme can be inhibited to the same extent by the polyphenols (table 3.2, figure 3.19).

The docking studies revealed that strong inhibitors of salivary α-amylase activity (arbitrarily defined as molecules with IC₅₀ <100 μM) bind in the active site next to, and interacting with, the catalytic residues Asp¹⁹⁷ (nucleophile), Glu²³³ (acid-base) and Asp³⁰⁰ (acid-base) through H-bonds (figure 3.20). These interactions occur between OH groups present in position R3' and R4' of the B ring in the flavonoid skeleton. The number of H-bond formed varied among polyphenols and they seem to predict the potency of the inhibitor according to the *in vitro* results. For instance, the R3' and R4'-OH groups of quercetin form H-bonds with Asp¹⁹⁷ residue (figure 3.20B) while luteolin and apigenin form only one H-bond through the OH group of R4' and R3' positions, respectively (figure 3.20D, E and I). A similar conclusion can be drawn for the most potent inhibitor identified in this study 'EGCG' where the R3'-OH and R4'-OH group form an H-bond with Asp¹⁹⁷ and Asp³⁰⁰ respectively.

From the selected conformations, the binding pose of EGCG, quercetin, apigenin and luteolin to the catalytic pocket of human salivary α-amylase is characterised by intramolecular hydrophobic π-π stacking interactions between the A, B and C-ring of the flavonoid core and the aromatic ring of Tyr⁶² and the indole ring of Trp⁵⁹ (a 3D illustration of the π-π stacking interactions is shown in figure 3.20B). These hydrophobic interactions are thought to be critical for the inhibition of salivary (Lo Piparo *et al.*, 2008) and human pancreatic α-amylase (Williams *et al.*, 2015) by polyphenols since they provide optimal alignment of the OH groups for prime hydrogen bonding with the catalytic residues (Williams *et al.*, 2015). A final feature of potent inhibitors is that they-

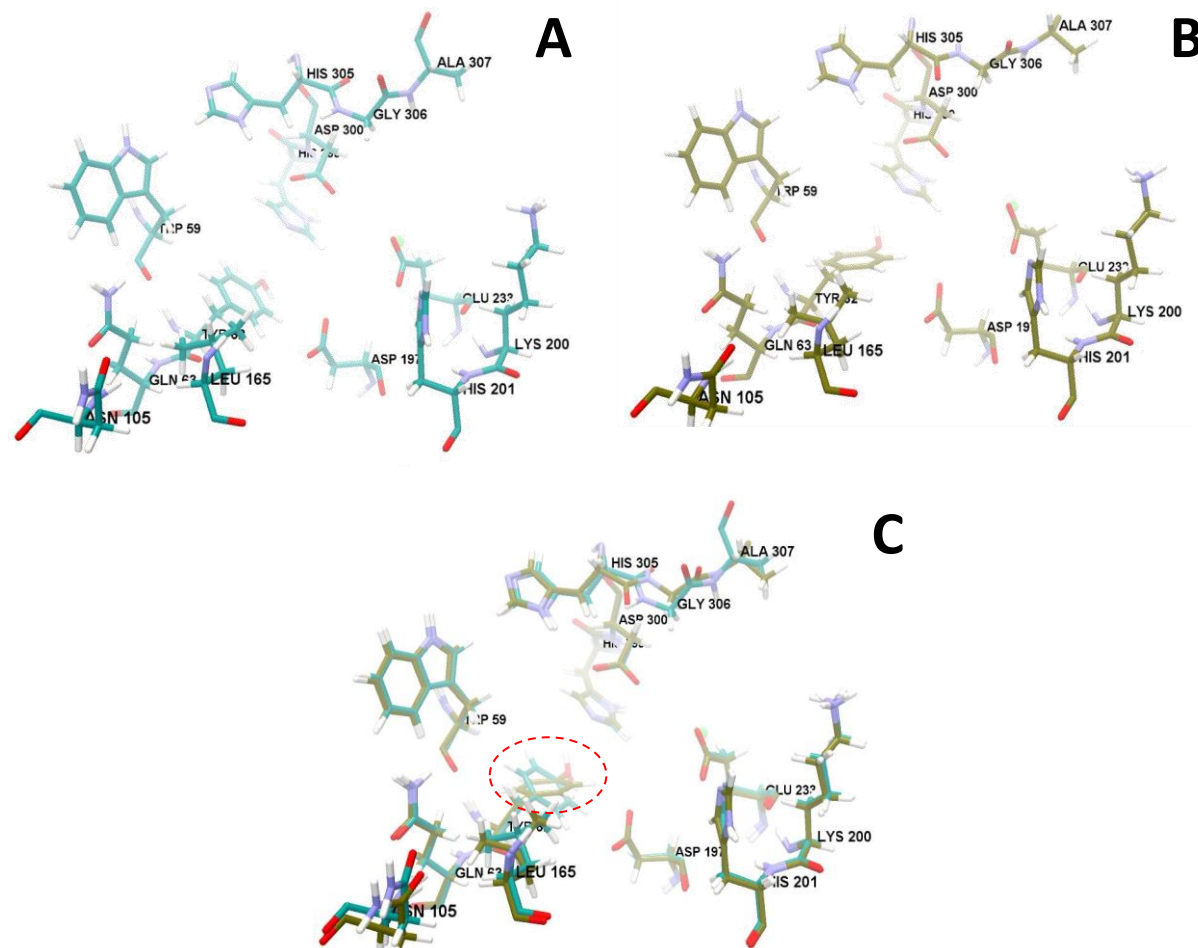


Figure 3.19 Structural comparison between the residues forming chemical interactions with the co-crystal structures of human salivary (1MFV) and human pancreatic α -amylase (1CPU). (A) Structural conformation of the binding pocket of salivary α -amylase. (B) Structural conformation of the binding pocket of pancreatic α -amylase. (C) Structural alignment of the binding pocket salivary (in turquoise) and pancreatic α -amylase (in dark green). As can be observed from the individual figures and from the superimposition, the only residue that has a different pose is Tyr⁶² (spherical red dotted line in panel C).

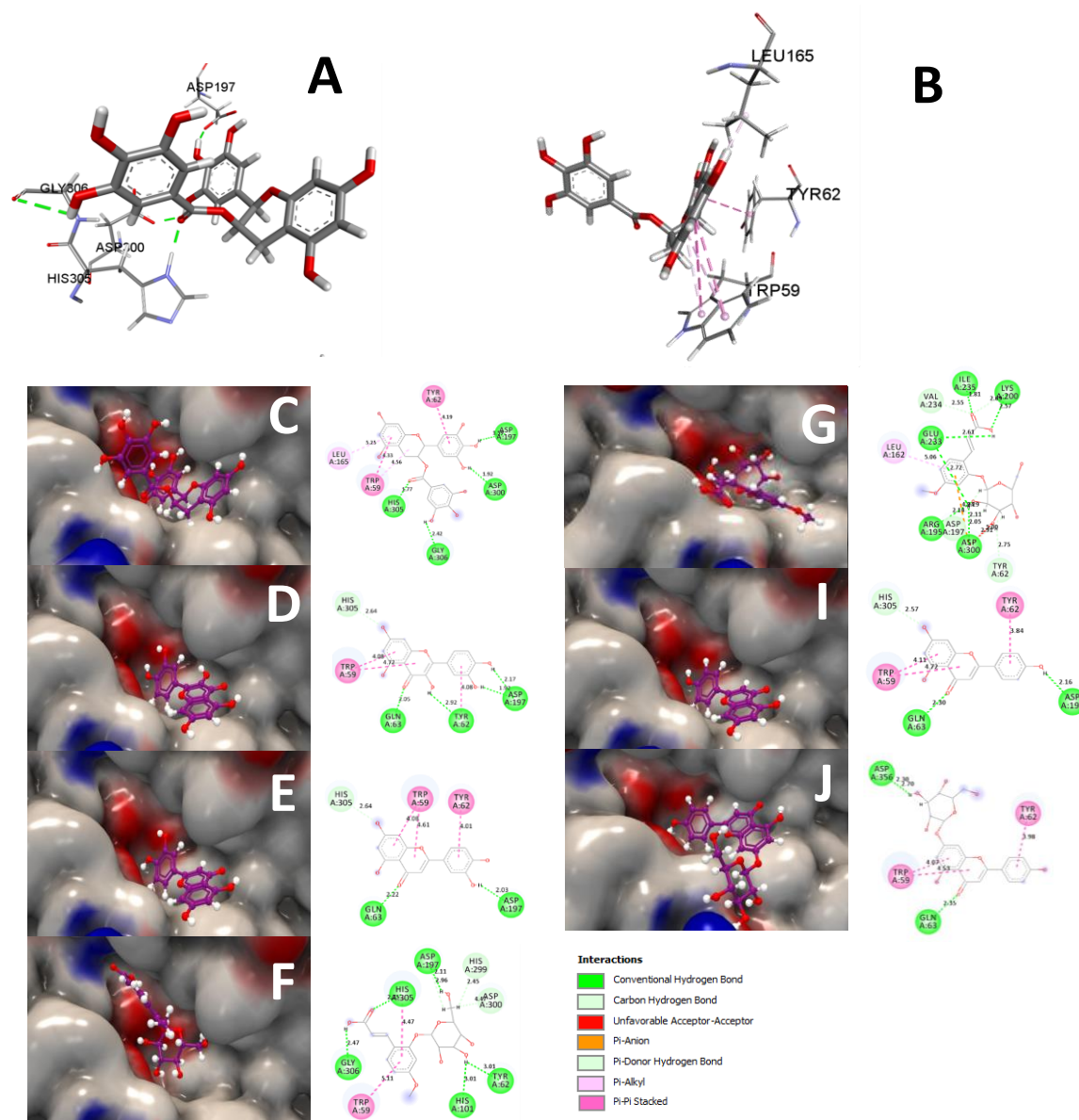


Figure 3.20 The binding pose and chemical interactions of polyphenols with human salivary α -amylase.

(A) and (B) Close-up 3D view illustrating the H-bond and π - π stacking interactions of EGCG adjacent to α -amylase active site residues respectively. (C-J) Charge surface representation (in blue and red) of α -amylase binding cavity with respective ligands displayed in stick format (in purple); (C) EGCG, (D) quercetin, (E) luteolin, (F) (Z)-MCAG, (G), (E)-MCAG, (I) apigenin and (J), apigenin 7-O-glucoside. Next to each 3D complex are schematic representations of the 2D interactions between each ligand and α -amylase amino acid residue including the length of each interaction (in Å) as displayed by Discovery Studio software.

occupy the same binding subsites in the catalytic pocket on salivary α -amylase (figure 3.21B and C). In these binding conformations, the flavonoid skeleton of EGCG, quercetin, apigenin and luteolin is directed towards subsites -1 and -2 according to the established nomenclature for acarbose substructures oriented in the active site spanning subsites -3 to +2 (Brayer *et al.*, 2000) (figure 3.21A).

EGCG shows a slightly different pose which favours a better orientation towards subsite -2. Subsites -1, -2 and -3 have been reported to be the centre of the catalytic reaction in human pancreatic α -amylase (Brayer *et al.*, 2000). This, along with the number of H-bonds formed with catalytic residues and the strength of the interaction (indicated by the length of the H-bonds) would explain the stronger effect observed in the *in vitro* experiments of EGCG to reduce human salivary α -amylase activity. Additional H-bonds were observed between the strong inhibitors with other residues that are not directly involved in the catalytic activity including Gln⁶³, His³⁰⁵ and Gly³⁰⁶ (figure 37).

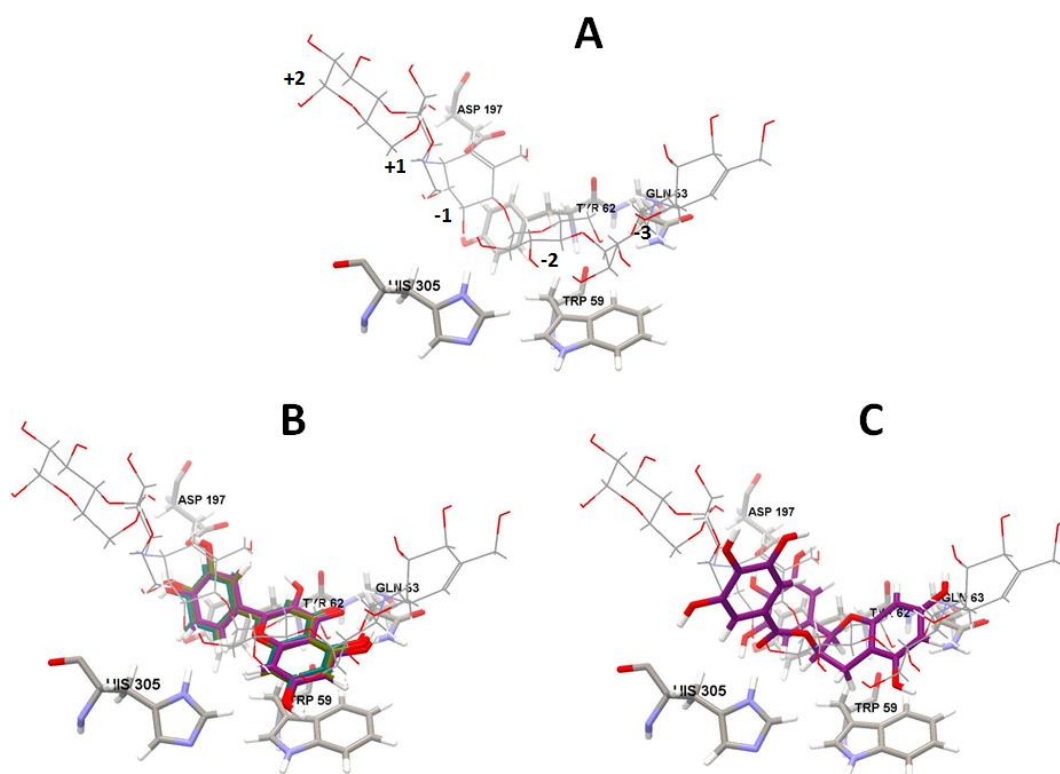


Figure 3.21 Subsite binding pose of strong polyphenol inhibitors of human salivary α amylase. (A) Illustration of the co-crystal modified acarbose molecule showing the binding subsites according to the reported nomenclature (Brayer *et al.*, 2000; Lo Piparo *et al.*, 2008; Al-Asri *et al.*, 2016). Binding subsites are denoted with negative and positive numbers. (B) Superim-

-position of the docking pose of quercetin (in purple), apigenin (in turquoise), luteolin (in dark green) and the docking pose of quercetin (in purple), apigenin (in turquoise), luteolin (in dark green) and (C) EGCG with the modified acarbose structure in amylase binding cavity. Surrounding residues are showed and labelled. Variable sizes of amino acid labelling correspond to their depth in the binding pocket.

Analysis of the docking conformation of polyphenols that presented modest inhibitory activity ((*Z*)-(*E*)-MCAG and apigenin 7-*O*-glucoside)) showed that they occupy the cavity in a completely different pose (figure 3.20F, G and J). Notably, (*Z*) and (*E*)-MCAG are able to form H-bonds with the catalytic residues. However, unlike apigenin, the H-bonds are formed mainly with the OH groups present in the glucose moiety and as might be expected, are weaker (as judged by the distance of H-bonds formed). Strong H-bonds would stabilise the substrate, keeping it in place and interfering with the catalytic activity.

In (*Z*)-MCAG, an H-bond is formed between the 6-OH group of the glucose unit with Asp¹⁹⁷ while (*E*)-MCAG present a more complex interaction. In (*E*)-MCAG, 2 covalent bonds are formed between the carbon at position 2 and Asp¹⁹⁷ (indicated as carbon-hydrogen bond in figure 3.20). Additionally, H-bond interactions occur between the 6-OH group and Glu²³³ and Asp³⁰⁰ and an additional H-bond is formed between the Glu²³³ and the OH-present in the carboxylic group of the phenolic skeleton. These additional interactions would explain the slightly higher inhibition observed by the (*E*)-isomer *in vitro*, and perhaps they account for its stability in the binding pocket due to the lack of π - π stacking interactions.

Apigenin 7-*O*-glucoside is able to form π - π stacking interactions with Trp⁵⁹ and Tyr⁶² however, it does not form the H-bond with the catalytic residue Asp¹⁹⁷ resulting in a ~ 8-12-fold decrease in its inhibitory activity as compared with luteolin, apigenin and quercetin and ~45-fold with EGCG. The side chain residue of Asp¹⁹⁷ is believed to act as nucleophile during the catalytic reaction of α -amylase and its substitution dramatically decreased (10⁶-fold) its catalytic activity (Brayer *et al.*, 2000) which explains its lower potency as observed *in vitro*. Thus, H-bond between OH groups of B ring and catalytic residues and π - π staking interactions appear to be requirements for an optimal inhibition

of human α -amylase by polyphenols acting via a competitive mechanism. Indeed, in a previous study, Lo Piparo *et al.* (2008) observed similar features; polyphenols showing $IC_{50} < 100 \mu M$ were anchored in the active through π - π interactions with Trp⁵⁹ and formed H-bonds with residues Asp¹⁹⁷ and Glu²³³ through OH groups in A and B ring. This mechanism is further supported by X-ray structural analyses of the polyphenols myricetin and montbretin A with human pancreatic α -amylase (Williams *et al.* 2012; Williams *et al.*, 2015).

Taken together, the combination of *in vitro* and molecular docking studies has revealed that apigenin and apigenin 7-*O*-glucoside are primarily responsible for the inhibition of ChE. This arises from (a) their ability to form H-bonds between the R3' and R4'-OH groups of B ring and the catalytic residues, mainly Asp¹⁹⁷, (b) the formation π - π stacking interactions with Trp⁵⁹ and Tyr⁶² and (c) their stacking at the binding subsides -1 and -2.

3.5 Conclusion.

Chamomile provide an interesting mixture of polyphenols and recent scientific evidence support its effectiveness against hyperglycaemia and other metabolic abnormalities observed in type 2 diabetes. The results of this study shows that ChE as botanical extract that combines (*Z*)-(*E*)-MCAG, apigenin and apigenin 7-*O*-glucoside can potentially be used to modulate postprandial blood glucose levels by restricting starch degradation in the GI tract. To further explore the potential of ChE and polyphenols to blunt sugar absorption at the GI site, the inhibition on sugar transport was next assessed (chapter 4).

Chapter 4 Chamomile, apigenin and apigenin 7-*O*-glucoside attenuate monosaccharide transport across Caco-2/TC7 cell monolayers: a mechanistic study for the identification of the target transporter.

4.1 Abstract.

Persistent high postprandial glycaemia has been associated with the development of insulin resistance and type 2 diabetes. A strategy to reduce postprandial sugar levels is to partially reduce glucose and fructose transport from the gut lumen to the blood stream. This chapter focuses on characterising the effect of ChE and its major individual polyphenols on monosaccharide transport using the well characterised differentiated Caco-2/TC7 cell model. Apigenin 7-*O*-glucoside was a very effective inhibitor of D-[U-¹⁴C]-glucose (IC₅₀ = 175 μM) and D-[U-¹⁴C]-sucrose (IC₅₀ = 194 μM) apical to basolateral transport while moderate inhibition was observed for D-[U-¹⁴C]-fructose (IC₂₀ at 200 μM). A stronger inhibition was observed under Na⁺-depleted conditions suggesting an interaction mainly with the GLUT2 transporter. Both (*Z*) and (*E*)-MCAG did not inhibit D-[U-¹⁴C]-glucose, D-[U-¹⁴C]-sucrose or D-[U-¹⁴C]-fructose transport. Mechanistic studies using specific inhibitors binding at the exofacial and endofacial site of GLUT2 transporter indicate interaction of apigenin and apigenin 7-*O*-glucoside at the exofacial-binding site. Moreover, the effect appears to be solely acute since chronic co-incubation of chamomile, apigenin and apigenin 7-*O*-glucoside did not affect the rate of D-[U-¹⁴C]-glucose across the cell monolayers. These findings highlight the effect of chamomile containing apigenin and apigenin 7-*O*-glucoside on attenuation sugar transport and its potential application in dietary and/or complementary strategies to manage postprandial hyperglycaemia.

4.2 Introduction.

The gastrointestinal tract represents the first site of interaction between energy-dense nutrients such as glucose and fructose and the host. The small intestine absorbs ~ 90 % of these nutrients (Chan and Leung, 2015) initiating crucial negative feedback systems to control whole body energy homeostasis through the action of other metabolic tissues such as the liver, adipose tissue and skeletal muscle (discussed in chapter 1). Therefore attenuation of postprandial sugar levels at the small intestinal site has been seen as a prominent strategy to prevent and manage metabolic dysregulations. In addition to the reduction or delay of glucose release from starch by intestinal enzymes, the inhibition of transporters responsible for absorption of dietary monosaccharides (figure 4.1) is another promising strategy to blunt postprandial hyperglycaemia and the two mechanisms together could provide an effective way to manage postprandial sugar levels.

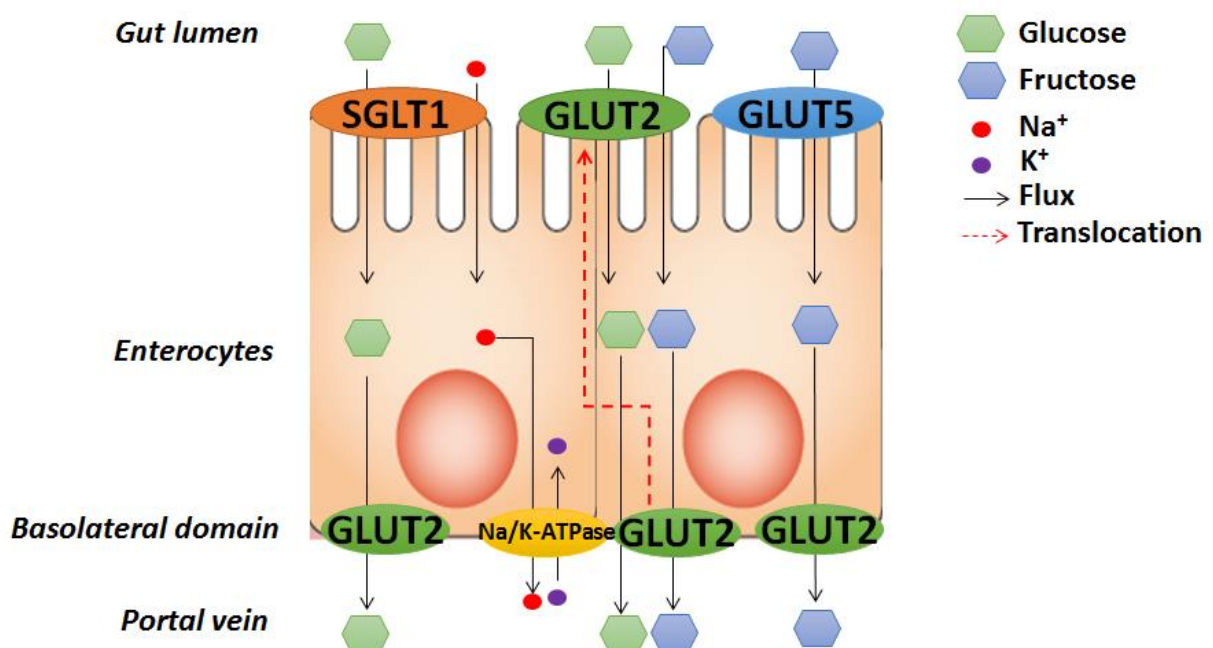


Figure 4.1 Schematic representation of glucose and fructose absorption in the small intestine. Glucose uptake from the intestinal lumen is mediated through SGLT1 expressed in the apical membrane of enterocytes which utilises the energy derived from moving Na⁺ down its concentration gradient. The Na⁺ that enters the cell is then transported out into blood *via* de portal vein by the Na/K-pump in the basolateral domain, so maintaining the driving force for glucose transport (Wright *et al.*, 2007, Cura and Carruthers, 2012). The resulting accumulation of cytoplas-

-mic glucose allows for the facilitative transport of glucose down a concentration gradient across the basolateral domain *via* GLUT2 (Wright *et al.*, 2007). Fructose is taken up from the intestinal lumen by the apically-located transporter GLUT5 (Cura and Carruthers, 2012, Burant *et al.*, 1992). Since GLUT2 also transport fructose, its localisation at the basolateral domain provides the exit pathway for fructose into the bloodstream (Cheeseman, 1993). The discovery of apical GLUT2 in diabetic rats (Corpe *et al.*, 1996) along with the observation that GLUT2 can translocate from the basolateral to the apical domain (Helliwell *et al.*, 2000; Tobin *et al.*, 2008)) and that it poses a high transport constant led to hypothesised that GLUT2 provides the main route for glucose uptake during the postprandial phase in humans (Kellett *et al.*, 2008). Studies in animal models have shown that at postprandial luminal concentrations (>30 mM), GLUT2 is translocated to the apical membrane and mediates the uptake of ~75 % of glucose and fructose (Gouyon *et al.*, 2003).

There are not yet commercially available glucose-lowering agents targeting monosaccharide transporters. Some pharmacological compounds are under development which have shown promising results in lowering postprandial glucose with overall positive effects on metabolic biomarkers. For instance, the compound LX4211 improved glycaemic control, lowered triglycerides and produced downward trends in weight over 4 weeks of once-daily dosing in type 2 diabetic subjects (Zambrowicz *et al.*, 2012). These effects were mediated through the inhibition of SGLT1 activity which attenuated the postprandial glucose appearance after an oral glucose challenge in both healthy and type 2 diabetics (Zambrowicz *et al.*, 2013b, Zambrowicz *et al.*, 2013a). Like the compound LX4211, some polyphenols interact with intestinal transporters and could potentially blunt sugar absorption (discussed in chapter 1, section 1.7.2) suggesting that either as food components or their co-administration with foods could help to attenuate high postprandial sugar excursions and hormonal responses.

Despite the promising progress achieved on the potential of polyphenols to interact with sugar transporters, some gaps still remain to be explored. For example, the information of which intestinal glucose transporters are inhibited by different polyphenols, polyphenol-rich foods and extracts is scarce and uncertain, which polyphenols are the most potent inhibitors of glucose transport and their active concentrations, and whether there is selectivity for inhibition of transport of different substrates have not been established.

Furthermore, most of the studies on the characterisation of polyphenols to blunt sugar postprandial rise has focused on studying a single metabolic pathway of the carbohydrate digestion and absorption process and so, information of compounds capable of acting at different steps of this pathway is lacking.

The generation of this information would serve as the foundation for the rational design of human intervention studies to study the effectiveness of polyphenols on sugar absorption, and to establish the potential mechanism of action of polyphenol-rich foods and extracts that have shown positive effect in relevant biomarkers. For instance apigenin, a major polyphenol constituent of chamomile have shown antihyperglycaemic effects in type 2 diabetic rats in both baseline and postprandial glucose levels and decreased insulin resistance after 6 weeks of treatment (Ren *et al.*, 2016). Therefore, it is possible that the antihyperglycaemic effect of chamomile observed in animal models and humans (Kato *et al.*, 2008; Weidner *et al.*, 2013; Rafraf *et al.*, 2015; Zemestani *et al.*, 2016) is mediated mainly through the presence of apigenin and its derivatives, and such effect can be partially elicited by their complementary action on both carbohydrate digestion (described in chapter 3) and sugar absorption.

Here, the potential of apigenin and other three major polyphenol constituents of chamomile to blunt intestinal glucose absorption in Caco-2/TC7 cells was assessed. Transporter specificity was delineated by the use of well-established SGLT1 inhibitor and GLUT2 while GLUT5 inhibition and specificity was assessed with the use of fructose. The Caco-2/TC7 cell model have been extensively characterised, and have been utilised for studies on sugar transport as a model for the small intestine, since the expression and membrane location of GLUTs and SGLT1 is well known under a wide variety of conditions (Robayo–Torres *et al.*, 2006; Sim *et al.*, 2010).

4.3 Materials and methods.

4.3.1 Materials.

The ChE and authentic standards of apigenin and apigenin 7-*O*-glucoside were obtained from PhytoLab as a lyophilised powder. D-glucose, D-sucrose, D-fructose, cytochalasin B from *Drechslera dematioidea*, 4,6-*O*-Ethylidene- α -D-glucose and Dulbecco's Modified Eagle's Medium, (including 1000 and 4500 mg glucose/L, L-glutamine, NaHCO₃ and pyridoxine HCl) and Bradford reagent were all purchased from Sigma-Aldrich. Co., Ltd., Dorset, UK. D-[U-¹⁴C]-Glucose and D-[U-¹⁴C]-sucrose were purchased from Perkin Elmer (Boston, USA) and D-[U-¹⁴C]-fructose was obtained from American Radiolabelled Chemicals (St. Louis, MO, USA). Cy3-conjugated donkey anti-rabbit IgG was obtained from Jackson Immuno Research (West Grove, USA), fluorescein conjugated wheat germ agglutinin (WGA) from Vector laboratories (Burlingame, USA), ProLong Gold anti-fade reagent mounting medium from molecular probes (Life Technologies, Paisley, UK) and GLUT2 polyclonal antibody from Abcam (ab95256), Cambridge, U.K. GLUT5 monoclonal antibody was from Santa Cruz Biotechnology. Claudin-1 (2H10D10) antibody, SLC2A5 and TATA-box binding protein (TBP) FAMTM-labelled TaqMan primers (Hs01086390_m1) were from Fisher Scientific, Leicestershire, UK. RNAqueous-4PCR (AM1912) and a high capacity RNA-to cDNA master mix kits were obtained from Applied Biosystems, Warrington, UK. The Caco-2/TC7 cell line was obtained from Dr M. Rousset, U178 INSERM, Villejuif, France. Caco-2 cells (HTB-37) were obtained from the American Type Culture Collection (LGC Promochem, Middlesex, UK). Distilled water was used for all the experiments (Millipore UK Ltd., Hertfordshire, UK). All the reagents were of the highest purity and standards were $\geq 98\%$.

4.3.2 Methods.

4.3.2.1 Preparation of ChE for bioactivity studies.

ChE was prepared as previously described in chapter 2 section 2.3.2.1.

4.3.2.2 Cell culture.

Caco-2 and Caco-2/TC7 cells were cultured in a humidified CO₂ incubator (Sanyo, MCO-18AIC) in an atmosphere of 10 % CO₂-90 % air at 37 °C. Cells were routinely

grown in Dulbecco's Modified Eagle's Medium (1000 and 4500 mg/L glucose), supplemented with 20 % heat-inactivated fetal calf serum, 2 % L-alanyl-L-glutamine, 200 mM, 2 % non-essential amino acids and 100 U/mL penicillin-streptomycin. Every other day, the growth medium was replaced with fresh medium. When cells reached 80-90 % confluence, they were detached from the flask using 0.25% trypsin-EDTA solution and propagated in new 75 cm² cell culture plastic flasks at a ratio of 1.2 x 10⁶ cells/flask. All experiments were carried out on cells of passage number from 36 and 50 and 30 to 42 for Caco-2 and Caco-2/TC7 respectively.

4.3.2.3 Transport assay of monosaccharides in Caco-2/TC7 cells.

The effect of ChE and polyphenols to blunt sugar absorption was investigated in Caco-2/TC7 cells. These cells undergo a process of spontaneous differentiation leading to the formation of a cell monolayer expressing several morphological and functional characteristics of human enterocyte, and more homogenous expression of differentiation traits and stability than the parent cell line Caco-2 (Robayo-Torres *et al.*, 2006). Both Caco-2 and Caco-2/TC7 cells are considered as one of the most appropriate *in vitro* models for the investigation of a number of intestinal functions including the uptake and transport of nutrients such as sugars, ions, lipids, vitamins, polyphenols and drugs (for a comprehensive review see Sambuy *et al.* (2006)). Multiple studies have shown that Caco-2 and Caco-2/TC7 differentiated monolayers are fully appropriate for the study of glucose, sucrose and fructose absorption (Tobin *et al.*, 2008; Manzano and Williamson, 2010; Grefner *et al.*, 2012; Zheng *et al.*, 2012) since they express the apically-located proteins SGLT1, sucrase-isomaltase and GLUT5 (Robayo-Torres *et al.*, 2006; Hayeshi *et al.*, 2008). Importantly, when seeded on porous filters (Transwell), Caco-2/TC7 cells permit access to both sides of the bipolar intestinal epithelium. The apical and basolateral compartments represent the intestinal lumen or serosal circulation respectively (figure 4.2), better reproducing the steric conditions of the intestine *in vivo*. Therefore, the Caco-2/TC7 cell model has been recognised to be a good alternative to human and animal studies to predict *in vivo* intestinal uptake and transport and to study mechanistic aspects of nutrient absorption, such as the case of polyphenols and sugar transporters.

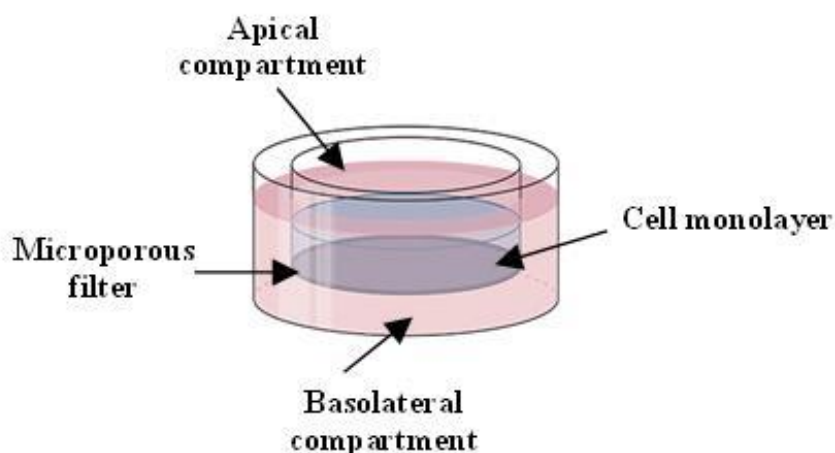


Figure 4.2 Schematic representation of Transwell® permeable support. The inserts provide independent access to both sides of the cell monolayer which allows study of the transport of nutrients and other molecules *in vitro*.

Transport experiments were performed according to the method published by Manzano and Williamson (2010) with minor modifications. Briefly, Caco-2/TC7 cells were seeded to 12-well plates (Costar, polycarbonate membrane, pore size 0.4 μm , 12 mm diameter) at 7×10^4 cells/well and cultured for 21-23 d at 37 °C. After 7 days, cells were changed to asymmetric conditions with a serum-free medium in the apical side for the remainder of the culturing period. Glucose transport was assessed by replacement of growth medium with transport buffer solution (TBS). TBS contained 5.4 mM KCl, 4.2 mM NaHCO_3 , 137 mM NaCl, 20 mM HEPES buffer solution and 1.8 mM CaCl_2 and pH was adjusted to 7.4. After washing cells, 1 mL TBS was added to both apical and basolateral sides and the plate was pre-incubated for 30 min at 37 °C under a humidified atmosphere. After equilibration, TEER values were recorded to assess the integrity of the monolayer and the TBS was carefully aspirated to waste from the apical and basolateral sides. For experiments, 0.5 mL TBS containing 5 mM glucose, sucrose or fructose including D-[U- ^{14}C]-glucose 0.15 $\mu\text{Ci/mL}$, D-[U- ^{14}C]-sucrose 1.8 $\mu\text{Ci/mL}$, or D-[U- ^{14}C]-fructose 1.0 $\mu\text{Ci/mL}$ with or without inhibitor at varying concentrations (adjusted pH 7.4 with HCl or NaOH) was added to the apical side (for asymmetric transport, solution was added at the basolateral side) and 1 mL TBS to the basolateral compartment. Then, cells were incubated for 25 min for glucose and 60 min for sucrose and fructose at 37 °C and

transport was stopped by washing each membrane twice with ice-cold PBS. Transport values were obtained by adding the apical and basolateral solution to scintillation vials containing 5 mL of scintillation liquid. The radioactivity was estimated from an 8-point linear calibration curve using scintillation counting (Packard Liquid Scintillation Analyser 1600TR). A schematic representation of the method used to assess monosaccharide transport is depicted in figure 4.3.

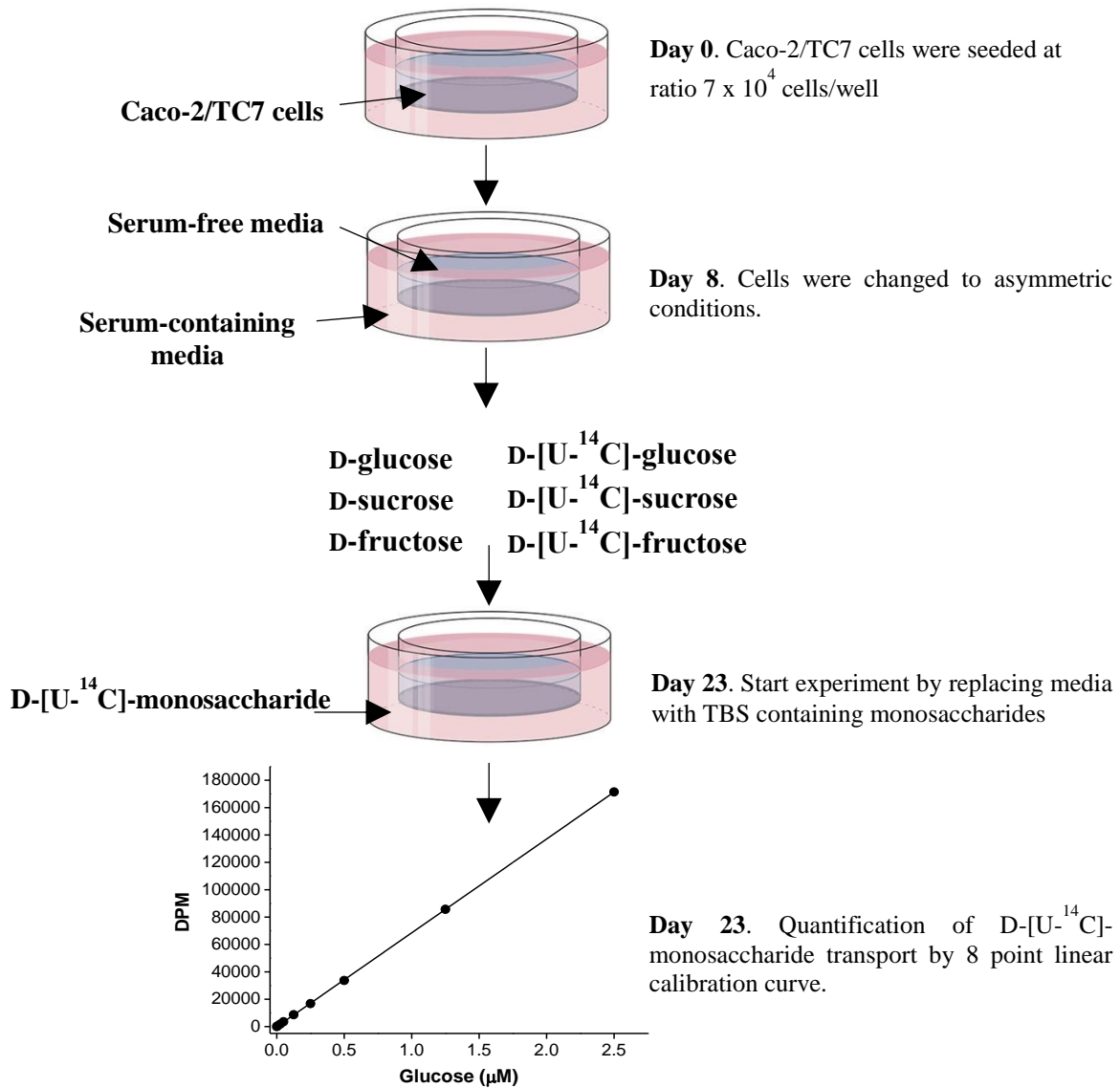


Figure 4.3 Schematic representation of the experimental design for assessing the inhibition of D-[U-¹⁴C]-monosaccharide transport across differentiated Caco-2/TC7 cell monolayers. The assay was conducted with and without inhibitors and the D-[U-¹⁴C]-glucose and D-[U-¹⁴C]-fructose transported from apical to basolateral was quantified using a standard of the corresponding radiolabelled monosaccharide.

4.3.2.4 Differential mRNA and protein expression levels of GLUT5 in CaCo-2 and CaCo-2/TC7 cells.

For GLUT5 mRNA and protein expression analysis, Caco-2 and Caco-2/TC7 cells were seeded onto solid supports (6.43×10^4 cells/cm²) and maintained for 23 days before harvesting for expression analysis. RNA isolation was performed using an RNAqueous-4PCR kit and its quality (260/280 ratio) and quantity (280 nm) determined with a Nanodrop 1000ND spectrophotometer (Thermo Scientific, Labtech, East Sussex, UK). 1 μ g of RNA was reverse transcribed to cDNA using a High Capacity RNA-to cDNA master mix kit. Quantitative gene expression was conducted using a QX100 Droplet digital PCR (ddPCR) system (Bio-Rad). In brief, 20 μ L of stock sample containing 9 μ L of transcribed DNA (21.5 ng), 1 μ L SLC2A5 FAMTM-labelled TaqMan primer and 10 μ L of digital droplet PCR Supermix for Probes (Bio-Rad) were introduced in the assay well. TBP was used as a reference. Droplets were generated according to the manufacturer's procedure with the QX100 Droplet generator (Bio-Rad) before cycling in a C1000 Touch thermal cycler (Bio-Rad) at optimal temperature for every primer for 30 min followed by 95 °C (10 min), 40 cycles of 94 °C (0.5 min) followed by 60 °C (60 min), and 98 °C (10 min). The average number of accepted droplets was 14781 ± 981 (see example in figure 4.4) and the concentration of the target DNA in copies/ μ L was calculated from the fraction of positive reactions using Poisson distribution analysis. The Data was analysed with the QuantaSoft software (Kosice, Slovakia). The ddPCR data for each target gene are captured independently based on fluorescence signal and copy numbers are reported for all (figure 4.4). Thus, the housekeeping gene expression can be monitored but is not essential for data evaluation and quantitative determination. Since Caco-2 and Caco/TC7 cells showed high variation in TBP expression, the quantitative data is presented as copy numbers/ng of cDNA and TBP was used solely as a reference for the same group of samples to compare performance between ddPCR runs.

For analysis of GLUT5 protein levels, Caco-2 and Caco-/TC7 cells were washed three times with ice-cold PBS, scraped from trans well filters and lysed in RIPA buffer containing 0.5% protease inhibitor mixture by gently rocking the samples on ice for 30 min. The lysate was centrifuged at 14,000 *g* for 10 min, and the total protein concentration of the supernatant was determined by BCA microplate assay according to the manufacturer's instructions. GLUT5 protein levels were quantified using the

automated capillary ProteinSimple system “Wes” (figure 4.5) according to the protocol of the manufacturer with primary antibody incubation time of 30 min.

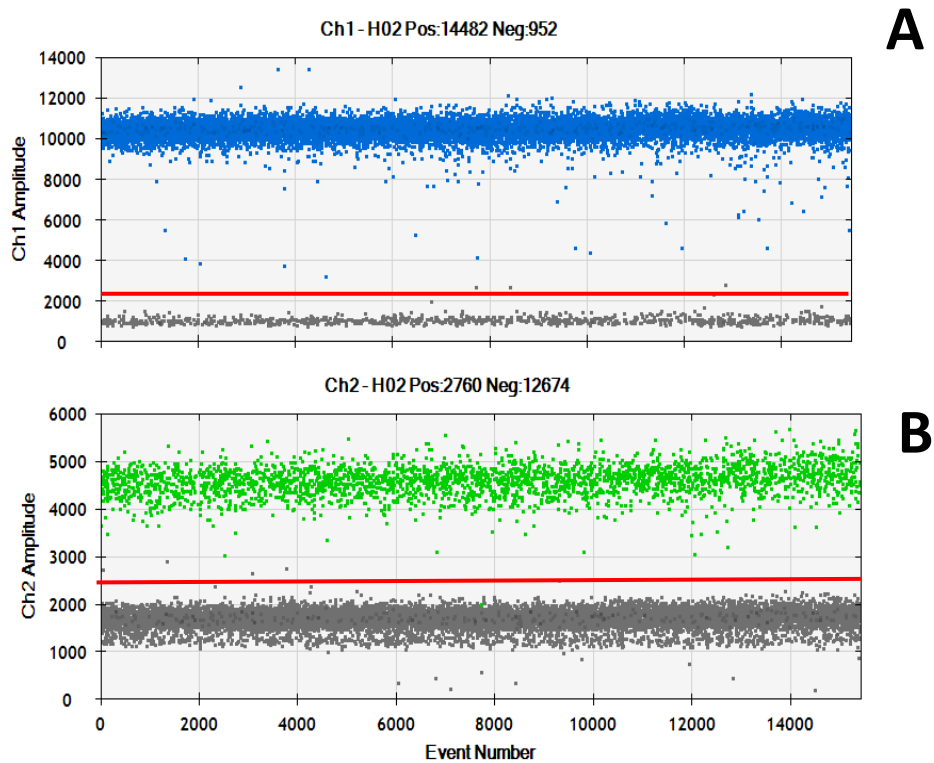


Figure 4.4 Representative example of ddPCR data viewed as a 1-D plot with each droplet from a sample plotted on the graph of fluorescence intensity vs droplet number. All positive droplets, those above the threshold (red line), are scored as positive and each is assigned a value of 1. All negative droplets, those below the red threshold line, are scored as negative and each is assigned a value of 0. QuantaSoft™ software measures the number of positive and negative droplets for each fluorophore in each sample. The software then fits the fraction of positive droplets to a Poisson algorithm to determine the starting concentration of the target DNA molecule in units of copies/ μ L. (A) In blue are the positive droplets obtained for a Caco-2 cell lysate containing GLUT5. (B) In green are the positives droplets obtained for a Caco-2 cell lysate containing TBP.

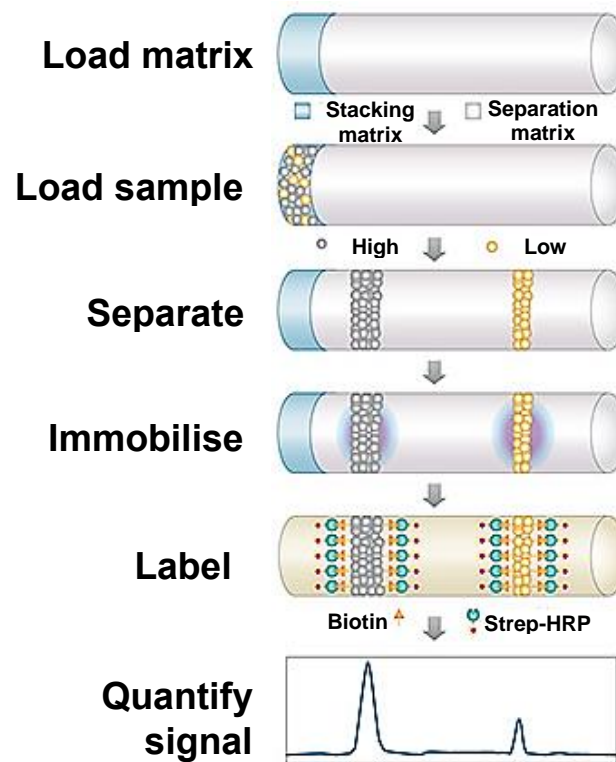


Figure 4.5 Schematic representation of the integration of all steps equivalent to a traditional Western blot in the automated capillary ProteinSimple system ‘Wes’. Samples and reagents are loaded into an assay plate and placed in the system and proteins are resolved as they migrate through a stacking and separation matrix in capillary columns based on size. After separation, the proteins are immobilized onto the interior wall by a proprietary photoactivated cross-linkage. Thereafter, the matrix is removed by the rinsing step and the capillary lumen is filled with primary antibody against the target protein, followed by the incubation of horseradish peroxidase (HRP)-conjugated secondary antibody. Chemiluminescent signal representing the protein of interest is generated by HRP-catalysed reaction as it occurs in traditional Western blot. The diagram was adapted from proteinsimple website (<https://www.proteinsimple.com>).

Different concentrations of cell lysates were tested for linearity of GLUT5 and Claudin-1 antibodies (both antibodies used with a dilution of 1:50) and a standard curve was generated for both cell lines (figure 4.6).

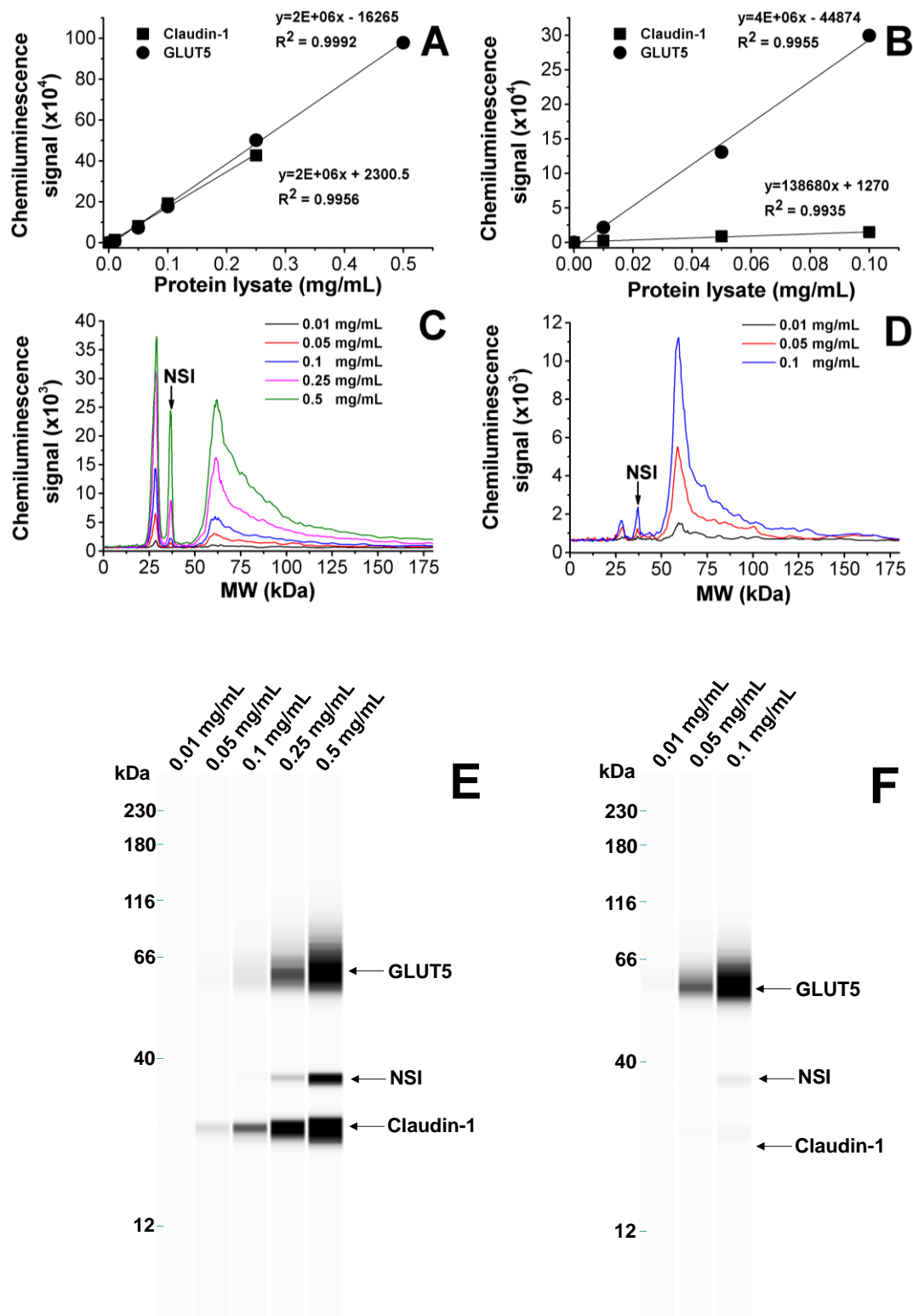


Figure 4.6 Concentration-dependent detection of multiplexed claudin-1 and GLUT5 in whole cell lysate. Panel A and B show the standard curve of multiplex claudin-1 and GLUT5. The concentration-dependent detection of Claudin-1 and GLUT5 is shown as electropherograms in panel C and D. Panel E and F shows the data as gel-like image. For quantitative analysis, 0.25 and 0.05 mg/mL were selected as the optimal lysate concentration for for Caco-2 and Caco/2 TC7

cells respectively. A, C and E- differentiated *Caco-2 cells*; B, D and F-differentiated *Caco-2/TC7 cells*. NSI: non- specific interaction. Three biological replicates in two seeding experiments were pooled and analysed four times. Data is expressed as mean \pm SEM. When not visible, the error bars are smaller than the data point.

Optimal loading concentration was 0.1 and 0.05 mg/mL for *Caco-2* and *Caco-2/TC7* cells, respectively (figure 4.6A and B). For assigning the molecular weight of target proteins, assay samples contained molecular weight fluorescence-labelled standards which were loaded and run in individual capillaries. Quantification of peak areas and gel-like image transformations were carried out using ProteinSimple Compass software. Given the large difference in protein expression of Claudin 1 between the two cell lines (13-fold), for quantitation, the peak areas of GLUT5 in *CaCo-2* and *CaCo-2/ TC7* cells are presented without normalisation to Claudin 1, but normalised to total protein.

4.3.2.5 Characterisation of the main glucose transporter in *Caco-2/TC7* cells and its inhibition by ChE, apigenin and apigenin 7-O-glucoside.

D-[U-¹⁴C]-glucose transport experiments were conducted as previously described in section 4.3.2.2. The assays were conducted under Na⁺ and Na⁺-free conditions to ascertain the involvement of SGLT1 and GLUT2 on glucose transport respectively. To validate the model, phloridzin and phloretin, well known inhibitors of SGLT1 and GLUT2 respectively, were used to determine the specific contribution of each transporter to the total glucose transport across *Caco-2/TC7* cell monolayers.

4.3.2.6 Detection of GLUT2 in *Caco-2/TC7* cells by immunofluorescence staining.

Caco-2/TC7 cells were seeded on 12 well Millicell cell culture inserts (PET 0.4 mm pore size, Millipore) at 7×10^4 cells/well and cultured for 21-23 d at 37 °C. For staining, cells were fixed with 4% para-formaldehyde in PBS and incubated with wheat germ agglutinin (WGA, 1 mg/mL) for 10 min at 37 °C. Following permeabilisation with 0.1% Triton-X100 for 20 min at room temperature, cells were incubated without (control) and with GLUT2 antibody at a dilution of 1:50 for 1 h. After washing with PBS, cells were further incubated with Cy3-conjugated donkey anti-rabbit IgG at a 1:300 dilution. Cell layers

were stained with 0.002 mg/mL 4,6-diamidino-2-phenylindole (DAPI) and mounted on microscopy slides with ProLong Gold antifade reagent mounting medium and imaged using a Zeiss LSM700 confocal microscope.

4.3.2.7 *In vitro* conversion of apigenin 7-*O*-glucoside to apigenin by Caco-2/TC7 cells.

Cells were seeded on 6-well plates (Costar, 22.1 mm diameter) at 2.4×10^5 cells/well and cultured for 21-23 d at 37 °C under the conditions previously described. Cells were exposed to 150 μ M apigenin 7-*O*-glucosid for 25 and 60 min. After the treatment, media was collected and subjected to HPLC analysis as described in chapter 2, section 2.3.2.2.

4.3.3 Statistical analysis.

Statistical analysis was performed by one-way analysis of variance using the Number Cruncher Statistical System version 6.0 software (NCSS, LLC). Significant differences were assessed with Tukey-Kramer multiple comparison test ($p < 0.05$). Independent samples *t* test was used to compare means of the contribution of apigenin 7-*O*-glucoside and apigenin to the total inhibition of sugar transport and between incremental concentration of inhibitors. Data are expressed as the mean \pm SEM.

4.4 Results and discussion.

4.4.1 Inhibitory effect of ChE and polyphenols on glucose, sucrose and fructose transport.

Excess dietary sugars such as glucose and fructose are responsible for altering whole system energy balance contributing to a coordinate breakdown of cellular functions. In order to be absorbed, glucose and fructose must be transported from the intestinal lumen into the blood, and so the small intestine has been suggested as a prime target for preventive and therapeutic actions against metabolic diseases by attenuating the activity of sugar transporters (Williamson, 2013; Stringer *et al.*, 2015).

In the presence of Na⁺ where the three sugar transporters SGLT1 and facilitated transporters GLUT2 and GLUT5 are active, Caco-2/TC7 cells transported 0.08 mmol of D-[U-¹⁴C]-glucose from the apical to basolateral compartment across the cell monolayers (figure 4.7A).

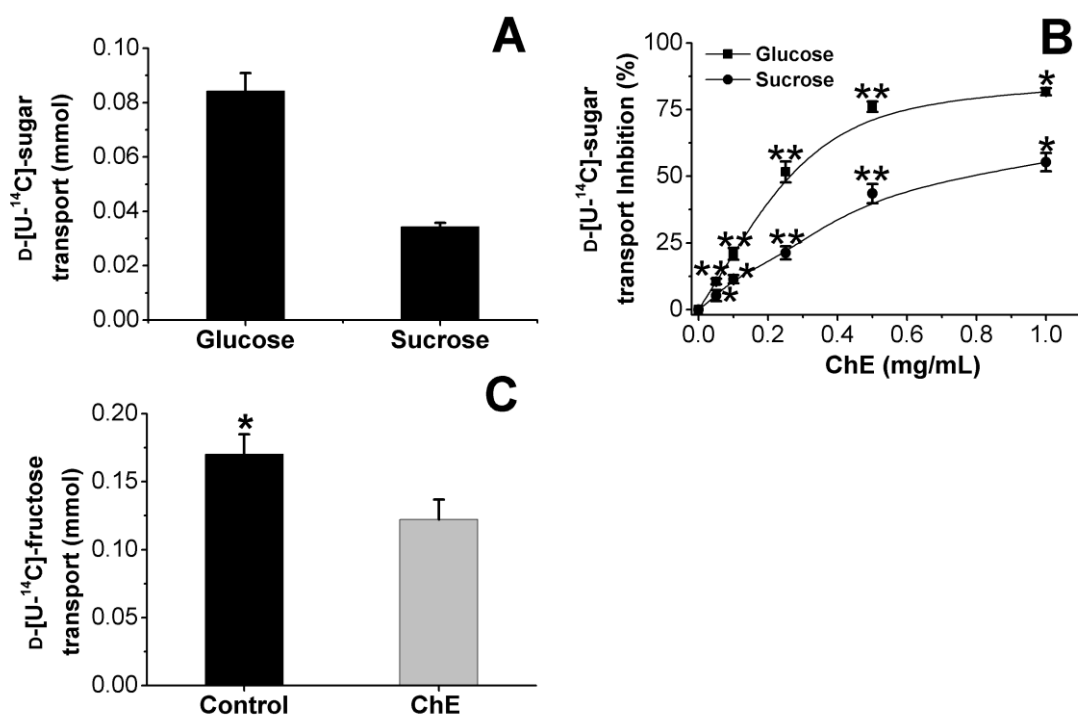


Figure 4.7 Monosaccharide transport under Na⁺ conditions across differentiated Caco-2/TC7 cells monolayers. (A) Transport D-[U-¹⁴C]-glucose and D-[U-¹⁴C]-sucrose in the absence of inhibitors. (B) Dose-dependent inhibition of D-[U-¹⁴C]-glucose and D-[U-¹⁴C]-sucrose transport

by ChE. (C) Inhibition of D-[U-¹⁴C]-fructose by ChE at a single concentration (1 mg/mL). For D-[U-¹⁴C]-glucose and D-[U-¹⁴C]-sucrose transport the IC₅₀ values were calculated as 0.24 ± 0.02 and 0.91 ± 0.06 mg/mL respectively. For D-[U-¹⁴C]-fructose the maximum inhibition at the concentration tested was 28 %. Each data point represents the mean ± SEM of at three independent experiments with six technical replicates each (n = 3). In figure (B), the reduction of D-[U-¹⁴C]-sugar transport is expressed as % compared to the transported sugars in control incubations (no inhibitor normalised to 100 %). When not visible, the error bars are smaller than the data point. In figure (B) statistical difference is indicated vs incremental concentration of ChE. **p*<0.05, ***p*<0.01.

D-[U-¹⁴C]-sucrose has to be hydrolysed by brush border sucrase and the resulting products, fructose and glucose, are transported across the cells. After incubation with D-[U-¹⁴C]-sucrose, Caco-2/TC7 cells transported 0.035 mmol from the apical to the basolateral compartment (figure 4.7A).

The addition of ChE to Caco-2/TC7 cells led to a dose-dependent inhibition of D-[U-¹⁴C]-glucose transport and labelled-derived sugars from D-[U-¹⁴C]-sucrose, with maximum inhibitions of ~ 78 and 55 % respectively at the highest concentration tested (1 mg/mL). The IC₅₀ value of ChE for D-[U-¹⁴C]-glucose transport was ~0.24 mg/mL while the inhibition when D-[U-¹⁴C]-sucrose was added was ~3.8-fold lower with an IC₅₀ value of 0.91 mg/mL (figure 4.7B). On the other hand, although D-[U-¹⁴C]-fructose was also transported in the apical to basolateral direction, the addition of 1 mg/mL of ChE did not reach 50 % of the inhibition (figure 4.7C); the addition of ChE had a lower but significant inhibitory effect (~28 %, *p*<0.05).

A previous study has been conducted in an attempt to identify plant extracts with the potential to attenuate monosaccharide uptake and transport in the intestinal cell line Caco-2 (Aydin, 2015). While the IC₅₀ values obtained for the inhibition D-[U-¹⁴C]-glucose (IC₅₀= 0.32 ± 0.05) and D-[U-¹⁴C]-sucrose (IC₅₀= 0.32 ± 0.05) transport were similar to those obtained in the clone cell line Caco-2/TC7, a different trend was observed for the inhibition of D-[U-¹⁴C]-fructose transport. Contrary to the experimental results obtained in this work, the addition of ChE inhibited the transport of D-[U-¹⁴C]-fructose (1 mM)

from apical to basolateral compartment in a competitive manner in Caco-2 cells (figure 4.8).

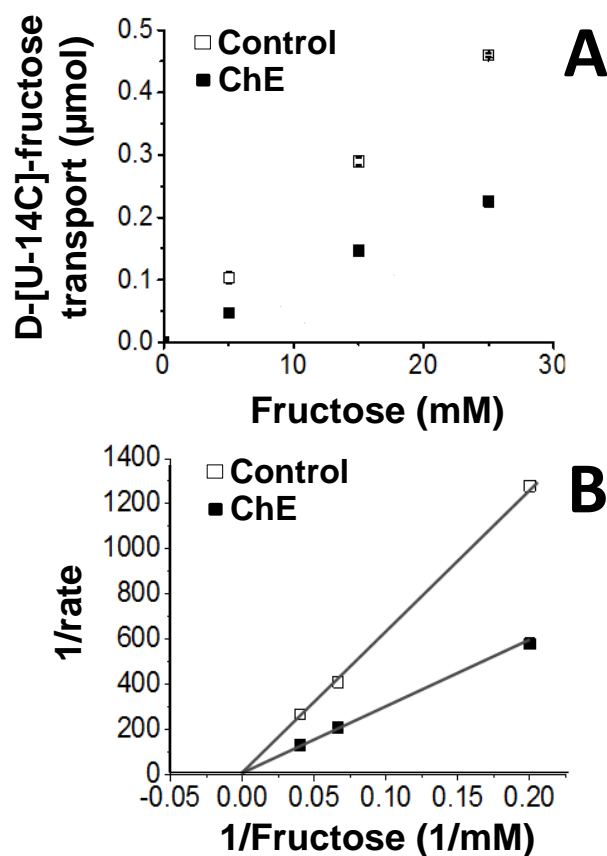


Figure 4.8 Inhibition of D-[U-¹⁴C]-fructose transport by ChE across differentiated Caco-2 cell monolayers.(A) Inhibition of D-[U-¹⁴C]-fructose transport by the addition of 1 mg/mL of ChE at different concentrations of apical fructose. (B) Lineweaver-Burk plot for transport of D-[U-¹⁴C]-fructose with and without ChE at 1 mg/mL; the intercept suggests competitive inhibition. The graph was adapted from Villa-Rodriguez *et al.* (2017).

The discrepancies in the inhibition values are likely due to differences between the protein expression levels of GLUT5 among the intestinal cell lines, since the morphological and functional phenotype tend to vary among cell lines from different passages and different clones (Sambuy *et al.*, 2005). Therefore, differences in the mRNA and protein expression levels of fructose transporter GLUT5 were investigated in Caco2/TC7 cells and in the parental cell line Caco-2 to clarify the differences in the inhibition obtained (figure 4.9). In accordance with the D-[U-¹⁴C]-fructose transport

observation, GLUT5 mRNA expression levels were ~2.5-fold higher ($p<0.01$) in the Caco-2 TC7 clone (figure 4.9A), which is translated into a ~2.0-fold increase ($p<0.01$) in GLUT5 protein levels in the apical membrane (figure 4.9B).

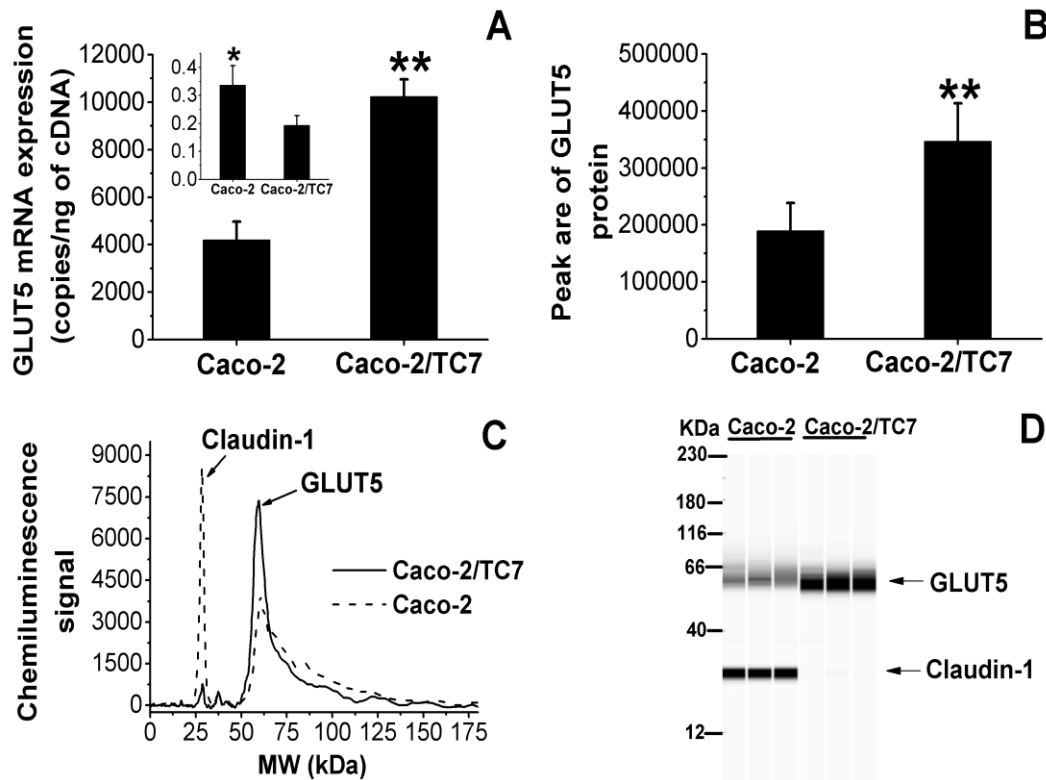


Figure 4.9 Differential mRNA and protein expression levels of GLUT5 in differentiated Caco-2 and Caco-2/TC7 cell monolayers. (A) Exact copy numbers of GLUT5 are shown per ng of cDNA since changes were also observed for TBP copy numbers (insert figure) when multiplexed with each cell line. (B) GLUT5 protein levels as quantified by automated capillary Western, with optimal protein lysate concentrations based on standard curves of multiplexed GLUT5 and Claudin-1 for both cell lines. (C) Data is shown as electropherograms. (D) Data is shown as gel-like image at equal concentration of cell lysate (0.1 mg/mL). Three biological replicates in two seeding experiments were pooled and analysed six times. Data is expressed as mean \pm SEM. * $p<0.05$, ** $p<0.01$.

These data indicate that the differences in the inhibition constants obtained between the two cell lines regarding D-[U-¹⁴C]-fructose transport from the apical to the basolateral compartment is due to a higher transport capacity due to a higher expression of GLUT5 transporter protein. The apical protein expression levels of GLUT5 in the Caco-2 cell line

has been shown to be similar to that noted in an adult small intestine (Mahraoui *et al.*, 1992), thus the inhibition value obtained for fructose in the Caco-2 cell line is underestimated.

In order to elucidate whether the four major polyphenols in ChE were responsible and /or participate in the inhibition of monosaccharide transport, they were tested for their potential to attenuate D-[U-¹⁴C]-monosaccharide flux across Caco-2/TC7 cell monolayers. Among individual polyphenols tested, apigenin 7-*O*-glucoside was a very effective inhibitor of D-[U-¹⁴C]-glucose and D-[U-¹⁴C]-sucrose transport, and IC₅₀ values were obtained. Apigenin 7-*O*-glucoside dose-dependently inhibited (0-200 μM) D-[U-¹⁴C]-glucose transport with a maximum inhibition of ~60 % and IC₅₀ of ~173 μM. The same range of concentrations were effective to attenuate D-[U-¹⁴C]-sucrose transport and the IC₅₀ was obtained around the highest concentration tested (IC₅₀= 197 μM) (figure 4.10A).

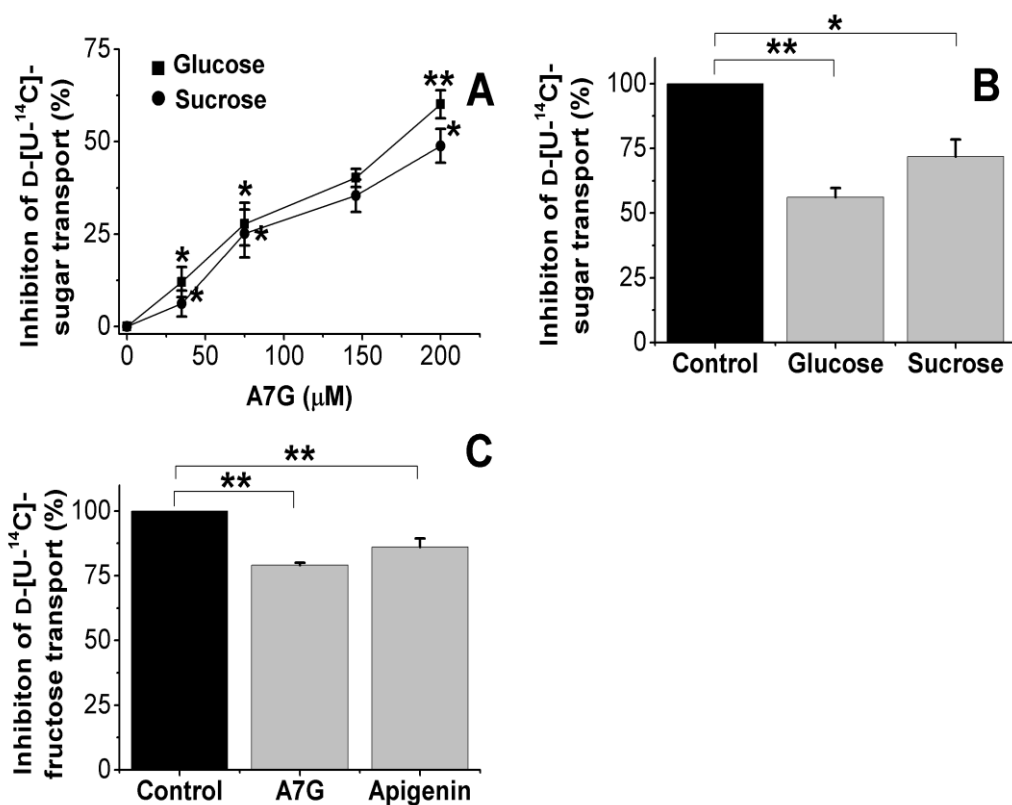


Figure 4.10 Inhibition of monosaccharide transport under Na⁺ conditions across differentiated Caco-2/TC7 cell monolayers by individual polyphenols. (A) Concentration-dependent inhibition of D-[U-¹⁴C]-glucose and D-[U-¹⁴C]-sucrose by apigenin 7-*O*-glucoside (A7G). (B) Inhibition of D-[U-¹⁴C]-glucose and D-[U-¹⁴C]-sucrose by apigenin at a single concentration (50 μM). (C) Inhibition of D-[U-¹⁴C]-fructose by A7G and apigenin at a single con-

-centration; A7G (200 μ M), apigenin (50 μ M). Results are expressed as % compared to the transported sugars in control incubations (no inhibitor: normalised to 100%). Each data point represents the mean \pm SEM of three independent experiments with six technical replicates ($n = 3$). In figure (A), statistical significance is indicated between incremental concentrations of A7G. * $p < 0.05$.

Apigenin was also an effective inhibitor of D-[U- 14 C]-glucose and D-[U- 14 C]-sucrose transport, although IC₅₀ values could not be obtained at the highest soluble concentration tested (50 μ M). However it can be deduced that it is a more potent inhibitor based on the substantial \sim 3-fold higher-effect when compared with apigenin 7-*O*-glucoside at the same concentration (figure 4.10B). On the other hand, as expected, apigenin and its precursor apigenin 7-*O*-glucoside weakly inhibited the transport of D-[U- 14 C]-fructose across the cell monolayers with maximum inhibitions of \sim 21 and 13 % at the maximum soluble concentrations tested (figure 4.10C). (*Z*) and (*E*)-MCAG did not inhibit D-[U- 14 C]-glucose, D-[U- 14 C]-sucrose nor D-[U- 14 C]-fructose transport.

To test whether apigenin and apigenin 7-*O*-glucoside were solely responsible for the inhibition of monosaccharide transport observed by the ChE, they were combined at the concentrations equivalent to those present in the extract and transport experiments were carried out. As depicted in figure 4.11, apigenin and apigenin 7-*O*-glucoside were responsible for \sim 62 %, 80 and 89 of the total D-[U- 14 C]-glucose, D-[U- 14 C]-sucrose and D-[U- 14 C]-fructose transport inhibition respectively.

The results on monosaccharide transport clearly show that ChE has the potential to attenuate the amount of glucose and, to a lesser extent, the amount of fructose that can be transported across the enterocytes, which is mainly driven by the presence of apigenin and apigenin 7-*O*-glucoside. This activity represents an advantage over acarbose which acts primarily (and perhaps solely) by inhibiting starch and disaccharide digestion (shown in chapter 2), thus decreasing and delaying the subsequent amount of free monosaccharides available for absorption. However, a previous study has indicated a direct effect of acarbose on free glucose absorption in the jejunal epithelium of rats (Hirsh

et al., 1997). Therefore acarbose was next assessed for its potential to attenuate D-[U-¹⁴C]-glucose, D-[U-¹⁴C]-sucrose and D-[U-¹⁴C]-fructose transport across Caco-2/TC7 cell

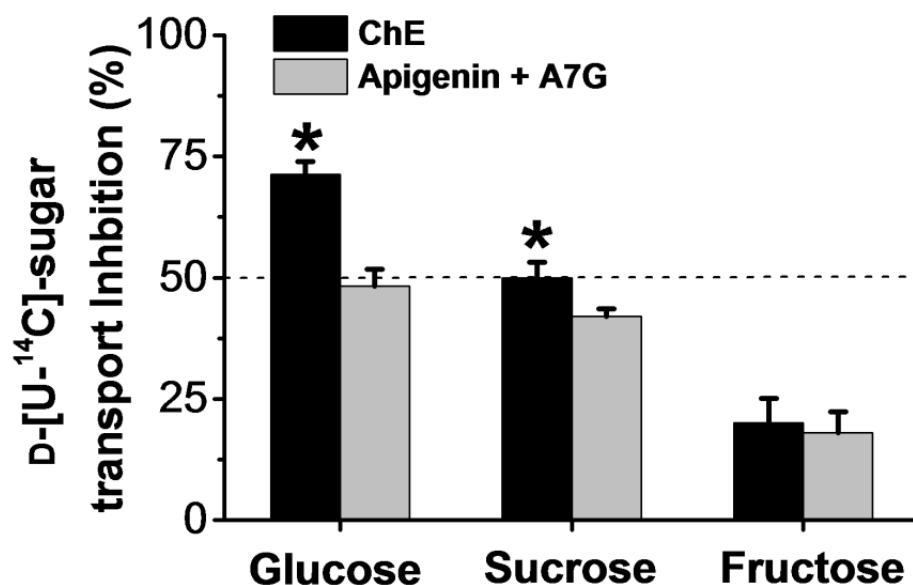


Figure 4.11 Inhibition of monosaccharide transport by ChE and combined inhibition of apigenin and apigenin 7-*O*-glucoside (A7G). D-[U-¹⁴C]-sugar transport assay was conducted under Na⁺ conditions. Apigenin, 12 μM; A7G 148 μM. Results are expressed as % compared to the transported sugars in control incubations (no inhibitor; normalised to 100 %). Each data point represents the mean ± SEM of three independent experiments with six technical replicates (n = 3). **p*<0.05; ***p*<0.01.

monolayers at varying concentrations ranging from 0-500 μM. Acarbose inhibited D-[U-¹⁴C]-sucrose transport effectively in a dose-dependent manner with an IC₅₀ value of ~7 μM (figure 4.12), but did not inhibit glucose nor fructose transport across cells monolayers even at a concentration of 500 μM. These results show that the enzyme sucrase, located at the apical membrane of Caco-2/TC7 cells, is sensitive to acarbose but neither SGLT1, GLUT2 nor GLUT5 are, since D-[U-¹⁴C]-glucose and D-[U-¹⁴C]-fructose transport was unaffected by its presence. The lack of effect of acarbose on GLUT2 and GLUT5 has been further confirmed in *Xenopus* Oocytes expressing the transporter proteins where acarbose did not attenuate the uptake of D-[U-¹⁴C]-glucose or D-[U-¹⁴C]-fructose up to a concentration of 5 mM (Villa-Rodriguez *et al.* 2017). Moreover, these

data suggest that the inhibition observed for D-[U-¹⁴C]-sucrose is due to the interaction of ChE constituents, apigenin and apigenin 7-*O*-glucoside, with the glucose transporter SGLT1 and/or GLUT2 since they showed a modest effect at impairing α -glucosidase activity (discussed in chapter 3, section 3.4.5).

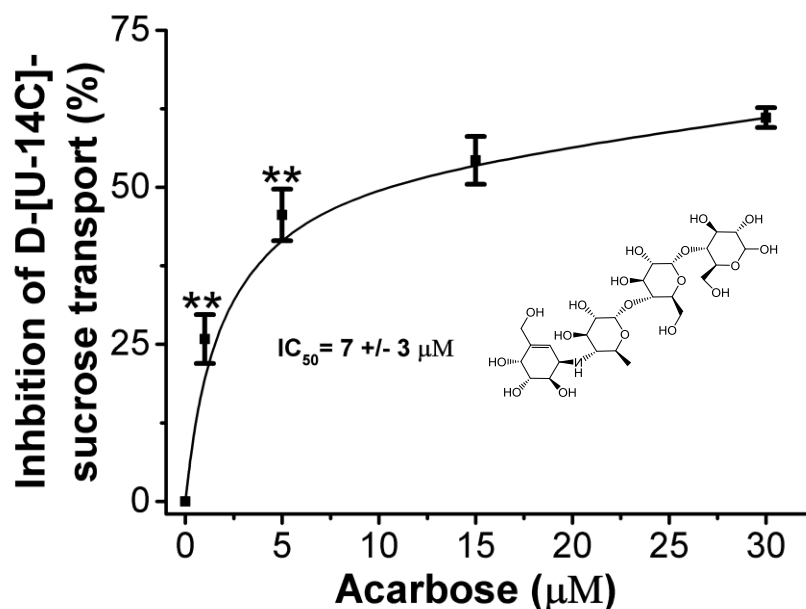


Figure 4.12 Concentration-dependent inhibition of D-[U-¹⁴C]-sucrose transport by the antidiabetic drug acarbose across differentiated Caco-2/TC7 cell monolayers. Insert shows the chemical structure of acarbose and the calculated IC₅₀ value. Each data point represents the mean \pm SEM of three independent experiments with six technical replicates (n = 3). Results are expressed as % compared to the transported sucrose in control incubations (no inhibitor; normalised to 100 %). When not visible, the error bars are smaller than the data point. Statistical difference is indicated vs incremental concentration of acarbose. * p <0.05, ** p <0.01.

4.4.2 Identification of the main glucose transporter protein in Caco-2/TC7 cells and the effect of ChE, apigenin and apigenin 7-*O*-glucoside on its activity.

At low concentrations, the uptake of glucose and fructose is *via* SGLT1 and the facilitated transporter GLUT5, respectively. However, after a high sugar meal, their concentration may be elevated to 50-300 mM, and consequently it has been suggested that the facilitated transporter GLUT2 is translocated to the apical membrane, and then accounts

for ~75 % of glucose and ~60 % of fructose total uptake (Gouyon *et al.*, 2003; Kellett *et al.*, 2008). To delineate whether the inhibition observed by ChE, apigenin and apigenin 7-*O*-glucoside on D-[U-¹⁴C]-glucose transport was predominantly through their interaction with SGLT1 or GLUT2, transport assays were carried out under Na⁺ (where both transporters are active) and Na⁺-free conditions (only GLUT2 is active).

Caco-2/TC7 cells transported 0.075 mmol of D-[¹⁴C]-glucose when Na⁺ was present. Removing Na⁺ from the TBS reduced the transport of D-[¹⁴C]-glucose to 0.049 mmol (figure 4.13A), implying that SGLT1 was responsible for ~35 % of the total D-[U-¹⁴C]-glucose transported across the monolayer. This was corroborated by two observations; phloridzin (a well-known specific inhibitor of SGLT1 transporter) showed no inhibition of D-[U-¹⁴C]-glucose transport under Na⁺-free conditions (Figure 4.13A) and D-[U-¹⁴C]-glucose transport was dose-dependently affected by phloretin (Figure 4.13B). Both findings also attest to the role of GLUT2 as the main glucose transporter in Caco-2/TC7 cells.

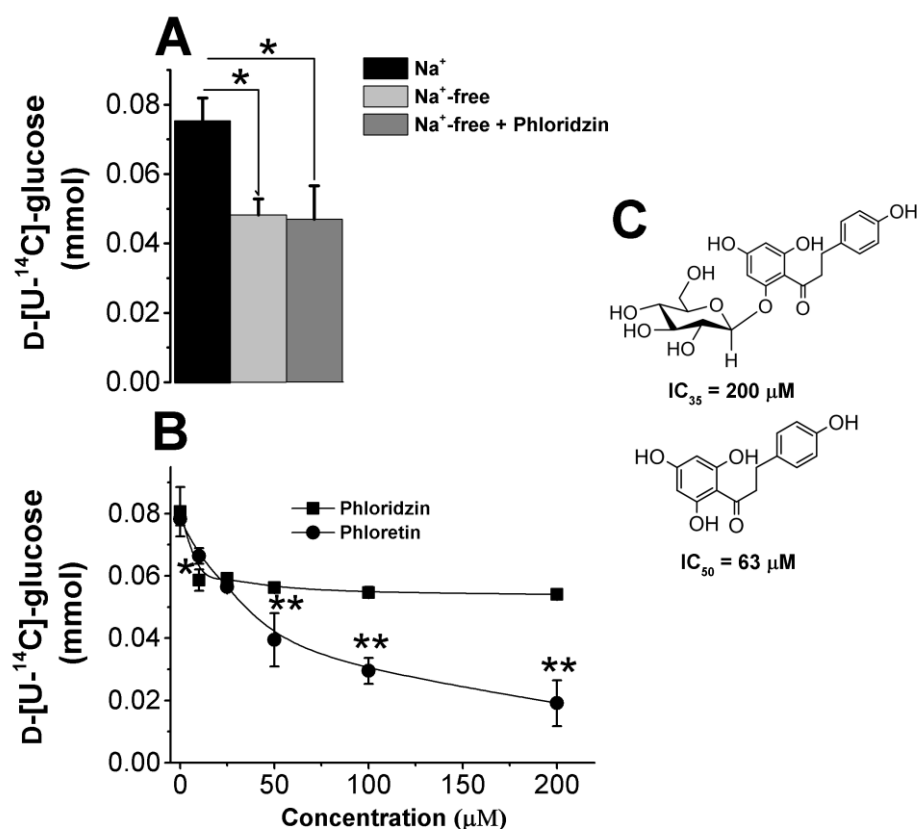


Figure 4.13 Characterisation of the main D-[U-¹⁴C]-glucose transporter in Caco-2/TC7 cell monolayers. (A) D-[U-¹⁴C]-glucose transport with and without Na⁺ and Na⁺-free with co-incuba-

-tion of 200 μM phlorizin. (B) Dose-dependent inhibition of D-[U- ^{14}C]-glucose by phlorizin and phloretin with TBS containing Na^+ . (C) Chemical structures of phlorizin and phloretin and their respective inhibition constants. Each data point represents the mean \pm SEM of three independent experiments with six technical replicates. When not visible, the error bars are smaller than the data point. In figure (B) statistical difference are indicated between phloridzin and phloretin. * $p < 0.05$, ** $p < 0.05$.

The inhibition of D-[U- ^{14}C]-glucose transport by ChE, apigenin and apigenin 7-*O*-glucoside under Na^+ conditions suggest that they interact mainly with GLUT2 transporter protein since these values were all above the maximum D-[U- ^{14}C]-glucose transported through SGLT1. Indeed, when D-[U- ^{14}C]-glucose transport was assessed under Na^+ -free conditions and ChE, apigenin or apigenin 7-*O*-glucoside were added as inhibitors, an increase in the inhibitory activity ($\sim 50\%$) was observed as evidenced by the decrease in their inhibition constants when compared in the presence of Na^+ (figure 4.14).

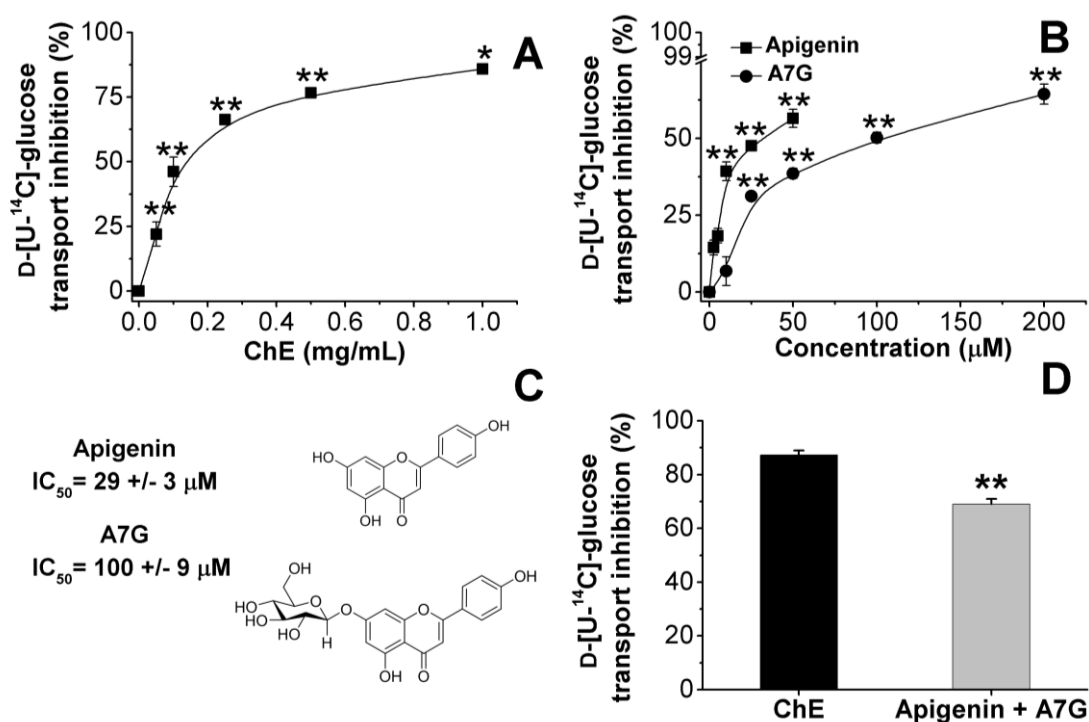


Figure 4.14 Inhibition D-[U- ^{14}C]-glucose transport across differentiated Caco-2/TC7 cell monolayers under Na^+ -free conditions. (A) Concentration-dependence inhibition of ChE, $\text{IC}_{50} = 0.138 \pm 0.018 \text{ mg/mL}$. (B) Concentration-dependence inhibition of apigenin and apigenin 7-*O*-glu

-coside (A7G) respectively. (C) Chemical structures of apigenin and A7G and their respective inhibition constants. (D) Combined inhibition of apigenin and A7G; apigenin, 12 μM ; A7G, 148 μM . Each data point represents the mean \pm SEM of three independent experiments with six technical replicates ($n=3$). Results are expressed as % compared to the transported sugars in control incubations (no inhibitor; normalised to 100 %). When not visible, the error bars are smaller than the data point. In figure (A) and (B) statistical difference is indicated vs incremental concentration of each inhibitor. * $p<0.05$, ** $p<0.05$.

The IC_{50} values for ChE, apigenin and apigenin 7-*O*-glucoside under Na^+ -free conditions were 0.13 mg/mL, 29 and 100 μM respectively. Moreover, when tested in combination, apigenin and apigenin 7-*O*-glucoside were responsible for ~80 % of the inhibitory activity (figure 4.14D). This indicates that there are other compound(s) present in the ChE which are responsible for the remaining inhibitory activity and are active on both SGLT1 and GLUT2 transporters. Nonetheless, overall apigenin and apigenin 7-*O*-glucoside are the main active compounds since they are the main contributors under Na^+ and Na^+ -free conditions.

Next, it was evaluated whether Caco-2/TC7 cells have the capability to convert apigenin-7-*O*-glucoside to apigenin. Glycosylated polyphenols can be hydrolysed by exogenous (luminal) β -glucosidase enzymes, such as lactase phlorizin hydrolase, present in the brush border of the enterocytes, and the aglycone released. Therefore, there was a possibility that the inhibition observed by apigenin-7-*O*-glucoside was due to the presence of apigenin after enzymic release. For these studies, Caco-2/TC7 cells were incubated with 150 μM apigenin 7-*O*-glucoside for 25 and 60 min as in the inhibition assays. Figure 4.15 shows that the *in vitro* conversion of apigenin 7-*O*-glucoside to apigenin is negligible at both incubation times confirming that both polyphenols interact with GLUT2 transporter protein. This is of primary importance since the release of apigenin from apigenin 7-*O*-glucoside in the small intestine is expected in humans which may increase the efficacy.

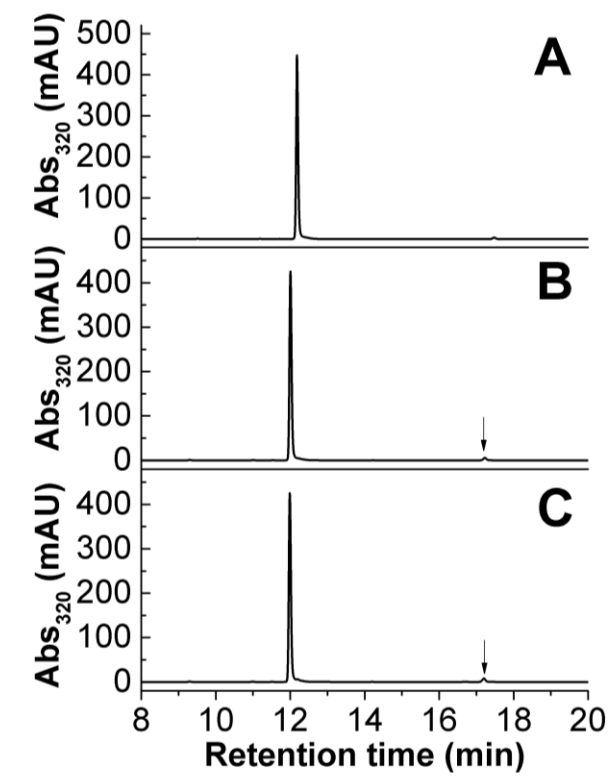


Figure 4.15 *In vitro* conversion of apigenin 7-*O*-glucoside to apigenin by Caco-2/TC7 cells. (A) Apigenin 7-*O*-glucoside standard (150 μ M). (B) Incubation of apigenin 7-*O*-glucoside (150 μ M) with Caco-2/TC7 cells/TC7 cells for 25 min. (C) Incubation of apigenin 7-*O*-glucoside (150 μ M) with Caco-2/TC7 cells/TC7 cells for 60 min. The detection of apigenin at both incubation times is indicated with the arrow.

Studies were conducted to explore the binding affinities of apigenin and apigenin 7-*O*-glucoside to GLUT2 in order to get a better insight on their interaction. Immunostaining of GLUT2 showed that the protein was present on both apical and basolateral sides of differentiated Caco-2/TC7 cell monolayers (figure 4.16). This was also confirmed by functional assays where the rate of D-[U-¹⁴C]-glucose transport under Na⁺-free conditions was the same from apical to basolateral compartments and *vice versa* (figure 4.17A). Having confirmed the localisation of GLUT2, inhibition constants for the exofacial glucose transporter inhibitor 4,6-*O*-ethylidene glucose and the endofacial glucose transporter inhibitor cytochalasin B on asymmetric D-[U-¹⁴C]-glucose transport were compared to those for apigenin and apigenin 7-*O*-glucoside (figure 4.17B,C and D). The results suggest that the two polyphenols apigenin and apigenin 7-*O*-glucoside bind at the

exofacial cavity of the transport channel since a 4-fold lower maximum inhibition was observed when the D-[U-¹⁴C]-glucose transport was assessed from basolateral to apical side which was also hold for the exofacial inhibitor 4,6-*O*-ethylidene glucose.

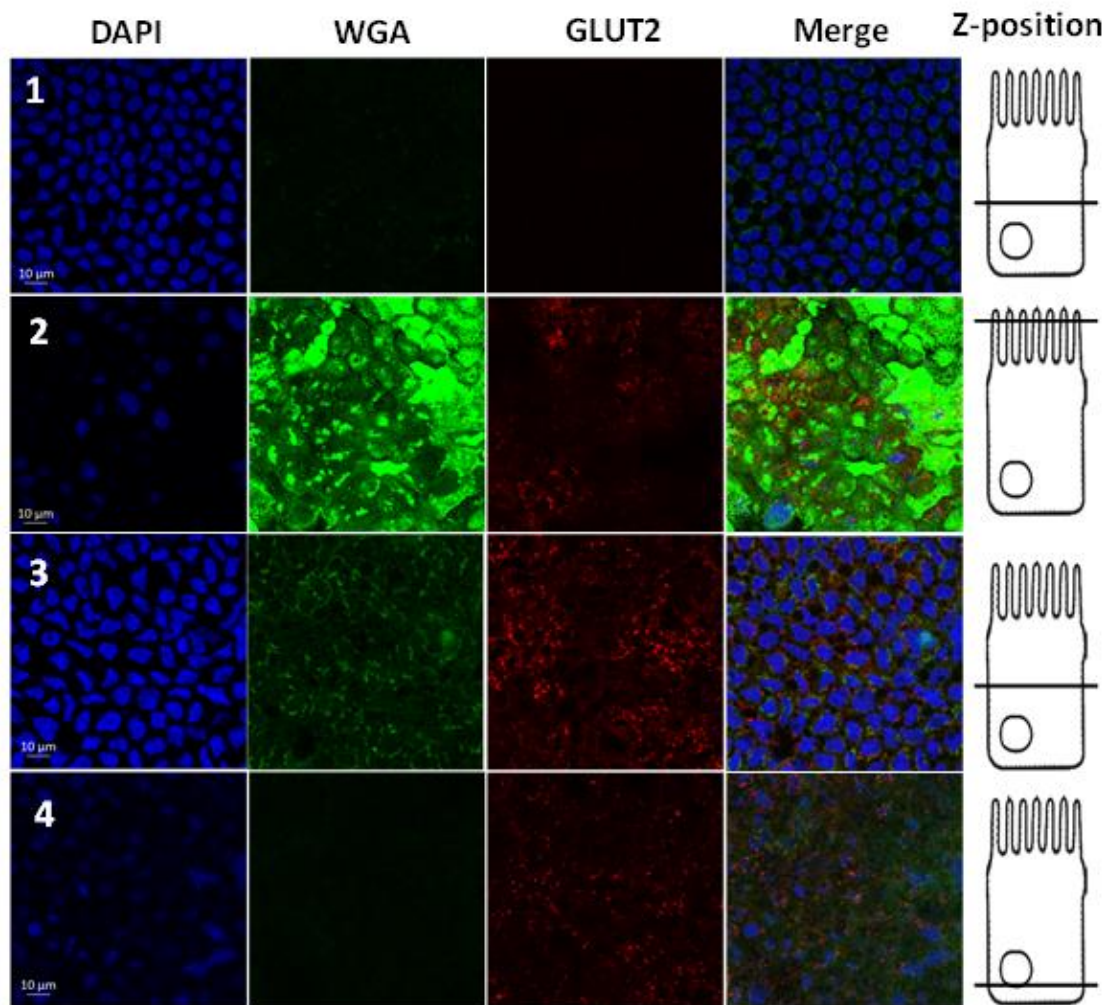


Figure 4.16. Immunofluorescence detection of GLUT2 in differentiated Caco-2/TC7 cell monolayers. Row 1 shows control cell layer incubated with 4',6-diamidino-2-phenylindole (DAPI) and Cy3-conjugated donkey anti-rabbit secondary antibody only. In rows 2-4 cells were incubated with DAPI, membrane marker wheat germ agglutinin (WGA), GLUT2 primary antibody and Cy3-conjugated donkey anti-rabbit secondary antibody. GLUT2 is shown in red, appearing orange when co-localising with DAPI and WGA shown in blue and green respectively. Staining revealed the presence of GLUT2 in the lateral and basal plasma membrane. Scale bars (10 μm) are shown in the lower left corner of DAPI images. Scale bar applies to all the images corresponding to each row. Images are representative examples of 3 independent immunostaining experiments (n=3).

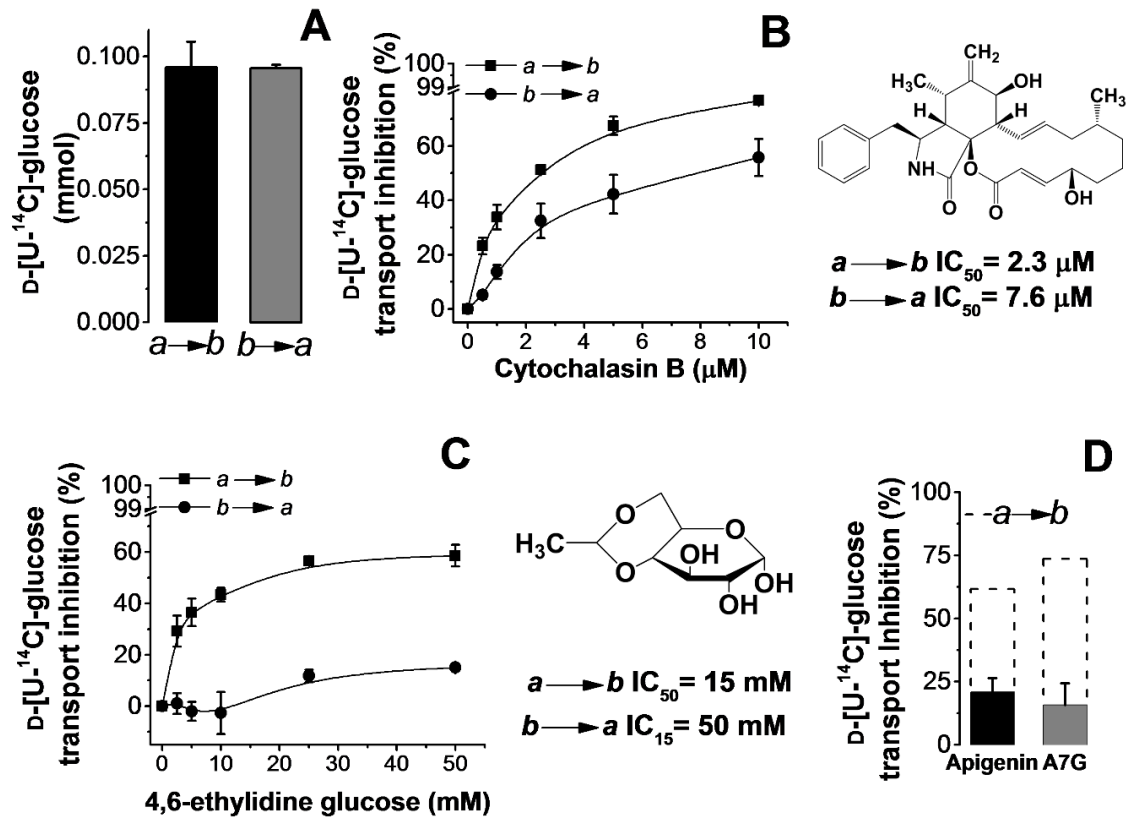


Figure 4.17 Characterisation of the potential binding site of apigenin and apigenin 7-*O*-glucoside (A7G) on GLUT2. Transport experiments were conducted under Na⁺-free conditions. (A) Asymmetric D-[U-¹⁴C]-glucose transport without inhibitor. (B) Asymmetric D-[U-¹⁴C]-glucose transport in the presence of cytochalasin B and inhibition constants. (C) Asymmetric D-[U-¹⁴C]-glucose transport in the presence of 4,6-ethylidene glucose and inhibition constants. (D) Inhibition of asymmetric D-[U-¹⁴C]-glucose transport by apigenin and A7G. Dotted line represents the inhibition values obtained at the maximum concentration tested when D-[U-¹⁴C]-glucose transport was assessed from apical (*a*) to basolateral (*b*) (data replotted from Fig 6C-2). Each data point represents the mean ± SEM (n = 3). In panel (B-C) results are expressed as % compared to the transported glucose in control incubations (no inhibitor; normalised to 100 %). When not visible, the error bars are smaller than the data point. In panel (B) and (C) statistical difference is indicated against incremental concentration of cytochalasin B and 4,6-ethylidene glucose respectively. **p* < 0.05, ***p* < 0.05.

Intestinal cells have the ability to adapt functionally to environmental stimuli such as diet (Drozdowski and Thomson, 2006). Therefore, ChE and apigenin was administered to Caco-2/TC7 cells for 96 h in order to assess whether the chronic treatment would affect

the D-[U-¹⁴C]-glucose transport by altering the intestinal expression of glucose transporters. Figure 4.18 shows that D-[U-¹⁴C]-glucose transport was unaffected implying that ChE and apigenin can potentially have an antihyperglycaemic effect exclusively by attenuating the activity of sugar transporters through physical interaction (acute effect). This means that an effect on postprandial glycaemia would only be possible when consumed at the same time as the carbohydrate or sugar source.

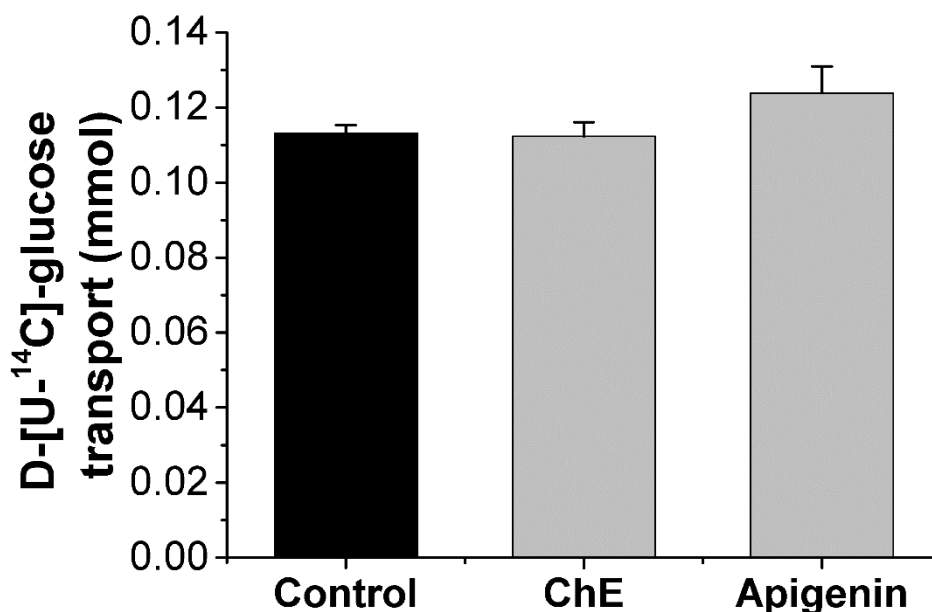


Figure 4.18 Effects of ChE and apigenin on D-[U-¹⁴C]-glucose transport across differentiated Caco-2/TC7 cell monolayers. Caco-2/TC7 cells were incubated with media (5 mM glucose) without (control) and with ChE (1 mg/mL) and apigenin (50 μ M) for 96 h (every 24 h, the media was replaced with fresh one). After the incubation period ended, media was discarded D-[U-¹⁴C]-glucose transport was assessed as described in section 4.3.2.2. Each data point represents the mean \pm SEM of three independent experiments with six technical replicates. No significant differences were found between control incubations and treatments.

The inhibition constants observed for apigenin and apigenin 7-*O*-glucoside on D-[U-¹⁴C]-glucose and D-[U-¹⁴C]-sucrose transport are realistic as intestinal intraluminal concentrations of polyphenols where they can be present in the mM range (Williamson, 2013). For instance, if 3 g of chamomile flowers are typically added to ~100 ml boiling water, then the concentration of extracted matter in the drink would be about 3 mg/mL assuming at least 10 % extraction. This would yield a content of apigenin and apigenin 7-

O-glucoside 60 and 20-fold higher than the necessary for 50% inhibition respectively. In the case of designed supplements and functional foods, the concentrations can be significantly higher depending on the type and the dose consumed. Thus, the individual intake of apigenin and apigenin 7-*O*-glucoside or their mixture as a botanical preparation (i.e. chamomile) could possibly inhibit, up to some extent, the glucose and fructose influx into the enterocyte and circulation, and could partially contribute to the positive effects recently observed by chamomile in type 2 diabetics subjects (Rafraf *et al.*, 2015; Zemestani *et al.*, 2016) and experimental diabetes (Cemek *et al.*, 2008; Weidner *et al.*, 2013).

4.5 Conclusion.

The findings of this work provide some mechanistic insights about the potential antidiabetic effects of chamomile, apigenin and apigenin 7-*O*-glucoside acting at the small intestinal site. Such a mechanism is mediated by acting at the different steps of carbohydrate digestion (described in chapter 3) and absorption. It is shown here that the drug acarbose does not affect glucose and fructose transport, and so would be ineffective against fructose and glucose absorption from, for example, high fructose corn syrups composed of free glucose and fructose and widely used as sweetener in fruit juices and beverages. Therefore botanical preparations such as chamomile and/or individual polyphenols such as apigenin and apigenin 7-*O*-glucoside can be exploited to develop food-based nutritional approaches which will diversify solutions spanning from preventive and complementary approaches for managing hyperglycaemia.

Chapter 5 Glucose stimulates cholesterol uptake in Caco-2 cells *via* upregulation of NPC1L1 protein receptor and this response is attenuated by the acute inhibition of glucose absorption by Chamomile and apigenin 7-*O*-glucoside.

5.1 Abstract.

Cholesterol uptake and chylomicron synthesis, which contribute to dyslipidaemia and cardiovascular risk factors, have been shown to be upregulated by high glucose levels in both healthy and diabetic individuals during the postprandial phase. The goal of this study was to determine the role of reducing glucose availability with polyphenols on Niemann-Pick C1 Like 1 protein expression and cholesterol uptake in simulated postprandial conditions using the intestinal cell model Caco-2. Cells incubated with glucose concentrations >5 mM showed an increase in [4-¹⁴C]-cholesterol uptake, however no significant differences were observed in concentrations ranging from 10-25 mM. Time-dependent studies indicated that this response is acute since the raise of [4-¹⁴C]-cholesterol uptake was observed at least 3 h post-incubation. The glucose-mediated increased uptake was parallel to an upregulation of Niemann-Pick C1 Like 1 protein receptor and this response was attenuated by the use of GLUT2 inhibitors ChE and apigenin 7-*O*-glucoside in a dose-dependent manner. Caco-2 cells did not express the efflux cholesterol transporter proteins ABCG5/G8 indicating that the attenuation of [4-¹⁴C]-cholesterol uptake relied solely on Niemann-Pick C1 Like 1. These data indicate that attenuation of intestinal glucose uptake with polyphenols may have pleiotropic effects on chylomicron-rich cholesterol synthesis with potential positive effects on postprandial lipemia in health and disease states.

5.2 Introduction.

Cholesterol is an indispensable component in the body as it forms part of most biological membranes. It plays a fundamental role in several physiological functions such as embryonic development, cell differentiation, nerve conduction and membrane fluidity; it also serves as precursor for the synthesis of steroid hormones and bile acids (Ge *et al.*, 2008; Yu *et al.*, 2014). However, high circulating levels of cholesterol cause severe problems including cardiovascular disease (Grundy *et al.*, 2004) and may be involved in liver (deOgburn *et al.*, 2012) and adipose tissue dysfunction (Aguilar and Fernandez, 2014). Blood cholesterol levels are regulated by several processes, including *de novo* synthesis from acetyl-CoA, cholesterol uptake from the intestinal lumen, and biliary clearance and excretion (figure 5.1).

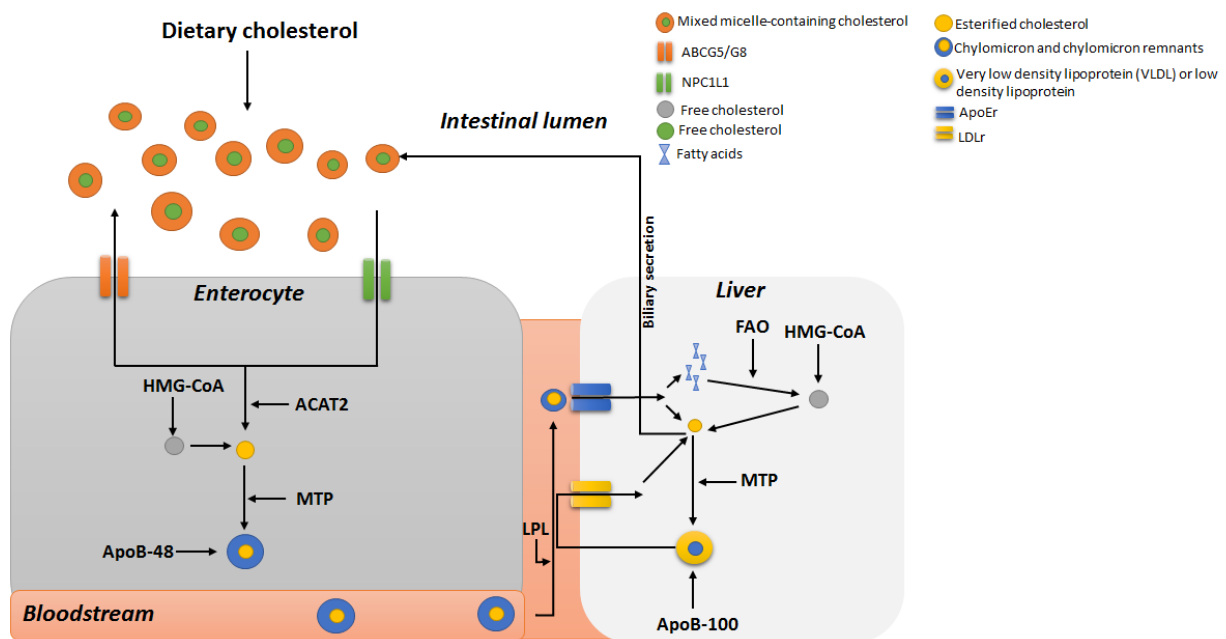


Figure 5.1 Cholesterol metabolism in the human body. After solubilisation in the mixed-micelles, dietary and biliary cholesterol is transported across the unstirred layer towards the brush-border membrane to facilitate its uptake by the apically-located receptor NPC1L1 (Wang, 2007). Both luminal free cholesterol and that produced by *de novo* synthesis (HMG-CoA-mediated) can either be exported back to the lumen *via* ABCG5/8 transporter proteins or move to the endoplasmic reticulum where it undergoes esterification by ACAT2. Cholesteryl esters are incorporated into ApoB-48 and exported to the lymph forming part of chylomicron particles (Dash *et al.*, 2015). Once in circulation, the chylomicron-triglyceride component is hydrolysed by

LPL expressed on the surface of adipocytes, myocytes, and macrophages, producing cholesterol remnants. The triglyceride component is used for energy production, stored in the liver or adipocytes *via* lipogenesis or exported back into circulation as a VLDL component (Bays *et al.*, 2016). Cholesterol remnants are conjugated with ApoE and cleared by the liver *via* the ApoE receptor (Tomkin and Owens, 2011). In the liver, cholesteryl esters are either exported back to the lumen through the enterohepatic circulation of bile acids or excreted as VLDL with Apo-B100 as the solubilising protein. As chylomicrons, VLDL are hydrolysed by LPL giving rise to LDL which are taken back into the liver by LDLr, representing another source of cholesteryl esters and cholesterol for further processing (Tomkin and Owens, 2011; Bays *et al.*, 2016). NPC1L1: Niemann-Pick C1 Like 1 protein receptor; HMG-CoA: 3-hydroxy-3-methylglutaryl-CoA; ACAT2: acetyl-CoA:cholesterol acyltransferase isoform 2; MTP: microsomal transfer protein; LPL: lipoprotein lipase; FAO: fatty acid oxidation; LDLr: low density lipoprotein receptor; ApoEr: ApoE receptor.

The use of statin, a drug reducing the *de novo* synthesis of cholesterol by inhibiting the activity of 3-hydroxy-3-methylglutaryl-CoA reductase (HMG-CoA), has been widely prescribed to reduce the levels of low density lipoprotein cholesterol (LDL-C) in subjects at risk of atherosclerosis or coronary heart disease (Kastelein, 2014; Nordestgaard and Varbo, 2014). However, in a substantial number of cases, statin therapy does not lower LDL-C levels to the desired goal and residual risk factors such as high levels of remnant cholesterol remain (Nordestgaard and Varbo, 2014; Kones and Rumana, 2015). It is well established that there is a positive and significant correlation between circulating levels of LDL-C and dietary and biliary cholesterol absorption (Wang, 2007), pointing out the importance of this metabolic pathway to manage whole body cholesterol homeostasis, independently of *de novo* synthesis.

NPC1L1 transmembrane protein receptor located on apical enterocytes has been identified as a critical player to take up readily available cholesterol from the gut lumen across species (Altmann *et al.*, 2004; Davis and Veltri, 2007; Jia *et al.*, 2011). NPC1L1-deficient mice demonstrated a drastic reduction of dietary cholesterol absorption (~70 %) (Altmann *et al.*, 2004). Like other transmembrane protein transporters, NPC1L1 activity is influenced by surrounding nutrients and cell-intrinsic nutrient sensors. For instance, *in vitro* studies have shown that NPC1L1 is translocated from the endocytic recycling

compartment to the apical membrane after cholesterol depletion (Yu *et al.*, 2006; Brown *et al.*, 2007); this response is thought to be controlled by the sterol response element binding protein 2 (SREBP2) (Alrefai *et al.*, 2007) which senses cholesterol levels and activates appropriated intracellular responses to maintain homeostasis (Horton *et al.*, 2002).

Like cholesterol, glucose also controls the expression of NPC1L1 gene and protein levels. In Caco-2 cells, chronic treatment with high glucose (25 mM, 24 h) upregulated the apical localisation of NPC1L1 resulting in an increased cholesterol uptake (~30-50 %) compared to cells incubated under physiological fasting glucose levels (Ravid *et al.*, 2008). In a subsequent study using the same *in vitro* model, it was shown that glucose directly modulates NPC1L1 expression *via* transcriptional mechanisms and this effect was dependent of glucose metabolism (Malhotra *et al.*, 2013). These studies were inspired by the recognised feature of dyslipidaemia in diabetics where NPC1L1 expression, concomitant with chylomicron production, is increased (Lally *et al.*, 2006; Adeli and Lewis, 2008), and this has been proposed as an important risk factor for cardiovascular disease in this population (Tomkin, 2010; Tomkin and Owens, 2015; King and Grant, 2016). Interestingly, *in vivo* evidence suggest that increased chylomicron production can occur in healthy individuals during the postprandial phase in response to glucose and insulin levels (Harbis *et al.*, 2001; Xiao *et al.*, 2013; Xiao *et al.*, 2016). This could contribute to the metabolic dysregulation observed during this period such as endothelial dysfunction and low grade inflammation with important long-term metabolic consequences on insulin resistance and type 2 diabetes onset.

Several lines of evidence including epidemiological studies, human intervention studies as well as mechanistic studies in animal and *in vitro* models have highlighted the potential of polyphenols to confer cardioprotection (Hertog *et al.*, 1997; McCullough *et al.*, 2012; Kishimoto *et al.*, 2013). Due to the potential of polyphenols to attenuate carbohydrate digestion and sugar absorption and to the intrinsic link between glucose metabolism and luminal cholesterol uptake, it can be hypothesised that polyphenols can reduce chylomicron-rich cholesterol particles by downregulating apical NPCL1 expression in the enterocytes. This mechanism could have a positive knock on effect on insulin resistance, type 2 diabetes and cardiovascular health and may partially explain the modulatory

effects of polyphenols on postprandial lipid metabolism observed in some human intervention studies (Pal and Naissides, 2004; Annuzzi *et al.*, 2014). Therefore, the present study was undertaken to examine for the first time the regulation of NPC1L1 and cholesterol uptake by glucose in intestinal Caco2 cells during postprandial conditions and to assess the potential of polyphenols to modulate this metabolic pathway by inhibiting the glucose transporter protein GLUT2.

5.3 Materials and methods.

5.3.1 Materials.

The ChE and authentic standards of apigenin and apigenin 7-*O*-glucoside were obtained from PhytoLab Co. KG.h as a lyophilised powder. D-glucose, cholesterol, L- α -phosphatidylcholine, oleic acid, taurocholic acid sodium salt hydrate, cytochalasin B from *Drechslera dematioidea*, Dulbecco's Modified Eagle's Medium (including L-glutamine, NaHCO₃ and pyridoxine HCl) and phosphate buffer saline (PBS) were all purchased from Sigma-Aldrich. Co., Ltd., Dorset, UK. [4-¹⁴C]-cholesterol was purchased from Perkin Elmer (Boston, USA). TATA-box binding protein (TBP, Hs01086390_m1), NPC1L1 (Hs00905233_m1), ABCG5 (Hs00223686_m1) and ABCG8 (Hs00223690_m1) FAMTM-labelled TaqMan primers and RIPA lysis buffer and Dulbecco's Modified Eagle's Medium without glucose (including L-glutamine) were from Thermo Fisher Scientific, Leicestershire, UK. RNAqueous-4PCR (AM1912) and high capacity RNA-to cDNA master mix kits were obtained from Applied Biosystems, Warrington, UK. Caco-2 cell line (HTB-37) was obtained from the American Type Culture Collection (LGC Promochem, Middlesex, UK). Distilled water was used for all the experiments (Millipore UK Ltd., Hertfordshire, UK). All the reagents were of the highest purity and standards were $\geq 98\%$.

5.3.2 Methods.

5.3.2.1 Preparation of ChE for bioactivity studies.

ChE was prepared as previously described in chapter 2 section 2.3.2.1.

5.3.2.2 Cell culture.

Caco-2 cells were cultured as described in chapter 4, section 4.3.2.1.

5.3.2.3 Preparation of mixed-micelles.

Stock solutions of micelle components including oleic acid, L- α -phosphatidylcholine, cholesterol, taurocholic acid and [4-¹⁴C]-cholesterol were prepared on the day of the experiment in ethanol (100 %) and mixed in pre-defined molar ratios. After drying with a stream of N₂, serum-free supplemented medium containing varying concentrations of glucose (5, 10, 15, 20 and 25 mM) was added to the lipid layer and stirred vigorously at

37 °C for 45 min. The final concentrations of the individual micelle components were as follows: 0.05 mM cholesterol, 0.3 mM oleic acid, 0.01 mM L- α -phosphatidylcholine, 5 mM taurocholic acid and 0.12 μ Ci/mL of [4- 14 C]-cholesterol. The incorporation of cholesterol into the mixed-micelles was confirmed by measuring their size using light scattering. For this experiment, a solution containing only cholesterol was prepared to assess the formation of the lipid-self-assembly mixed-micelles. Additionally, mixed-micelles were prepared as described above with and without cholesterol to measure its incorporation into the self-assembly bodies. For each measurement, ~1 mL of micellar mixture was placed in plastic cuvettes in a Zetasizer NanoSeries Nano ZS (Malvern, U.K.) particle characterisation system and particle size distribution was measured using a standard protocol. The confirmation of the formation of mixed-micelles and the incorporation of cholesterol is shown in figure 5.2.

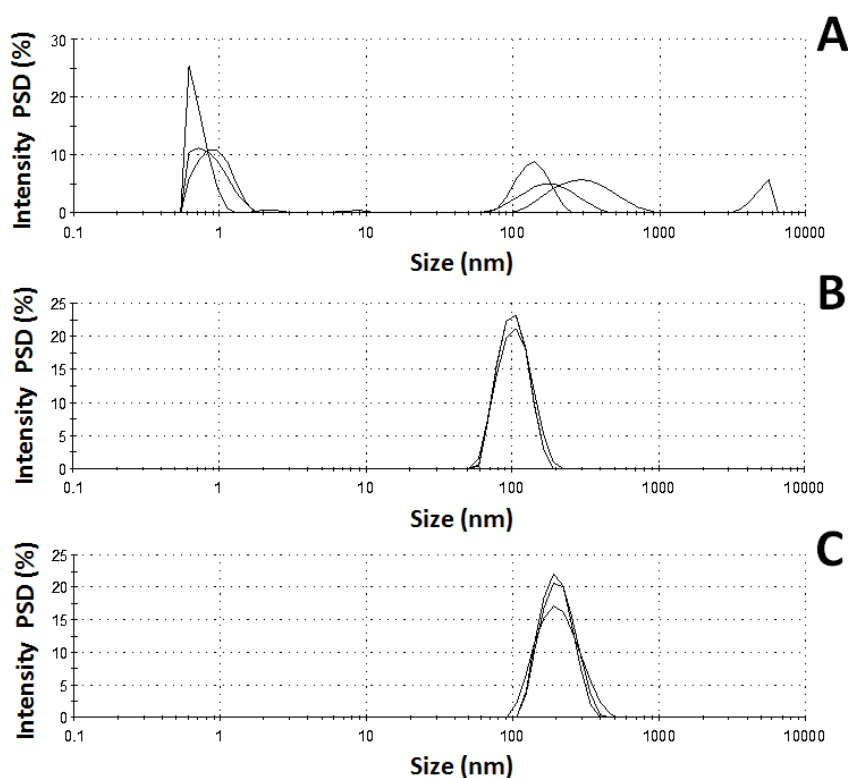


Figure 5.2 Formation of mixed-micelle containing cholesterol as assessed by particle size and distribution. (A) Insoluble cholesterol in solution, B) mixed-micelle formation without cholesterol and C) mixed-micelle containing cholesterol. The formation of self-assembly micelles can be observed by the homogenous distribution of size particle when comparing with insoluble cholesterol. Micelles containing-cholesterol presented an increase in particle size of more than-

100 %. Three individual experiments were conducted and the average particle size was analysed in triplicate. PSD: particle size distribution.

For initial experiments, Caco-2 cells (between passages 48–60) were seeded in transwell and flat bottom 6-well plates at a density of 6.43 and 5.6×10^4 cells/cm² per well respectively. Cells were grown under a humidified atmosphere containing 5 % CO₂ at 37 °C, Dulbecco's Modified Eagle's Medium (1000 mg/L glucose), supplemented with 15 % heat-inactivated fetal calf serum, 2 % L-alanyl-L-glutamine (200 mM) and 1 % penicillin-streptomycin (100 U/mL). The media in the apical (1.5 mL) and basal (2 mL) compartments was replaced every other day for 21 days; the time at which cells are completely differentiated and ready for uptake experiments. In cells seeded on transwell plates, the integrity of the monolayer was assessed by measuring the TEER values obtaining an average value of 500 ohms. On day 21, cells were washed three times with PBS solution (37 °C) and incubated in a glucose-free supplemented media containing the final concentration of 5 mM glucose added to the apical and basolateral compartments for 24 h. After, cells were washed twice with PBS and uptake assay was initiated by incubating the cells at 37 °C for 60 min with a mixed-micelle solution (1.5 mL) containing 5 mM glucose (for transwell plates, serum-free supplemented medium with 5 mM glucose was added to the basal compartment). At the end of the incubation, the unincorporated radiolabelled cholesterol was removed by washing the cells four times with 1.5 ml of ice-cold PBS, scraped in 0.1 (transwell plates) and 0.2 (bottom flat plates) mL of RIPA lysis buffer (25 mM Tris•HCl pH 7.6, 150 mM NaCl, 1% NP-40, 1% sodium deoxycholate, 0.1% SDS) followed with dilution (1:3 v/v) with ice-cold PBS and centrifugation at 14000 g for 10 min to remove cell debris. The radioactivity was estimated from an 8-point linear calibration curve using scintillation counting and normalised to the concentration of protein in the sample to represent total cholesterol uptake. Protein content was determined by Bradford according to the manufacturer procedure. As depicted in figure 5.3, there were no differences in the total [4-¹⁴C]-cholesterol uptake between transwell plates and flat bottom plates, implying that the formation of the basolateral side is not required for the synthesis of cholesterol transporter proteins.

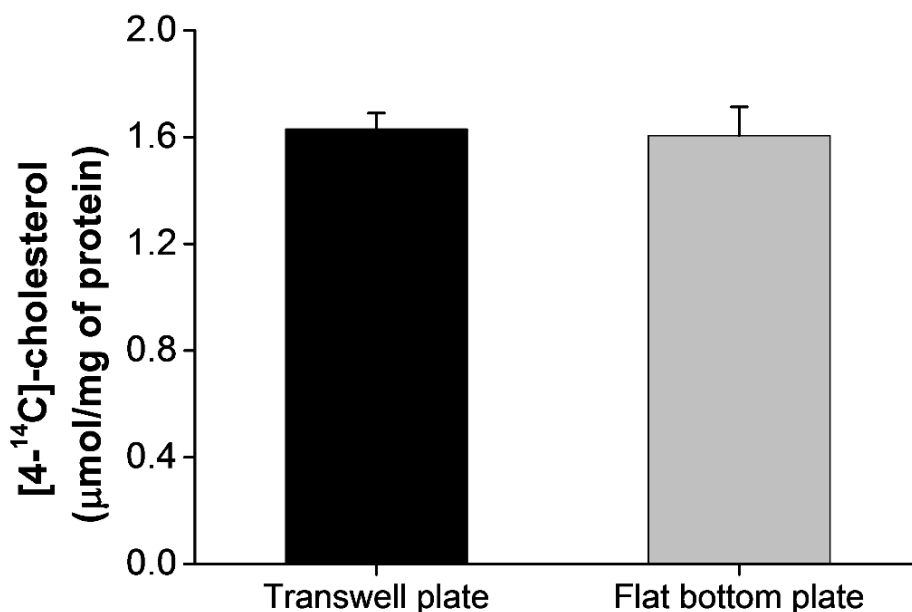


Figure 5.3 Effect of type of plate on [4-¹⁴C]-cholesterol uptake in Caco-2 cells. Differentiated Caco-2 cells were cultured for 24 h in media containing 5 mM glucose. At the end of the preincubation time, cells were exposed to micelle solution spiked with [4-¹⁴C]-cholesterol in the presence of the same concentrations of glucose for 60 min. No differences in uptake were observed regardless of the plate used ($p < 0.05$). Three biological replicates with three technical replicates were employed. Results are expressed as mean values \pm SEM.

Further assays looking at the influence of glucose concentration on [4-¹⁴C] cholesterol uptake and the effect of glucose inhibitors on this pathway were conducted on 6-well flat bottom plates after cells were completely differentiated.

5.3.2.4 Acute inhibition of D-[U-¹⁴C]-glucose uptake.

For D-[U-¹⁴C]-glucose uptake, cells were grown and treated with different glucose concentrations as described above for [4-¹⁴C]-cholesterol uptake assays with an incubation period of 3 h in the presence and absence of the GLUT2 inhibitors. Then the uptake assay was initiated by adding 1.5 µL of radiolabelled glucose (0.15 µCi/mL) and stopped after 1 h with ice-cold PBS. Cells were processed and D-[U-¹⁴C]-glucose uptake estimated with an 8-point linear calibration curve as indicated for [4-¹⁴C]-cholesterol experiments. For this experiment, the GLUT2 inhibitors Cytochalasin B, ChE and apigenin 7-*O*-glucoside were used since this protein is the main active transporter of

glucose at concentrations ≥ 10 mM in Caco-2 cells (Grefner *et al.*, 2012; Zheng *et al.*, 2012). Cytochalasin B was used as a positive control due to its higher capacity to inhibit GLUT2 than polyphenols. To assess the potential of polyphenols, ChE and apigenin 7-*O*-glucoside were employed.

5.3.2.5 Gene expression analysis of cholesterol flux transporters.

RNA isolation and quantitative gene expression analysis of cholesterol flux transporter proteins were conducted as described in chapter 4 section 4.3.2.3 with the appropriate primers. The average number of accepted droplets was 14130 ± 2130 (n= 27).

5.3.3 Statistical analysis.

Statistical analysis was performed by one-way analysis of variance using the Number Cruncher Statistical System version 6.0 software (NCSS, LLC). Significant differences were assessed with Tukey-Kramer multiple comparison test and *t* test when appropriate ($p < 0.05$). Data is expressed as the mean \pm SEM.

5.4 Results and discussion.

5.4.1 Glucose promote [4-¹⁴C]-cholesterol uptake in Caco-2 cells.

Cardiovascular disease represents the main cause of morbidity and mortality in diabetes (King and Grant, 2016). The typical dyslipidaemia that is associated with insulin resistance has been proposed to play an important role in the atherogenic process mediated by cholesterol-rich lipoproteins (Nordestgaard and Varbo, 2014). Furthermore, the now established observation that Apo-B48-containing remnant lipoproteins are elevated in insulin resistant and type 2 diabetes (Adeli and Lewis, 2008; Tomkin and Owens, 2011; Veilleux *et al.*, 2014; Tomkin and Owens, 2015) has encouraged the study of the metabolic events that promote cholesterol rich-lipoprotein overproduction in the small intestine. Special attention has been put on the contribution of NPC1L1 to this condition, since elevated expression levels have been found under these pathophysiological conditions in both animal and human subjects (Lally *et al.*, 2007; Levy *et al.*, 2010), suggesting it represents an important control point for the assembly of cholesterol-rich ApoB-48 particles and whose expression can be regulated by glucose levels. Indeed, mechanistic studies in Caco-2 cells employing experimental settings that resemble chronic exposure to elevated glucose levels, have shown that glucose upregulates the expression of NPC1L1 increasing the uptake of cholesterol (Ravid *et al.*, 2008; Malhotra *et al.*, 2013) corroborating the observations found *in vivo*.

In order to confirm the previous observations and validate the model for subsequent studies, two concentrations of glucose on [4-¹⁴C]-cholesterol uptake were examined. Following pre-incubation (24 h) of differentiated Caco-2 cell monolayers on solid supports with medium containing 5 or 25 mM glucose, [4-¹⁴C]-cholesterol uptake was determined with short- and long-term incubation. As shown in figure 5.4, [4-¹⁴C] cholesterol uptake was linear as a function of time up to 1 and 2 h in cells treated with 25 and 5 mM glucose respectively.

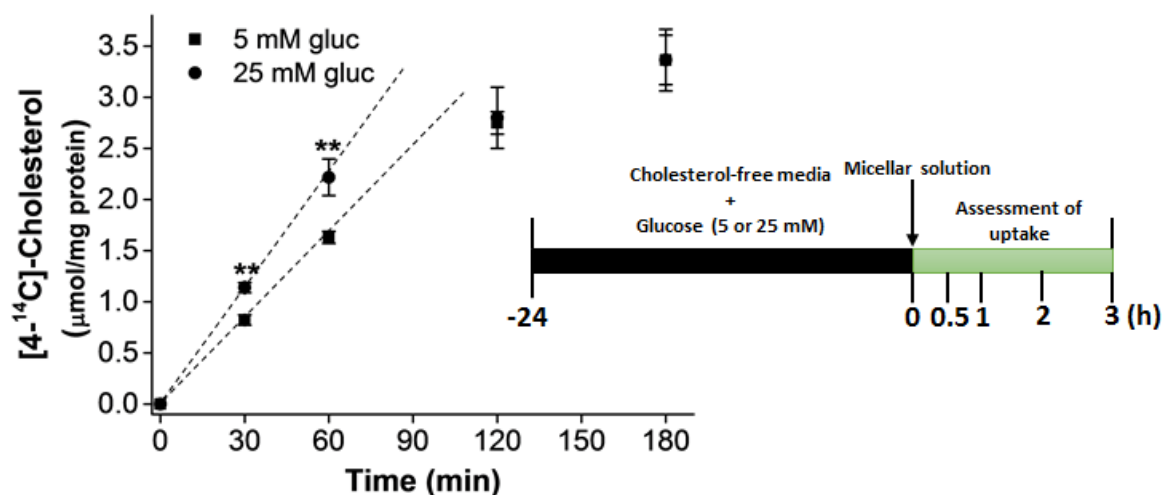


Figure 5.4 Effect of glucose concentration and incubation time on [4-¹⁴C]-cholesterol uptake in Caco-2 cells. Differentiated Caco-2 cells were cultured for 24 h in media containing either 5 or 25 mM glucose. At the end of the pre-incubation time, cells were exposed to a micelle solution spiked with [4-¹⁴C]-cholesterol in the presence of the same concentrations of glucose (either 5 or 25 mM) for the indicated time (30-180 min). Linear uptake of [4-¹⁴C]-cholesterol is indicated with dotted lines. The diagram showing the procedure used to treat the cells is presented next to the panel. The data represent the mean value of three seeding experiments with at least 3 technical replicates. Results are expressed as mean values \pm SEM. ** $p < 0.01$ compared with cells incubated with 5 mM glucose. When not visible, the error bars are smaller than the data point.

Caco-2 cells incubated with 25 mM glucose showed an increase of total [4-¹⁴C]-cholesterol uptake with an absorption rate of 0.04 $\mu\text{mol/mg}$ of protein/min which was higher than when cells were incubated with 5 mM glucose (0.026 $\mu\text{mol/mg}$ of protein/min) after 60 min. In contrast, no differences were observed in [4-¹⁴C]-cholesterol uptake at 120 and 180 min between cells incubated at 5 and 25 mM glucose indicating that equilibrium was reached at those time points. These data confirm previous observations on glucose-mediated increase of cholesterol uptake in Caco-2 cells, validating the suitability of the model for the subsequent studies (Ravid *et al.*, 2008; Malhotra *et al.*, 2013).

The majority of the studies conducted in cell models looking at the effect of glucose concentration on different biomarkers, including cholesterol uptake, normally have employed 25 mM glucose (Ravid *et al.*, 2008; Malhotra *et al.*, 2013) which represents a value that might not be achieved under physiological circumstances, even in type 2 diabetic subjects. Therefore [4-¹⁴C]-cholesterol uptake assays were conducted using varying concentrations of glucose to reveal if the promoting effect on uptake can be maintained at concentrations below 25 mM (figure 5.5). The results indicate that the uptake of [4-¹⁴C]-cholesterol in Caco-2 cells is stimulated at concentrations above 5 mM (control conditions). However, no significant changes ($p < 0.05$) in uptake induction were observed at concentrations between 10-25 mM glucose which showed an overall increase ~28 % as compared to cells incubated in 5 mM glucose.

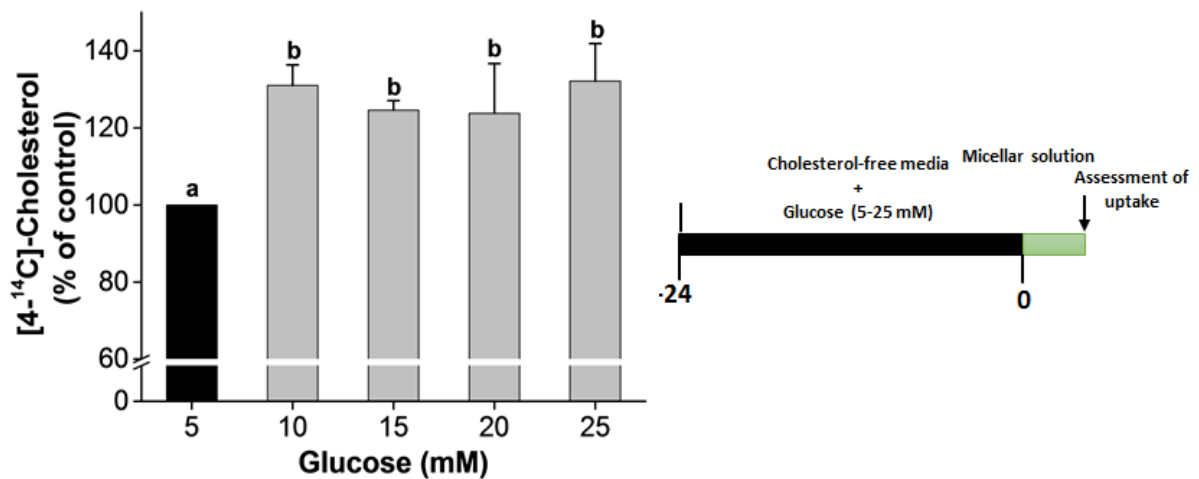


Figure 5.5 Effect of glucose concentration on [4-¹⁴C]-cholesterol uptake in Caco-2 cells. Differentiated Caco-2 cells were cultured for 24 h with different concentrations of glucose. At the end of the pre-incubation time, cells were exposed to a micelle solution spiked with [4-¹⁴C]-cholesterol in the presence of the same concentration of glucose before uptake was assessed. The diagram showing the procedure used to treat the cells is presented next to the panel. The data represent the mean value of three seeding experiments with at least 3 technical replicates. Results are expressed as mean values \pm SEM. Different letters denote significant differences ($p < 0.05$) between treatments. When not visible, the error bars are smaller than the data point.

The experiments in figure 5.4 and 5.5 were conducted by incubating the cells in varying concentrations of glucose for 24 h before [4-¹⁴C]-cholesterol uptake was assessed. However, the observed changes in uptake influenced by glucose may occur at shorter

incubation times, which would prove the relevance of glucose concentrations on cholesterol uptake during the postprandial period using an *in vitro* model. In order to elucidate this, Caco-2 cells were incubated at different times with 10 mM glucose and [4-¹⁴C]-cholesterol uptake was examined. As illustrated in figure 5.6, exposure to 10 mM glucose compared with 5 mM resulted in a significant increase in the uptake as soon as 3 h postincubation time and, in general, the effect was maintained constant over a period of 24 h with a maximum increase in uptake ~25 % with regard to control incubations (5 mM). Moreover, there was a slight but significant effect of glucose concentration on the initial uptake.

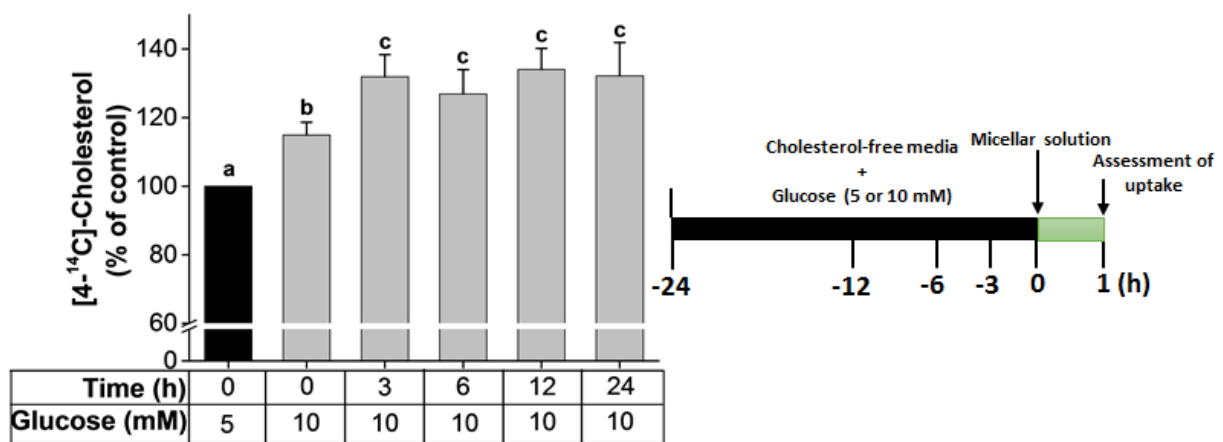


Figure 5.6 Time-dependence effect of glucose concentration on [4-¹⁴C]-cholesterol uptake in Caco-2 cells. Caco-2 cells were incubated with 10 mM glucose at different times and uptake examined and compared with those incubated with 5 mM glucose. The diagram showing the procedure used to treat the cells is presented next to the panel. The data represent the mean value of three seeding experiments with at least 3 technical replicates. Results are expressed as mean values \pm SEM. Different letters denote significant differences ($p < 0.05$) between treatments. When not visible, the error bars are smaller than the data point.

Importantly, these results suggest that increased uptake of cholesterol *via* NPC1L1 is not exclusively of insulin resistance and type 2 diabetes, it could also occur in response to acute glucose excursions in healthy individuals. In support of this statement, acute infusion of glucose alongside with a lipid emulsion directly into the duodenum or through intravenous administration, and under conditions of a pancreatic clamp (to avoid any confounding effect of insulin), stimulated the production and increased plasma

concentration of Apo-B48 lipoproteins (~2-2.5-fold) compared to a saline infusion in healthy subjects over a period of 10 h (Xiao *et al.*, 2013; Xiao *et al.*, 2016). Furthermore, glucose triggered the release of lipids from the enterocytes increasing Apo-B48 levels in serum compared to water intake in healthy individuals (Robertson *et al.*, 2003). Although the content of cholesterol contained in the chylomicrons was not evaluated in these studies, based on these results, it can be predicted a higher concentration in the test subjects than controls. Therefore further studies are warranted looking at the impact of glucose on the concentration of cholesterol in chylomicrons during the postprandial phase.

5.4.2 [4-¹⁴C]-cholesterol uptake in Caco-2 cells is attenuated by acute inhibition of glucose absorption by ChE and apigenin 7-*O* glucoside.

The observation that glucose control the expression of intestinal NPC1L1 and therefore, the uptake of luminal cholesterol during the postprandial phase, led us to hypothesise that polyphenols can have a positive knock-on effect on cardiovascular health by attenuating glucose availability within the enterocyte. This may represent a mechanism through which polyphenols in general and ChE in particular confer cardioprotection as observed *in vivo* in mice (Weidner *et al.*, 2013) and humans (Rafraf *et al.*, 2015).

Caco-2 cells were incubated with 10 and 25 mM glucose in the presence of varying concentrations of previously characterised inhibitors of glucose absorption ChE and apigenin 7-*O*-glucoside (figure 5.7). In general, pre-incubation of cells with ChE and apigenin 7-*O*-glucoside resulted in an attenuation of [4-¹⁴C]-cholesterol uptake by Caco-2 cells. ChE was effective at attenuating [4-¹⁴C]-cholesterol uptake in a dose-dependent manner, with the greatest effect shown at concentrations above 0.1 mg/mL and maintained up to 1 mg/mL and this effect was irrespective of the glucose concentration used to pre-treat the cells (figure 5.7A and B). The overall response induced by ChE was comparable to that obtained for the positive control cytochalasin B (~82 %) (figure 5.7C and D).

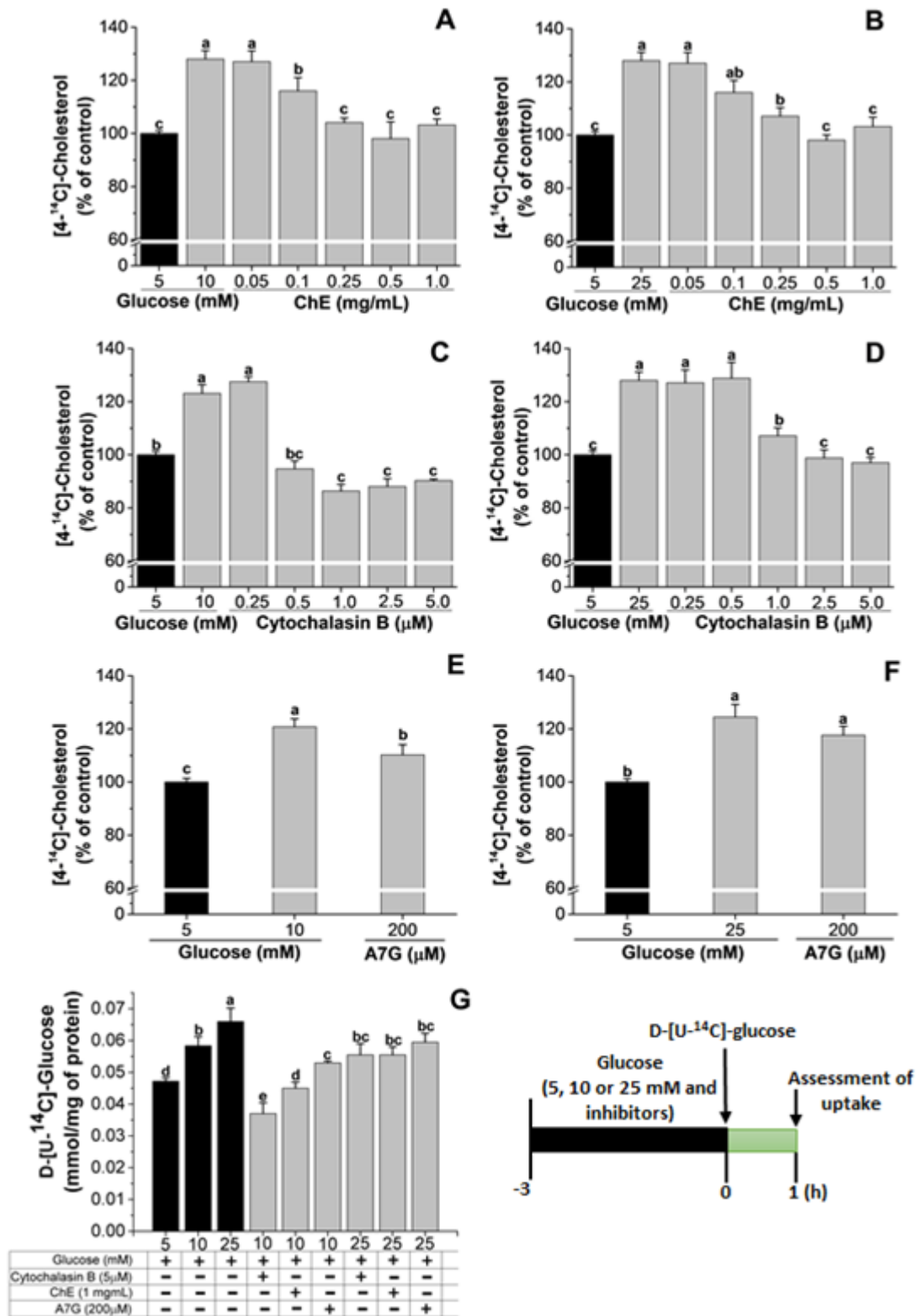


Figure 5.7 Effect of acute inhibitors of glucose absorption on [4-¹⁴C]-cholesterol uptake.

Caco-2 cells were cultured for 3 h in media containing either 10 or 25 mM glucose in the presence of varying concentration of glucose inhibitors. At the end of the preincubation time, cells were exposed to micelle solution spiked with [4-¹⁴C]-cholesterol in the presence of the same

concentrations of glucose (10 or 25 mM) for the indicated period of time. (A and B) Uptake of [4-¹⁴C]-cholesterol after preincubation of cells with ChE. (C and D) Uptake of [4-¹⁴C]-cholesterol after preincubation of cells with cytochalasin B. (E and F) Uptake of [4-¹⁴C]-cholesterol after preincubation of cells with apigenin 7-*O*-glucoside (A7G). (G) After the preincubation period with glucose and inhibitors as indicated in the adjacent diagram, D-[U-¹⁴C]-glucose was directly added to the media and uptake was assessed over a period of 1 h. In all the experiments, cells incubated with 5 mM glucose were used as general control. In panel (A-F), inhibition is expressed as % compared to control incubations (5 mM glucose; normalised to 100 %). The data represent the mean value of three seeding experiments with at least 3 technical replicates. Results are expressed as mean values ± SEM. Different letters indicate significant differences ($p < 0.05$) between treatments. When not visible, the error bars are smaller than the data point.

Previous characterisation studies on the effect of apigenin 7-*O*-glucoside to reduce glucose absorption revealed an IC₅₀ value around its maximum soluble concentration (~200 μM). Therefore in the present experiment Caco-2 cells were pre-incubated only with a single concentration of apigenin 7-*O*-glucoside. The results show that apigenin 7-*O*-glucoside was effective at reducing glucose-induced [4-¹⁴C]-cholesterol uptake with a decrease of ~50 and 30 % when incubated in 10 and 25 mM glucose respectively (figure 5.7E and F). Although apigenin 7-*O*-glucoside showed a much more modest effect at attenuating [4-¹⁴C]-cholesterol uptake by Caco-2 cells, based on the results, a more pronounced reduction of cholesterol uptake can be predicted if higher concentrations are used. A direct evidence between the attenuation of [4-¹⁴C]-cholesterol uptake in Caco-2 cells and reduction of glucose availability was established by measuring D-[U-¹⁴C]-glucose uptake. As expected, ChE and cytochalasin B showed the strongest inhibitory effect on D-[U-¹⁴C]-glucose absorption regardless of the concentration of glucose employed to incubate the cells (figure 5.7G). ChE was effective at reducing D-[U-¹⁴C]-glucose uptake when cells were incubated in 10 mM glucose showing reductions comparable to control incubations (5 mM). However in cells incubated in 25 mM glucose the effect is clearly reduced, which was reflected in a lower attenuation of [4-¹⁴C]-cholesterol uptake by Caco-2 cells; this observation was also held for Cytochalasin B. Apigenin 7-*O*-glucoside showed the lowest attenuation effect of D-[U-¹⁴C]-glucose uptake with an overall reduction of ~50 and 35 % in cells incubated with 10 and 25 mM glucose respectively.

The levels of cholesterol uptake into the enterocyte are dictated by the balance of the expression and function of apically-located transporter proteins responsible for cholesterol flux. Therefore the reduction of [4-¹⁴C]-cholesterol uptake exhibited by Caco-2 cells incubated in the presence of ChE and apigenin 7-*O*-glucoside may be due to an up- and downregulation in the expression of cholesterol efflux and influx transporters ABCG5/G8 and NPC1L1, respectively. To test this hypothesis, the protein expression of cholesterol transporters present in intestinal epithelial cells was examined. As shown in figure 5.8, Caco-2 cells did not show any expression of the efflux transporters ABCG5 and ABCG8 which is in line with previous observations reporting no expression of these proteins in Caco-2 cells from 10 different laboratories (Hayeshi *et al.*, 2008). The results indicate that the attenuation of [4-¹⁴C]-cholesterol uptake may be caused solely by the lowered expression levels of the influx transporter receptor NPC1L1. Indeed, cells exposed to ChE, apigenin 7-*O*-glucoside and Cytochalasin B presented reduced expression levels of this protein than their counterparts exposed to 10 and 25 mM glucose (figure 5.9).

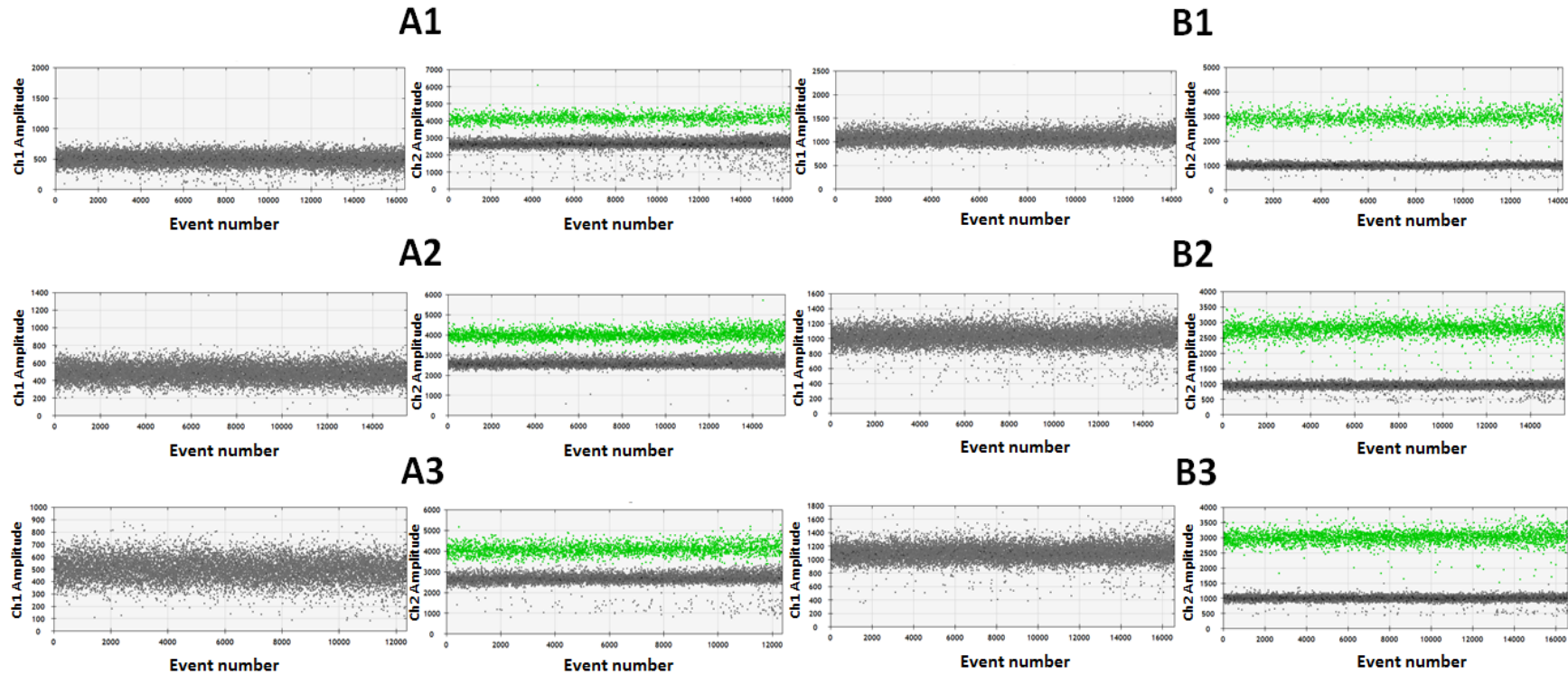


Figure 5.8 Representative examples of ABCG5/G8 and TBP ddPCR expression analysis following incubation in media with different glucose concentrations. (A1-A3) Quantitative expression analysis of ABCG5. (B1-B3) Quantitative expression analysis of ABCG8. (A1-B1), 5 mM glucose, (A2-B2), 10 mM glucose and (A3-B3), 25 mM glucose. Data viewed as a 1-D plot with each droplet from a sample plotted on the graph of fluorescence intensity vs droplet number. Left panels represent the droplets recorded for either ABCG5 or ABCG8. Right panels represent the droplets recorded for TBP. Positive and negative droplets are indicated in green and grey respectively for TBP. For ABCG5/8 only negative droplets were recorded indicating null expression of these proteins. Three biological replicates in three seeding experiments were pooled and analysed six times.

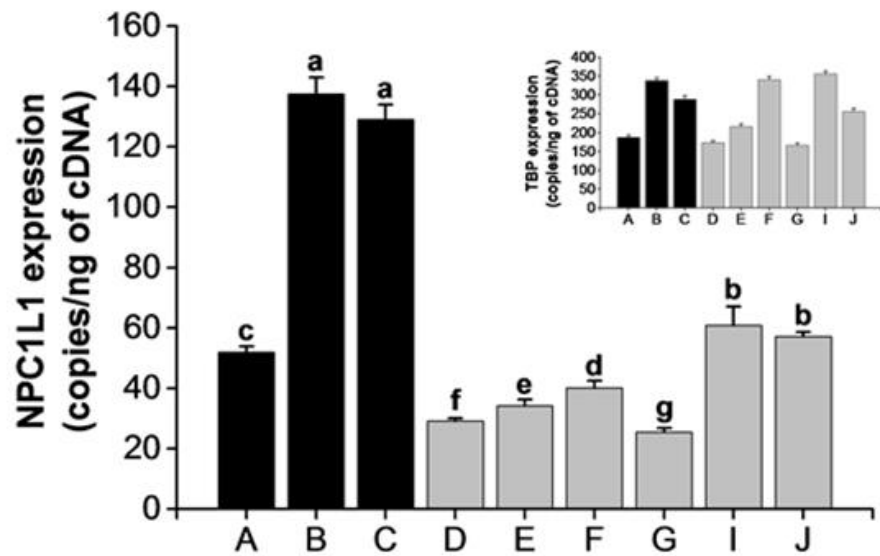
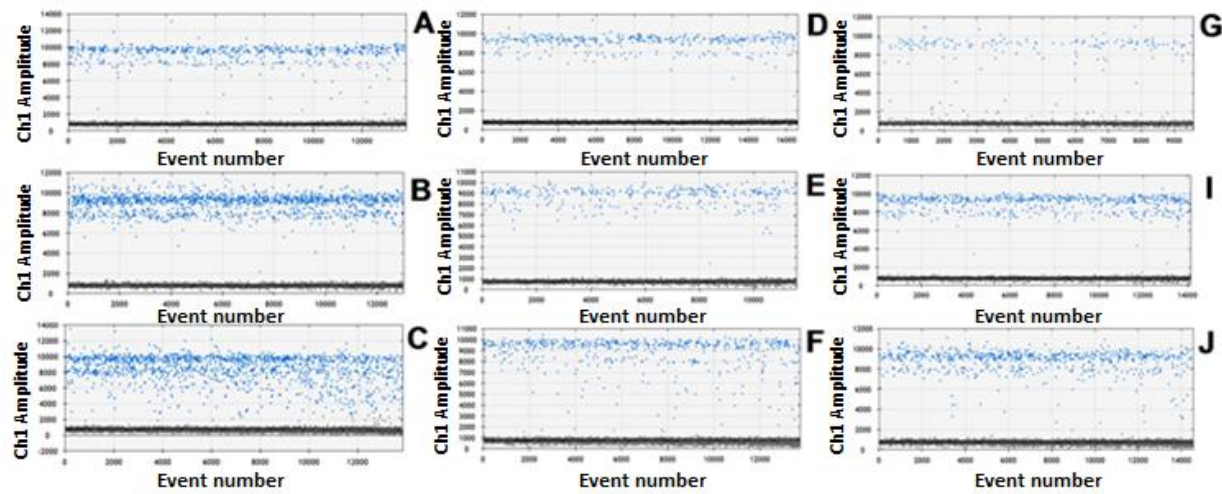


Figure 5.9 Quantitative mRNA expression analysis of NPC1L1 in differentiated Caco-2 cells following incubation in media containing 5, 10 and 25 mM glucose and with and without inhibitors of glucose uptake. (A) 5 mM glucose, (B) 10 mM glucose, (C) 25 mM glucose, (D) 10 mM glucose + 5 μ M cytochalasin B, (E) 10 mM glucose + 1 mg/mL ChE, (F) 10 mM glucose + 200 μ M apigenin 7-*O*-glucoside (A7G), (G) 25 mM glucose + 5 μ M cytochalasin B, (I) 25 mM glucose + 1 mg/mL ChE, (J) 25 mM glucose + 200 μ M A7G. Top panels show data as a 1-D plot with each droplet from a sample plotted on the graph of fluorescence intensity vs droplet number. Positive and negative droplets are indicated in blue and grey respectively for NPC1L1. Exact copy numbers of NPC1L1 are indicated per ng of cDNA since changes were also observed for TBP copy numbers (insert figure) when multiplexed with each cell line. Three biological replicates in three seeding experiments were combined and analysed six times. Results are expressed as mean values \pm SEM. Different letters indicate significant differences ($p < 0.05$) between treatments.

In general, the results on NPC1L1 mRNA expression are in line with [4-¹⁴C]-cholesterol uptake where cells showing higher expression of this transporter protein presented greater uptake rates indicating higher protein expression levels of NPC1L1 at the apical membrane.

Increase in NPC1L1 mRNA expression levels by glucose were attenuated with ChE and apigenin 7-*O*-glucoside irrespective of the concentration of glucose used, although the glucose concentration determined the extent of the reduction. The presence of ChE and apigenin 7-*O*-glucoside reduced NPC1L1 mRNA expression causing reductions of ~3.5- and ~3-fold respectively when incubated with 10 mM glucose. However, this effect was decreased when cells were exposed to 25 mM glucose showing a reduction of ~50 % in their effectiveness to attenuate NPC1L1 expression. Due to its higher potency to attenuate glucose transport, cytochalasin B showed the strongest effect on reducing NPC1L1 mRNA expression causing a ~4-fold decrease compared to cells incubated in 10 and 25 mM glucose. This result suggests that the use of higher concentrations and a combination of polyphenols, which presumably can happen after dietary exposure could maximise the response observed for ChE and apigenin 7-*O*-glucoside.

The atherogenic process has been proposed to be a postprandial event caused by the accumulation of remnant cholesterol into sub-endothelial space, leading to inflammation and vascular injury (Nordestgaard and Varbo, 2014) increasing the risk of cardiovascular disease (Jørgensen *et al.*, 2012; Varbo *et al.*, 2013). Therefore overproduction of cholesterol-rich Apo-B48 lipoproteins might be implicated in the low-grade inflammation and endothelial dysfunction observed during the postprandial phase mediated by hyperglycaemia and the concomitant hyperinsulinemia. In this sense, reducing postprandial glycaemic impact by the intake of polyphenols could be linked with previous observations stating an association between diet rich in polyphenols and cardioprotection (Kishimoto *et al.*, 2013). This is further supported by a human intervention study where the consumption of a polyphenol-rich diet reduced the postprandial levels of cholesterol-rich chylomicrons (Annuzzi *et al.*, 2014).

This work has proved for the first time that individual polyphenols and polyphenol-rich extracts capable of inhibiting glucose absorption, as exemplified with ChE and apigenin

7-O-glucoside, can reduce the expression of intestinal NPCL1, which is associated with lower rates of cholesterol uptake in Caco-2 cells. Although speculative, the findings of this work may be to some extent linked with the reduction of cardiovascular disease risk (49 %) found by the STOP-NIDDM study in impaired glucose tolerant subjects after acarbose treatment (Chiasson *et al.*, 2003). For instance, under pathophysiological conditions, acarbose reduced the activity and nuclear localization of the pro-inflammatory transcription factor NF- κ B (Rudofsky Jr *et al.*, 2004), possibly due to a reduction of atherogenesis (Inoue *et al.*, 2006). Like acarbose, polyphenols have been related with cardioprotective effects *via* multiple mechanism.

5.5 Conclusion

In summary, this study provides evidence that acute attenuation of glucose absorption has a positive effect in reducing cholesterol uptake and polyphenols are able to mediate this response. This could have important implication in modulating metabolic abnormalities observed during the postprandial phase such as endothelial dysfunction and inflammation with long-term health benefits by polyphenol-rich diets.

Chapter 6 Polyphenols and type 2 diabetes : perspectives and conclusion.

Over the last 3 decades, research in the area of polyphenols and health has expanded significantly. Polyphenols have been identified as the most likely class of small molecules present in plant-derived products capable of affecting physiological processes that protect against cardiometabolic diseases including type 2 diabetes (Arts and Hollman, 2005; Bertoina *et al.*, 2016).

Consistent outcomes from large epidemiological and dietary intervention studies greatly suggest the likelihood of a robust and potentially causal relationship of the intake of diets rich in polyphenols with a reduced risk of developing type 2 diabetes (Knekt *et al.*, 2002; Wedick *et al.*, 2012; van Dam *et al.*, 2013; Bertoina *et al.*, 2016). For instance in a prospective cohort of 40,011 participants with a mean follow-up of 10 years, the consumption of coffee or tea (3 cups/day) were both inversely associated with the onset of type 2 diabetes by ~42 % where blood pressure, intake of magnesium, potassium and caffeine did not explain this relationship (Van Dieren *et al.*, 2009). Results from the PREDIMED study showed a 40 % risk reduction in type 2 diabetes in a population at high cardiovascular risk (cohort of 3541 participants) consuming a Mediterranean diet (i.e. high intake of olive oil, fruit, nuts, vegetables, and cereals) in comparison with a diet low in fats after a follow-up of 4.1 years without specific restrictions in energy intake or an increase of physical activity (Salas-Salvadó *et al.*, 2014).

Based on mechanistic evidence from animal and *in vitro* studies, the connection of polyphenols with the reduction of type 2 diabetes risk is likely through potential multiple mechanisms; these have been proposed and reviewed elsewhere (Hanhineva *et al.*, 2010; Williamson, 2013; Carpena *et al.*, 2015; Kim *et al.*, 2016) and exemplified with polyphenols in chamomile and apigenin in this thesis (chapter 1). These include attenuation of post-prandial glycaemic responses by inhibiting digestion and/or sugar transport, improved fasting blood glucose levels by enhancing insulin secretion and

improving insulin sensitivity in peripheral tissues *via* activation of insulin receptors, protection of pancreatic β -cell function, modification of hepatic glucose release and modulation of signalling pathways and gene expression.

Certainly, when linking the epidemiological evidence with bioavailability studies, logic suggest that mammalian -and bacterial-derived metabolites should be the compounds mediating the health effects since they are the most abundant chemical forms present in circulation. However, it is important to point out that most of the mechanistic evidence existing so far have been generated using supramolecular doses of aglycones and so, there is limited evidence supporting the bioactivity of mammalian and bacterial metabolites. For instance, resveratrol but not its sulphated (trans-3-*O*-sulfate) nor glucuronidated (trans-*O*- β -D-glucuronide) forms had an antilipolytic effect on adipocytes at physiological doses (0.3-3 μ M) (Gheldof *et al.*, 2017). In one study, only 2 phenolic metabolites (protocatechuic acid-3-sulfate and isovanillic acid) out of 20 had an effect on reducing soluble vascular cell adhesion molecule 1(VCAM-1) expression with a minimum active dose of 10 μ M in activated human umbilical vein endothelial cells (Warner *et al.*, 2016). Furthermore, there was no synergistic or additive effects in this response when tested at equimolar doses (Warner *et al.*, 2016). In contrast, a mixture of cyanidin-3-glucoside-derived metabolites reflecting dietary concentrations and ratios after the intake of 500 mg, reduced VCAM-1 and IL-6 production in in human endothelial cells and this effect was sustained even when the dose was reduced 10-fold (Warner *et al.*, 2017). Similarly, 4 combinations of phenolic metabolites out of 29 reduced TNF α secretion in human THP-1 monocytes (di Gesso *et al.*, 2015).

Based on the information above and making a simple extrapolation without taking into account interactions with other molecules present in serum, which may affect their activity, it seems that only certain mixtures present in a defined ratios may have some beneficial effects. This pose a practical challenge to unravel the active compounds and their molecular targets since there is a wide interpersonal variation in the production of these metabolites (Manach *et al.*, 2017; Milenkovic *et al.*, 2017) and some changes in their profile can be also predicted from meal to meal in free living subjects. With numerous possible combinations of metabolites, there are multiple and complex metabolic pathways affected making almost an impossible task to establish a clear

association between plasma metabolites and the range of claimed metabolic changes in tissues such as the pancreas, liver, skeletal muscle and adipose tissue (Hollman, 2014). Although it has not been decisively proven, undoubtedly, plasma metabolites contribute to some extent to the cardiometabolic protection of polyphenols observed in epidemiological studies, however, what if circulating metabolites were not the big part of the story?

6.2 Advances in polyphenol research: the GI tract as a prime site of action?

Given the importance of high metabolic tissues such as the liver, adipose tissue, pancreas and skeletal muscle and their cross-talk in handling energy, it is not surprising that a great number of studies have tried to unravel the potential modulatory effects of polyphenols in these tissues, while the metabolic capabilities of the GI tract and its influence in energy homeostasis have not been fully appreciated. However, an increasing number of studies are starting to establish that the GI tract initiate direct and anticipatory metabolic control of distant organs including those regulating energy uptake and utilisation. Thus, the GI is far from being a simple absorptive and excretory organ as it was previously thought (Stringer *et al.*, 2015; Tomkin and Owens, 2015; Fändriks, 2016; Bhat and Kapila, 2017) and its metabolic relevance is now recognised by 45 professional societies proposing that the GI tract and, particularly, the bariatric surgery should be considered as a standard treatment for type 2 diabetes (Brito *et al.*, 2017). This procedure has the potential to reverse obesity, type 2 diabetes and the associated cardiovascular risk factors by modulating energy sensing and availability in the GI tract (Rubino *et al.*, 2006) together with a shift of the gut microbiota ecology (Liou *et al.*, 2013).

Polyphenols are found in plant-based diets at high concentrations, even comparable to those of pharmacological doses (Williamson, 2017). According to some bioavailability studies in mice and humans, after intake, most of the active chemical forms (unmetabolised aglycones) stay in the intestinal mucosa up to 24 h before absorption (Patel *et al.*, 2013; Ferrars *et al.*, 2014). Furthermore, their concentration can be 1000-times higher than the one in circulation with an estimated total concentration of 1 mM

reaching the colon (Williamson, 2017). Thus, even though the action of parent polyphenols in peripheral tissues is limited by its low bioavailability, their persistence in the GI tract after ingestion may indicate that this tissue is a key site for cardiometabolic protection by modulating GI functions. This notion is further supported by previous findings demonstrating that polyphenols can favour chemical interactions with proteins altering the digestion and absorption process of nutrients (Williamson, 2013) and exert cellular modulatory effects such as secretion of GI hormones (McCarty, 2005; Panickar, 2013; Song *et al.*, 2015), tight junction (TJ) proteins (Suzuki and Hara, 2011) and gut microbiota ecology (Tzounis *et al.*, 2011; Anhê *et al.*, 2015; Roopchand *et al.*, 2015; Most *et al.*, 2017). Some of these metabolic actions are similar to the ones observed after the bariatric surgery so, the GI tract may represent the missing link between the consumption of polyphenol-rich diets and the maintenance of cardiometabolic.

The gastrointestinal tract is the body's principal nutrient provider and therefore, it represents a cellular link to metabolic disorders caused by excessive and readily nutrient supply. As discussed in chapter 1, continuous acute supply of carbohydrates and simple sugars triggers a sharp increase in blood glucose and insulin concentration and these events have been considered prime factors in the pathogenesis of insulin resistance and type 2 diabetes *via* altered energy partitioning (Brand-Miller *et al.*, 2002), increased oxidative stress, low-grade inflammation and endothelial dysfunction (Kawano *et al.*, 1999; Ceriello *et al.*, 2004). More gentle responses by the consumption of low GI diets have shown to prevent these metabolic disturbances and they are inversely associated with insulin resistance and type 2 diabetes risks (Bhupathiraju *et al.*, 2014) and to help in the management of type 2 diabetes (Brand-Miller *et al.*, 2003).

The content of naturally occurring polyphenols has been linked with low GI response since ~30 years ago when Thompson *et al.* (1984) observed a negative correlation between polyphenol content in legumines, and blood glucose response in normal and diabetic individuals after intake of 50 g of available carbohydrates. This study and many others suggest that polyphenols added as part of a meal or during it, could be used to mimic the slow release of glucose into the blood of low GI foods and/or acarbose without altering the carbohydrate and sugar composition of diets. However, after ~35 years of the first observation, there is not consensus on the potential of polyphenols to affect

postprandial glycaemic impact. This is due in part to the wide variations in *in vitro* experimental settings and outcomes, which have produced inconsistent findings, limiting the identification and recognition of plant extracts or specific polyphenols to attenuate glycaemic response in a consistent manner.

In order to narrow the bridge that connects the identification of polyphenol-rich extracts and specific polyphenols with further development of human intervention studies, we have improved a method to accurately measure their potency to inhibit human α -amylase activity *in vitro* (described in chapter 3). Using this method along with the use of human cell lines (described in chapter 4) we have demonstrated that apigenin and apigenin 7-*O*-glucoside present in Chamomile are effective modulators of the carbohydrate digestion and sugar absorption process. These metabolic actions may be related with the cardiometabolic protection reported for chamomile in animal and human intervention studies by mimicking the effect of low glycaemic index diets and the antidiabetic drug acarbose. Therefore this research work not only contributes to decipher plausible molecular targets of chamomile polyphenols but also provides robust evidence for the inclusion of apigenin in acute and long-term animal and human intervention studies. Furthermore, although it remains to be demonstrated *in vivo*, the attenuation of postprandial glycaemia by polyphenols might reduce the atherogenesis process (discussed in chapter 5) and conferring protection against the risk of developing cardiovascular disease.

6.2.1 Perspective

It has been widely acknowledge that part of the metabolic effects of polyphenols at the GI tract is due to the reduction of glucose influx into circulation attenuating postprandial hyperglycaemia, as demonstrated in this research work. However, adding to, and complementing, the effect of polyphenols could be related with the maintenance of an adequate intestinal AMP-activated protein kinase (AMPK) activity and related signalling pathways, thus preserving the chemosensory functions of the GI tract and preventing aberrant metabolism in absorptive cells. This statement is based on two main recent findings, i) activation of duodenal-AMPK activity by antidiabetic drug metformin and AICAR (an AMPK agonist) lowered hepatic glucose release in rat models of

hyperglycaemia (high-fat diet and streptozotocin-induced prediabetes), an effect that was suppressed when duodenal AMPK was blocked or by intravenous administration of metformin (Duca *et al.*, 2015) and ii) maintenance of AMPK-signalling pathway in enterocytes of insulin resistant and type 2 diabetes mice improved insulin sensitive and decreased dyslipidaemia (Harmel *et al.*, 2014).

Some dietary polyphenols have been reported to be agonist of AMPK in the liver and skeletal muscle (Zang *et al.*, 2006; Collins *et al.*, 2007; Lin *et al.*, 2007; Hwang *et al.*, 2009; Price *et al.*, 2012), although whether polyphenols can mediate this metabolic action in the GI remains largely unexplored. A pioneering study was conducted by Cote *et al.* (Côté *et al.*, 2015) showing that acute infusion of resveratrol into the duodenum attenuated hepatic glucose release in insulin resistant rats *via* a vagal gut-brain neuronal axis improving hypothalamic insulin sensitivity, an effect that required the AMPK-SIRT1 cycle in this tissue (Ruderman *et al.*, 2013). Interestingly, chronic feeding with high fat diet decreased the mRNA and protein expression of SIRT1 and this was immediately normalised to those of chow-fed rats with resveratrol infusion, enhancing insulin sensitivity and lowering hepatic glucose release (Côté *et al.*, 2015). Similarly, an acute and chronic administration of chlorogenic acid improved fasting glucose level and postprandial glucose tolerance in *Lepr^{db/db}* mice which was related with AMPK activation and attenuation of gluconeogenesis (Ong *et al.*, 2013). Although the later study did not established a direct relationship between duodenal AMPK and hepatic gluconeogenesis, the fact that chlorogenic acid was tested directly to a liver cell line raise the possibility that the metabolic improvements were mediated *via* the gut-brain-liver axis. These results suggest that chronic perturbation of the intestinal physiology disrupts the chemosensory capacity of the duodenum, impairing the glucoregulatory function of the GI tract and liver. This disruption may also be acute and independent of a pathological state since healthy subjects supplemented with a single oral dose of saturated fat increased hepatic gluconeogenesis by 70% with a net decline in glycogenesis of 20% concomitant with an increase in hepatic lipid storage and insulin resistance (Hernández *et al.*, 2017).

Maintaining AMPK activity by polyphenols in absorptive cells either by reducing glucose influx (inhibition of GLUT2 and/or SGLT1) or direct signalling. i.e SIRT1 activation (Chung *et al.*, 2010) could reduce the postprandial processing of lipids and maintain a

functional insulin signalling pathway (Harmel *et al.*, 2014). For instance, in the study of Ong *et al.* (2013) the chronic intake of chlorogenic acid in *Lepr^{db/db}* mice improved systemic insulin sensitivity, lipid profile and lowered dyslipidemia. However, whether the metabolic effects triggered by chlorogenic acid intake were mediated by regulating GI functions in this study is uncertain.

The glucoregulatory capacity of the duodenum seems to be mediated in part by an increase of GLP-1 as observed with the antidiabetic drug metformin and the polyphenol resveratrol (Côté *et al.*, 2015; Duca *et al.*, 2015). It has been suggested that GLP-1 has different actions depending whether is released by EECs in the small intestine or in the colon (Greiner and Bäckhed, 2016). Given the short-half of active GLP-1 (Holst, 2007) and that GLP-1 receptors are expressed on nerves in the intestinal submucosa and the liver (Richards *et al.*, 2014), it has been proposed that GLP-1 secreted in the small intestine signals directly to GLP-1 receptor expressed on vagal afferent nerves that relay signals to the brain (Vahl *et al.*, 2007; Richards *et al.*, 2014; Greiner and Bäckhed, 2016) (for a comprehensive review of these pathways see (Holst, 2007)) rather than to boost insulin secretion from pancreatic β -cells (Smith *et al.*, 2014). This is in line with the observation that chlorogenic acids in coffee induce GLP-1 secretion along with a reduction of postprandial glucose but without changes in insulin levels (Jokura *et al.*, 2015). Although it remains to be demonstrated, perhaps chlorogenic acids acts as ligands on GLP-1-secreting cells localized in the small intestine since this activity has been observed *in vitro* (Fujii *et al.*, 2015); thus reducing hepatic glucose production with a global effect in serum glucose levels. The inhibition of SGLT1 transporter in GLP-1-secreting cells would reduce the flux of Na^+ into the cells blocking membrane depolarisation and Ca^{+2} entry (Parker *et al.*, 2012; Psichas *et al.*, 2015) suppressing the release of GLP-1, an effect that has been observed by polyphenol supplementation (Castro-Acosta *et al.*, 2016). Therefore polyphenols could induce and suppress GLP-1 secretion depending on their molecular targets and this may explain the discrepancies on GLP-1 secretion by polyphenol intervention (Burton-Freeman, 2010).

The evidence presented underscores the possible role of polyphenols to maintain the energy sensing capacity in the small intestine, which is complementary to their role to attenuate carbohydrate digestion and sugar absorption, both contributing to maintain

energy homeostasis and cardiometabolic health. These mechanisms may partially clarify the debated explanation behind the antidiabetic effects of some polyphenols such as resveratrol (Timmers *et al.*, 2011; Bhatt *et al.*, 2012; Crandall *et al.*, 2012). Further studies are warranted to identify other polyphenols capable of maintaining the chemosensory capacity of the small intestine which could act in cohort with the inhibition of glucose transporters.

Dietary molecules that escape absorption in the small intestine reach the colon where they are metabolised by the resident microbiota producing a series of microbial metabolites and affecting microbiota ecology with an impact on metabolic process locally, and in the periphery (Cani *et al.*, 2013; Greiner and Bäckhed, 2016). For instance, propionate, and butyrate are well characterised microbial metabolites derived from fermentable carbohydrates that regulate energy metabolism in both animals and humans. Propionate has beneficial effects on β -cell function in humans and *in vitro* analyses with human islets suggest that it acts synergistically on glucose-stimulated insulin release which was independent of GLP-1 secretion (Pingitore *et al.*, 2017). Butyrate regulates glucose and energy metabolism in mice, an effect that has been ascribed to partially be mediated *via* a gut–brain axis (De Vadder *et al.*, 2014), once again highlighting the significance of the GI tract on controlling global energy homeostasis. There are plausible many other microbial-derived metabolites with the potential to regulate energy balance remained to be discovered and characterised. For instance, it has been recently reported that *N*-acyl amides activate intestinal GPCRs and improve glucose tolerance in mice (Cohen *et al.*, 2017).

On the other hand, diets rich in fats and simple sugars alters the gut microbiota affecting metabolic pathways implicated in insulin resistance, type 2 diabetes and cardiovascular disease such as inflammation and adiposity (Turnbaugh *et al.*, 2006; Samuel *et al.*, 2008). Experimental data has confirmed that microbiota is actively involved in the development of local and systemic inflammation through a lipopolysaccharide (LPS)-dependent mechanism which may acts *via* an impaired mucosal barrier (Cani *et al.*, 2007; Cani *et al.*, 2008; Cani *et al.*, 2009). Indeed, significant endotoxaemia was found in individuals with metabolic syndrome (Lassenius *et al.*, 2011) and type 2 diabetes (Pussinen *et al.*, 2011) and it could represent the root cause of altered adipose tissue and liver metabolism

characteristic of these phenotypes (Cani *et al.*, 2008; Cani *et al.*, 2009). While microbial metabolites such as butyrate and propionate could regulate energy metabolism by preserving intestinal barrier function and downregulated immune local responses and inflammation (Postler and Ghosh, 2017), a particular ‘healthy’ bacteria signature may also be required. i.e *Akkermansia muciniphila* (Everard *et al.*, 2013; Derrien *et al.*, 2017; Plovier *et al.*, 2017). Moreover, the microbiota seems to have a high degree of plasticity in response to diet (Cotillard *et al.*, 2013; Carmody *et al.*, 2015), suggesting that dietary manipulation can be used to prevent and/or manage metabolic disorders.

The interaction of polyphenols with intestinal proteins, such as the sugar transporter SGLT1 has presumed to be reversible (Schulze *et al.*, 2014), indicating that polyphenols can reach the colon and affect GI metabolism, maximising any modulatory effect on energy homeostasis. The connection of polyphenols with microbiota is more intricate than initially thought. Polyphenols may exert a ‘prebiotic effect’ promoting the growth of intestinal health-associated bacteria.

Several human intervention studies have observed an increase in bifidobacteria and lactobacillus population after dietary intervention with different polyphenol sources including cocoa, red wine, blueberries, grape seeds, oranges, apples, virgin olive oil, pomegranate and green tea (Yamakoshi *et al.*, 2001; Tzounis *et al.*, 2011; Vendrame *et al.*, 2011; Jin *et al.*, 2012; Queipo-Ortuño *et al.*, 2012; Boto-Ordóñez *et al.*, 2014; Cuervo *et al.*, 2015; Li *et al.*, 2015; Martín-Peláez *et al.*, 2017). Most of these studies focused on establishing a relationship between changes in microbiota ecology with the production of colonic catabolites that might benefit the host after absorption, thus is uncertain whether this changes can be related with improvement in cardiometabolic health in humans, although some evidence do exist. For instance, in a randomised, cross-over study, the intake of cocoa flavonols for 4 weeks (494 mg cocoa flavanols/day) increased the bifidobacterial and lactobacilli populations and decreased clostridia counts which was related with reductions in plasma triacylglycerols and C-reactive protein concentrations (Tzounis *et al.*, 2011). *Akkermansia muciniphila* has been identified as a beneficial microbiota signature and has been positively associated with the attenuation of pathological conditions such as obesity, type 2 diabetes, inflammatory bowel diseases and liver diseases (Cani and De Vos, 2017). Interestingly, intervention with a pomegranate

extract for 4 weeks (1000 mg/day) increased the population of bacteria in healthy subjects (Li *et al.*, 2015). This observation also has been reported in animal models after polyphenol intervention (Anhê *et al.*, 2015; Roopchand *et al.*, 2015; Zhang *et al.*, 2017).

Two independent studies evaluated the metabolic effects of polyphenol-rich extracts, cranberry and concord grape on mice fed a high fat/high sugar and high fat diet respectively (Anhê *et al.*, 2015; Roopchand *et al.*, 2015). In both studies *A. muciniphila* was a strong biomarker of cranberry and grape extracts supplementation, and 16S rRNA gene sequencing of faecal samples revealed a striking ~30 and 50 % increase in the relative abundance of this bacteria. At the functional level, polyphenol supplementation decreased body and liver weight gain in mice, improved insulin and glucose tolerance, lowered hepatic, intestinal, and plasma triglycerides and attenuated intestinal and hepatic inflammation alongside with reduced serum LPS. Although the increase in *A. muciniphila* and the improvement of metabolic biomarkers in these studies was merely correlative, a body of evidence suggest that *A. muciniphila* protects against cardiometabolic diseases (Everard *et al.*, 2013; Schneeberger *et al.*, 2015; Dao *et al.*, 2016). Chlorogenic acids have also been reported to increase *A. muciniphila* in mice resulting in a lower intestinal and systemic inflammation (Zhang *et al.*, 2017), outlined another potential mechanism of the protection of coffee against type 2 diabetes.

Gut permeability has been shown to be a key component in the dysregulation of energy metabolism. A direct link of *A. muciniphila* with an improved gut barrier function which prevents metabolic endotoxemia and inflammatory tone averting the disruption of junctional proteins has been established, possibly via an outer-membrane protein (Amuc_1100*) which signals toll-like receptor 2 (Plovier *et al.*, 2017). There is evidence underlying the potential of polyphenols to preserve intestinal barrier function (Amasheh *et al.*, 2008; Suzuki and Hara, 2011; Suzuki *et al.*, 2011), targeting signal transduction pathways involved in tight junction regulation such as PKC δ (Suzuki *et al.*, 2011) and cytokine signalling, thus decreasing inflammatory tone and maintaining tight-junction protein structure. In Caco-2/15 cell line, cranberry extract offset LPS-mediated inflammation *via* inhibition of nuclear factor κ B activation and production of pro-inflammatory cytokines along with an increased expression of tight junction proteins (Denis *et al.*, 2015). In the study of Ahne *et al.* (2015) cranberry polyphenols completely

suppressed NF κ B activation in the intestine of mice. This functional overlap between polyphenols and *A. muciniphila* makes not possible to distinguish who is responsible for keeping intestinal barrier function intact after the high-fat high-sugar challenge, although a synergistic effect cannot be ruled out.

As highlighted before, there might be a number of microbiota-encoded small molecules that influence energy metabolism. Although it remains to be tested, it is possible that microbial catabolites derived from dietary polyphenols influence energy balance before colonic absorption in a manner similar to the short chain fatty acids butyrate and propionate. The fact that some these catabolites present a t_{\max} after 6 h suggest that they remain in the colon long enough to act as functional and signalling molecules. Moreover, the problem of having a great chemical diversity of polyphenols in the diet and those of circulating metabolites is drastically reduced in the colon. The microbiota transform the most abundant dietary polyphenols in the same set of catabolites while other catabolites are a signature of the intake of a particular polyphenol from the diet (Williamson and Clifford, 2017). Therefore unravelling whether some microbial polyphenol-derived metabolites are involved in energy homeostasis acting locally may provide a clearer pathway of how dietary polyphenols positively influence cardiometabolic health.

6.2.2 Concluding comments.

Given the evidence supporting the critical role of the GI tract on glucose and energy homeostasis, it is intuitive that polyphenols may have a key role in metabolic control acting at this site since they reach concentrations that are several orders of magnitude higher than in the serum in the appropriate chemical form.

The mechanistic evidence generated with non-mammalian metabolites whose action is questionable in peripheral tissues and the liver (i.e activation of AMPK, downregulation of inflammatory pathways, maintenance of insulin signalling pathway), supports the potential modulatory role of polyphenols at the GI tract. Therefore, it is reasonable that a two-compartment model where cardiometabolic of polyphenols comes from a cooperative action of the chemical forms present at the GI tract and the circulating metabolites

derived after mammalian and bacterial metabolism. However whether polyphenols acting at the GI tract play a more crucial role than circulating metabolites needs to be determined.

List of references.

- Acker, M.G., and D.S. Auld, 2014. Considerations for the design and reporting of enzyme assays in high-throughput screening applications. *Perspectives in Science*, 1(1): 56-73.
- Adeli, K. and G.F. Lewis, 2008. Intestinal lipoprotein overproduction in insulin-resistant states. *Current Opinion in Lipidology*, 19(3): 221-228.
- Ademiluyi, A.O. and G. Oboh, 2013. Aqueous extracts of roselle (*Hibiscus sabdariffa* linn.) varieties inhibit α -amylase and α -glucosidase activities *in vitro*. *Journal of Medicinal Food*, 16(1): 88-93.
- Aguilar, D., and M.L. Fernandez, 2014. Hypercholesterolemia induces adipose dysfunction in conditions of obesity and nonobesity. *Advances in Nutrition*, 5(5): 497-502.
- Ahmed, D., V. Kumar, M. Sharma and A. Verma, 2014. Target guided isolation, *in vitro* antidiabetic, antioxidant activity and molecular docking studies of some flavonoids from *Albizia lebeck Benth* Bark. *BMC Complementary and Alternative Medicine*, 14(1): 155.
- Ait-Omar, A., M. Monteiro-Sepulveda, C. Poitou, M. Le Gall, A. Cotillard, J. Gilet, K. Garbin, A. Houllier, D. Chateau, A. Lacombe, N. Veyrie, D. Hugol, J. Tordjman, C. Magnan, P. Serradas, K. Clement, A. Leturque and E. Brot-Laroche, 2011. GLUT2 accumulation in enterocyte apical and intracellular membranes: a study in morbidly obese human subjects and ob/ob and high fat-fed mice. *Diabetes*, 60(10): 2598-2607.
- Al-Asri, J, G. Gyémánt, E. Fazekas, G. Lehoczki, M.F. Melzig, G. Wolber and J. Mortier, 2016. α -amylase modulation: discovery of inhibitors using a multi-pharmacophore approach for virtual screening. *ChemMedChem*, 11(21): 2372-2377.
- Alrefai, W.A, F. Annaba, Z. Sarwar, A. Dwivedi, S. Saksena, A. Singla, P.K. Dudeja and R.K. Gill, 2007. Modulation of human Niemann-Pick C1-Like 1 gene expression by sterol: role of sterol regulatory element binding protein 2. *American Journal of Physiology-Gastrointestinal and Liver Physiology*, 292(1): G369-G376.
- Altmann, S.W., H.R. Davis, L.-j. Zhu, X. Yao, L.M. Hoos, G. Tetzloff, S.P.N. Iyer, M. Maguire, A. Golovko and M. Zeng, 2004. Niemann-Pick C1-Like 1 protein is critical for intestinal cholesterol absorption. *Science*, 303(5661): 1201-1204.
- Alvarado, F., and R.K. Crane, 1962. Phlorizin as a competitive inhibitor of the active transport of sugars by hamster small intestine, *in vitro*. *Biochimica et Biophysica Acta*, 56: 170-172.
- Amasheh, M., S. Schlichter, S. Amasheh, J. Mankertz, M. Zeitz, M. Fromm and J.D. Schulzke, 2008. Quercetin enhances epithelial barrier function and increases claudin-4 expression in Caco-2 cells. *The Journal of Nutrition*, 138(6): 1067-1073.
- Amiot, M C, Riva and A. Vinet, 2016. Effects of dietary polyphenols on metabolic syndrome features in humans: A systematic review. *Obesity Reviews*, 17(7): 573-586.

- Andreasen, M.F, L.P. Christensen, A.S. Meyer and Å. Hansen, 2000. Content of phenolic acids and ferulic acid dehydrodimers in 17 rye (*secale cereale* L.) varieties. *Journal of Agricultural and Food Chemistry*, 48(7): 2837-2842.
- Anhê, F.F., D. Roy, G. Pilon, S. Dudonné, S. Matamoros, T.V. Varin, C. Garofalo, Q. Moine, Y. Desjardins and E. Levy, 2015. A polyphenol-rich cranberry extract protects from diet-induced obesity, insulin resistance and intestinal inflammation in association with increased *Akkermansia* spp. Population in the gut microbiota of mice. *Gut*, 64(6): 872-883.
- Annuzzi, G., L. Bozzetto, G. Costabile, R. Giacco, A. Mangione, G. Anniballi, M. Vitale, C. Vetrani, P. Cipriano and G. Della Corte, 2014. Diets naturally rich in polyphenols improve fasting and postprandial dyslipidemia and reduce oxidative stress: A randomized controlled trial. *The American Journal of Clinical Nutrition*, 99(3): 463-471.
- Ansar, S., J. Koska and P.D. Reaven, 2011. Postprandial hyperlipidemia, endothelial dysfunction and cardiovascular risk: focus on incretins. *Cardiovascular Diabetology*, 10(1): 61.
- Arts, I.C. and P.C. Hollman, 2005. Polyphenols and disease risk in epidemiologic studies. *The American Journal of Clinical Nutrition*, 81(1): 317S-325S.
- Aslam, M., S. Aggarwal, K.K. Sharma, V. Galav and S.V. Madhu, 2016. Postprandial hypertriglyceridemia predicts development of insulin resistance glucose intolerance and type 2 diabetes. *PloS One*, 11(1): e0145730.
- Atanasov, A.G., B. Waltenberger, E.-M. Pferschy-Wenzig, T. Linder, C. Wawrosch, P. Uhrin, V. Temml, L. Wang, S. Schwaiger and E.H. Heiss, 2015. Discovery and resupply of pharmacologically active plant-derived natural products: a review. *Biotechnology Advances*, 33(8): 1582-1614.
- Avula, B., Y.-H. Wang, M. Wang, C. Avonto, J. Zhao, T.J. Smillie, D. Rua and I.A. Khan, 2014. Quantitative determination of phenolic compounds by UHPLC-UV-MS and use of partial least-square discriminant analysis to differentiate chemotypes of chamomile/chrysanthemum flower heads. *Journal of Pharmaceutical and Biomedical Analysis*, 88: 278-288.
- Aydin, E., 2015. Effects of natural products on sugar metabolism and digestive enzymes. *The University of Leeds, School of Food Science and Nutrition*. Thesis ©.
- Barbosa, A.C.L., M.d.S. Pinto, D. Sarkar, C. Ankolekar, D. Greene and K. Shetty, 2010. Varietal influences on antihyperglycemia properties of freshly harvested apples using *in vitro* assay models. *Journal of Medicinal Food*, 13(6): 1313-1323.
- Barclay, A.W., P. Petocz, J. McMillan-Price, V.M. Flood, T. Prvan, P. Mitchell and J.C. Brand-Miller, 2008. Glycemic index, glycemic load, and chronic disease risk—a meta-analysis of observational studies. *The American Journal of Clinical Nutrition*, 87(3): 627-637.
- Bays, H., S.N. Kothari, D.E. Azagury, J.M. Morton, N.T. Nguyen, P.H. Jones, T.A. Jacobson, D.E. Cohen, C. Orringer and E.C. Westman, 2016. Lipids and bariatric procedures part 2 of 2: Scientific statement from the american society for metabolic and bariatric surgery (ASMBS), the national lipid association (NLA), and obesity medicine association (OMA). *Surgery for Obesity and Related Diseases*, 12(3): 468-495.
- Bertoia, M.L., E.B. Rimm, K.J. Mukamal, F.B. Hu, W.C. Willett and A. Cassidy, 2016. Dietary flavonoid intake and weight maintenance: Three prospective cohorts of 124 086 US men and women followed for up to 24 years. *British Medical Journal*, 352: i17.

- Bethel, M., W. Xu and M. Theodorakis, 2015. Pharmacological interventions for preventing or delaying onset of type 2 diabetes mellitus. *Diabetes, Obesity and Metabolism*, 17(3): 231-244.
- Bhaskaran, N., J.K. Srivastava, S. Shukla and S. Gupta, 2013. Chamomile confers protection against hydrogen peroxide-induced toxicity through activation of nrf2-mediated defense response. *Phytotherapy Research*, 27(1): 118-125.
- Bhat, M.I. and R. Kapila, 2017. Dietary metabolites derived from gut microbiota: Critical modulators of epigenetic changes in mammals. *Nutrition Reviews*, 75(5): 374-389.
- Bhatt, J.K., S. Thomas and M.J. Nanjan, 2012. Resveratrol supplementation improves glycemic control in type 2 diabetes mellitus. *Nutrition Research*, 32(7): 537-541.
- Bhupathiraju, S.N., D.K. Tobias, V.S. Malik, A. Pan, A. Hruby, J.E. Manson, W.C. Willett and F.B. Hu, 2014. Glycemic index, glycemic load, and risk of type 2 diabetes: results from 3 large us cohorts and an updated meta-analysis. *The American Journal of Clinical Nutrition*, 100(1): 218-232.
- Bisswanger, H., 2014. Enzyme assays. *Perspectives in Science*, 1(1): 41-55.
- Blaak, E., J.M. Antoine, D. Benton, I. Björck, L. Bozzetto, F. Brouns, M. Diamant, L. Dye, T. Hulshof and J. Holst, 2012. Impact of postprandial glycaemia on health and prevention of disease. *Obesity Reviews*, 13(10): 923-984.
- Boath, A.S., D. Stewart and G.J. McDougall, 2012. Berry components inhibit α -glucosidase *in vitro*: Synergies between acarbose and polyphenols from black currant and rowanberry. *Food Chemistry*, 135(3): 929-936.
- Boey, D., A. Sainsbury and H. Herzog, 2007. The role of peptide YY in regulating glucose homeostasis. *Peptides*, 28(2): 390-395.
- Boto-Ordóñez, M., M. Urpi-Sarda, M.I. Queipo-Ortuño, S. Tulipani, F.J. Tinahones and C. Andres-Lacueva, 2014. High levels of bifidobacteria are associated with increased levels of anthocyanin microbial metabolites: a randomized clinical trial. *Food & Function*, 5(8): 1932-1938.
- Brand-Miller, J., S. Hayne, P. Petocz and S. Colagiuri, 2003. Low-glycemic index diets in the management of diabetes. *Diabetes Care*, 26(8): 2261-2267.
- Brand-Miller, J.C., S.H. Holt, D.B. Pawlak and J. McMillan, 2002. Glycemic index and obesity. *The American Journal of Clinical Nutrition*, 76(1): 281S-285S.
- Brayer, G.D., G. Sidhu, R. Maurus, E.H. Rydberg, C. Braun, Y. Wang, N.T. Nguyen, C.M. Overall and S.G. Withers, 2000. Subsite mapping of the human pancreatic α -amylase active site through structural, kinetic, and mutagenesis techniques. *Biochemistry*, 39(16): 4778-4791.
- Brito, J.P., V.M. Montori and A.M. Davis, 2017. Metabolic surgery in the treatment algorithm for type 2 diabetes: a joint statement by International Diabetes Organizations. *Journal of the American Medical Association*, 317(6): 635-636.
- Brown, J.M., L.L. Rudel and L. Yu, 2007. NPC1L1 (niemann-pick c1-like 1) mediates sterol-specific unidirectional transport of non-esterified cholesterol in mcardle-rh7777 hepatoma cells. *Biochemical Journal*, 406(2): 273-283.
- Brown, L., H. Poudyal and S. Panchal, 2015. Functional foods as potential therapeutic options for metabolic syndrome. *Obesity Reviews*, 16(11): 914-941.
- Brun, J., C. Fedou, O. Bouix, E. Raynaud and A. Orsetti, 1995. Evaluation of a standardized hyperglucidic breakfast test in postprandial reactive hypoglycaemia. *Diabetologia*, 38(4): 494-501.
- Burton-Freeman, B., 2010. Postprandial metabolic events and fruit-derived phenolics: a review of the science. *British Journal of Nutrition*, 104(S3): S1-S14.

- Butterworth, P.J., F.J. Warren and P.R. Ellis, 2011. Human α -amylase and starch digestion: an interesting marriage. *Starch-Stärke*, 63(7): 395-405.
- Cahill Jr, G.F., 1970. Starvation in man. *New England Journal of Medicine*, 282(12): 668-675.
- Cani, P.D., A.M. Neyrinck, F. Fava, C. Knauf, R.G. Burcelin, K.M. Tuohy, G. Gibson and N.M. Delzenne, 2007. Selective increases of bifidobacteria in gut microflora improve high-fat-diet-induced diabetes in mice through a mechanism associated with endotoxaemia. *Diabetologia*, 50(11): 2374-2383.
- Cani, P.D., R. Bibiloni, C. Knauf, A.M. Neyrinck, A.M. Neyrinck, N.M. Delzenne and R. Burcelin, 2008. Changes in gut microbiota control metabolic endotoxemia-induced inflammation in high-fat diet-induced obesity and diabetes in mice. *Diabetes*, 57(6): 1470-1481.
- Cani, P.D., S. Possemiers, T. Van de Wiele, Y. Guiot, A. Everard, O. Rottier, L. Geurts, D. Naslain, A. Neyrinck and D.M. Lambert, 2009. Changes in gut microbiota control inflammation in obese mice through a mechanism involving GLP-2-driven improvement of gut permeability. *Gut*, 58(8): 1091-1103.
- Cani, P.D., A. Everard and T. Duparc, 2013. Gut microbiota, enteroendocrine functions and metabolism. *Current Opinion in Pharmacology*, 13(6): 935-940.
- Cani, P.D. and W.M. De Vos, 2017. Next-generation beneficial microbes: the case of *Akkermansia muciniphila*. *Frontiers in Microbiology*, 8: 1765.
- Carmody, R.N., G.K. Gerber, J.M. Luevano, D.M. Gatti, L. Somes, K.L. Svenson and P.J. Turnbaugh, 2015. Diet dominates host genotype in shaping the murine gut microbiota. *Cell Host & Microbe*, 17(1): 72-84.
- Carpene, C., S. Gomez-Zorita, S. Deleruyelle and M. Carpena, 2015. Novel strategies for preventing diabetes and obesity complications with natural polyphenols. *Current Medicinal Chemistry*, 22(1): 150-164.
- Castro-Acosta, M.L., L. Smith, R.J. Miller, D.I. McCarthy, J.A. Farrimond and W.L. Hall, 2016. Drinks containing anthocyanin-rich blackcurrant extract decrease postprandial blood glucose, insulin and incretin concentrations. *The Journal of Nutritional Biochemistry*, 38: 154-161.
- Cemek, M., S. Kağa, N. Şimşek, M.E. Büyükokuroğlu and M. Konuk, 2008. Antihyperglycemic and antioxidative potential of *Matricaria Chamomilla* L. in streptozotocin-induced diabetic rats. *Journal of Natural Medicines*, 62(3): 284-293.
- Ceriello, A., L. Quagliaro, L. Piconi, R. Assaloni, R. Da Ros, A. Maier, K. Esposito and D. Giugliano, 2004. Effect of postprandial hypertriglyceridemia and hyperglycemia on circulating adhesion molecules and oxidative stress generation and the possible role of simvastatin treatment. *Diabetes*, 53(3): 701-710.
- Ceriello, A. and S. Colagiuri, 2008. International Diabetes Federation Guideline for management of postmeal glucose: a review of recommendations. *Diabetic Medicine*, 25(10): 1151-1156.
- Chan, L.K.Y. and P.S. Leung, 2015. Multifaceted interplay among mediators and regulators of intestinal glucose absorption: Potential impacts on diabetes research and treatment. *American Journal of Physiology-Endocrinology and Metabolism*, 309(11): E887-E899.
- Chavez-Jauregui, R.N., R.D. Mattes and E.J. Parks, 2010. Dynamics of fat absorption and effect of sham feeding on postprandial lipemia. *Gastroenterology*, 139(5): 1538-1548.

- Cheng, Y.-S., O. Seibert, N. Klötting, A. Dietrich, K. Straßburger, S. Fernández-Veledo, J.J. Vendrell, A. Zorzano, M. Blüher and S. Herzig, 2015. PPP2R5C couples hepatic glucose and lipid homeostasis. *PLoS Genetics*, 11(10): e1005561.
- Chiasson, J.L., R.G. Josse, R. Gomis, M. Hanefeld, A. Karasik, M. Laakso and S.-N.T.R. Group, 2002. Acarbose for prevention of type 2 diabetes mellitus: The STOP-NIDDM randomised trial. *The Lancet*, 359(9323): 2072-2077.
- Chiasson, J.L., R.G. Josse, R. Gomis, M. Hanefeld, A. Karasik, M. Laakso and S.-N.T.R. Group, 2003. Acarbose treatment and the risk of cardiovascular disease and hypertension in patients with impaired glucose tolerance: The STOP-NIDDM randomised trial. *Journal of the American Medical Association*, 290(4): 486-494.
- Cho, S.Y., Y.K. Song, J.G. Kim, S.Y. Oh and C.M. Chung, 2009. Photoconversion of *o*-hydroxycinnamates to coumarins and its application to fluorescence imaging. *Tetrahedron Letters*, 50(33): 4769-4772.
- Clifford, M.N., 2004. Diet-derived phenols in plasma and tissues and their implications for health. *Planta Medica*, 70(12): 1103-1114.
- Clifford, M.N. and N.E. Madala, 2017. Surrogate standards: a cost-effective strategy for identification of phytochemicals. *Journal of Agricultural and Food Chemistry*, 65(18): 3589-3590.
- Coe, S. and L. Ryan, 2016. Impact of polyphenol-rich sources on acute postprandial glycaemia: a systematic review. *Journal of Nutritional Science*, 5: e24.
- Cohen, L.J., D. Esterhazy, S.-H. Kim, C. Lemetre, R.R. Aguilar, E.A. Gordon, A.J. Pickard, J.R. Cross, A.B. Emiliano and S.M. Han, 2017. Commensal bacteria make GPCR ligands that mimic human signalling molecules. *Nature*, 549(7670): 48-53.
- Collins, Q.F., H.-Y. Liu, J. Pi, Z. Liu, M.J. Quon and W. Cao, 2007. Epigallocatechin-3-gallate (EGCG), a green tea polyphenol, suppresses hepatic gluconeogenesis through 5'-AMP-activated protein kinase. *Journal of Biological Chemistry*, 282(41): 30143-30149.
- Côté, C.D., B.A. Rasmussen, F.A. Duca, M. Zadeh-Tahmasebi, J.A. Baur, M. Daljeet, D.M. Breen, B.M. Filippi and T.K. Lam, 2015. Resveratrol activates duodenal SIRT1 to reverse insulin resistance in rats through a neuronal network. *Nature Medicine*, 21(5): 498-505.
- Cotillard, A., S.P. Kennedy, L.C. Kong, E. Prifti, N. Pons, E. Le Chatelier, M. Almeida, B. Quinquis, F. Levenez, N. Galleron, S. Gougis, S. Rizkalla, J.M. Batto, P. Renault, J. Dore, J.D. Zucker, K. Clement, S.D. Ehrlich and A.N.R.M. Consortium, 2013. Dietary intervention impact on gut microbial gene richness. *Nature*, 500(7464): 585-588.
- Courts, F., 2011. Human absorption and metabolism of aspalathin, a C-glycosyl dihydrochalcone from rooibos tea. *The University of Leeds, School of Food Science and Nutrition*. Thesis ©.
- Crandall, J.P., V. Oram, G. Trandafirescu, M. Reid, P. Kishore, M. Hawkins, H.W. Cohen and N. Barzilai, 2012. Pilot study of resveratrol in older adults with impaired glucose tolerance. *Journals of Gerontology Series A: Biomedical Sciences and Medical Sciences*, 67(12): 1307-1312.
- Crozier, A., I.B. Jaganath and M.N. Clifford, 2009. Dietary phenolics: chemistry, bioavailability and effects on health. *Natural Product Reports*, 26(8): 1001-1043.
- Cuervo, A., A. Hevia, P. López, A. Suárez, B. Sánchez, A. Margolles and S. González, 2015. Association of polyphenols from oranges and apples with specific intestinal

- microorganisms in systemic lupus erythematosus patients. *Nutrients*, 7(2): 1301-1317.
- D'Aquila, T., Y.-H. Hung, A. Carreiro and K.K. Buhman, 2016. Recent discoveries on absorption of dietary fat: Presence, synthesis, and metabolism of cytoplasmic lipid droplets within enterocytes. *Biochimica et Biophysica Acta (BBA)-Molecular and Cell Biology of Lipids*, 1861(8): 730-747.
- Dao, M.C., A. Everard, J. Aron-Wisnewsky, N. Sokolovska, E. Prifti, E.O. Verger, B.D. Kayser, F. Levenez, J. Chilloux and L. Hoyles, 2016. *Akkermansia muciniphila* and improved metabolic health during a dietary intervention in obesity: relationship with gut microbiome richness and ecology. *Gut*, 65(3): 426-436.
- Dash, S., C. Xiao, C. Morgantini and G.F. Lewis, 2015. New insights into the regulation of chylomicron production. *Annual Review of Nutrition*, 35: 265-294.
- Davis, H.R. and E.P. Veltri, 2007. Zetia: inhibition of Niemann-Pick C1 like 1 (NPC1L1) to reduce intestinal cholesterol absorption and treat hyperlipidemia. *Journal of Atherosclerosis and Thrombosis*, 14(3): 99-108.
- Day, A.J., F.J. Cañada, J.C. Díaz, P.A. Kroon, R. Mclauchlan, C.B. Faulds, G.W. Plumb, M.R. Morgan and G. Williamson, 2000. Dietary flavonoid and isoflavone glycosides are hydrolysed by the lactase site of lactase phlorizin hydrolase. *FEBS Letters*, 468(2-3): 166-170.
- Day, A.J., M.S. DuPont, S. Ridley, M. Rhodes, M.J. Rhodes, M.R. Morgan and G. Williamson, 1998. Deglycosylation of flavonoid and isoflavonoid glycosides by human small intestine and liver β -glucosidase activity. *FEBS Letters*, 436(1): 71-75.
- de Bock, M., J.G. Derraik and W.S. Cutfield, 2012. Polyphenols and glucose homeostasis in humans. *Journal of the Academy of Nutrition and Dietetics*, 112(6): 808-815.
- De Vadder, F., P. Kovatcheva-Datchary, D. Goncalves, J. Vinera, C. Zitoun, A. Duchamp, F. Bäckhed and G. Mithieux, 2014. Microbiota-generated metabolites promote metabolic benefits via gut-brain neural circuits. *Cell*, 156(1): 84-96.
- Denis, M.-C., Y. Desjardins, A. Furtos, V. Marcil, S. Dudonné, A. Montoudis, C. Garofalo, E. Delvin, A. Marette and E. Levy, 2015. Prevention of oxidative stress, inflammation and mitochondrial dysfunction in the intestine by different cranberry phenolic fractions. *Clinical Science*, 128(3): 197-212.
- deOgburn, R., J.O. Leite, J. Ratliff, J.S. Volek, M.M. McGrane and M.L. Fernandez, 2012. Effects of increased dietary cholesterol with carbohydrate restriction on hepatic lipid metabolism in guinea pigs. *Comparative Medicine*, 62(2): 109-115.
- Derrien, M., C. Belzer and W.M. de Vos, 2017. *Akkermansia muciniphila* and its role in regulating host functions. *Microbial Pathogenesis*, 106: 171-181.
- di Gesso, J.L., J.S. Kerr, Q. Zhang, S. Raheem, S.K. Yalamanchili, D. O'hagan, C.D. Kay and M.A. O'connell, 2015. Flavonoid metabolites reduce tumor necrosis factor- α secretion to a greater extent than their precursor compounds in human THP-1 monocytes. *Molecular Nutrition & Food Research*, 59(6): 1143-1154.
- Ding, M., S.N. Bhupathiraju, M. Chen, R.M. van Dam and F.B. Hu, 2014. Caffeinated and decaffeinated coffee consumption and risk of type 2 diabetes: a systematic review and a dose-response meta-analysis. *Diabetes Care*, 37(2): 569-586.
- Dixon, M., 1953. The determination of enzyme inhibitor constants. *Biochemical Journal*, 55(1): 170.
- Drozdowski, L. and A.B. Thomson, 2006. Intestinal mucosal adaptation. *World Journal of Gastroenterology*, 12(29): 4614.

- Drummond, E.M., N. Harbourne, E. Marete, D. Martyn, J. Jacquier, D. O'riordan and E.R. Gibney, 2013. Inhibition of proinflammatory biomarkers in THP-1 macrophages by polyphenols derived from Chamomile, Meadowsweet and Willow bark. *Phytotherapy Research*, 27(4): 588-594.
- Duca, F.A., C.D. Côté, B.A. Rasmussen, M. Zadeh-Tahmasebi, G.A. Rutter, B.M. Filippi and T.K. Lam, 2015. Metformin activates a duodenal ampk-dependent pathway to lower hepatic glucose production in rats. *Nature Medicine*, 21(5): 506-511.
- Dueñas, M., F. Surco-Laos, S. González-Manzano, A.M. González-Paramás, E. Gómez-Orte, J. Cabello and C. Santos-Buelga, 2013. Deglycosylation is a key step in biotransformation and lifespan effects of quercetin-3-O-glucoside in *Caenorhabditis elegans*. *Pharmacological Research*, 76: 41-48.
- El-Osta, A., D. Brasacchio, D. Yao, A. Poci, P.L. Jones, R.G. Roeder, M.E. Cooper and M. Brownlee, 2008. Transient high glucose causes persistent epigenetic changes and altered gene expression during subsequent normoglycemia. *Journal of Experimental Medicine*, 205(10): 2409-2417.
- Escande, C., V. Nin, N.L. Price, V. Capellini, A.P. Gomes, M.T. Barbosa, L. O'Neil, T.A. White, D.A. Sinclair and E.N. Chini, 2013. Flavonoid apigenin is an inhibitor of the NAD⁺ase CD38. *Diabetes*, 62(4): 1084-1093.
- Etxeberria, U., A.L. de la Garza, J. Campión, J.A. Martinez and F.I. Milagro, 2012. Antidiabetic effects of natural plant extracts via inhibition of carbohydrate hydrolysis enzymes with emphasis on pancreatic α -amylase. *Expert Opinion on Therapeutic Targets*, 16(3): 269-297.
- Everard, A., C. Belzer, L. Geurts, J.P. Ouwerkerk, C. Druart, L.B. Bindels, Y. Guiot, M. Derrien, G.G. Muccioli and N.M. Delzenne, 2013. Cross-talk between *Akkermansia muciniphila* and intestinal epithelium controls diet-induced obesity. *Proceedings of the National Academy of Sciences*, 110(22): 9066-9071.
- Fändriks, L., 2016. Roles of the gut in the metabolic syndrome: an overview. *Journal of Internal Medicine*, 281(4): 319-336.
- Ferrars, R., C. Czank, Q. Zhang, N. Botting, P. Kroon, A. Cassidy and C. Kay, 2014. The pharmacokinetics of anthocyanins and their metabolites in humans. *British Journal of Pharmacology*, 171(13): 3268-3282.
- Forester, S.C., Y. Gu and J.D. Lambert, 2012. Inhibition of starch digestion by the green tea polyphenol, (-)-epigallocatechin-3-gallate. *Molecular Nutrition & Food Research*, 56(11): 1647-1654.
- Forouzanfar, M.H., L. Alexander, H.R. Anderson, V.F. Bachman, S. Biryukov, M. Brauer, R. Burnett, D. Casey, M.M. Coates and A. Cohen, 2015. Global, regional, and national comparative risk assessment of 79 behavioural, environmental and occupational, and metabolic risks or clusters of risks in 188 countries, 1990–2013: a systematic analysis for the global burden of disease study 2013. *The Lancet*, 386(10010): 2287-2323.
- Fujii, Y., N. Osaki, T. Hase and A. Shimotoyodome, 2015. Ingestion of coffee polyphenols increases postprandial release of the active glucagon-like peptide-1 (GLP-1 (7–36)) amide in C57bl/6J mice. *Journal of Nutritional Science*, 4: UNSP e9
- Ge, L., J. Wang, W. Qi, H.-H. Miao, J. Cao, Y.-X. Qu, B.-L. Li and B.-L. Song, 2008. The cholesterol absorption inhibitor ezetimibe acts by blocking the sterol-induced internalization of NPC1L1. *Cell Metabolism*, 7(6): 508-519.

- Gheldof, N., S. Moco, C. Chabert, T. Teay, D. Barron and J. Hager, 2017. Role of sulfotransferases in resveratrol metabolism in human adipocytes. *Molecular Nutrition & Food Research*, 61(10): 1700020.
- Gossiau, A., S. Li, C.-T. Ho, K.Y. Chen and N.E. Rawson, 2011. The importance of natural product characterization in studies of their anti-inflammatory activity. *Molecular Nutrition & Food Research*, 55(1): 74-82.
- Goto, T., M. Horita, H. Nagai, A. Nagatomo, N. Nishida, Y. Matsuura and S. Nagaoka, 2012. Tiliroside, a glycosidic flavonoid, inhibits carbohydrate digestion and glucose absorption in the gastrointestinal tract. *Molecular Nutrition & Food Research*, 56(3): 435-445.
- Gouyon, F., L. Caillaud, V. Carriere, C. Klein, V. Dalet, D. Citadelle, G.L. Kellett, B. Thorens, A. Leturque and E. Brot-Laroche, 2003. Simple-sugar meals target GLUT2 at enterocyte apical membranes to improve sugar absorption: a study in GLUT2-null mice. *Journal of Physiology-London*, 552(3): 823-832.
- Grefner, N., L. Gromova, A. Gruzdkov and Y.Y. Komissarchik, 2012. Caco-2 cell culture as an intestinal epithelium model to study hexose transport. *Cell and Tissue Biology*, 6(4): 335-340.
- Greiner, T.U. and F. Bäckhed, 2016. Microbial regulation of GLP-1 and L-cell biology. *Molecular Metabolism*, 5(9): 753-758.
- Grundy, S.M., J.I. Cleeman, C.N.B. Merz, H.B. Brewer, L.T. Clark, D.B. Hunninghake, R.C. Pasternak, S.C. Smith and N.J. Stone, 2004. Implications of recent clinical trials for the national cholesterol education program adult treatment panel iii guidelines. *Circulation*, 110(2): 227-239.
- Guariguata, L., D. Whiting, I. Hambleton, J. Beagley, U. Linnenkamp and J. Shaw, 2014. Global estimates of diabetes prevalence for 2013 and projections for 2035. *Diabetes Research and Clinical Practice*, 103(2): 137-149.
- Guimarães, R., L. Barros, M. Dueñas, R.C. Calhella, A.M. Carvalho, C. Santos-Buelga, M.J.R. Queiroz and I.C. Ferreira, 2013. Infusion and decoction of wild German Chamomile: bioactivity and characterization of organic acids and phenolic compounds. *Food Chemistry*, 136(2): 947-954.
- Guimarães, R., L. Barros, M. Dueñas, R.C. Calhella, A.M. Carvalho, C. Santos-Buelga, M.J.R. Queiroz and I.C. Ferreira, 2013. Nutrients, phytochemicals and bioactivity of wild Roman Chamomile: a comparison between the herb and its preparations. *Food Chemistry*, 136(2): 718-725.
- Guzmán-Maldonado, H., O. Paredes-López and C.G. Biliaderis, 1995. Amyolytic enzymes and products derived from starch: a review. *Critical Reviews in Food Science & Nutrition*, 35(5): 373-403.
- Hanhineva, K., R. Törrönen, I. Bondia-Pons, J. Pekkinen, M. Kolehmainen, H. Mykkänen and K. Poutanen, 2010. Impact of dietary polyphenols on carbohydrate metabolism. *International Journal of Molecular Sciences*, 11(4): 1365-1402.
- Hanske, L., G. Loh, S. Sczesny, M. Blaut and A. Braune, 2009. The bioavailability of apigenin-7-glucoside is influenced by human intestinal microbiota in rats. *The Journal of Nutrition*, 139(6): 1095-1102.
- Harbis, A., C. Defoort, H. Narbonne, C. Juhel, M. Senft, C. Latgé, B. Delenne, H. Portugal, C. Atlan-Gepner and B. Vialettes, 2001. Acute hyperinsulinism modulates plasma apolipoprotein B-48 triglyceride—rich lipoproteins in healthy subjects during the postprandial period. *Diabetes*, 50(2): 462-469.
- Harman, D., 1956. Aging: A theory based on free radical and radiation chemistry. *Journal of Gerontology*, 11(3): 298-300.

- Harmel, E., E. Grenier, A. Bendjoudi Ouadda, M. El Chebly, E. Ziv, J.F. Beaulieu, A. Sané, S. Spahis, M. Laville and E. Levy, 2014. AMPK in the small intestine in normal and pathophysiological conditions. *Endocrinology*, 155(3): 873-888.
- Harwood, H.J., 2012. The adipocyte as an endocrine organ in the regulation of metabolic homeostasis. *Neuropharmacology*, 63(1): 57-75.
- Hayeshi, R., C. Hilgendorf, P. Artursson, P. Augustijns, B. Brodin, P. Dehertogh, K. Fisher, L. Fossati, E. Hovenkamp and T. Korjamo, 2008. Comparison of drug transporter gene expression and functionality in Caco-2 cells from 10 different laboratories. *European Journal of Pharmaceutical Sciences*, 35(5): 383-396.
- He, W., Y. Barak, A. Hevener, P. Olson, D. Liao, J. Le, M. Nelson, E. Ong, J.M. Olefsky and R.M. Evans, 2003. Adipose-specific peroxisome proliferator-activated receptor γ knockout causes insulin resistance in fat and liver but not in muscle. *Proceedings of the National Academy of Sciences*, 100(26): 15712-15717.
- Hernández, E.Á., S. Kahl, A. Seelig, P. Begovatz, M. Irmeler, Y. Kupriyanova, B. Nowotny, P. Nowotny, C. Herder and C. Barosa, 2017. Acute dietary fat intake initiates alterations in energy metabolism and insulin resistance. *The Journal of Clinical Investigation*, 127(2): 695-708.
- Hertog, M.G., E.J. Feskens and D. Kromhout, 1997. Antioxidant flavonols and coronary heart disease risk. *The Lancet*, 349(9053): 699-699.
- Hirsh, A.J., S. Yao, J.D. Young and C.I. Cheeseman, 1997. Inhibition of glucose absorption in the rat jejunum: a novel action of α -D-glucosidase inhibitors. *Gastroenterology*, 113(1): 205-211.
- Ho, G.T.T., E.T. Kase, H. Wangenstein and H. Barsett, 2017. Phenolic elderberry extracts, anthocyanins, procyanidins, and metabolites influence glucose and fatty acid uptake in human skeletal muscle cells. *Journal of Agricultural and Food Chemistry*, 65(13): 2677-2685.
- Hollman, P.C., 2014. Unravelling of the health effects of polyphenols is a complex puzzle complicated by metabolism. *Archives of Biochemistry and Biophysics*, 559: 100-105.
- Holst, J.J., 2007. The physiology of glucagon-like peptide 1. *Physiological Reviews*, 87(4): 1409-1439.
- Horton, J.D., J.L. Goldstein and M.S. Brown, 2002. SREBPs: Activators of the complete program of cholesterol and fatty acid synthesis in the liver. *The Journal of Clinical Investigation*, 109(9): 1125-1131.
- Hossain, S.J., H. Kato, H. Aoshima, T. Yokoyama, M. Yamada and Y. Hara, 2002. Polyphenol-induced inhibition of the response of Na⁺/glucose cotransporter expressed in *Xenopus oocytes*. *Journal of Agricultural and Food Chemistry*, 50(18): 5215-5219.
- Hwang, J.-T., D.Y. Kwon and S.H. Yoon, 2009. Amp-activated protein kinase: a potential target for the diseases prevention by natural occurring polyphenols. *New Biotechnology*, 26(1): 17-22.
- Ifie, I., L.J. Marshall, P. Ho and G. Williamson, 2016. *Hibiscus sabdariffa* (roselle) extracts and wine: phytochemical profile, physicochemical properties, and carbohydrase inhibition. *Journal of Agricultural and Food Chemistry*, 64(24): 4921-4931.
- Imamura, F., L. O'Connor, Z. Ye, J. Mursu, Y. Hayashino, S.N. Bhupathiraju and N.G. Forouhi, 2015. Consumption of sugar sweetened beverages, artificially sweetened beverages, and fruit juice and incidence of type 2 diabetes: Systematic review,

- meta-analysis, and estimation of population attributable fraction. *British Medical Journal*, 351: h3576.
- Inoue, I., Y. Shinoda, T. Nakano, M. Sassa, S.-i. Goto, T. Awata, T. Komoda and S. Katayama, 2006. Acarbose ameliorates atherogenicity of low-density lipoprotein in patients with impaired glucose tolerance. *Metabolism*, 55(7): 946-952.
- Jia, L., J.L. Betters and L. Yu, 2011. Niemann-pick c1-like 1 (NPC1L1) protein in intestinal and hepatic cholesterol transport. *Annual Review of Physiology*, 73: 239-259.
- Jin, J.S., M. Touyama, T. Hisada and Y. Benno, 2012. Effects of green tea consumption on human fecal microbiota with special reference to bifidobacterium species. *Microbiology and Immunology*, 56(11): 729-739.
- Johnston, K., P. Sharp, M. Clifford and L. Morgan, 2005. Dietary polyphenols decrease glucose uptake by human intestinal Caco-2 cells. *Febs Letters*, 579(7): 1653-1657.
- Johnston, K.L., M.N. Clifford and L.M. Morgan, 2002. Possible role for apple juice phenolic compounds in the acute modification of glucose tolerance and gastrointestinal hormone secretion in humans. *Journal of the Science of Food and Agriculture*, 82(15): 1800-1805.
- Jokura, H., I. Watanabe, M. Umeda, T. Hase and A. Shimotoyodome, 2015. Coffee polyphenol consumption improves postprandial hyperglycemia associated with impaired vascular endothelial function in healthy male adults. *Nutrition Research*, 35(10): 873-881.
- Jørgensen, A.B., R. Frikke-Schmidt, A.S. West, P. Grande, B.G. Nordestgaard and A. Tybjaerg-Hansen, 2012. Genetically elevated non-fasting triglycerides and calculated remnant cholesterol as causal risk factors for myocardial infarction. *European Heart Journal*: ehs431.
- Josic, J., A.T. Olsson, J. Wickeberg, S. Lindstedt and J. Hlebowicz, 2010. Does green tea affect postprandial glucose, insulin and satiety in healthy subjects: a randomized controlled trial. *Nutrition Journal*, 9(1): 63.
- Joven, J., V. Micol, A. Segura-Carretero, C. Alonso-Villaverde and J.A. Menéndez, 2013. Polyphenols and the modulation of gene expression pathways: Can we eat our way out of the danger of chronic disease? *Critical Reviews in Food Science and Nutrition*, 54(8): 985-1001.
- Kadouh, H.C., S. Sun, W. Zhu and K. Zhou, 2016. α -glucosidase inhibiting activity and bioactive compounds of six red wine grape pomace extracts. *Journal of Functional Foods*, 26: 577-584.
- Kastelein, J.J., 2014. Dyslipidaemia in perspective. *The Lancet*, 384(9943): 566-568.
- Kato, A., Y. Minoshima, J. Yamamoto, I. Adachi, A.A. Watson and R.J. Nash, 2008. Protective effects of dietary chamomile tea on diabetic complications. *Journal of Agricultural and Food Chemistry*, 56(17): 8206-8211.
- Kawano, H., T. Motoyama, O. Hirashima, N. Hirai, Y. Miyao, T. Sakamoto, K. Kugiyama, H. Ogawa and H. Yasue, 1999. Hyperglycemia rapidly suppresses flow-mediated endothelium-dependent vasodilation of brachial artery. *Journal of the American College of Cardiology*, 34(1): 146-154.
- Kellett, G.L., E. Brot-Laroche, O.J. Mace and A. Leturque, 2008. Sugar absorption in the intestine: the role of GLUT2. *Annual Review of Nutrition*, 28: 35-54.
- Kennedy, J.F., P. Methacanon and L.L. Lloyd, 1999. The identification and quantitation of the hydroxycinnamic acid substituents of a polysaccharide extracted from maize bran. *Journal of the Science of Food and Agriculture*, 79(3): 464-470.

- Kerimi, A. and G. Williamson, 2016. At the interface of antioxidant signalling and cellular function: key polyphenol effects. *Molecular Nutrition & Food Research*.
- Kim, Y., J.B. Keogh and P.M. Clifton, 2016. Polyphenols and glycemic control. *Nutrients*, 8(1): 17.
- King, R. and P. Grant, 2016. Diabetes and cardiovascular disease: pathophysiology of a life-threatening epidemic. *Herz*, 41(3): 184-192.
- Kishimoto, Y., M. Tani and K. Kondo, 2013. Pleiotropic preventive effects of dietary polyphenols in cardiovascular diseases. *European Journal of Clinical Nutrition*, 67(5): 532-535.
- Kitchen, D.B., H. Decornez, J.R. Furr and J. Bajorath, 2004. Docking and scoring in virtual screening for drug discovery: methods and applications. *Nature Reviews. Drug Discovery*, 3(11): 935.
- Knekt, P., J. Kumpulainen, R. Järvinen, H. Rissanen, M. Heliövaara, A. Reunanen, T. Hakulinen and A. Aromaa, 2002. Flavonoid intake and risk of chronic diseases. *The American Journal of Clinical Nutrition*, 76(3): 560-568.
- Kobayashi, Y., M. Suzuki, H. Satsu, S. Arai, Y. Hara, K. Suzuki, Y. Miyamoto and M. Shimizu, 2000. Green tea polyphenols inhibit the sodium-dependent glucose transporter of intestinal epithelial cells by a competitive mechanism. *Journal of Agricultural and Food Chemistry*, 48(11): 5618-5623.
- Koh, L.W., L.L. Wong, Y.Y. Loo, S. Kasapis and D. Huang, 2009. Evaluation of different teas against starch digestibility by mammalian glycosidases. *Journal of Agricultural and Food Chemistry*, 58(1): 148-154.
- Kones, R. and U. Rumana, 2015. Current treatment of dyslipidemia: evolving roles of non-statin and newer drugs. *Drugs*, 75(11): 1201-1228.
- Korem, T., D. Zeevi, N. Zmora, O. Weissbrod, N. Bar, M. Lotan-Pompan, T. Avnit-Sagi, N. Kosower, G. Malka and M. Rein, 2017. Bread affects clinical parameters and induces gut microbiome-associated personal glycemic responses. *Cell Metabolism*, 25(6): 1243-1253. e1245.
- Kotra, G. and H. Daniel, 2007. Flavonoid glycosides are not transported by the human Na⁺/glucose transporter when expressed in *Xenopus laevis* oocytes, but effectively inhibit electrogenic glucose uptake. *Journal of Pharmacology and Experimental Therapeutics*, 322(2): 829-835.
- Kováčik, J. and M. Repčák, 2008. Accumulation of coumarin-related compounds in leaves of *Matricaria Chamomilla* related to sample processing. *Food Chemistry*, 111(3): 755-757.
- Lally, S., D. Owens and G.H. Tomkin, 2007. Genes that affect cholesterol synthesis, cholesterol absorption, and chylomicron assembly: the relationship between the liver and intestine in control and streptozotocin diabetic rats. *Metabolism*, 56(3): 430-438.
- Lally, S., C. Tan, D. Owens and G. Tomkin, 2006. Messenger RNA levels of genes involved in dysregulation of postprandial lipoproteins in type 2 diabetes: the role of Niemann–Pick C1-Like 1, ATP-binding cassette, transporters G5 and G8, and of microsomal triglyceride transfer protein. *Diabetologia*, 49(5): 1008-1016.
- Lev-Ran, A. and R.W. Anderson, 1981. The diagnosis of postprandial hypoglycemia. *Diabetes*, 30(12): 996-999.
- Levy, E., G. Lalonde, E. Delvin, M. Elchebly, L.P. Précourt, N.G. Seidah, S. Spahis, R. Rabasa-Lhoret and E. Ziv, 2010. Intestinal and hepatic cholesterol carriers in diabetic *Psammomys obesus*. *Endocrinology*, 151(3): 958-970.

- Ley, S.H., O. Hamdy, V. Mohan and F.B. Hu, 2014. Prevention and management of type 2 diabetes: dietary components and nutritional strategies. *The Lancet*, 383(9933): 1999-2007.
- Li, Z., S.M. Henning, R.-P. Lee, Q.-Y. Lu, P.H. Summanen, G. Thames, K. Corbett, J. Downes, C.-H. Tseng and S.M. Finegold, 2015. Pomegranate extract induces ellagitannin metabolite formation and changes stool microbiota in healthy volunteers. *Food & Function*, 6(8): 2487-2495.
- Lin, H.C., W.Y. Chey and X.T. Zhao, 2000. Release of distal gut peptide YY (PYY) by fat in proximal gut depends on CCK. *Peptides*, 21(10): 1561-1563.
- Lin, H.C. and I.L. Taylor, 2004. Release of peptide yy by fat in the proximal but not distal gut depends on an atropine-sensitive cholinergic pathway. *Regulatory Peptides*, 117(1): 73-76.
- Lin, C.L., H.-C. Huang and J.-K. Lin, 2007. Theaflavins attenuate hepatic lipid accumulation through activating ampk in human HEPG2 cells. *Journal of Lipid Research*, 48(11): 2334-2343.
- Lin, L.-Z. and J.M. Harnly, 2012. LC-PDA-ESI/MS identification of the phenolic components of three compositae spices: Chamomile, Tarragon, and Mexican Arnica. *Natural Product Communications*, 7(6): 749-752.
- Liou, A.P., M. Paziuk, J.M. Luevano, S. Machineni, P.J. Turnbaugh and L.M. Kaplan, 2013. Conserved shifts in the gut microbiota due to gastric bypass reduce host weight and adiposity. *Science Translational Medicine*, 5(178).
- Liu, K., R. Zhou, B. Wang, K. Chen, L.-Y. Shi, J.-D. Zhu and M.-T. Mi, 2013. Effect of green tea on glucose control and insulin sensitivity: a meta-analysis of 17 randomized controlled trials. *The American Journal of Clinical Nutrition*, 98(2): 340-348.
- Livesey, G., R. Taylor, T. Hulshof and J. Howlett, 2008. Glycemic response and health— a systematic review and meta-analysis: relations between dietary glycemic properties and health outcomes. *The American Journal of Clinical Nutrition*, 87(1): 258S-268S.
- Lo Piparo, E., H. Scheib, N. Frei, G. Williamson, M. Grigorov and C.J. Chou, 2008. Flavonoids for controlling starch digestion: structural requirements for inhibiting human α -amylase. *Journal of Medicinal Chemistry*, 51(12): 3555-3561.
- Lochocka, K., J. Bajerska, A. Glapa, E. Fidler-Witon, J.K. Nowak, T. Szczapa, P. Grebowiec, A. Lisowska and J. Walkowiak, 2015. Green tea extract decreases starch digestion and absorption from a test meal in humans: a randomized, placebo-controlled crossover study. *Scientific Reports*, 5: 12015
- Lotito, S.B., W.J. Zhang, C.S. Yang, A. Crozier and B. Frei, 2011. Metabolic conversion of dietary flavonoids alters their anti-inflammatory and antioxidant properties. *Free Radical Biology and Medicine*, 51(2): 454-463.
- Ludwig, D.S., 2002. The glycemic index: physiological mechanisms relating to obesity, diabetes, and cardiovascular disease. *Journal of the American Medical Association*, 287(18): 2414-2423.
- Lumeng, C.N. and A.R. Saltiel, 2011. Inflammatory links between obesity and metabolic disease. *The Journal of Clinical Investigation*, 121(6): 2111-2117.
- Lv, Y., X. Yang, Y. Zhao, Y. Ruan, Y. Yang and Z. Wang, 2009. Separation and quantification of component monosaccharides of the tea polysaccharides from *Gynostemma pentaphyllum* by HPLC with indirect UV detection. *Food Chemistry*, 112(3): 742-746.

- Mace, O.J., J. Affleck, N. Patel and G.L. Kellett, 2007. Sweet taste receptors in rat small intestine stimulate glucose absorption through apical GLUT2. *Journal of Physiology-London*, 582(1): 379-392.
- Mahraoui, L., M. Rousset, E. Dussaulx, D. Darmoul, A. Zweibaum and E. Brot-Laroche, 1992. Expression and localization of GLUT5-5 in Caco-2 cells, human small intestine, and colon. *American Journal of Physiology-Gastrointestinal and Liver Physiology*, 263(3): G312-G318.
- Mahraoui, L., A. Rodolosse, A. Barbat, E. Dussaulx, A. Zweibaum, M. Rousset and E. Brot-Laroche, 1994. Presence and differential expression of SGLT1, GLUT1, GLUT2, GLUT3 and GLUT5 hexose-transporter mRNAs in Caco-2 cell clones in relation to cell growth and glucose consumption. *Biochemical Journal*, 298(3): 629-633.
- Makarova, E., P. Górnaś, I. Konrade, D. Tirzite, H. Cirule, A. Gulbe, I. Pugajeva, D. Seglina and M. Dambrova, 2015. Acute anti-hyperglycaemic effects of an unripe apple preparation containing phlorizin in healthy volunteers: a preliminary study. *Journal of the Science of Food and Agriculture*, 95(3): 560-568.
- Malhotra, P., C.S. Boddy, V. Soni, S. Saksena, P.K. Dudeja, R.K. Gill and W.A. Alrefai, 2013. D-glucose modulates intestinal Niemann-Pick C1-Like 1 (NPC1L1) gene expression via transcriptional regulation. *American Journal of Physiology-Gastrointestinal and Liver Physiology*, 304(2): G203-G210.
- Manach, C., D. Milenkovic, T. de Wiele, A. Rodriguez-Mateos, B. Roos, M.T. Garcia-Conesa, R. Landberg, E.R. Gibney, M. Heinonen and F. Tomás-Barberán, 2016. Addressing the inter-individual variation in response to consumption of plant food bioactives—towards a better understanding of their role in healthy ageing and cardiometabolic risk reduction. *Molecular Nutrition & Food Research*, 61(6): 1600557 (1-16).
- Manzano, S. and G. Williamson, 2010. Polyphenols and phenolic acids from strawberry and apple decrease glucose uptake and transport by human intestinal Caco-2 cells. *Molecular Nutrition & Food Research*, 54(12): 1773-1780.
- Margolskee, R.F., J. Dyer, Z. Kokrashvili, K.S. Salmon, E. Ilegems, K. Daly, E.L. Maillet, Y. Ninomiya, B. Mosinger and S.P. Shirazi-Beechey, 2007. T1R3 and gustducin in gut sense sugars to regulate expression of Na⁺-glucose cotransporter 1. *Proceedings of the National Academy of Sciences*, 104(38): 15075-15080.
- Martel, J., D.M. Ojcius, C.-J. Chang, C.-S. Lin, C.-C. Lu, Y.-F. Ko, S.-F. Tseng, H.-C. Lai and J.D. Young, 2016. Anti-obesogenic and antidiabetic effects of plants and mushrooms. *Nature Reviews Endocrinology*, 13(3): 149-160.
- Martín-Peláez, S., J.I. Mosele, N. Pizarro, M. Farràs, R. de la Torre, I. Subirana, F.J. Pérez-Cano, O. Castañer, R. Solà and S. Fernandez-Castillejo, 2017. Effect of virgin olive oil and thyme phenolic compounds on blood lipid profile: implications of human gut microbiota. *European Journal of Nutrition*, 56(1): 119-131.
- Matić, I.Z., Z. Juranić, K. Šavikin, G. Zdunić, N. Nađvinski and D. Godevac, 2013. Chamomile and marigold tea: chemical characterization and evaluation of anticancer activity. *Phytotherapy Research*, 27(6): 852-858.
- McCarty, M.F., 2005. A chlorogenic acid-induced increase in GLP-1 production may mediate the impact of heavy coffee consumption on diabetes risk. *Medical Hypotheses*, 64(4): 848-853.

- McCullough, M.L., J.J. Peterson, R. Patel, P.F. Jacques, R. Shah and J.T. Dwyer, 2012. Flavonoid intake and cardiovascular disease mortality in a prospective cohort of US adults. *The American Journal of Clinical Nutrition*, 95(2): 454-464.
- McKay, D.L. and J.B. Blumberg, 2006. A review of the bioactivity and potential health benefits of chamomile tea (*Matricaria recutita* L.). *Phytotherapy Research*, 20(7): 519-530.
- Menendez, C., M. Dueñas, P. Galindo, S. González-Manzano, R. Jimenez, L. Moreno, M.J. Zarzuelo, I. Rodríguez-Gómez, J. Duarte and C. Santos-Buelga, 2011. Vascular deconjugation of quercetin glucuronide: the flavonoid paradox revealed? *Molecular Nutrition & Food Research*, 55(12): 1780-1790.
- Meng, X.-Y., H.-X. Zhang, M. Mezei and M. Cui, 2011. Molecular docking: a powerful approach for structure-based drug discovery. *Current Computer-Aided Drug Design*, 7(2): 146-157.
- Milenkovic, D., C. Morand, A. Cassidy, A. Konic-Ristic, F. Tomás-Barberán, J.M. Ordovas, P. Kroon, R. De Caterina and A. Rodriguez-Mateos, 2017. Interindividual variability in biomarkers of cardiometabolic health after consumption of major plant-food bioactive compounds and the determinants involved. *Advances in Nutrition: An International Review Journal*, 8(4): 558-570.
- Most, J., J. Penders, M. Lucchesi, G. Goossens and E. Blaak, 2017. Gut microbiota composition in relation to the metabolic response to 12-week combined polyphenol supplementation in overweight men and women. *European Journal of Clinical Nutrition*, 71(9): 1040-1045.
- Mulinacci, N., A. Romani, P. Pinelli, F. Vincieri and D. Prucher, 2000. Characterization of *Matricaria recutita* L. flower extracts by HPLC-MS and HPLC-DAD analysis. *Chromatographia*, 51(5-6): 301-307.
- Muoio, D.M. and C.B. Newgard, 2008. Molecular and metabolic mechanisms of insulin resistance and β -cell failure in type 2 diabetes. *Nature Reviews Molecular Cell Biology*, 9(3): 193-205.
- Murase, T., Y. Yokoi, K. Misawa, H. Ominami, Y. Suzuki, Y. Shibuya and T. Hase, 2012. Coffee polyphenols modulate whole-body substrate oxidation and suppress postprandial hyperglycaemia, hyperinsulinaemia and hyperlipidaemia. *British Journal of Nutrition*, 107(12): 1757-1765.
- Murumkar, P.R., R. Giridhar and M.R. Yadav, 2013. Novel methods and strategies in the discovery of tace inhibitors. *Expert Opinion on Drug Discovery*, 8(2): 157-181.
- Nakamura, K., T. Miyoshi, K. Yunoki and H. Ito, 2016. Postprandial hyperlipidemia as a potential residual risk factor. *Journal of Cardiology*, 67(4): 335-339.
- Nordestgaard, B.G. and A. Varbo, 2014. Triglycerides and cardiovascular disease. *The Lancet*, 384(9943): 626-635.
- Nyambe-Silavwe, H., 2016. Effect of polyphenol-rich extracts on glycaemic response in humans. *The University of Leeds, School of Food Science and Nutrition*. Thesis ©.
- Nyambe-Silavwe, H., J.A. Villa-Rodriguez, I. Ifie, M. Holmes, E. Aydin, J.M. Jensen and G. Williamson, 2015. Inhibition of human α -amylase by dietary polyphenols. *Journal of Functional Foods*, 19: 723-732.
- Ohe, C., M. Minami, C. Hasegawa, K. Ashida, M. Sugino and H. Kanamori, 1994. Seasonal variation in production of the head and accumulation of glycosides in the head of *matricaria chamomilla*. In: *Internat. Symposium on Medicinal and Aromatic Plants* 390: pp: 75-82.

- Ong, K.W., A. Hsu and B.K.H. Tan, 2013. Anti-diabetic and anti-lipidemic effects of chlorogenic acid are mediated by ampk activation. *Biochemical pharmacology*, 85(9): 1341-1351.
- Pal, S. and M. Naissides, 2004. Polyphenolics and fat absorption. *International Journal of Obesity & Related Metabolic Disorders*, 28(2): 324-326.
- Panickar, K.S., 2013. Effects of dietary polyphenols on neuroregulatory factors and pathways that mediate food intake and energy regulation in obesity. *Molecular Nutrition & Food Research*, 57(1): 34-47.
- Parker, H., A. Adriaenssens, G. Rogers, P. Richards, H. Koepsell, F. Reimann and F. Gribble, 2012. Predominant role of active versus facilitative glucose transport for glucagon-like peptide-1 secretion. *Diabetologia*, 55(9): 2445-2455.
- Patel, K.R., C. Andreadi, R.G. Britton, E. Horner-Glister, A. Karmokar, S. Sale, V.A. Brown, D.E. Brenner, R. Singh and W.P. Steward, 2013. Sulfate metabolites provide an intracellular pool for resveratrol generation and induce autophagy with senescence. *Science Translational Medicine*, 5(205): 205ra133.
- Payne, M.J., W.J. Hurst, K.B. Miller, C. Rank and D.A. Stuart, 2010. Impact of fermentation, drying, roasting, and dutch processing on epicatechin and catechin content of cacao beans and cocoa ingredients. *Journal of Agricultural and Food Chemistry*, 58(19): 10518-10527.
- Perry, G.H., N.J. Dominy, K.G. Claw, A.S. Lee, H. Fiegler, R. Redon, J. Werner, F.A. Villanea, J.L. Mountain and R. Misra, 2007. Diet and the evolution of human amylase gene copy number variation. *Nature Genetics*, 39(10): 1256-1260.
- Pingitore, A., E.S. Chambers, T. Hill, I.R. Maldonado, B. Liu, G. Bewick, D.J. Morrison, T. Preston, G.A. Wallis and C. Tedford, 2017. The diet-derived short chain fatty acid propionate improves β -cell function in humans and stimulates insulin secretion from human islets *in vitro*. *Diabetes, Obesity and Metabolism*, 19(2): 257-265.
- Plovier, H., A. Everard, C. Druart, C. Depommier, M. Van Hul, L. Geurts, J. Chilloux, N. Ottman, T. Duparc and L. Lichtenstein, 2017. A purified membrane protein from *Akkermansia muciniphila* or the pasteurized bacterium improves metabolism in obese and diabetic mice. *Nature Medicine*, 23(1): 107-113.
- Porter, L., Z. Ma and B. Chan, 1991. Cacao procyanidins: Major flavanoids and identification of some minor metabolites. *Phytochemistry*, 30(5): 1657-1663.
- Postler, T.S. and S. Ghosh, 2017. Understanding the holobiont: how microbial metabolites affect human health and shape the immune system. *Cell Metabolism*, 26(1): 110-130.
- Price, N.L., A.P. Gomes, A.J. Ling, F.V. Duarte, A. Martin-Montalvo, B.J. North, B. Agarwal, L. Ye, G. Ramadori and J.S. Teodoro, 2012. SIRT1 is required for AMPK activation and the beneficial effects of resveratrol on mitochondrial function. *Cell metabolism*, 15(5): 675-690.
- Psichas, A., F. Reimann and F.M. Gribble, 2015. Gut chemosensing mechanisms. *The Journal of Clinical Investigation*, 125(3): 908-917.
- Pussinen, P.J., A.S. Havulinna, M. Lehto, J. Sundvall and V. Salomaa, 2011. Endotoxemia is associated with an increased risk of incident diabetes. *Diabetes Care*, 34(2): 392-397.
- Qin, W., B. Ren, S. Wang, S. Liang, B. He, X. Shi, L. Wang, J. Liang and F. Wu, 2016. Apigenin and naringenin ameliorate PKC β II-associated endothelial dysfunction via regulating ROS/caspase-3 and NO pathway in endothelial cells exposed to high glucose. *Vascular Pharmacology*, 85: 39-49.

- Queipo-Ortuño, M.I., M. Boto-Ordóñez, M. Murri, J.M. Gomez-Zumaquero, M. Clemente-Postigo, R. Estruch, F.C. Diaz, C. Andrés-Lacueva and F.J. Tinahones, 2012. Influence of red wine polyphenols and ethanol on the gut microbiota ecology and biochemical biomarkers. *The American Journal of Clinical Nutrition*, 95(6): 1323-1334.
- Raal, A., A. Orav, T. Püssa, C. Valner, B. Malmiste and E. Arak, 2012. Content of essential oil, terpenoids and polyphenols in commercial Chamomile (*Chamomilla recutita* L. Rauschert) teas from different countries. *Food Chemistry*, 131(2): 632-638.
- Rafraf, M., M. Zemestani and M. Asghari-Jafarabadi, 2015. Effectiveness of chamomile tea on glycemic control and serum lipid profile in patients with type 2 diabetes. *Journal of Endocrinological Investigation*, 38(2): 163-170.
- Ramasubbu, N., C. Ragnath and P.J. Mishra, 2003. Probing the role of a mobile loop in substrate binding and enzyme activity of human salivary amylase. *Journal of Molecular Biology*, 325(5): 1061-1076.
- Raskin, I., D.M. Ribnický, S. Komarnytsky, N. Ilic, A. Poulev, N. Borisjuk, A. Brinker, D.A. Moreno, C. Ripoll and N. Yakoby, 2002. Plants and human health in the twenty-first century. *Trends in Biotechnology*, 20(12): 522-531.
- Ravid, Z., M. Bendayan, E. Delvin, A.T. Sané, M. Elchebly, J. Lafond, M. Lambert, G. Mailhot and E. Levy, 2008. Modulation of intestinal cholesterol absorption by high glucose levels: impact on cholesterol transporters, regulatory enzymes, and transcription factors. *American Journal of Physiology-Gastrointestinal and Liver Physiology*, 295(5): G873-G885.
- Reimann, F., G. Tolhurst and F.M. Gribble, 2012. G-protein-coupled receptors in intestinal chemosensation. *Cell Metabolism*, 15(4): 421-431.
- Ren, B., W. Qin, F. Wu, S. Wang, C. Pan, L. Wang, B. Zeng, S. Ma and J. Liang, 2016. Apigenin and naringenin regulate glucose and lipid metabolism, and ameliorate vascular dysfunction in type 2 diabetic rats. *European Journal of Pharmacology*, 773: 13-23.
- Repčák, M., A. Pastírová, J. Imrich, V. Š Vehlíková and P. Mártonfi, 2001. The variability of (Z)-and (E)-2-β-d-glucopyranosyloxy-4-methoxycinnamic acids and apigenin glucosides in diploid and tetraploid *Chamomilla recutita*. *Plant Breeding*, 120(2): 188-190.
- Rice-Evans, C.A., N.J. Miller and G. Paganga, 1996. Structure-antioxidant activity relationships of flavonoids and phenolic acids. *Free Radical Biology and Medicine*, 20(7): 933-956.
- Robayo-Torres, C.C., R. Quezada-Calvillo and B.L. Nichols, 2006. Disaccharide digestion: clinical and molecular aspects. *Clinical Gastroenterology and Hepatology*, 4(3): 276-287.
- Robertson, M., M. Parkes, B. Warren, D. Ferguson, K. Jackson, D. Jewell and K. Frayn, 2003. Mobilisation of enterocyte fat stores by oral glucose in humans. *Gut*, 52(6): 834-839.
- Roopchand, D.E., R.N. Carmody, P. Kuhn, K. Moskal, P. Rojas-Silva, P.J. Turnbaugh and I. Raskin, 2015. Dietary polyphenols promote growth of the gut bacterium *Akkermansia muciniphila* and attenuate high-fat diet-induced metabolic syndrome. *Diabetes*, 64(8): 2847-2858.
- Roowi, S., A. Stalmach, W. Mullen, M.E.J. Lean, C.A. Edwards and A. Crozier, 2010. Green tea flavan-3-ols: colonic degradation and urinary excretion of catabolites by humans. *Journal of Agricultural and Food Chemistry*, 58(2): 1296-1304.

- Ross, S.M., 2008. Chamomile: a spoonful of medicine. *Holistic Nursing Practice*, 22(1): 56-57.
- Rubino, F., A. Forgione, D.E. Cummings, M. Vix, D. Gnuli, G. Mingrone, M. Castagneto and J. Marescaux, 2006. The mechanism of diabetes control after gastrointestinal bypass surgery reveals a role of the proximal small intestine in the pathophysiology of type 2 diabetes. *Annals of Surgery*, 244(5): 741-749.
- Rudofsky Jr, G., P. Reismann, S. Schiekofer, D. Petrov, M. Von Eynatten, P. Humpert, B. Isermann, C. Müller-Hoff, T.-P. Thai and S. Lichtenstein, 2004. Reduction of postprandial hyperglycemia in patients with type 2 diabetes reduces NF- κ B activation in PBMCS. *Hormone and Metabolic Research*, 36(09): 630-638.
- Salas-Salvadó, J., M. Bulló, R. Estruch, E. Ros, M.-I. Covas, N. Ibarrola-Jurado, D. Corella, F. Arós, E. Gómez-Gracia and V. Ruiz-Gutiérrez, 2014. Prevention of diabetes with mediterranean diets: a subgroup analysis of a randomized trial. *Annals of Internal Medicine*, 160(1): 1-10.
- Sambuy, Y., I. De Angelis, G. Ranaldi, M. Scarino, A. Stammati and F. Zucco, 2005. The Caco-2 cell line as a model of the intestinal barrier: influence of cell and culture-related factors on Caco-2 cell functional characteristics. *Cell Biology and Toxicology*, 21(1): 1-26.
- Samuel, B.S., A. Shaito, T. Motoike, F.E. Rey, F. Backhed, J.K. Manchester, R.E. Hammer, S.C. Williams, J. Crowley and M. Yanagisawa, 2008. Effects of the gut microbiota on host adiposity are modulated by the short-chain fatty-acid binding g protein-coupled receptor, GPR41. *Proceedings of the National Academy of Sciences*, 105(43): 16767-16772.
- Samuel, V.T., K.F. Petersen and G.I. Shulman, 2010. Lipid-induced insulin resistance: unravelling the mechanism. *The Lancet*, 375(9733): 2267-2277.
- Schneeberger, M., A. Everard, A.G. Gómez-Valadés, S. Matamoros, S. Ramírez, N.M. Delzenne, R. Gomis, M. Claret and P.D. Cani, 2015. *Akkermansia muciniphila* inversely correlates with the onset of inflammation, altered adipose tissue metabolism and metabolic disorders during obesity in mice. *Scientific reports*, 5: 16643.
- Schulze, C., A. Bangert, G. Kottra, K.E. Geillinger, B. Schwanck, H. Vollert, W. Blaschek and H. Daniel, 2014. Inhibition of the intestinal sodium-coupled glucose transporter 1 (SGLT1) by extracts and polyphenols from apple reduces postprandial blood glucose levels in mice and humans. *Molecular Nutrition & Food Research*, 58(9): 1795-1808.
- Schulze, C., A. Bangert, B. Schwanck, H. Vollert, W. Blaschek and H. Daniel, 2015. Extracts and flavonoids from onion inhibit the intestinal sodium-coupled glucose transporter 1 (SGLT1) *in vitro* but show no anti-hyperglycaemic effects *in vivo* in normoglycaemic mice and human volunteers. *Journal of Functional Foods*, 18: 117-128.
- Seimon, R.V., I.M. Brennan, A. Russo, T.J. Little, K.L. Jones, S. Standfield, J.M. Wishart, M. Horowitz and C. Feinle-Bisset, 2013. Gastric emptying, mouth-to-cecum transit, and glycemic, insulin, incretin, and energy intake responses to a mixed-nutrient liquid in lean, overweight, and obese males. *American Journal of Physiology-Endocrinology and Metabolism*, 304(3): E294-E300.
- Shen, X. and H. Perreault, 1998. Characterization of carbohydrates using a combination of derivatization, high-performance liquid chromatography and mass spectrometry. *Journal of Chromatography*, 811(1): 47-59.

- Shirosaki, M., T. Koyama and K. Yazawa, 2012. Apple leaf extract as a potential candidate for suppressing postprandial elevation of the blood glucose level. *Journal of Nutritional Science and Vitaminology*, 58(1): 63-67.
- Shukla, S. and S. Gupta, 2010. Apigenin: a promising molecule for cancer prevention. *Pharmaceutical Research*, 27(6): 962-978.
- Sim, L., C. Willemsma, S. Mohan, H.Y. Naim, B.M. Pinto and D.R. Rose, 2010. Structural basis for substrate selectivity in human maltase-glucoamylase and sucrase-isomaltase N-terminal domains. *Journal of Biological Chemistry*, 285(23): 17763-17770.
- Singh, M., M. Arseneault, T. Sanderson, V. Murthy and C. Ramassamy, 2008. Challenges for research on polyphenols from foods in alzheimer's disease: bioavailability, metabolism, and cellular and molecular mechanisms. *Journal of Agricultural and Food Chemistry*, 56(13): 4855-4873.
- Smith, E.P., Z. An, C. Wagner, A.G. Lewis, E.B. Cohen, B. Li, P. Mahbod, D. Sandoval, D. Perez-Tilve and N. Tamarina, 2014. The role of β cell glucagon-like peptide-1 signaling in glucose regulation and response to diabetes drugs. *Cell metabolism*, 19(6): 1050-1057.
- Song, W.-Y., Y. Aihara, T. Hashimoto, K. Kanazawa and M. Mizuno, 2015. (-)-epigallocatechin-3-gallate induces secretion of anorexigenic gut hormones. *Journal of Clinical Biochemistry and Nutrition*, 57(2): 164-169.
- Srivastava, J.K. and S. Gupta, 2007. Antiproliferative and apoptotic effects of Chamomile extract in various human cancer cells. *Journal of Agricultural and Food Chemistry*, 55(23): 9470-9478.
- Srivastava, J.K. and S. Gupta, 2009. Extraction, characterization, stability and biological activity of flavonoids isolated from chamomile flowers. *Molecular and Cellular Pharmacology*, 1(3): 138.
- Srivastava, J.K., M. Pandey and S. Gupta, 2009. Chamomile, a novel and selective COX-2 inhibitor with anti-inflammatory activity. *Life Sciences*, 85(19): 663-669.
- Srivastava, J.K., E. Shankar and S. Gupta, 2010. Chamomile: a herbal medicine of the past with a bright future (review). *Molecular Medicine Reports*, 3(6): 895-901.
- Sternini, C., L. Anselmi and E. Rozengurt, 2008. Enteroendocrine cells: a site of 'taste' in gastrointestinal chemosensing. *Current Opinion in Endocrinology Diabetes and Obesity*, 15(1): 73-78.
- Stringer, D.M., P. Zahradka and C.G. Taylor, 2015. Glucose transporters: cellular links to hyperglycemia in insulin resistance and diabetes. *Nutrition Reviews*, 73(3): 140-154.
- Su, Q., C. Baker, P. Christian, M. Naples, X. Tong, K. Zhang, M. Santha and K. Adeli, 2014. Hepatic mitochondrial and ER stress induced by defective PPAR α signaling in the pathogenesis of hepatic steatosis. *American Journal of Physiology-Endocrinology and Metabolism*, 306(11): E1264-E1273.
- Suksomboon, N., N. Poolsup, S. Boonkaew and C.C. Suthisisang, 2011. Meta-analysis of the effect of herbal supplement on glycemic control in type 2 diabetes. *Journal of Ethnopharmacology*, 137(3): 1328-1333.
- Suzuki, T. and H. Hara, 2011. Role of flavonoids in intestinal tight junction regulation. *The Journal of Nutritional Biochemistry*, 22(5): 401-408.
- Suzuki, T., S. Tanabe and H. Hara, 2011. Kaempferol enhances intestinal barrier function through the cytoskeletal association and expression of tight junction proteins in Caco-2 cells. *The Journal of Nutrition*, 141(1): 87-94.

- Švehlíková, V., R.N. Bennett, F.A. Mellon, P.W. Needs, S. Piacente, P.A. Kroon and Y. Bao, 2004. Isolation, identification and stability of acylated derivatives of apigenin 7-*O*-glucoside from Chamomile (*Chamomilla recutita* [L.] Rauschert). *Phytochemistry*, 65(16): 2323-2332.
- Takii, H., K. Matsumoto, T. Kometani, S. Okada and T. Fushiki, 1997. Lowering effect of phenolic glycosides on the rise in postprandial glucose in mice. *Bioscience, Biotechnology, and Biochemistry*, 61(9): 1531-1535.
- Tallon, M., 2015. Authorised EU health claim for cocoa flavanols. In *Foods, Nutrients and Food Ingredients with Authorised EU Health Claims*, 2(4): 83.
- Tarling, C.A., K. Woods, R. Zhang, H.C. Brastianos, G.D. Brayer, R.J. Andersen and S.G. Withers, 2008. The search for novel human pancreatic α -amylase inhibitors: high-throughput screening of terrestrial and marine natural product extracts. *ChemBioChem*, 9(3): 433-438.
- Taylor, R., 2013. Type 2 diabetes etiology and reversibility. *Diabetes Care*, 36(4): 1047-1055.
- Te Morenga, L., S. Mallard and J. Mann, 2013. Dietary sugars and body weight: systematic review and meta-analyses of randomised controlled trials and cohort studies. *British Medical Journal*, 346: e7492.
- Teng, Z., C. Yuan, F. Zhang, M. Huan, W. Cao, K. Li, J. Yang, D. Cao, S. Zhou and Q. Mei, 2012. Intestinal absorption and first-pass metabolism of polyphenol compounds in rat and their transport dynamics in caco-2 cells. *PLoS One*, 7(1): e29647.
- Thompson, L.U., J.H. Yoon, D. Jenkins, T. Wolever and A.L. Jenkins, 1984. Relationship between polyphenol intake and blood glucose response of normal and diabetic individuals. *The American Journal of Clinical Nutrition*, 39(5): 745-751.
- Timmers, S., E. Konings, L. Bilet, R.H. Houtkooper, T. van de Weijer, G.H. Goossens, J. Hoeks, S. van der Krieken, D. Ryu and S. Kersten, 2011. Calorie restriction-like effects of 30 days of resveratrol supplementation on energy metabolism and metabolic profile in obese humans. *Cell Metabolism*, 14(5): 612-622.
- Tobin, V., M. Le Gall, X. Fioramonti, E. Stolarczyk, A.G. Blazquez, C. Klein, M. Prigent, P. Serradas, M.-H. Cuif and C. Magnan, 2008. Insulin internalizes GLUT2 in the enterocytes of healthy but not insulin-resistant mice. *Diabetes*, 57(3): 555-562.
- Tomkin, G.H., 2010. Atherosclerosis, diabetes and lipoproteins. *Expert review of Cardiovascular Therapy*, 8(7): 1015-1029.
- Tomkin, G.H. and D. Owens, 2011. The chylomicron: relationship to atherosclerosis. *International Journal of Vascular Medicine*, 2012: 784536
- Tomkin, G.H. and D. Owens, 2015. Dyslipidaemia of diabetes and the intestine. *World Journal of Diabetes*, 6(7): 970-977.
- Turnbaugh, P.J., R.E. Ley, M.A. Mahowald, V. Magrini, E.R. Mardis and J.I. Gordon, 2006. An obesity-associated gut microbiome with increased capacity for energy harvest. *Nature*, 444(7122): 1027-1031.
- Tzounis, X., A. Rodriguez-Mateos, J. Vulevic, G.R. Gibson, C. Kwik-Urbe and J.P. Spencer, 2011. Prebiotic evaluation of cocoa-derived flavanols in healthy humans by using a randomized, controlled, double-blind, crossover intervention study. *The American Journal of Clinical Nutrition*, 93(1): 62-72.
- Vacca, M., M. Allison, J.L. Griffin and A. Vidal-Puig, 2015. Fatty acid and glucose sensors in hepatic lipid metabolism: Implications in NAFLD. *Seminars in Liver Disease*, 35(3): 250-261.

- Vahl, T.P., M. Tauchi, T.S. Durler, E.E. Elfers, T.M. Fernandes, R.D. Bitner, K.S. Ellis, S.C. Woods, R.J. Seeley and J.P. Herman, 2007. Glucagon-like peptide-1 (GLP-1) receptors expressed on nerve terminals in the portal vein mediate the effects of endogenous GLP-1 on glucose tolerance in rats. *Endocrinology*, 148(10): 4965-4973.
- van Dam, R.M., N. Naidoo and R. Landberg, 2013. Dietary flavonoids and the development of type 2 diabetes and cardiovascular diseases: review of recent findings. *Current Opinion in Lipidology*, 24(1): 25-33.
- van der Flier, L.G. and H. Clevers, 2009. Stem cells, self-renewal, and differentiation in the intestinal epithelium. *Annual Review of Physiology*, 71: 241-260.
- Van Dieren, S., C. Uiterwaal, Y. Van der Schouw, J. Boer, A. Spijkerman, D. Grobbee and J. Beulens, 2009. Coffee and tea consumption and risk of type 2 diabetes. *Diabetologia*, 52(12): 2561-2569.
- Varbo, A., M. Benn, A. Tybjærg-Hansen and B.G. Nordestgaard, 2013. Elevated remnant cholesterol causes both low-grade inflammation and ischemic heart disease, while elevated low-density lipoprotein cholesterol causes ischemic heart disease without inflammation. *Circulation*, 128(12): 1298-1309.
- Veilleux, A., É. Grenier, P. Marceau, A.C. Carpentier, D. Richard and E. Levy, 2014. Intestinal lipid handling. *Arteriosclerosis, Thrombosis, and Vascular Biology*. 34(3): 644-653.
- Vendrame, S., S. Guglielmetti, P. Riso, S. Arioli, D. Klimis-Zacas and M. Porrini, 2011. Six-week consumption of a wild blueberry powder drink increases bifidobacteria in the human gut. *Journal of Agricultural and Food Chemistry*, 59(24): 12815-12820.
- Vick, H., D. Diedrich and K. Baumann, 1973. Reevaluation of renal tubular glucose transport inhibition by phlorizin analogs. *American Journal of Physiology-Legacy Content*, 224(3): 552-557.
- Villa-Rodriguez, J.A., E. Aydin, J.S. Gauer, A. Pyner, G. Williamson and A. Kerimi, 2017. Green and chamomile teas, but not acarbose, attenuate glucose and fructose transport via inhibition of GLUT2 and GLUT5. *Molecular Nutrition & Food Research*. doi: 10.1002/mnfr.201700566
- Vinoy, S., M. Laville and E.J. Feskens, 2016. Slow-release carbohydrates: Growing evidence on metabolic responses and public health interest. Summary of the symposium held at the 12th European Nutrition Conference (FENS 2015). *Food & Nutrition Research*, 60: 31662
- Wang, D.Q.-H., 2007. Regulation of intestinal cholesterol absorption. *Annual Review of Physiology*, 69: 221-248.
- Warner, E.F., Q. Zhang, K.S. Raheem, D. O'Hagan, M.A. O'Connell and C.D. Kay, 2016. Common phenolic metabolites of flavonoids, but not their unmetabolized precursors, reduce the secretion of vascular cellular adhesion molecules by human endothelial cells. *The Journal of Nutrition*, 146(3): 465-473.
- Warner, E.F., M.J. Smith, Q. Zhang, K.S. Raheem, D. O'Hagan, M.A. O'Connell and C.D. Kay, 2017. Signatures of anthocyanin metabolites identified in humans inhibit biomarkers of vascular inflammation in human endothelial cells. *Molecular Nutrition & Food Research*, 61(9): 1600053.
- Weber, B., M. Herrmann, B. Hartmann, H. Joppe, C.O. Schmidt and H.-J. Bertram, 2008. HPLC/MS and hPLC/NMR as hyphenated techniques for accelerated characterization of the main constituents in chamomile (*Chamomilla recutita* [L.] Rauschert). *European Food Research and Technology*, 226(4): 755-760.

- Wedick, N.M., A. Pan, A. Cassidy, E.B. Rimm, L. Sampson, B. Rosner, W. Willett, F.B. Hu, Q. Sun and R.M. van Dam, 2012. Dietary flavonoid intakes and risk of type 2 diabetes in US men and women. *The American Journal of Clinical Nutrition*, 95(4): 925-933.
- Weidner, C., S.J. Wowro, M. Rousseau, A. Freiwald, V. Kodelja, H. Abdel-Aziz, O. Kelber and S. Sauer, 2013. Antidiabetic effects of Chamomile flowers extract in obese mice through transcriptional stimulation of nutrient sensors of the peroxisome proliferator-activated receptor (PPAR) family. *PloS One*, 8(11): e80335.
- WHO, 2016. Global report on diabetes. *World Health Organization*. <http://www.who.int>.
- Willett, W.C., 2002. Balancing life-style and genomics research for disease prevention. *Science*, 296(5568): 695-698.
- Williams, L.K., C. Li, S.G. Withers and G.D. Brayer, 2012. Order and disorder: differential structural impacts of myricetin and ethyl caffeate on human amylase, an antidiabetic target. *Journal of Medicinal Chemistry*, 55(22): 10177-10186.
- Williams, L.K., X. Zhang, S. Caner, C. Tysoe, N.T. Nguyen, J. Wicki, D.E. Williams, J. Coleman, J.H. McNeill and V. Yuen, 2015. The amylase inhibitor montbretin a reveals a new glycosidase inhibition motif. *Nature Chemical Biology*. 11(9): 691-696.
- Williamson, G., 2013. Possible effects of dietary polyphenols on sugar absorption and digestion. *Molecular Nutrition & Food Research*, 57(1): 48-57.
- Williamson, G. and M.N. Clifford, 2017. Role of the small intestine, colon and microbiota in determining the metabolic fate of polyphenols. *Biochemical Pharmacology*. 139(1): 24-39.
- Williamson, G., 2017. Bioavailability and anti-diabetic action of naturally-occurring flavonoids and phenolic acids. *Biochemical Pharmacology*, 139: 106-106.
- Wojdyło, A., P. Nowicka, Á.A. Carbonell-Barrachina and F. Hernández, 2016. Phenolic compounds, antioxidant and antidiabetic activity of different cultivars of *Ficus Carica* L. Fruits. *Journal of Functional Foods*, 25: 421-432.
- Wong, C.C., W. Meinel, H.R. Glatt, D. Barron, A. Stalmach, H. Steiling, A. Crozier and G. Williamson, 2010. *In vitro* and *in vivo* conjugation of dietary hydroxycinnamic acids by UDP-glucuronosyltransferases and sulfotransferases in humans. *The Journal of Nutritional Biochemistry*, 21(11): 1060-1068.
- Wright, E., B. Hirayama and D. Loo, 2007. Active sugar transport in health and disease. *Journal of Internal Medicine*, 261(1): 32-43.
- Xiao, C., S. Dash, C. Morgantini and G.F. Lewis, 2013. Novel role of enteral monosaccharides in intestinal lipoprotein production in healthy humans. *Arteriosclerosis, Thrombosis, and Vascular Biology*, 33(5): 1056-1062.
- Xiao, C., S. Dash, C. Morgantini and G.F. Lewis, 2016. Intravenous glucose acutely stimulates intestinal lipoprotein secretion in healthy humans. *Arteriosclerosis, Thrombosis, and Vascular Biology*, 36(7): 1457-1463.
- Xiao, J., G. Kai, K. Yamamoto and X. Chen, 2013. Advance in dietary polyphenols as α -glucosidases inhibitors: a review on structure-activity relationship aspect. *Critical Reviews in Food Science and Nutrition*, 53(8): 818-836.
- Yamagata, K., A. Miyashita, M. Chino and H. Matsufuji, 2011. Apigenin inhibits tumor necrosis factor alpha plus high glucose-induced LOX-1 expression in human endothelial cells. *Microvascular Research*, 81(1): 60-67.

- Yamakoshi, J., S. Tokutake, M. Kikuchi, Y. Kubota, H. Konishi and T. Mitsuoka, 2001. Effect of proanthocyanidin-rich extract from grape seeds on human fecal flora and fecal odor. *Microbial Ecology in Health and Disease*, 13(1): 25-31.
- Yasuda, M., K. Yasutake, M. Hino, H. Ohwatari, N. Ohmagari, K. Takedomi, T. Tanaka and G.-i. Nonaka, 2014. Inhibitory effects of polyphenols from water chestnut (*Trapa japonica*) husk on glycolytic enzymes and postprandial blood glucose elevation in mice. *Food Chemistry*, 165: 42-49.
- Young, R.L., B. Chia, N.J. Isaacs, J. Ma, J. Khoo, T.Z. Wu, M. Horowitz and C.K. Rayner, 2013. Disordered control of intestinal sweet taste receptor expression and glucose absorption in type 2 diabetes. *Diabetes*, 62(10): 3532-3541.
- Yu, L., S. Bharadwaj, J.M. Brown, Y. Ma, W. Du, M.A. Davis, P. Michaely, P. Liu, M.C. Willingham and L.L. Rudel, 2006. Cholesterol-regulated translocation of NPC1L1 to the cell surface facilitates free cholesterol uptake. *Journal of Biological Chemistry*, 281(10): 6616-6624.
- Yu, X.-H., K. Qian, N. Jiang, X.-L. Zheng, F.S. Cayabyab and C.-K. Tang, 2014. ABCG5/ABCG8 in cholesterol excretion and atherosclerosis. *Clinica Chimica Acta*, 428: 82-88.
- Zambrowicz, B., Z.-M. Ding, I. Ogbaa, K. Frazier, P. Banks, A. Turnage, J. Freiman, M. Smith, D. Ruff and A. Sands, 2013. Effects of LX4211, a dual SGLT1/SGLT2 inhibitor, plus sitagliptin on postprandial active GLP-1 and glycemic control in type 2 diabetes. *Clinical Therapeutics*, 35(3): 273-285.
- Zambrowicz, B., J. Freiman, P. Brown, K. Frazier, A. Turnage, J. Bronner, D. Ruff, M. Shadoan, P. Banks and F. Mseeh, 2012. Lx4211, a dual SGLT1/SGLT2 inhibitor, improved glycemic control in patients with type 2 diabetes in a randomized, placebo- controlled trial. *Clinical Pharmacology & Therapeutics*, 92(2): 158-169.
- Zambrowicz, B., I. Ogbaa, K. Frazier, P. Banks, A. Turnage, J. Freiman, K.A. Boehm, D. Ruff, D. Powell and A. Sands, 2013. Effects of LX4211, a dual sodium-dependent glucose cotransporters 1 and 2 inhibitor, on postprandial glucose, insulin, glucagon-like peptide 1, and peptide tyrosine tyrosine in a dose-timing study in healthy subjects. *Clinical Therapeutics*, 35(8): 1162-1173.
- Zang, M., S. Xu, K.A. Maitland-Toolan, A. Zuccollo, X. Hou, B. Jiang, M. Wierzbicki, T.J. Verbeuren and R.A. Cohen, 2006. Polyphenols stimulate Amp-activated protein kinase, lower lipids, and inhibit accelerated atherosclerosis in diabetic LDL receptor-deficient mice. *Diabetes*, 55(8): 2180-2191.
- Zemestani, M., M. Rafrat and M. Asghari-Jafarabadi, 2016. Chamomile tea improves glycemic indices and antioxidants status in patients with type 2 diabetes mellitus. *Nutrition*, 32(1): 66-72.
- Zhang, Z., X. Wu, S. Cao, M. Cromie, Y. Shen, Y. Feng, H. Yang and L. Li, 2017. Chlorogenic acid ameliorates experimental colitis by promoting growth of *Akkermansia* in mice. *Nutrients*, 9(7): 677.
- Zheng, Y., J.S. Scow, J.A. Duenes and M.G. Sarr, 2012. Mechanisms of glucose uptake in intestinal cell lines: Role of GLUT2. *Surgery*, 151(1): 13-25.

Appendix A. Assay parameters used for measuring the inhibition of human salivary α -amylase by polyphenols. Adapted from Nyambe-Silavwe *et al.* (2015).

Method of detection	Inhibitor	Substrate		Enzyme (mg/mL)	Buffer	Incubation time (min)	Temperature (°C)	Kinetic parameters	IC ₅₀ (µg/ml)	Acarbose (µM)	Reference
		Source	Concentration (mg/mL)								
DNS reagent	Almond nut seeds skin polyphenols	*	5	*	Sodium phosphate (100 mM, 17 mM NaCl, pH 6.9)	30	37	*	2.74	*	Tsujita, Shintani, and Sató (2013)
DNS reagent	Chestnut extract (tannins and procyanidins)	*	5	*	Sodium phosphate NaCl (17 mM pH 6.8)	30	37	*	3.17	*	Tsujita <i>et al.</i> (2011)
EnzChek Ultra Amylase Assay Kit		DQ starch from corn	0.005	0.0000025	NH ₂ PO ₄ 50 mM, NaCl, 0.5 mM CaCl ₂ , and 0.1% bovine serum (50 mM pH 6.0)	30	25	*	Grape seed 8.7 Green tea 34.9 Catechin 160 EGC 27 EGCG 24 GCG 17	6.9	Yilmazer-Musa, Griffith, Michels, Schneider, and Frei (2012)
DNS reagent	Phlorotannins	Corn starch	0.0476	0.0083	Sodium phosphate (20 mM, NaCl 6.7 mM, pH 6.9)	10	20	*	2.8	*	Roy <i>et al.</i> (2011)
DNS reagent	Black tea Green tea Oolong tea Catechins Theaflavins	Rice starch	0.16	0.0044	Sodium phosphate (50 mM, 6.85 mM NaCl, pH 6.9)	12	37	*	Black tea 420 TDG 2.2 EGCG 642	5.7	Koh <i>et al.</i> (2010)
Nelson-Somogyi	Flavonoids	Potato starch	*	*	50 mM NH ₂ PO ₄ , 50 mM NaCl, 0.5 mM CaCl ₂ , and 0.1% bovine serum albumin, pH 6.0	10	25	*	Scutellarein 2.75 Quercetagetin 3.24 Luteolin 5.26 Fisetin 5.61 Quercetin 6.46 Myricetin 9.61 Eupafolin 15.18	0.9	Lo Piparo <i>et al.</i> (2008)
DNS reagent	Chestnut extract	*	5	Pancreatic*	Sodium phosphate (100 mM, 17 mM NaCl, pH 6.8)	30	37	*	9.4	*	Tsujita, Takaku, and Suzuki (2008)
DNS reagent	Chestnut extract	*	5	*	Sodium phosphate (100 mM, 17 mM NaCl, pH 6.8)	30	37	*	7.5	*	Tsujita <i>et al.</i> (2008)
DNS reagent	Polyphenol-rich pine bark extract	*	*	*	Phosphate*	5	37	*	1.7	3.9 µM	Kim, Jeong, Wang, Lee, and Rhee (2005)
Nelson-Somogyi	Catechins	Maize starch	0.2	4.95	Phosphate* (0.2 M, pH 5.2)	15	37	*	GCG 503.8 EGC 618.8 EGCG 1053 EGC 11689 Epicatechin 11745 Catechin 13310	*	Miao <i>et al.</i> (2014)
DNS reagent	Almond nut seed skin polyphenols	*	5	*	Sodium phosphate (100 mM, 17 mM NaCl, pH 6.8)	30	37	*	2.74	*	Tsujita <i>et al.</i> (2013)

* Not stated or clearly defined.
DQ starch is a starch-derived substrate labelled with a fluorescent group (BODIPY® FL dye).
TDG: theaflavin digallate.

Appendix B. Assay parameters used for measuring the inhibition of porcine α -amylase by polyphenols. Adapted from Nyambe-Silavwe *et al.* (2015).

Method of detection	Inhibitor	Substrate		Enzyme (mg/mL)	Buffer	Incubation time (min)	Temperature (°C)	Kinetic parameters	IC ₅₀ (µg/mL)	Acarbose (µM)	Reference
		Source	Concentration (mg/mL)								
DNS reagent	<i>Phaleria macrocarpa</i> fruit extracts	*	*	0.16	Sodium phosphate (0.02 M, pH 6.9)	10	25	*	n-butanol fraction 58.5 Methanol extract 43.90	49.6	Ali et al. (2013)
DNS reagent	Almond nut seeds skin polyphenols	*	5	*	Sodium phosphate (100 mM, 17 mM NaCl, pH 6.8)	30	37	*	2.2	*	Tsujita et al. (2013)
Chromogenic red starch method	EGCG	Red starch	7	*	Sodium phosphate (20 mM, 6.7 mM NaCl, pH 6.9)	10	37	*	9.2 (IC ₅₀)	*	Forester, Gu, and Lambert (2012)
DNS reagent	Polyphenol rich extracts of <i>C. olitorius</i> leaf	*	0.01	0.25	Sodium phosphate (0.02M, 0.006 M NaCl, pH 6.9)	10	25	*	26.8	*	Oboh et al. (2012)
DNS reagent	Cyanidin-3-O-rutinoside	*	*	*	Phosphate buffer saline (0.1M, pH 6.9)	10	*	*	15.4	18.1	S. Akkarachiyasit, Yibchok-Anun, Wacharasindhu, and Adisakwattana (2011)
*	Rowanberry extract Raspberry extract Red raspberry extract Yellow raspberry extract	Potato starch	0.003	0.025	Synthetic saliva buffer	*	*	*	**	1.24	Grussu, Stewart, and McDougall (2011)
DNS reagent	Polyphenols from chestnut	*	5	*	Sodium phosphate (100 mM, NaCl 17 mM, pH 6.8)	30	37	*	5.71	*	Tsujita et al. (2011)
DNS reagent	Cyanidin Cyanidin-3-O-glucoside	*	1	*	Sodium phosphate (pH 6.9)	10	*	*	Cyanidin 109 Cyanidin-3-glucoside 145	120	Sarinya Akkarachiyasit, Charoenlertkul, Yibchok-anun, and Adisakwattana (2010)
DNS reagent	Dinkum raspberry extract	*	*	0.167	Sodium phosphate (0.02M, 6 mM NaCl, pH 6.9)	10	25	*	16.8	*	Zhang et al. (2010)
DNS reagent	<i>Andrographis paniculata</i> extract Andrographolide	*	*	0.17	Phosphate (20 mM, pH 6.9)	10	25	*	<i>Andrographis paniculata</i> extract 50,900 Andrographolide 11,300	23,079	Subramanian, Asmawi, and Sadikun (2008)
Starch iodine test	Cyanidin-3-O-sambubioside	*	0.0036	*	Sodium phosphate (pH 7)	*	37	*	592	*	Iwai, Kim, Onodera, and Matsue (2006)
Liberation of p-nitrophenol	Quercetin Luteolin Myricetin EGCG Apigenin	Synthetic substrate non-reducing end blocked p-nitrophenyl maltoheptaoside (BFNPG7)	*	0.03	HEPES buffer (pH 6.9)	10	37	*	Quercetin 151 Luteolin 103 Myricetin 98 EGCG >229 Apigenin >135		Tadera, Minami, Takamatsu, and Matsuoka (2006)
DNS reagent	Polyphenol-rich Pine bark extract	*	*	*	Sodium phosphate (pH 6.9)	5	37	*	1.69	2.71	Y. M. Kim et al. (2005)
Reducing termini using FAHBAH	Berry extracts	Potato starch	0.003	0.025	Synthetic saliva	*	*	*	***		McDougall et al. (2005)
Detecting the release of chromophore from synthetic substrate	Flavonoids	p-nitrophenyl- α -D-maltopentaglycoside	1.05	*	Phosphate buffer (100 mM, 0.2 % w/v bovine serum albumin, 1.80 mM CaCl ₂ , pH 7)	5	*	*	Luteolin (50–500) Luteolin-7-O-glucoside 4540 (IC ₁₀₀) Kaempferol-3-O-glucoside 4540 (IC ₁₀₀)	7.74–77.44	J. S. Kim, Kwon, and Son (2000)

* Not stated or clearly defined.
** Inhibition values reported as µg of gallic acid equivalent/mL.
*** Inhibition values reported as µg of phenols/assay.
Where IC₅₀ not given, data are presented as IC_n, where n = % of inhibition reported.

Appendix C. Assay parameters used for measuring the inhibition of microorganism α -amylase by polyphenols. Adapted from Nyambe-Silavwe *et al.* (2015).

Method of detection	Inhibitor	Substrate		Enzyme (mg/mL)	Buffer	Incubation time (min)	Temperature (°C)	Kinetic parameters	IC ₅₀ (µg/mL)	Acarbose (µM)	Reference
		Source	Concentration (mg/mL)								
DNS reagent	Phenolics from the pericarp of red pepper	Potato starch	0.005	*	Phosphate buffer (20 mM, 6.7 mM NaCl, pH 6.9)	3	25	*	Pericarp A 3000 (IC ₃₆) Pericarp B 5000 (IC ₃₆)	*	Chen and Kang (2014)
DNS reagent	Geraldone, isookanin and luteolin	*	0.001	*	Sodium phosphate buffer (20 mM, pH 6.7)	5	37	*	Geraldone 10,000 (IC ₉₄) Isookanin 10,000 (IC ₈₄) Luteolin 10,000 (IC ₉₀)	15,480	Ahmed, Kumar, Sharma, and Verma (2014)
DNS reagent	Almond nut seeds skin polyphenols	*	5	*	Sodium phosphate (100 mM, 17 mM NaCl, pH 6.8)	30	37	*	200 – 50 kDa (49.5)	*	Tsujita <i>et al.</i> (2013)
Starch-iodine method	Tannins from cocoa, pomegranates, cranberries and grapes	Potato starch	*	*	*	2	55	*	Cranberry 5000 (IC ₅₅) Pomegranate 5000 (IC < 50) Grapes 5000 (IC < 50) Cocoa 5000 (IC < 50)	*	Barrett <i>et al.</i> (2013)
DNS reagent	Polyphenols from chestnut	*	5	*	Sodium phosphate (100 mM, 17 mM NaCl, pH 6.8)	30	37	*	300 – 100 kDa (23.95)	*	Tsujita <i>et al.</i> (2011)
Starch iodine method	Polyphenols from different Bangladesh fruits	*	*	0.019	Phosphate buffer (0.02 M, 0.006 M NaCl, pH 7.0)	10	37	*	<i>D. indica</i> (410) polyphenols from other fruits had < 50%	*	Hossain <i>et al.</i> (2008)
DNS reagent	Polymers and oligomers from proanthocyanidins of persimmon peel	*	*	*	Phosphate buffer (20 mM, pH 6.7)	3	20	*	Polymers 100 (IC ₅₃) Oligomers 100 (IC < 50)	*	Lee, Cho, Tanaka, and Yokozawa, (2007)

* Not stated or clearly defined.
Where IC₅₀ is not given, data are presented as IC_n, where n = % of inhibition reported.